WARWICK
THE UNIVERSITY OF WARWICK

Development of Organocatalytic Strategies for Controlled Ring-Opening Polymerisation for Producing Biodegradable Polyesters and Polycarbonates

Paula Kishi Kuroishi

Submitted for the degree of Doctor of Philosophy in Chemistry

University of Warwick, Department of Chemistry

January 2019

Table of Contents

List of Figures

List of Schemes

List of Tables

Acknowledgements

Firstly, I would like to thank my supervisor, Prof Andrew Dove, for giving me the opportunity to do my PhD in his group. Your valuable intellectual guidance, mentoring and encouragement during these years were fundamental for my professional growth and the work in this thesis. I also would like to thank the Brazilian National Council for Scientific and Technological Development (CNPq) for providing the funding through the Science without Border programme, which enabled this research to be carried out in the UK.

Thanks to all members of the Dove group, past and present, for the friendship and support. I will carry the good moments I had with each one of you for the rest of my life. A special thanks to Mathieu, Mar, Chiara and Josh for proof-reading the chapters of this thesis and contributing with valuable suggestions. Many thanks to the analytical facilities team at Warwick and Birmingham Universities for the technical support, ensuring that the studies were conducted at a high-quality standard.

Thank you very much to my parents, Atsushi and Miiaco, for supporting my dreams. Your dedication and love throughout my life have armed me with the resilience and strength required to face new challenges, including completing this PhD so far from home. Thank you to my sister, Carla, for our friendship: our differences are what make us stronger together.

A very special thank you to my partner, Felipe, for your steadfast support in this journey, and for always being so patient, caring and loving. Thank you very much to Denise, Cicaroni and Bá for your unconditional love and for accepting me so warmly in your family.

Declaration of Authorship

This thesis is submitted to the University of Warwick in support of my application for the degree of Doctor of Philosophy. It has been composed by myself and has not been submitted in any previous application for any degree. The work presented (including data generated and data analysis) was carried out by the author except in the case of the photobase generators used in Chapter 5 that were synthesised by Dr Nicolas Zivic, from Sardon's Research Group at the University of the Basque Country.

Summary

This thesis investigates organocatalytic ring-opening polymerisation (ROP) approaches for the controlled synthesis of biodegradable polymers by exploring the post-polymerisation modifications of pendent groups and by photochemical regulations.

Chapter 1 reviews the organocatalysts developed for ROP, including the mechanistic aspects involved in the polymerisation. In addition, an overview of photocatalysed ROPs and the photocatalysts that can be potentially applied for this strategy is presented.

Chapter 2 describes the selective carbonate ROP of trimethylenepropane oxirane ether carbonate monomer by using 1,5,7-triazabicyclo[4.4.0]dec-5-ene as organocatalyst. Post-polymerisation modifications of the pendent epoxide group with a range of nucleophiles demonstrate to be especially effective for benzylamine, chlorine and aromatic thiols.

Chapter 3 demonstrates the high catalytic activity of 1,1,3,3-tetramethylguanidine (TMG) towards the ROP of L-lactide, and of δ-valerolactone and ε-caprolactone when a thiourea cocatalyst is utilised. In addition, the photoinduced ROP is explored by protecting TMG with a photosensitive group and the system is shown to provide temporal control to the polymerisation.

Chapter 4 details the synthesis a bicyclic monomer analogue to lactide that would potentially crosslink *via* ROP to provide spatial resolution to the photocatalyst system. The monomer is obtained from the synthesis of an allyl-functional lactide, and subsequent thiol-ene reaction with a dithiol to form a bis(cyclic diester).

Chapter 5 describes the efforts in preparing a resin formulation composed of the bis(cyclic diester) prepared in Chapter 4 and the photocatalyst developed in Chapter 3 to achieve spatial control. Network materials with various mechanical properties could be obtained by using the crosslinker, poly(L-lactide) oligomers and TMG as a catalyst, although no curing was observed when utilising photocatalysts.

Chapter 6 summarises the key findings of Chapters 2 to 5 and presents opportunities for future investigations in the area of research of this thesis.

Chapter 7 provides the experimental protocols and characterisation data of the compounds and materials prepared in this thesis.

List of Publications

Publications resulted from this thesis:

1. *Synthesis and Properties of Polylactide Elastomers from a Bis(cyclic diester)*, P. K. Kuroishi, A. P. Dove, *Manuscript in preparation*. (**Chapters 4 and 5**)
2. *Recent Advances and Challenges in the Design of Organic Photoacid and Photobase Generators for Polymerizations*, N. Zivic, P. K. Kuroishi, F. Dumur, D. Gigmes, A. P. Dove, H. Sardon, *Angew. Chem. Int. Ed*., *DOI: 10.1002/anie.201810118*. (**Chapter 1**)
3. *Photoinduced Ring-Opening Polymerisation of L-Lactide via a Photocaged Superbase*, P. K. Kuroishi, A. P. Dove, *Chem. Commun*., 2018, **54**, 6264. (**Chapter 3**)
4. *Synthesis and Post-Polymerisation Modification of an Epoxy-Functional Polycarbonate*, P. K. Kuroishi, M. J. Bennison, A. P. Dove, *Polym. Chem*. 2016, **7**, 7108. (**Chapter 2**)

Other Publications:

1. *On Like a Light*, P. K. Kuroishi, A. P. Dove, *Nat. Catal.*, 2018, **1**, 486.
2. *Synthesis of Aliphatic Polycarbonates with a Tuneable Thermal Response,* A. W. Thomas, P. K. Kuroishi, M. M. Perez-Madrigal, A. K. Whittaker, A. P. Dove, *Polym. Chem*., 2017, **8**, 5082.
3. *The Total Synthesis of (−)-Cryptocaryol A*, L. C. Dias., P. K. Kuroishi, E. C. de Lucca Jr., *Org. Biomol. Chem.,* 2015, **13**, 3575.
4. *Enantioselective Total Synthesis of (−)-Ericanone*, L. C. Dias, P. K. Kuroishi, E. C. Polo, E. C. de Lucca Jr., *Tetrahedron Lett.*, 2013, **54**, 980.

List of Abbreviations

1,4-BDM	1,4-Benzenedimethanol
5,5'-BO	5,5'-Bis(oxepane-2-one)
δ	Chemical shift
δ-VL	δ-Valerolactone
ε	Molar absorption coefficient
ε-CL	ε-Caprolactone
λ	Wavelength
Φ	Quantum yield
$Đ_M$	Dispersity
ACE	Activated chain end
AcOH	Acetic acid
AIBN	2,2'-Azobis(isobutyronitrile)
AM	Activated monomer
BCP	2,2'-Bis-(3-caprolactone-4-yl)propane
BEMP	2-*tert*-Butylimino-2-diethylamino-1,3-dimethylperhydro-1,3,2-diazaphosphorine
BnSH	Benzyl mercaptan
BTLA	Bis(thiol-lactide)
DBU	1,8-Diazabicyclo[5.4.0]undec-7-ene
DMAP	4-Dimethylaminopyridine
DMF	*N,N*-Dimethylformamide
DMPA	2,2-Dimethoxy-2-phenylacetophenone
DMSO	Dimethylsulfoxide
DP	Degree of polymerisation
DPP	Diphenyl phosphate
DSC	Differential scanning calorimetry
DTGA	Dodecanethiol-glycolide
DTLA	Dodecanethiol-lactide
DXO	1,5-Dioxepan-2-one
EtOAc	Ethyl acetate
FT-IR	Fourier-transform infrared

HFA	Hexafluoroalcohol
$HNTf_2$	Trifluoromethanesulfonimide
$HNNf_2$	Nona-fluorobutanesulfonimide
HOTf	Trifluoromethanesulfonic acid
L-LA	L-Lactide
LS	Light scattering
NBS	*N*-Bromosuccinimide
MALDI-ToF	Matrix-assisted laser desorption/ionisation time-of-flight
$[M]_0$	Initial monomer concentration
$[M]_0/[I]_0$	Initial monomer-to-initiator concentration ratio
$([M]_0/[I]_0/[cat]_0)$	Initial monomer-to-initiator-to-catalyst
mCPBA	*meta*-Chloroperbenzoic acid
Me_6TREN	Tris[2-(dimethylamino)ethyl]amine
MLA	Methylene-functional lactide
M_n	Number average molecular weight
MS	Mass spectrometry
MSA	Methanesulfonic acid
MTBD	7-Methyl-1,5,7-triazabicyclo[4.4.0]dec-5-ene
M_w	Weight average molecular weight
MWt	Molecular weight
NBOC	*o*-Nitrobenzyloxycarbonyl
$NCyMe_2$	*N*,*N*-Dimethylcyclohexylamine
NHC	*N*-Heterocyclic carbene
NHO	*N*-Heterocyclic olefins
NMR	Nuclear magnetic resonance
NPEOC	2-(*O*-Nitrophenyl)ethoxycarbonyl
NPPOC	2-(2-Nitrophenyl)propoxycarbonyl
NVOC	*o*-Nitroveratryloxycarbonyl
OBS	*O*-Benzenedisulfonimide
OTf	Triflate
P_1-*t*-Bu	*N′*-*tert*-Butyl-*N*,*N*,*N′*,*N′*,*N″*,*N″*- hexamethylphosphorimidic triamide
P_2-*t*-Bu	1-*tert*-Butyl-2,2,4,4,4-pentakis(dimethylamino)-2Λ,^{5}4Λ^5-catenadi(phosphazene)

PAG	Photoacid generator
PBG	Photobase generator
PCL	Polycaprolactone
PDTGA	Poly(dodecanethiol-glycolide)
PDTLA	Poly(dodecanethiol-lactide)
PEG	Poly(ethylene glycol)
PGA	Polyglycolide
PGMA	Polyglycidylmethacrylate
PLA	Polylactide
PLLA	Poly(L-lactide)
PPG	Photolabile protecting group
PTSA	*p*-Toluenesulfonic acid
PVL	Polyvalerolactone
PyOH	1-Pyrenebutanol
QA	Quaternary ammonium salts
RDRP	Reversible-deactivation radical polymerisations
RI	Refractive index
ROMP	Ring-opening metathesis polymerisation
ROP	Ring-opening polymerisation
SEC	Size exclusion chromatography
SET	Single electron transfer
$Sn(Oct)_2$	Tin(II) 2-ethylhexanoate or stannous octanoate
TBAB	Tetrabutylammonium bromide
TBAF	Tetrabutylammonium fluoride
TBAI	Tetrabutylammonium iodide
TBD	1,5,7-Triazabicyclo[4.4.0]dec-5-ene
TCC	Triclocarban
T_d	Temperature of decomposition
T_g	Glass transition temperature
TGA	Thermogravimetric analysis
THF	Tetrahydrofuran
TMC	Trimethylene carbonate
TMG	1,1,3,3-Tetramethylguanidine
TMOC	Trimethylenepropane oxirane ether carbonate

TU	1-(3,5-Bis(trifuoromethyl)phenyl)-3-cyclohexylthiourea
UV	Ultraviolet
UV-Vis	Ultraviolet/visible

Chapter 1

Introduction

1.1 Introduction

Advances in polymers science and technology over the last century have transformed the way we live. Polymers have replaced traditional materials such as metals and ceramics in different areas (*e.g*. packaging, construction, and transport) as a consequence of properties such as light-weight, chemical resistance and durability.[1] More importantly, these versatile materials present unique properties thanks to their ability to be modified according to the specific application. This has enabled the use of polymers across a wide range of sectors, such as agriculture, textiles, electronics and medicine.[2-4] Nevertheless, the non-degradable nature of certain polymeric materials has become highly undesirable in several applications. This has not only resulted in serious environmental issues such as the accumulation of plastic in land and marine waters, but has also restricted the use of some polymers as biomaterials and in the pharmaceutical area.[5]

With the increasing need to promote sustainable practices in materials science, biodegradable polymers have been leading the evolution towards more environmentally-friendly products that tackle the challenges related to the use-phase and end of life of plastics. These materials have been recognized as promising alternatives in combating the plastic pollution problem, especially to replace short-term use plastics (*i.e*. single-use and packaging), since the polymer chains can be transformed by microorganisms and converted into simple units such as CO_2 and water in a short time frame.[6] In addition, studies of the whole life cycle (also known as life cycle assessment (LCA)) of these polymers have suggested the benefits of biodegradability over recovery of energy *via* incineration in terms of emissions.[7] In the biomedical field, the use of biodegradable polymers is advantageous as they can be eliminated from the body after completing their function, which avoids the removal of implants or sutures, and also allows for a controlled delivery of drugs as the polymeric carrier is degraded.[8]

Currently, aliphatic polyesters and polycarbonates are the most investigated biodegradable polymers, although the higher mechanical performance of aliphatic polyesters makes them more suitable for commodity applications.[9,10] In addition, both these polymers are biocompatible and produce non-toxic degradation products, which has also enabled their use in the biomedical area.[11,12] Given the relevance of these materials in the area of sustainable polymers, the following sections discuss how they

can be produced and further manipulated to present the features required for their specific applications.

1.2 Synthesis of Biodegradable Aliphatic Polyesters and Polycarbonates

Aliphatic polyesters and polycarbonates can be produced *via* different methodologies. For instance, the step growth polycondensation of diacids and diols or hydroxy acids provides polyesters,[13,14] while the copolymerisation of CO_2 and epoxides can be utilised to obtain polycarbonates.[15,16] However, these strategies provide reduced control over the molecular weight (MWt) and can also result in undesirable byproducts. Alternatively, both these polymers can be synthesised *via* the ring-opening polymerisation (ROP) of appropriate cyclic monomers.[17-19] This methodology provides great levels of control over the molecular weight, ranging from oligomers to high MWt polymers, while presenting low dispersity and high end-group fidelity.[20,21] In addition, this approach allows modifying the final properties of the resultant polymers, (*i.e*. mechanical, hydrophilic and degradation profiles) not only by applying copolymerisation strategies,[11,22,23] but also by varying the macromolecular architecture, such as star,[24,25] macrocyclic polymers,[26,27] and crosslinked networks.[28,29] However, most of the typical monomers, including lactide (LA), ε-caprolactone (ε-CL), and trimethylene carbonate (TMC), result in polymers without any functionalisable groups in the side chain, which are essential to allow further chemical modification and fine-tune their properties for a wider application (Scheme 1.1).

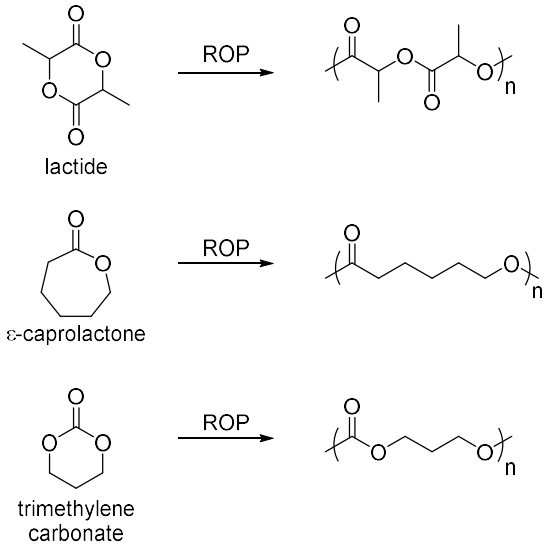

Scheme 1.1. ROP of typical commercially available cyclic monomers.

In this regard, functional groups have been incorporated into the polymer by synthesising and polymerising cyclic monomers containing different substituents.[30-32] Functionalised LA analogues, for instance, are typically prepared by the dimerization of α-hydroxy acids (Scheme 1.2a)[33,34] or the condensation of α-hydroxy acids with α-haloacyl halides, followed by a base mediated cyclisation (Scheme 1.2b).[35,36] However, these ring closure strategies require the use of high dilution conditions to avoid intermolecular reactions, which results in low yields (up to 60%). Alternatively, *O*-carboxyanhydride (OCA) or 1,3-dioxolan-4-ones (DOX) monomers result in a structurally identical polyester by eliminating small molecules during the polymerisation. These monomers are synthesised by ring-closure of α-hydroxy acids with phosgene derivatives in the case of OCA (Scheme 1.2c), or with more sustainable resources such as *p*-formaldehyde for DOX (Scheme 1.2d).[37,38] On the other hand, functionalised ε-caprolactones are prepared in relatively high yields (~85%) by the ring-expansion of the parent cyclohexanones by Baeyer-Villiger oxidation with *meta*-chloroperbenzoic acid (mCPBA) (Scheme 1.2e).[30] Finally, the synthesis of functional cyclic carbonate monomers is usually more straightforward and involves the ring-closure of diols with phosgene derivatives (Scheme 1.2f).[31,39] The commercial availability of 1,3-diols containing different functional groups have allowed the synthesis of a variety of 6-membered carbonate monomers, although 7-membered and *N*-functional 8-membered cyclic carbonates have also been explored as ROP monomers.[40,41]

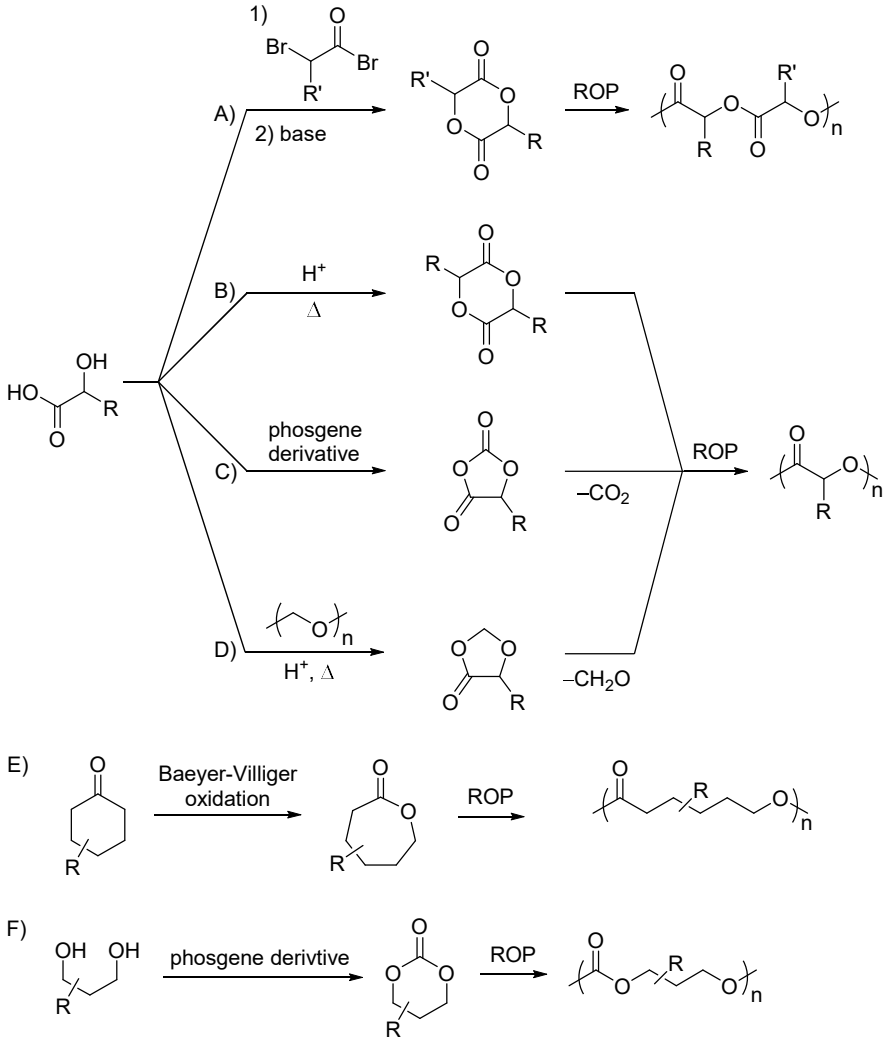

Scheme 1.2. Typical synthesis of functional A) and B) cyclic diesters, C) O-carboxy anhydride, D) 1,3-dioxolan-4-ones, E) ε-caprolactones, and F) cyclic carbonate monomers for ROP.

In order to promote the polymerisation of these cyclic monomers, a number of catalysts have been investigated, ranging from organometallic compounds to organocatalysts. However, both the nature of the monomer (*i.e*. ring functionality and size) and the presence of functional groups provide different reactivities towards ROP. Therefore, the screening of an appropriate catalyst is of critical relevance to obtain good control over the polymerisation for each monomer. As such, a series of ROP catalysts have been developed to provide alternatives with improved activities. Herein, the most common ROP catalysts will be summarised, and the mechanistic aspects of the polymerisation will be presented. Special attention has been placed to discuss those

works using lactide (LA), ε-caprolactone (ε-CL), δ-valerolactone (δ-VL) and cyclic carbonates, as these monomers were investigated in this thesis. Furthermore, an overview of alternative strategies (*i.e.* photocatalysis) applied to provide additional control over the polymerisation has also been included.

1.3 Catalysis for Ring-Opening Polymerisation

1.3.1 Metal Catalysis

The ROP of cyclic esters and carbonates is most commonly performed using organometallic catalysts, especially aluminium alkoxides and tin carboxylates.[42-45] In particular, tin(II) 2-ethylhexanoate ($Sn(Oct)_2$, stannous octanoate) is the ROP catalyst most utilised in industry to produce high MWt polymers as a consequence of its lower air sensitivity when compared to other organometallics and high activity.[43] The polymerisation using organometallic catalysts typically proceeds *via* a coordination-insertion mechanism that involves an initial formation of metal alkoxide species (Scheme 1.3). The carbonyl in the monomer is then activated by coordination with the metal centre and attack of the alkoxide into the carbonyl results in the acyl-oxygen bond cleavage to form a propagating metal alkoxide.

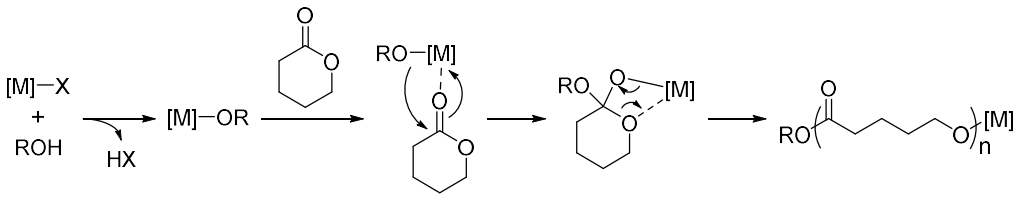

Scheme 1.3. Coordination-insertion mechanism for the ROP of cyclic monomers.

However, concerns have arisen from the presence of residual metal catalysts in the final polymers, especially for the application in the biomedical and microelectronic area.[21] In this regard, organocatalysts have been investigated to provide substitutes with comparable control and reactivities.

1.3.2 Organocatalysis

As an alternative to the metal-based catalysts, organocatalysts offer the advantage of being less sensitive to water and oxygen, providing long shelf lives.[46,47] Regarding the toxicity of such compounds, Nachtergael *et al*. investigated well-stablished organocatalysts (*e.g.* 4-dimethylaminopyridine (DMAP), (+)-sparteine, 1-(3,5-

bis(trifluoromethyl)phenyl)-3-cyclohexylthiourea, 1,8-diazabicyclo[5.4.0]undec-7-ene (DBU), 1,5,7-triazabicyclo[4.4.0]dec-5-ene (TBD)), and most of them showed low levels of cytotoxicity for the range of concentrations studied (up to 200 μM).[48] However, the functionalised thiourea presented more than 50% cell death at concentrations of 11 to 28 μM for the two cell models tested, therefore special care should be taken in removing this catalyst from the polymer and a more thorough investigation should be performed on its toxicity.

Since the first ROP organocatalyst was reported in 2001 by Hedrick and coworkers,[49] great advances have been achieved in the area such that organocatalysts have rivalled the activity of the traditional metal catalysts. An overview of the most utilised ROP organocatalysts will be presented, and the recent developments in the area that provided highly reactive and selective catalysts will also be described.

1.3.2.1 Nucleophilic Base Catalysts

1.3.2.1.1 4-Dimethylaminopyridine (DMAP)

Hedrick and coworkers reported the first organocatalytic ROP of LA utilising DMAP.[49] The polymerisations were initially performed in CH_2Cl_2 at 35 °C, with catalyst loadings of 2 to 4 equivalents to alcohol initiator. The polymerisation times varied from 24 to 64 hours depending on the target degree of polymerisation (DP) and the resultant polymers displayed narrow dispersity values ($Đ_M < 1.13$). Interestingly, the dispersity remained low even at prolonged reaction times (96 hours), which indicated the absence of undesirable transesterification reactions. In addition, polymers produced from pure L-LA revealed no epimerisation occurring during the polymerisation. Bulk polymerisations were also carried out and showed to reduce significantly the polymerisation times to 5 to 20 minutes while maintaining narrow dispersity values.

The ROP of LA catalysed by DMAP was proposed to occur through a monomer-activated mechanism, which involves the initial nucleophilic attack of DMAP to the monomer to produce an alkoxide zwitterion (Scheme 1.4). [49] The subsequent reaction with an initiating alcohol provides an open monomer with a hydroxide terminal group that further propagates by reacting with another lactide-DMAP complex. Later on, Bonduelle *et al*. proposed a mechanism based on computational studies where DMAP acts as a bifunctional catalyst (Scheme 1.5).[50] While the basic nitrogen activates the alcohol/hydroxy chain end *via* hydrogen bonding, the carbonyl in the monomer

interacts with the *ortho*-hydrogen atoms in the pyridinium ring. Although the nucleophilic mechanism was shown to be energetically less favoured than the alcohol activation, both pathways are possible, with the former becoming preferential when low concentrations of alcohol are utilised.

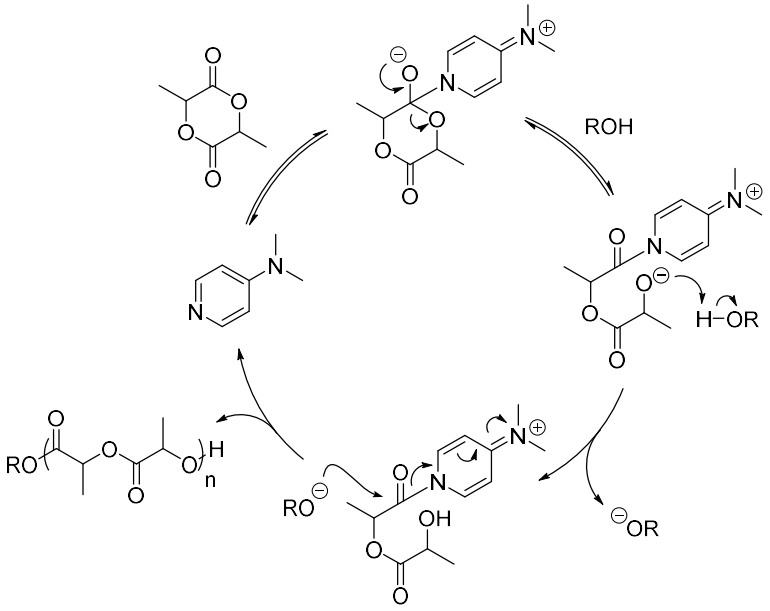

Scheme 1.4. Proposed monomer-activated mechanism for the DMAP catalysed ROP of LA.

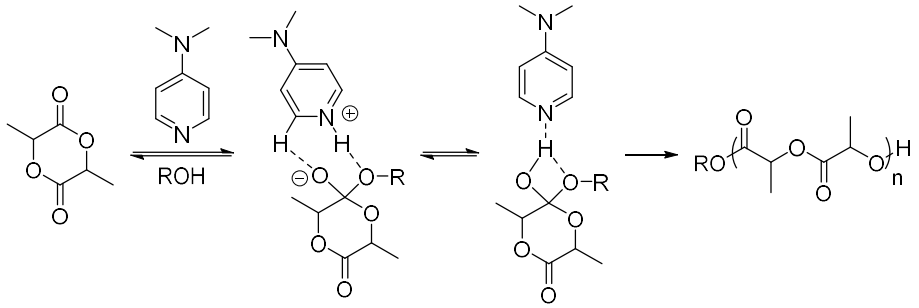

Scheme 1.5. Bifunctional mechanism for the DMAP catalysed ROP of LA.

1.3.2.1.2 *N*-Heterocyclic Carbenes

Hedrick and coworkers reported in 2002 the use of an *N*-heterocyclic carbene (NHC) in the ROP of cyclic monomers.[51] High reactivities were observed with NHC **1.1** (Figure 1.1), which allowed the polymerisation of L-LA in THF to reach 92% monomer conversion in 2 hours in the presence of an alcohol initiator (initial monomer-to-initiator-to-catalyst ($[M]_0/[I]_0/[cat]_0$) of 100:1:1.5). The polymerisation

showed living characteristics, and polymers with controllable molecular weights and low dispersity values were obtained ($Đ_M \leq 1.16$). This catalyst was also able to polymerise ε-CL, although 24 hours were necessary to reach completion and result in polymers with a molecular weight distribution of 1.33. Further investigation on the structure-activity relationship of NHCs revealed that less sterically hindered carbenes such as **1.2** provided increased reactivity, such that reduced catalyst loadings (0.5 equivalent to alcohol initiator) and concentrations below 1 M were required to maintain the control over the polymerisation.[52] Although quenching the polymerisation before full conversion was required to avoid undesirable transesterification of the polymer, the high activity of the NHCs has enabled the polymerisation of a range of lactones and cyclic carbonates with different macromolecular arquitectures.[53-55]

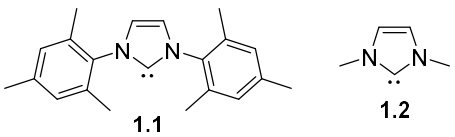

Figure 1.1. Examples of NHCs used as ROP catalysts.

The mechanism for the NHC-catalysed ROP was proposed to occur *via* a nucleophilic pathway, which is supported by the formation of cyclic polymers when the polymerisation is performed in the absence of an alcohol initiator.[26] In this mechanism, a nucleophilic attack of the carbene to the carbonyl of the monomer generates an alkoxide zwitterion that propagates and further cyclises to release NHC and a cyclic polymer (Scheme 1.6a).[56] While computational studies corroborated a nucleophilic mechanism when no initiator is utilised, an alcohol activation by hydrogen bond showed to be favoured when the polymerisation is performed in the presence of an alcohol (Scheme 1.6b).[57]

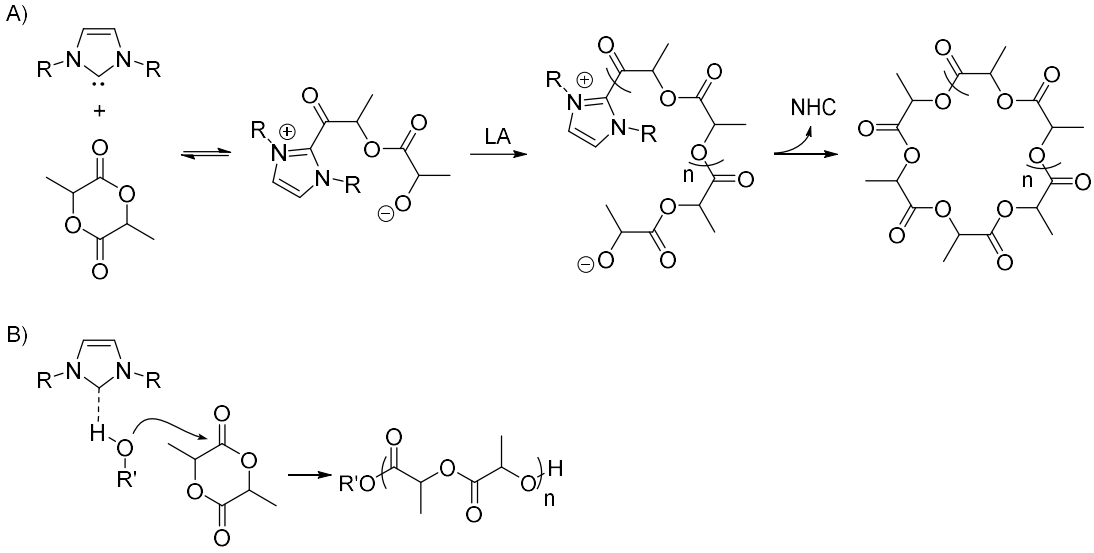

Scheme 1.6. A) Formation of cyclic polymers *via* nucleophilic mechanism and B) alcohol activated mechanism for the NHC catalysed ROP.

1.3.2.1.3 *N*-Heterocyclic Olefins

In 2016, Naumann *et al*. introduced *N*-heterocyclic olefins (NHO)s as a new class of catalyst for the ROP of cyclic esters and carbonates.[58] These compounds have a strongly polarised double bond with a high electron density in their exocyclic carbon (Figure 1.2a). The authors investigated NHOs with various structures and observed that, among the compounds with a terminal olefin (**1.3**–**1.5**), NHO **1.5** was the most active catalyst for ROP (Figure 1.2b). This fact was attributed to the aromatisation of the catalyst that favours a charge separation, thus increasing the nucleophilicity or basicity in the exocyclic carbon. However, the activity of NHO **1.5** was shown to decrease during the polymerisation, which was proposed to occur as a result of the deactivation of the catalyst by a proton transfer from the acidic CH_2 group in the zwitterion formed after NHO attacked the monomer (Scheme 1.7).

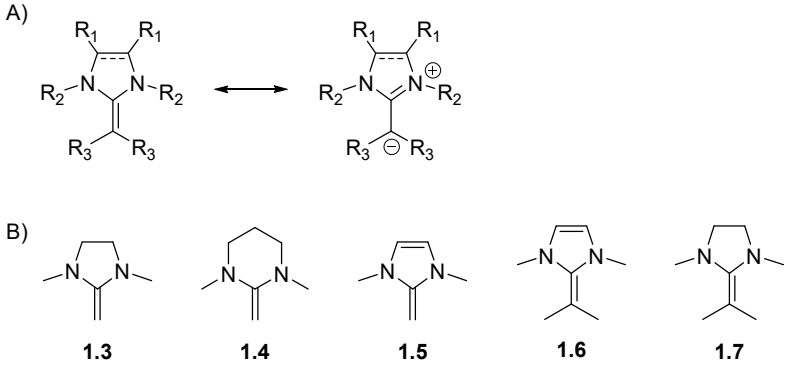

Figure 1.2. A) Resonance structures of NHOs and B) NHOs investigated by Naumann *et al*.

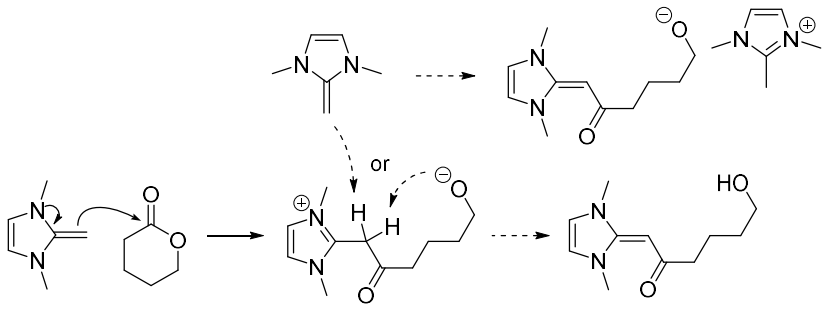

Scheme 1.7. Proposed deactivation of NHO by a proton transfer to either another NHO molecule or the alkoxide chain end.

To avoid the deactivation of the catalyst, NHO **1.6** was prepared by methylating the exocyclic carbon, which promoted the polymerisations of L-LA and TMC to high monomer conversions. For a target DP of 50 and using 1 mol% catalyst, the ROP of L-LA and TMC proceeded in 30 minutes and 25 seconds, respectively, and the resultant polymers presented reasonable dispersities ($Đ_M$ < 1.90). Interestingly, the ROP of δ-VL was shown to be uncontrolled in the presence of catalyst **1.6**, which was a result of a series of side reactions, including the formation of an enolate of δ-VL. The catalyst **1.7** was also investigated, and a lower catalytic activity was expected as a result of the lower polarisation of the double bond. Surprisingly, the polymerisation of L-LA reached 92% monomer conversion in less than 2 minutes, and lower dispersity values were obtained (target DP of 50, 1 mol% catalyst, $Đ_M$ = 1.18). In addition, the ROP of TMC with NHO **1.7** was considerably slower than that using catalyst **1.6** (76% conversion at 3.5 hours, target DP of 50, 1 mol% catalyst) and higher levels of control were obtained, resulting in polymers with lower dispersity ($Đ_M$ = 1.12). Although no insights on the differences in activities of **1.6** and **1.7** were provided, the ROP

catalysed by NHO **1.3** is believed to proceed *via* a nucleophilic mechanism, whereas the higher steric hindrance and basicity of catalysts **1.6** and **1.7** should favour an alcohol activation pathway in a similar manner as with NHCs.

1.3.2.2 Acid Catalysts

A series of carboxylic acids have demonstrated activity for ROP of ε-CL,[59,60] δ-VL,[61] and cyclic carbonates.[62] α-Hydroxy acids and α-amino acids were investigated in the ROP of ε-CL, and faster polymerisations were obtained with α-hydroxy acids, especially with tartaric acid (Figure 1.3).[60] For instance, the polymerisation under bulk conditions at 120 °C in the presence of tartaric acid and an alcohol initiator proceeded to high monomer conversions in 4 hours ($[M]_0/[I]_0/[cat]_0$) = 100:3:10). The resultant polymers presented relatively low dispersity ($Đ_M$ < 1.40) and high end-group fidelity, although initiation by the catalyst was observed in the absence of an alcohol initiator. Carboxylic acids were also investigated in the polymerisation of TMC, and trifluoroacetic acid (TFA) was shown to be an efficient catalyst.[62] The ROP of the cyclic carbonate performed in toluene at 50 °C with an alcohol initiator reached completion in 24 hours, and the polymers produced presented low dispersities ($[M]_0/[I]_0/[cat]_0$ = 100:1:1, $Đ_M$ < 1.25). An interaction of TFA and the monomer was observed by ^{1}H and ^{13}C NMR spectroscopy, which suggested the polymerisation occurred *via* an activated monomer (AM) mechanism, where the acid activates the carbonyl in the monomer to allow the nucleophilic attack by the alcohol/propagating chain end (Scheme 1.8).[62]

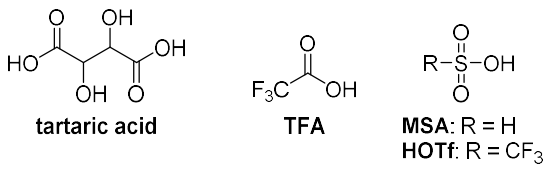

Figure 1.3. Example of carboxylic acids and sulfonic acids used as ROP catalysts.

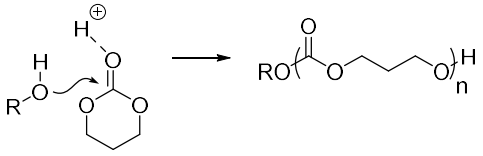

Scheme 1.8. Proposed AM mechanism for the carboxylic acid catalysed ROP of TMC.

While the polymerisation of lactones has been performed in the presence of weak carboxylic acids, the ROP of LA requires stronger acids, such as trifluoromethanesulfonic acid (HOTf) (Figure 1.3).[63,64] The polymerisation of LA in the presence of HOTf and water or an alcohol as initiator achieved high monomer conversions after over 2 hours ($[M]_0/[I]_0/[cat]_0$ = 10:1:1). Characterisation of the resultant polymers revealed relatively low dispersity ($Đ_M$ < 1.50), while mass spectrum analysis demonstrated high end-group fidelity and low degrees of transesterification side reactions. In addition, the linear increase of number-average molecular weight (M_n) with monomer conversion and $[M]_0/[I]_0$ demonstrated the controlled nature of the polymerisation.

HOTf has also been effective for the ROP of ε-CL, as demonstrated by the low dispersity values obtained when utilising 1:1 ratio of acid to initiator ($Đ_M$ = 1.07, 1.5 hours for a target DP of 40).[65] Interestingly, despite the lower acidity, methanesulfonic acid (MSA) showed reactivity similar to HOTf. In addition, the polymerisation times could be reduced to 30 minutes when increasing the MSA-to-initiator ratio to 3:1, which contrasts with the slower polymerisation observed when higher loadings of HOTF were applied. The difference in reactivities was proposed to be a result of the competitive alcohol deactivation by the excess of the stronger acid HOTf, whereas increasing amounts of MSA would promote a more efficient monomer activation (Scheme 1.9a). Computational studies on the polymerisation of ε-CL catalysed by sulfonic acids suggested a bifunctional mechanism, where the acidic proton activates the monomer and the basic oxygen atoms activate the alcohol initiator/propagating chain end (Scheme 1.9b).[66]

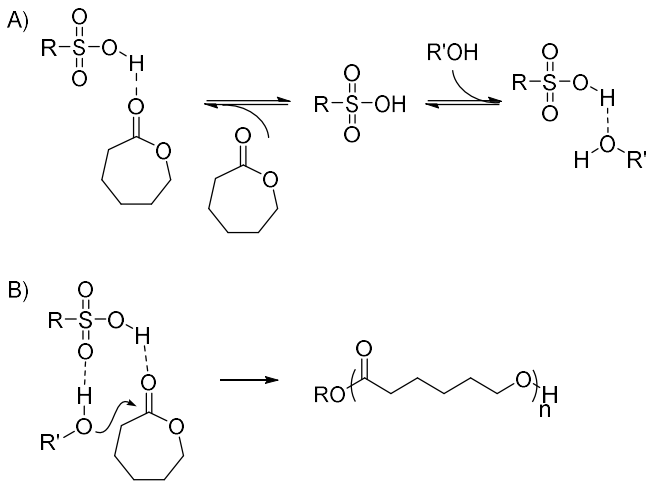

Scheme 1.9. A) Competitive monomer activation and alcohol deactivation with an excess of strong sulfonic acids and B) bifunctional activation of ε-CL and alcohol/propagating chain end by sulfonic acids.

The polymerisation of cyclic carbonate monomers have been investigated with sulfonic acids, and while HOTf provided undesirable decarboxylation with low catalyst loadings at room temperature, MSA showed no signs of mediating this side reaction even under harsher conditions (6 equivalents of catalyst or at temperatures of 80 °C).[67] The polymerisation of TMC with one equivalent MSA to water as initiator reached completion in 2.5 hours and the resultant polycarbonate presented narrow dispersity ($Đ_M$ = 1.08). Interestingly, when polymerisations were performed with *n*-pentanol as the initiator, bimodal distributions were observed at $[M]_0/[I]_0 > 10$, which was initially concluded to be a result of competitive AM and activated chain end (ACE) mechanisms. In the ACE pathway, a carbonate monomer attacks an activated monomer and results in a carbonic acid and an oxonium moiety (Scheme 1.10a).[67] While the carbonic acid undergoes spontaneous decarboxylation and generates a hydroxy group that can propagate *via* an AM mechanism, the oxonium chain end propagates by a consecutive attack of the carbonate unit. After hydrolysis of the oxonium group, a telechelic polymer is obtained. However, identical species are formed when the polymerisation of cyclic carbonates is initiated by water and propagated by an AM mechanism (Scheme 1.10b). Computational investigation with several acids (*i.e.* sulfonic, phosphate and carboxylic acids) revealed that the ACE pathway was unviable.[68] In addition, the authors concluded that the bimodality

observed previously was, in fact, a result of the water initiation from residual moisture in the catalysts, as sulfonic acids are highly hygroscopic.

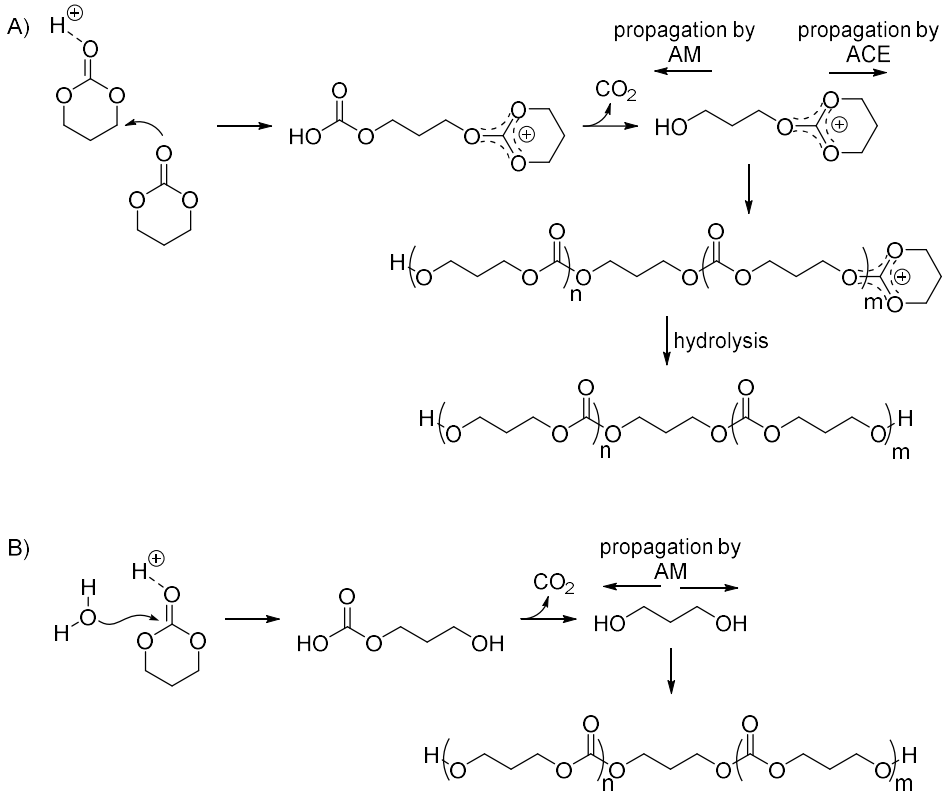

Scheme 1.10. A) Proposed ACE mechanism for the ROP of TMC and B) Proposed AM mechanism for the ROP of TMC initiated by water.

Sulfonimides are another class of strong acids that have shown high activity for lactones and TMC (Figure 1.4).[69-72] The ROP of δ-VL using 0.1 mol% of trifluoromethanesulfonimide ($HNTf_2$) using an alcohol initiator reached 93% monomer conversions in 9 hours for a target DP of 100.[69] The polymerisation was well controlled, and polymers with up to 13 kg mol^{-1} were synthesised with narrow molecular weight distributions ($Đ_M \leq 1.12$). The sulfonimides $HNTf_2$ and nona-fluorobutanesulfonimide ($HNNf_2$) were investigated in the ROP of ε-CL in toluene in the presence of ethanol as the initiator, and full monomer conversions were obtained in 8 hours at 25 °C ($[M]_0/[I]_0/[cat]_0 = 40:1:0.04$).[70] Faster polymerisations could be achieved by increasing the temperatures to 50 °C, while the dispersity remained relatively low ($Đ_M \leq 1.48$). Although similar performance was demonstrated by with *O*-benzenedisulfonimide (OBS) in the ROP of δ-VL and ε-CL, the low toxicity, water compatibility, and non-corrosive nature of OBS presented advantages over $HNTf_2$ and

$HNNf_2$.[71] In addition, OBS-catalysed ROP of TMC was shown to be well controlled and the use of different multifunctional initiators allowed the preparation of telechelic and star-shaped polycarbonates with low dispersities ($1.12 \leq Đ_M \leq 1.27$).[72]

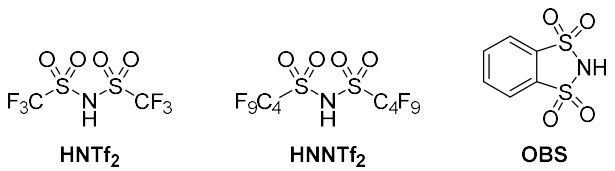

Figure 1.4. Structure of sulfonimides used as ROP catalysts.

Diphenyl phosphate (DPP) is a commercially available acid that besides the lower acidity, presents comparable reactivity to MSA.[73] For instance, the polymerisation of δ-VL and ε-CL in toluene reached completion in 1 and 8 hours, respectively, when using an alcohol initiator ($[M]_0/[I]_0/[cat]_0$ = 50:1:1). The controlled nature of the polymerisations was evidenced by the linear increase of M_n with monomer conversion, while the dispersity remained very low even at high monomer conversions ($Đ_M \leq$ 1.09). In addition, DPP efficiently catalysed the ROP of TMC and provided polymers of DP 50 in 36 hours with narrow molecular weight distribution ($[I]_0/[cat]_0$ = 1:1, $Đ_M \leq 1.13$).[74] Kinetic experiments showed that the polymerisation was well controlled, while analysis by matrix-assisted laser desorption/ionisation mass spectrometry (MALDI-ToF MS) revealed a high end-group fidelity, with no water initiation. These results demonstrated that, in contrast with sulfonates, DPP could be easily dried and remained under these conditions upon storage. Computational studies suggested a bifunctional mechanism for the DPP catalysed ROP, and that its relatively high activity was a result of the stronger hydrogen-bond accepting ability of DPP when compared to sulfonic acids or carboxylic acids, which provides a more efficient alcohol activation (Scheme 1.11).[68] Interestingly, Macdonald and Shaver have demonstrated that phosphoric acid catalysts are deactivated when polymerising β-butyrolactone.[75] The authors proposed the formation of a stable cyclic phosphorous structure by the elimination of a phenoxide group, which was evidenced by the non-deactivation of phosphinic acids that contain a stronger P–C bond. Overall, the acid catalysts have shown to be effective for the ROP of cyclic carbonate and lactones such as δ-VL and ε-CL, although less active for lactide.

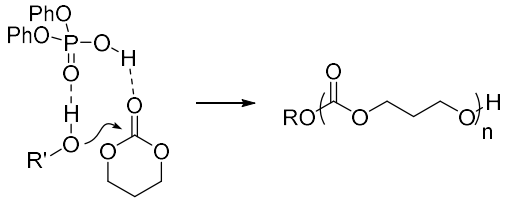

Scheme 1.11. Bifunctional activation of DPP in the ROP of TMC.

1.3.2.3 Superbase Catalysts

1.3.2.3.1 1,8-Diazabicyclo[5.4.0]undec-7-ene and 7-Methyl-1,5,7-triazabicyclo[4.4.0]dec-5-ene

The amidine DBU and guanidine 7-methyl-1,5,7-triazabicyclo[4.4.0]dec-5-ene (MTBD) are strong bases that have demonstrated high catalytic activity in the ROP of LA (Figure 1.5).[76] While the polymerisation of LA utilising 1 mol% DBU in the presence of an initiator reached completion in 1 hour for target DP of 100, the ROP using MTBD under similar conditions required 30 minutes. Both catalysts provided polymers with narrow dispersity ($Đ_M \leq 1.1$), although quenching the polymerisation by the addition of an acid was necessary to avoid undesirable transesterification. DBU also demonstrated activity for the ROP of TMC, although the polymerisation rate was lower than for LA (*i.e.* 8 hours for a $[M]_0/[I]_0 = 50$).[55] Nevertheless, the polymerisation was well controlled and generated polymers with very narrow molecular weight distribution ($Đ_M = 1.04$), which remained low at prolonged reaction times. However, these strong bases were shown to be inactive for the polymerisation of δ-VL and ε-CL.

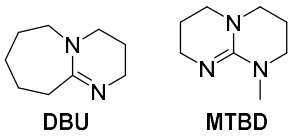

Figure 1.5. Structures of DBU and MTBD.

Mechanistic studies revealed that reactions of DBU or MTBD with vinyl acetate produced no acylated products, whereas the catalysts hydrogen bonded to benzyl alcohol, which suggested a polymerisation *via* an alcohol activated pathway (Scheme 1.12a).[76] However, the ROP of LA was shown to proceed with DBU in the absence of an alcohol as initiator, which indicated that a different pathway was taking place.[77] A nucleophilic mechanism was proposed, in which DBU attacks LA to form a zwitterion

intermediate that can then proceed *via* different pathways (Scheme 1.12b). The alkoxide in the zwitterion can react with another LA molecule and propagate to provide larger chains, which further cyclises by displacing DBU (path a). The second pathway involves the protonation of the alkoxide to form a ketene aminal (path b) that can undergo chain growth in the presence of DBU to provide either cyclic polymers (path c) or generate linear PLA upon quenching the polymerisation with an alcohol (path d). While this mechanism is favoured when the concentration of alcohol is reduced, the alcohol activated pathway might be predominant when the polymerisation is performed in the presence of an alcohol initiator.

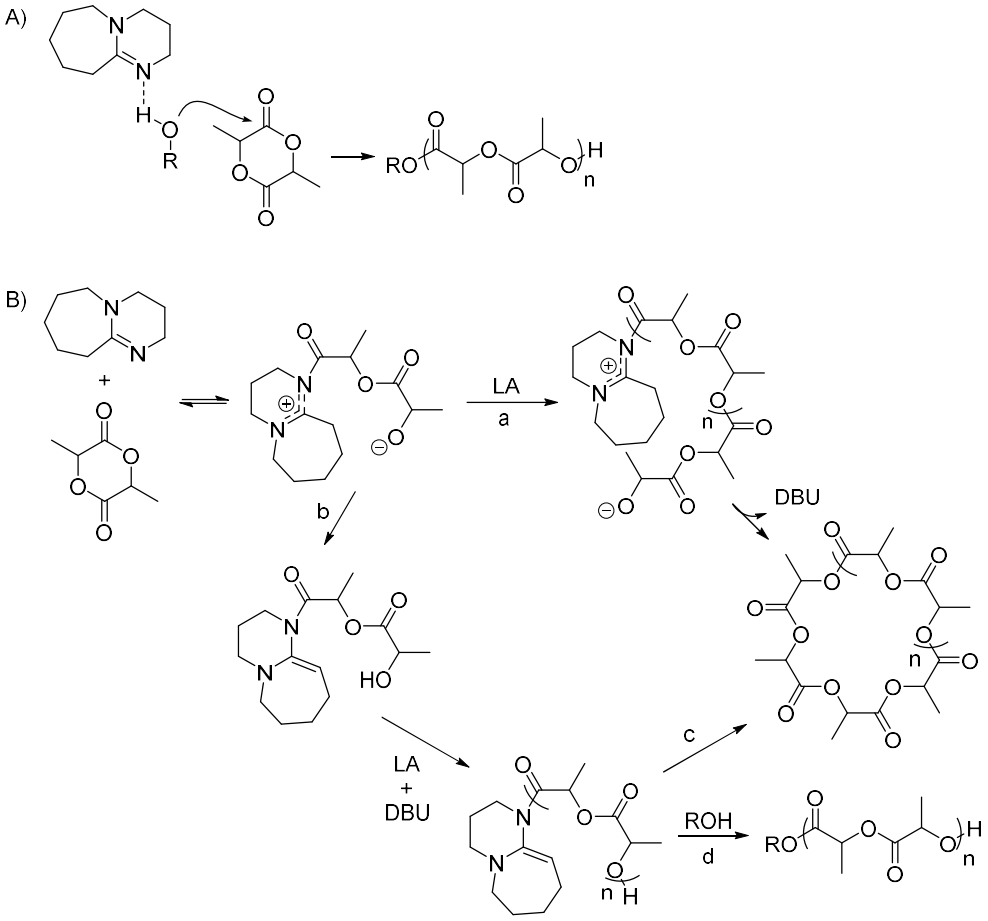

Scheme 1.12. ROP of LA catalysed by DBU *via* A) an alcohol activated mechanism in the presence of an alcohol initiator or B) a nucleophilic pathway in the absence of an alcohol initiator.

1.3.2.3.2 Phosphazenes

Phosphazenes are highly basic compounds with a general structure of $(R_2N)_3P{=}N\text{-}R$ that have been shown active as ROP catalysts (Figure 1.6). Initial studies involved

the use of 2-*tert*-butylimino-2-diethylamino-1,3-dimethylperhydro-1,3,2-diazaphosphorine (BEMP) or *N*′-*tert*-butyl-*N*,*N*,*N*′,*N*′,*N*″,*N*″-hexamethylphosphorimidic triamide (P_1-*t*-Bu) in the ROP of L-LA and δ-VL.[78] The polymerisation of L-LA was carried out with an alcohol initiator in toluene at room temperature and for a target DP of 100, ~80% monomer conversion was achieved in 23 hours when using BEMP (1 mol%) or in 70 hours with P_1-*t*-Bu (1 mol%). The resultant polymers presented low dispersities ($Đ_M$ < 1.10), although these values increased at conversions above ~70% as a result of transesterification of the polymer. The ROP of δ-VL was performed under neat conditions in the presence of an alcohol as initiator and reached 70% conversion with BEMP and 56% using P_1-*t*-Bu in ~70 hours. The polymerisation was proposed to occur *via* the alcohol activation by hydrogen bonding with the base in a similar way as described for DBU and MTBD (Scheme 1.13).

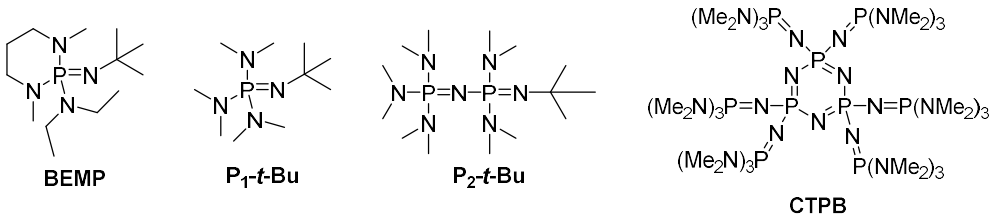

Figure 1.6. Phosphazenes used as ROP catalysts.

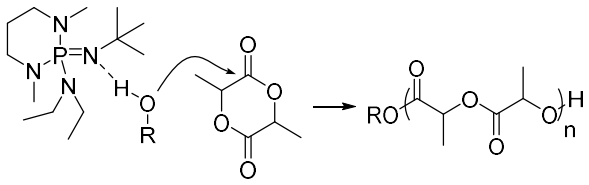

Scheme 1.13. Alcohol activation by phosphazene in the ROP of LA.

Zhang *et al*. reported a stronger phosphazene base, namely 1-*tert*-butyl-2,2,4,4,4-pentakis(dimethylamino)-2Λ,^{5}4Λ^5-catenadi(phosphazene) (P_2-*t*-Bu) in the ROP of LA.[79] The polymerisation in toluene at room temperature in the presence of an alcohol initiator reached completion in 10 seconds for a target DP of 100 and initial monomer concentration ($[M]_0$) of 0.32 M. Although the polymers presented high dispersities ($Đ_M$ = 1.23), this could be improved by reducing $[M]_0$ to 0.08 M, which resulted in the formation of polymer in 25 minutes with a molecular weight distribution of 1.08. However, as the monomer concentration was very low, the polymerisation could not

achieve full conversion. Decreasing the temperature to −75 °C, high monomer conversions were obtained in 3 hours, while the dispersity remained low ($Đ_M$ = 1.11). Interestingly, the polymers obtained at −75 °C from *rac*-LA presented a high degree of stereoregularity, with long isotactic poly(L-lactic acid) (PLLA) and poly(D-lactic acid) (PDLA) segments. Similar results were reported more recently by Liu *et al*., who demonstrated the preparation of highly isotactic PLA stereoblocks from *rac*-LA by utilising a cyclic trimeric phosphazene (CTPB, Figure 1.6).[80] A chain-end control mechanism was proposed to explain the stereoselectivity provided by these catalysts, where the chirality in the propagating chain end, combined with the high steric hindrance of the catalyst influences the insertion of the next monomer.

Phosphazene catalysts have also been applied in the ROP of ε-CL. Alamri *et al*. performed the polymerisation using P_2-*t*-Bu and observed 86% monomer conversion in 8 hours when utilising toluene as a solvent ($[M]_0$ = 3 M, $[M]_0/[I]_0/[cat]_0$ = 100/1/1), which resulted in polymers with low dispersity ($Đ_M$ = 1.11).[81] More recently, Li *et al*. demonstrated the high activity of CTPB in the ROP of ε-CL, with full monomer conversions being obtained in only 5 minutes for a target DP of 500.[82] Although the polymers presented broad molecular weight distribution ($Đ_M$ = 1.4 – 2.2), this catalyst allowed the preparation of high molecular weight PCL (M_n > 100 kg mol^{-1}) that is typically inaccessible by organocatalysts.

1.3.2.4 Bifunctional Catalysts

1.3.2.4.1 Thiourea/Base

The use of a thiourea-amine bifunctional catalyst system for the ROP of LA was firstly reported in 2005 by Dove *et al*.[83] The polymerisation was carried out in CH_2Cl_2 at 25 °C utilising an alcohol initiator and 5 mol% of thiourea **1.8**, and took 48 hours to reach 97% monomer conversion for a target DP of 100 (Scheme 1.14). The resultant polymers displayed very low dispersity values ($Đ_M$ = 1.05) that remained low after extending the polymerisation for a further 4 days, which indicated that minimal transesterification side reactions occurred. Moreover, ^{13}C NMR spectroscopy and differential scanning calorimetry analyses supported the absence of racemisation in the ROP of L-LA. The mechanism proposed involves a bifunctional activation, where the thiourea acts as a hydrogen-bond donor to the carbonyl in the monomer, and the tertiary amine, as a hydrogen-bond acceptor to the alcohol/propagating chain end (Scheme 1.14).[83] This mechanism was supported by the absence of polymerisations

when utilising THF or DMF, as these solvents are hydrogen-bond acceptors, and therefore, are likely to bind to the thiourea and hinder the monomer activation.

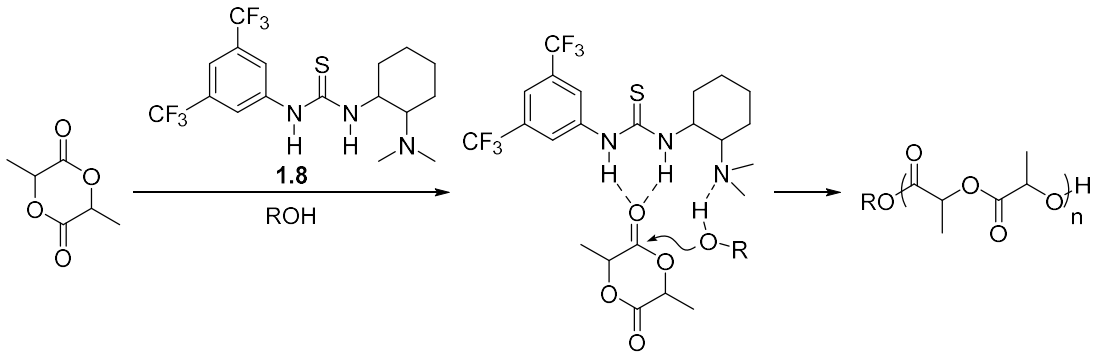

Scheme 1.14. Bifunctional hydrogen-bond activation of LA and alcohol initiator/propagating chain end by thiourea-amine **1.8**.

Further investigation on the bifunctional nature of the catalyst showed that the polymerisation could proceed when utilising both thiourea **1.9** and *N*,*N*-dimethylcyclohexylamine ($NCyMe_2$), although no polymers were obtained when these compounds were applied separately (Figure 1.7).[83] While this result demonstrated the requirement of both functionalities for a catalytic activity, the presence of a thiourea and an amine in the same molecule proved unnecessary. This characteristic facilitated the screening of other thioureas and amines to obtain more active catalyst systems. In this regard, studies with commercially available amines revealed that (−)-sparteine provided higher reaction rates when compared to **1.9**/$NCyMe_2$ (~35 fold), while maintaining the good control over the molecular weight and dispersity.[84] Similar performance was observed with tris[2-(dimethylamino)ethyl]amine (Me_6TREN), which was attributed to the chelative effect of both Me_6TREN and (−)-sparteine that provided an increased alcohol activation.[85] Superbases such as DBU and MTBD that, alone were inactive for the ROP of δ-VL or ε-CL, in the presence of thiourea **1.9**, the polymerisation of these lactones could proceed in a controlled manner to provide polyesters with low dispersities ($Đ_M \leq 1.06$).[76] While the ROP of δ-VL progressed to 95% monomer conversion in 4 hours ($[M]_0/[I]_0 = 100$), the polymerisation of ε-CL was slower and required 5 days to reach 78% monomer conversion. Although quenching the superbase catalysts with acid was necessary to avoid undesirable transesterification, the polymerisations were well controlled up to these conversions. Notably, the higher reactivity provided by the use

of thiourea **1.9** combined with chelating amines or stronger bases allowed the controlled polymerisation of TMC[55] and other functional cyclic carbonate monomers.[31,86]

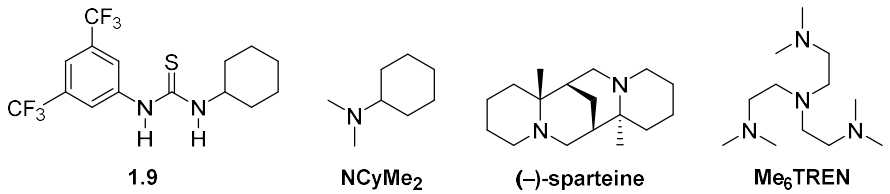

Figure 1.7. Chemical **s**tructures of thiourea **1.9**, $NCyMe_2$, (−)-sparteine and Me_6TREN.

Spink *et al*. demonstrated that increased polymerisation rates could be obtained by using the bis-thiourea **1.10** (Figure 1.8a).[87] For instance, while the ROP of L-LA showed to proceed in 50 minutes in the presence thiourea **1.9**/Me_6TREN (5 mol% each, target DP of 100), only 10 minutes were required when utilising **1.10**/Me_6TREN (2.5 mol% each), while producing polymers with very low dispersity ($Đ_M$ = 1.03). Similar behaviour was observed for the polymerisations of δ-VL or ε-CL using MTBD as a base, where the reaction times were especially reduced for ε-CL (45 hours with **1.9**/MTBD *vs* 10 hours with bis-thiourea **1.10**/MTBD, target DP of 50).[88] This enhancement in reactivity was suggested to occur *via* an activated-thiourea mechanism, which involves a monomer activation by a single thiourea moiety that is subsequently activated by the other thiourea (Figure 1.8b). This interaction was shown to be preferential over the dual thiourea activation where the monomer is activated simultaneously by both thiourea moieties.

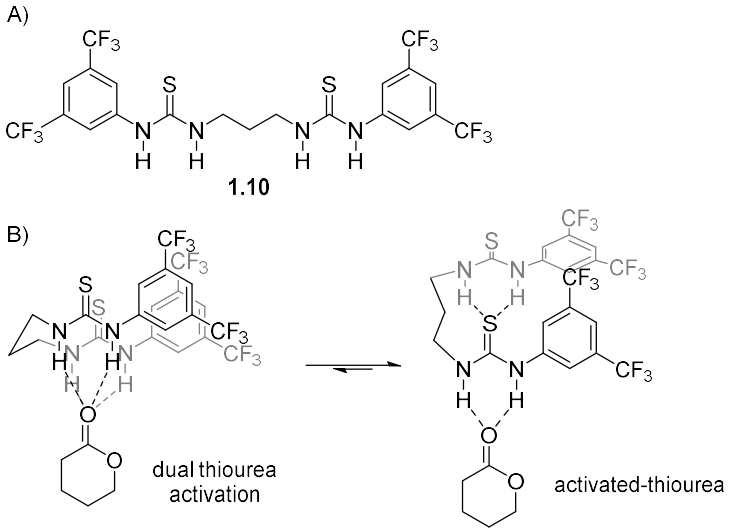

Figure 1.8. A) Structure of bis-thiourea **1.10** and B) proposed monomer activation by bis-thiourea **1.10**.

1.3.2.4.2 Urea/Base

The use of urea/base as catalysts for ROP was disclosed in 2016 by Kiesewetter and coworkers, who demonstrated the ability of ureas in activating the monomer in a similar manner as thioureas (Scheme 1.15).[88] In these studies, mono-, bis- and tris-(thio)ureas were investigated in the ROP of δ-VL in the presence of MTBD, and generally, ureas were shown to be more active than thioureas of similar structure (Figure 1.9). For instance, the polymerisation using thiourea **1.11S**/MTBD (5 mol% each) proceeded to 94% monomer conversion in 110 minutes for a target DP of 50, while similar conversions were obtained in 70 minutes when utilising urea **1.11O**/MTBD, while both catalyst systems provided polymers with low dispersity values ($Đ_M \leq 1.08$). The differences in catalytic activity were hypothesised to come from the higher polarity of ureas when compared to thioureas, which would provide a better hydrogen-bond activation. Interestingly, parallel studies by Kiesewetter and Waymouth have shown that the urea/base system remained highly active when utilising hydrogen-bond accepting solvents such as THF and acetone,[89,90] which is in contrast with a previous report that showed a complete inactivity of a thiourea/amine catalyst system in THF.[83] This characteristic would enable a broader application of ureas, as the low solubility in non-polar solvent had previously limited their use as ROP catalysts.[84]

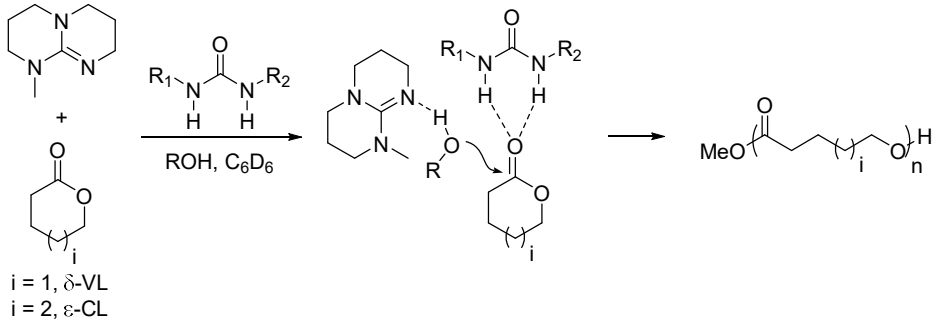

Scheme 1.15. Bifunctional hydrogen-bond activation of monomer by a urea and alcohol initiator/propagating chain end activation by MTBD.

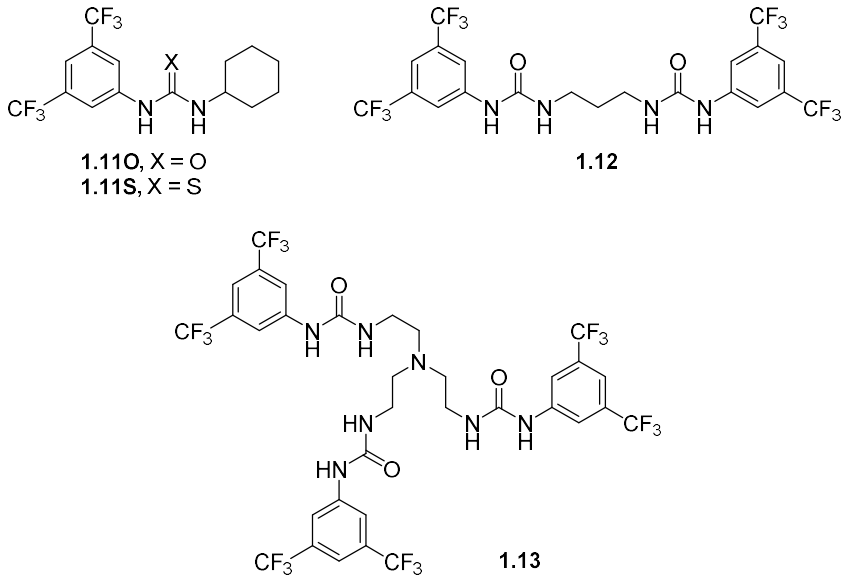

Figure 1.9. Structures of mono-, bis- and tris-(thio)ureas investigated by Kiesewetter and coworkers.

Kiesewetter and coworkers also observed that higher polymerisation rates were obtained as the number of urea moieties in the catalyst increased.[88] For instance, ~90% of δ-VL was converted into PVL in 34 minutes when using bis-urea **1.12**/MTBD (2.5 mol%) and in only 3 minutes with tris-urea **1.13**/MTBD (1.67 mol%) ($[M]_0/[I]_0 = 50$). With the high activity provided by the trifunctional catalyst, the **1.13**/MTBD system was applied in the ROP of ε-CL, and polymers with very narrow dispersities were observed at monomer conversions of 97% ($Đ_M = 1.05$). This level of control in the polymerisation of ε-CL catalysed by bifunctional catalysts (*e.g.* TBD or TU/DBU) is exceptional, as transesterification of PCL is frequently observed at monomer conversions above 80%.[76,91] Finally, this catalyst system also showed to promote the polymerisation of TMC, which proceeded to 97% monomer conversion in 1 minute

and the resultant polymers presented dispersity value of 1.05. The increase in activity of bis- and tris-ureas is proposed to occur by the successive intramolecular activation of the additional urea moiety that provides a stronger hydrogen bond to the carbonyl in the monomer (Figure 1.10).

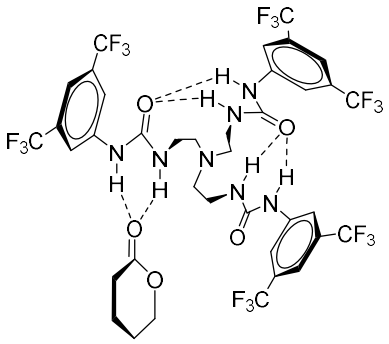

Figure 1.10. Hydrogen-bond activation of δ-VL by tris-urea **1.13** and successive intramolecular hydrogen bonding by other urea moieties.

1.3.2.4.3 Alternative Hydrogen-Bond Donors/Base

With the high polymerisation control provided by the (thio)urea/base system, a range of alternative hydrogen-bond donors was investigated as ROP catalysts in the presence of a base. However, despite the efforts, many of these catalysts have shown lower activity than the traditional thiourea **1.9**/base system.[92-97] Still, Liu *et al*. reported squaramides as hydrogen-bond donors for the ROP of LA, lactones and cyclic carbonates, and observed comparable reactivites to thioureas (Figure 1.11).[98,99] Squaramide **1.14** combined with (−)-sparteine was initially studied in the polymerisation of LA, and 96% monomer conversion was obtained in 9 hours (target DP of 100) and the synthesised polymers presented low dispersity values ($Đ_M$ < 1.08), while maintaining living characteristics.[98] In addition, squaramide **1.14** showed higher reactivity than a thiourea of similar structure, which was explained by the stronger hydrogen-bond interactions between LA and squaramide, as evidenced by computational studies. The catalyst system composed of squaramide **1.14**/(−)-sparteine also demonstrated activity in the ROP of TMC and provided high monomer conversions in 4 hours ($[M]_0/[I]_0/[cat]_0/[base]_0$ = 30:1:1.5:1.5).[99] The polymerisation of δ-VL and ε-CL was investigated using squaramide **1.15** and DBU, and high monomer conversions were achieved in 24 and 96 hours, respectively. The polymerisations of all monomers using squaramide catalysts were well controlled and

provided polymers with narrow dispersity. While other amino-functionalised squaramides were recently reported as bifunctional catalysts for the ROP of LA, low reactivities were observed with these catalysts.[100,101]

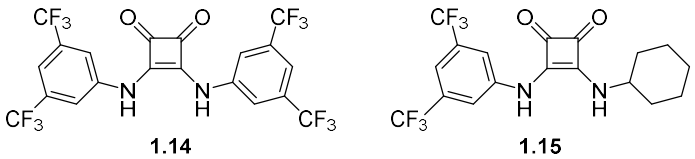

Figure 1.11. Squaramides used as a cocatalyst for ROP.

1.3.2.4.4 Guanidines

In 2006, Pratt *et al*. introduced TBD as a highly active ROP organocatalyst.[91] Although the p*K*a of the conjugate acid of TBD is very similar to that of DBU (TBD.H$^+$: p*K*a = 26.0 and DBU.H$^+$: p*K*a = 24.3 in MeCN),[102] the polymerisation of LA was shown to be much faster when applying TBD. For a target DP of 100 and using 0.1 mol% TBD in CH_2Cl_2, full monomer conversion was obtained in only 20 seconds, against 1 hour required utilising 1 mol% DBU. In addition, the polymers prepared from TBD presented low dispersity ($Đ_M$ = 1.19), although it broadened at extended reaction times, as a result of transesterification of the polymer. Nevertheless, this undesirable reaction could be avoided by quenching the catalyst with the addition of excess acid. TBD also demonstrated activity for δ-VL and ε-CL, although the polymerisations were slower and required higher catalyst loadings (0.5 mol%). While the ROP of δ-VL was shown to be well controlled and presented narrow dispersities throughout the polymerisation, the ROP of ε-CL presented an onset of transesterification at ~60% monomer conversions.

Preliminary mechanistic investigation on the TBD catalysed ROP showed that TBD was acetylated by vinyl acetate and, subsequent reaction with benzyl alcohol, displaced TBD and formed benzyl acetate.[91] Based on these studies, a mechanism for the ROP was proposed to occur through the acylation of TBD by the monomer (Scheme 1.16a). The alcohol/propagating hydroxide is then activated by the nitrogen in the intermediate *via* hydrogen bonding, which facilitates the nucleophilic attack to the carbonyl to regenerate TBD and form the polyester. However, further computational studies revealed that a dual hydrogen-bond activation was preferential over the nucleophilic pathway.[103,104] In this mechanism, the high activity provided by

TBD is explained by the simultaneous activation of the alcohol/propagating chain end by the basic nitrogen of TBD and the carbonyl in the monomer by the hydrogen attached to the other nitrogen atom (Scheme 1.16b).

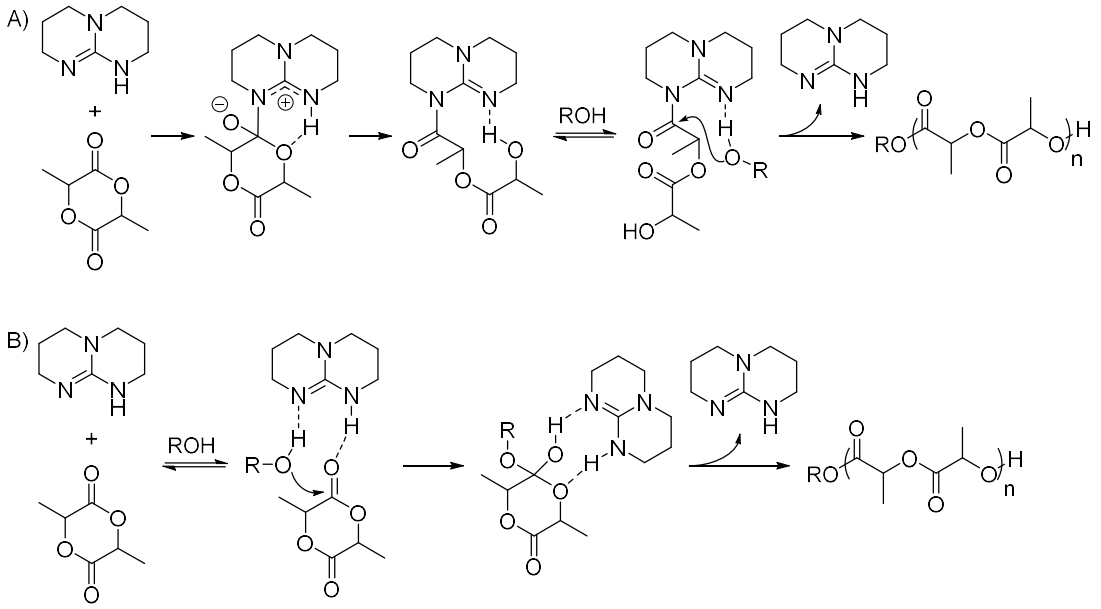

Scheme 1.16. A) Acetyl transfer pathway initially proposed for the TBD catalysed ROP of LA and B) bifunctional hydrogen-bond activation mechanism for the ROP of LA catalysed by TBD.

Considering the high reactivity displayed by TBD, acyclic guanidines were investigated as ROP organocatalysts, once the activity can be more easily tuned by varying the substituents. Zhang *et al*. reported the straightforward synthesis of such catalysts by the reaction of a carbodiimide with secondary amines to provide guanidines **1.16** and **1.17** (Figure 1.12).[105] The ROP of LA was performed using 1 mol% of guanidine **1.16** in the presence of an alcohol initiator, and 20 minutes were required to reach completion (target DP of 100). However, this polymerisation was poorly controlled, and the resultant polymers presented broad molecular weight distributions ($Đ_M$ = 1.49). Catalysts **1.17** was also investigated under similar conditions and the polymerisation of LA achieved full monomer conversion in 40 minutes. In this case, polymers with low dispersity values were obtained ($Đ_M$ < 1.15), and a linear increase of the M_n with the monomer conversion demonstrated the good control of the polymerisation. However, this catalyst presented lower activity than

TBD, which was attributed to the out-of-plane rotation of the pyrrolidine ring that attenuates the conjugation among the nitrogen atoms in the guanidine.

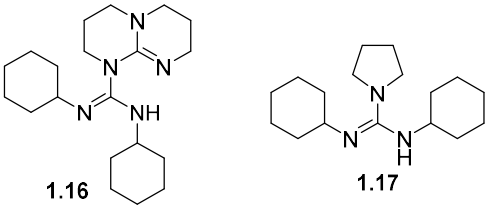

Figure 1.12. Acyclic guanidines investigated by Zhang *et al*.

Although the acyclic guanidines presented reduced reactivity, Eisenreich *et al*. demonstrated their versatility by varying the substituents in the aromatic ring to modulate their activity (Figure 1.13).[106] Initial investigation on the ROP of L-LA catalysed by guanidines **1.18a** and **1.19** showed a significant decrease in activity when compared to catalyst **1.17**, which was associated to the delocalisation of the electron density of the guanidine nitrogen atoms to the aromatic group. Further incorporation of an electron withdrawing group (CF_3, **1.18b**) in the aromatic ring of the guanidine demonstrated a drastic drop in activity. Nonetheless, the catalyst activities were increased by utilising electron donating groups. Specifically, the methoxy-substituted catalyst **1.18c** provided high monomer conversions in 20 hours, whereas the guanidine containing a dimethylamino group (**1.18d**) required 7 hours to reach similar conversions ($[M]_0/[I]_0 = 50$). In addition, good control over the polymerisation was observed, and the resultant polymers displayed low dispersity.

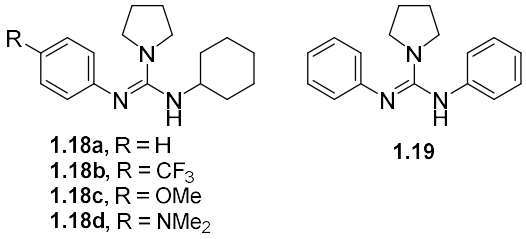

Figure 1.13. Aromatic acyclic guanidines investigated by Eisenreich *et al*.

1.3.2.4.5 (Thio)urea Anions

In 2016, Waymouth and coworkers reported a new highly active ROP catalyst system composed of a thiourea and sodium methoxide, potassium methoxide or NHC **1.1** that generate a thioimidate (Scheme 1.17).[107] Initial studies involving the ROP of

LA with either $NaOCH_3$ or $KOCH_3$ in the absence of a thiourea showed a slow polymerisation and the resultant polymers presented broad dispersity values ($Đ_M$ > 1.8). On the other hand, when the thiourea was initially treated with either sodium or potassium methoxide and then added to a solution of LA in CH_2Cl_2, the polymerisation was shown to be fast and provide polymers with predictable molecular weights based on the $[M]_0/[I]_0$. Specifically, the ROP of LA using $NaOCH_3$ and 1 to 10 equivalents of thiourea proceeded in up to 6 minutes for a target DP of 200, while the molecular weight distributions narrowed with the increase in thiourea content ($Đ_M$ = 1.55 to 1.16). On the other hand, more efficient polymerisation was achieved with $KOCH_3$ that, although displayed similar reaction rates, provided polymers with lower dispersity values using only 5 equivalents of thiourea in excess to the base ($Đ_M$ =1.09).

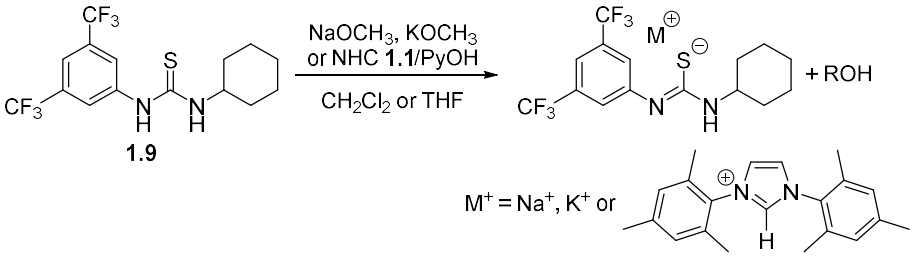

Scheme 1.17. Generation of a thioimidate by deprotonation of thiourea **1.9** with $NaOCH_3$, $KOCH_3$ or NHC **1.1**.

Waymouth and coworkers also investigated the use of carbene **1.1** to generate a thiourea anion (1 equivalent of **1.1** to thiourea) and polymerise LA in the presence of 1-pyrenebutanol (PyOH) as the initiator.[107] Although the polymerisation was considerably slower than the thiourea/alkoxide system (*e.g.* 22 minutes for a target DP of 200), the resultant polymers presented very low dispersity values ($Đ_M$ < 1.10), that surprisingly remained low after the reaction was completed. Analysis of the resultant polymers by MALDI-ToF MS revealed minimum or no transesterification of the polymers when utilising thiourea/$KOCH_3$ or thiourea/NHC **1.1**/PyOH systems, respectively, which demonstrated the high selectivity for ring-opening the monomer relative to transesterification of the polymer.[107] Finally, these catalyst systems demonstrated activity in the ROP of δ-VL, ε-CL and a benzyl-functional cyclic carbonate, although these monomers required hours to achieve high monomer conversions. Nonetheless, the polymerisations were shown to be well controlled and provided polymers with predictable molecular weight and narrow dispersities.

The mechanism for the ROP catalysed by thiourea anion was proposed to be *via* a bifunctional pathway in a similar manner to that of TBD, where the alcohol/propagating chain end and the monomer are activated simultaneously by hydrogen bonding with the catalyst (Scheme 1.18). This mechanism was supported by computational studies that further showed that LA has a stronger binding in **INT2** than the open-chain ester (**INT1**), which provides insights on the high selectivity of the catalyst system for ring-opening LA over transesterification of the polymer open chain.

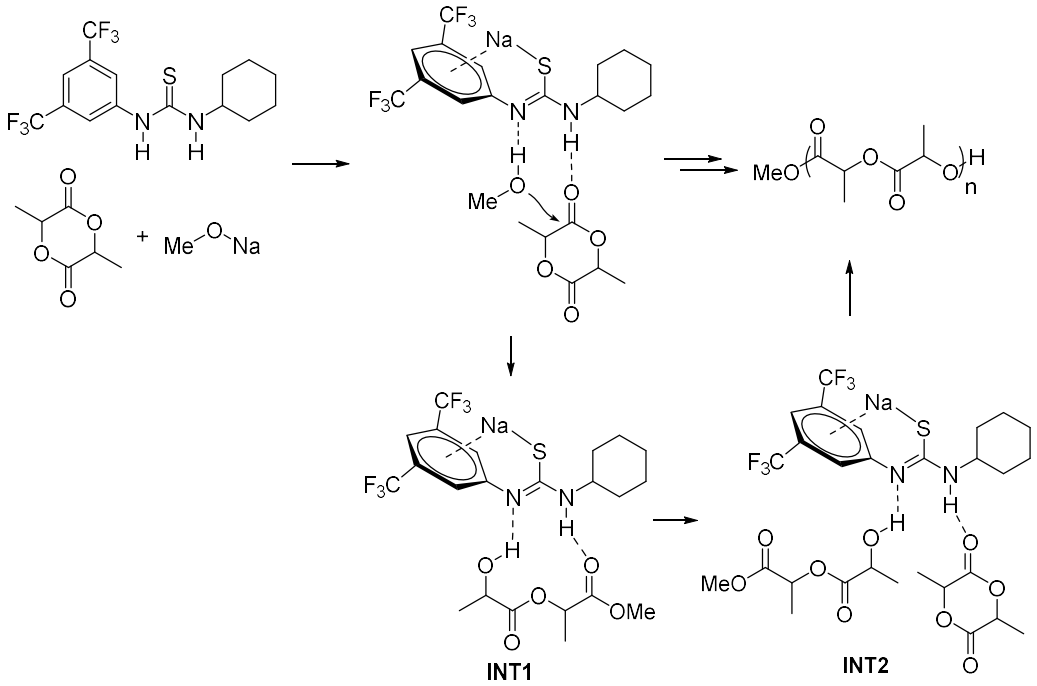

Scheme 1.18. Proposed mechanism for ROP of LA catalysed by a thiourea anion.

In 2017, Lin and Waymouth extended the studies to urea anions, which proved to be highly active and selective bifunctional ROP catalysts (Scheme 1.19).[108] The catalyst was initially prepared by mixing $KOCH_3$ and 3 equivalents of urea in THF to obtain a homogeneous solution and then added to a monomer solution to promote the polymerisation. Using urea **1.20**, the ROP of L-LA achieved 94% monomer conversion in only 6 seconds and provided PLLA with narrow dispersity (target DP of 100, $Đ_M$ = 1.06). In addition, homodecoupled ^{1}H NMR spectroscopy and DSC analysis demonstrated high isotacticity for the resultant polymers, whereas MALDI-ToF/MS revealed minimum transesterification. The urea **1.20**/$KOCH_3$ system was also utilised in the ROP of δ-VL and ε-CL, but low monomer conversions were

obtained. Nonetheless, using a stronger urea anion derived from **1.25** provided high monomer conversions in only 1 second for δ-VL and 12 seconds for ε-CL, while the resultant polymers presented low dispersity values ($Đ_M$ < 1.15).

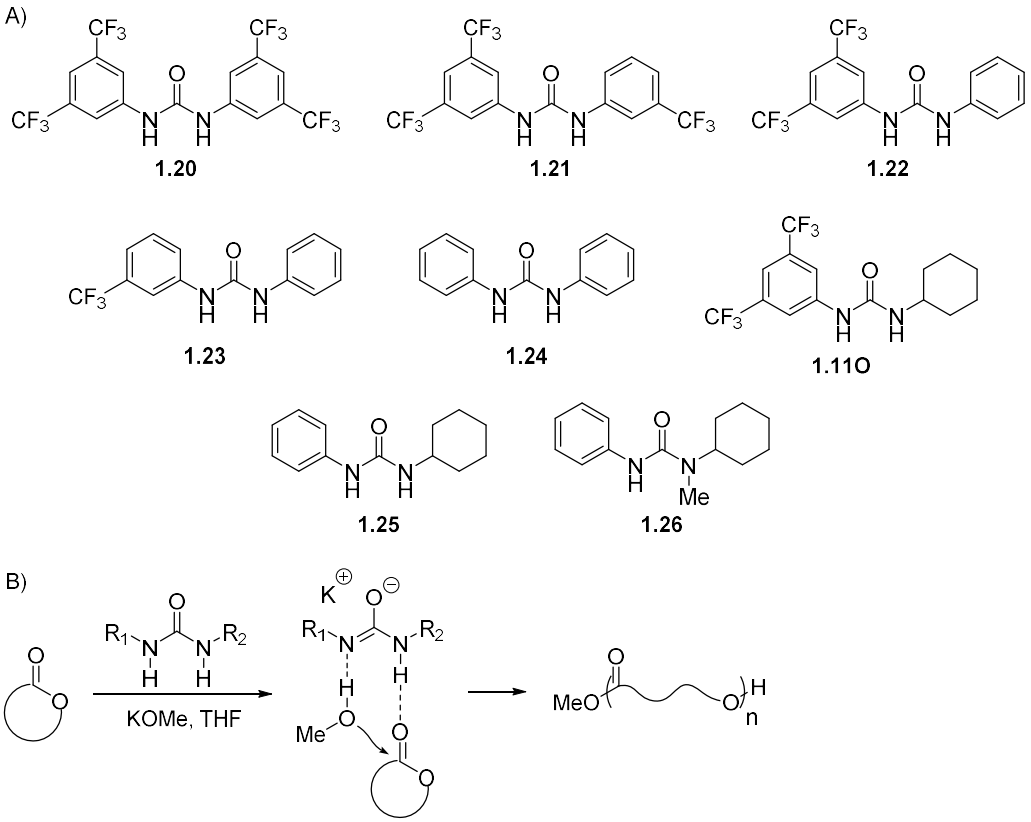

Scheme 1.19. A) Ureas investigated by Lin and Waymouth and B) ROP of cyclic monomers by bifunctional activation of a urea anion.

Further investigation on the activity of diaryl ureas bearing a different number of CF_3 substituents revealed that the rate of polymerisation increased linearly with the decrease in the number of CF_3 substituents (*i.e.* activity increased from **1.20** < **1.21** < **1.22** < **1.23** < **1.24**).[108] This observation was associated with the linear decrease in p*K*a of the urea as the number of CF_3 substituents is reduced, which demonstrated that less acidic ureas lead to more basic urea anions, and therefore, to faster polymerisation rates. While these studies showed the effect of basicity on alcohol activation, the use of a *N*-methylated urea **1.26** demonstrated the importance of the N–H bond for the monomer activation: the polymerisation of ε-CL using urea **1.26**/$KOCH_3$ system was slower than the nonmethylated urea **1.25** and provided polymers with a bimodal molecular weight distribution ($Đ_M$ = 1.30 at 35% monomer conversion).

More recently, Lin and Waymouth reported a detailed study with several (thio)ureas and bases and evaluated the effect of their p*K*a in the ROP activity.[90] The authors observed that for a given (thio)urea, faster rates were obtained as the basicity increased from DBU < MTBD < BEMP < NHC **1.1**, which was attributed to the higher activation of the alcohol by stronger bases. However, for a given base, the maximum catalytic activity is obtained when the acidity of the thiourea is closest to the basicity of the base. This observation was rationalised by the different mechanisms involved when neutral or anionic (thio)ureas are applied as catalysts. When strong bases are utilised with (thio)ureas of lower p*K*a, the (thio)ureas are deprotonated, and the polymerisation occurs *via* the anionic pathway proposed for thio(urea) anions. In this case, the activity increases as the acidity of the (thio)ureas decreases (or the basicity of the anions increases). On the other hand, for weaker bases that are unable to deprotonate the (thio)urea, the neutral (thio)urea activates the monomer by hydrogen bonding, while the base activates the alcohol. Under these conditions, the decrease in the (thio)urea acidity reduces the reactivity towards polymerisation, which is associated with the lower hydrogen-bonding capability of less acidic (thio)ureas. Therefore, considering the opposite trends for both mechanisms, the highest activity for the catalyst system will be achieved when the p*K*a of the (thio)urea is closest to that of the conjugate acid of the base.

In these studies, the authors observed no trends for the ROP activity of ureas and thioureas of analogous structure.[90] However, when a urea or thiourea with similar acidities is used in combination with a base of comparable basicity, the urea present higher activity than the thiourea. This observation goes in line with the studies on (thio)urea/base systems reported by Kiesewetter and coworkers,[88] and is supported by the stronger binding of ureas to carbonyl compounds than thioureas of similar acidities.[109] Further mechanistic insights on the (thio)urea catalysed ROP were provided by Kiesewetter and coworkers, who demonstrated that apolar solvents favour a neutral (thio)urea mechanism, whereas polar solvents favour an anionic pathway.[110]

The great developments in the field of organocatalysts for ROP have enabled the controlled polymerisation of a range of monomers to obtain biodegradable polyesters and polycarbonates. Remarkably, the recent disclosure of the ureas/base and (thio)urea anion systems have provided unprecedented activity and selectivity. As a result, organocatalysts have been progressively becoming a robust alternative to the traditional metal catalysts to facilitate those applications where metals are undesirable.

1.4 Photoinduced Organocatalysed Ring-Opening Polymerisation

While the significant developments on ROP organocatalysts have allowed the synthesis of polymers with good control over the molecular weight and dispersity, the combination of this strategy with an external stimulus would provide additional control to the polymerisation regarding time and space.[111] Remote regulations are widely found in complex processes in nature and are typically promoted by chemical stimuli. In the allosteric regulations, for example, the protein functions are changed by binding of molecules away from the active site and result in conformational changes, and therefore, in activities modulation.[112] As for polymer chemists, a series of stimuli have been investigated to mimic the control observed in nature.[113] For instance, the use of polymerisation catalysts that have different activities in two oxidation states has allowed the temporal control by either using chemicals to promote redox reactions,[114,115] or the application of a current to provide an electrochemical control.[116,117] However, while the first approach is invasive and requires the addition of redox species to modulate the catalyst activity, the last technique uses confined electrochemical cells and specific electrolytes that limit a wider application. A non-invasive strategy that has been reported for a series of polymerisation methodologies is by utilising thermal latent catalysts.[118] While this technique provides good temporal control, spatial resolutions becomes challenging as heat is quickly dissipated. On the other hand, the use of light as a stimulus offers not only a non-invasive characteristic, but a series of advantages: the choice of appropriate wavelengths enables the induction of a particular photochemical reaction, whereas the intrinsic ability of light in focusing a beam in defined areas, combined with great developments in optics, allows for a high spatial resolution.[119]

The spatial and temporal control provided by photochemical polymerisations has been applied in advanced techniques such as photolithography, which is used in the preparation of sophisticated materials for the microelectronic[120,121] or biomedical (*i.e.* DNA and peptides microarrays)[122-124] industries. In this approach, particular areas are exposed to light and allow the polymerisation to proceed in the irradiated regions, thus creating patterns on a surface.[125] Moreover, this principle can be further extended to additive manufacturing technologies to prepare three-dimensional structures for biomaterial application.[126,127] In particular, the use of light as a stimulus has been widely investigated in the preparation of non-biodegradable polymers by reversible-deactivation radical polymerisations (RDRP) to provide specific surface modifications

and create complex structures.[128-130] Metters and coworkers, for instance, reported the use of photo-RDRP to graft poly(methacrylic acid) (PMAA) into silicon wafers with a spatially defined gradient of density by varying the irradiation exposure time across the surface.[131] The PMAA films were then functionalised with arginine-glycine-aspartic acid (RGD) peptide sequence that allowed controlling the degree of specific cell adhesion by changing the RGD density. Despite the advances in photo-CRP techniques, the utilisation of photoinduced processes in the preparation of biodegradable polymers such as aliphatic polyesters and polycarbonates by ROP has been hardly explored.

In this context, photocaged catalysts (*i.e.* inactive catalyst precursors that are transformed into active species by an irreversible photoreaction) have been investigated as a means to promote chemical reactions upon irradiation.[111] Specifically, photocaged catalysts able to generate strong acids or bases (*i.e.* photoacid generators (PAGs) or photobase generators (PBGs)) have been demonstrated in ROP. The application of this concept was firstly reported in 2008 by Wang and coworkers who utilised a tetraphenylborate salt of TBD (TBD.HBPh$_4$) that comprises a protonated and hence inactive form of the base.[132] Upon UV irradiation at λ = 254 nm, the BPh_4^- chromophore undergoes a rearrangement, followed by abstraction of the acidic proton of $TBDH^+$, which releases the active base (quantum yield, Φ, *i.e.* the number of reactants consumed by the number of photons absorbed, of 0.18). By using this PBG, the authors were able to demonstrate the phototriggered bulk ROP of ε-CL using *n*-hexanol as the initiator and 1 mol% catalyst by irradiating the polymerisation mixture for 5 minutes, which proceeded for further 8 hours at 60 °C to reach a monomer conversion of 70% (Scheme 1.20). The polymerisation was shown to be well controlled, as illustrated by the linear increase of the molecular weight with monomer conversion.

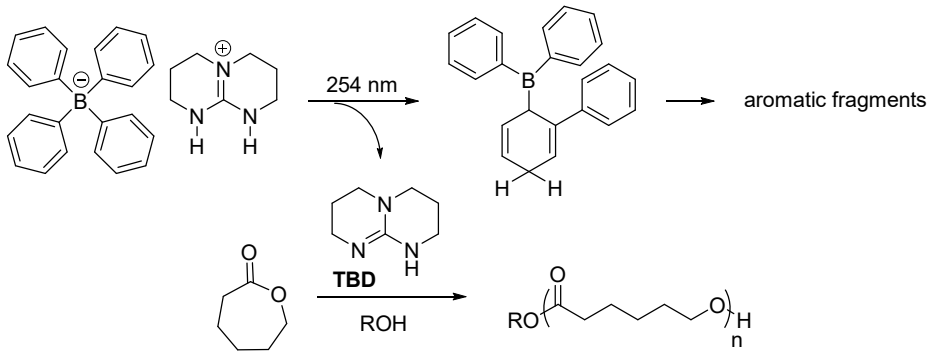

Scheme 1.20. Phototriggered ROP of ε-CL catalysed by TBD.HBPh$_4$ upon λ = 254 nm irradiation.

Following this work, our group demonstrated the use of triarylsulfonium hexafluorophosphate salts as a PAG in the cationic ROP of several cyclic monomers.[133] These salts undergo photocleavage at λ = 365 nm, which is followed by a series of rearrangements that finally leads to the release of a strong acid and aromatic byproducts.[134,135] When utilising 0.33% catalyst and irradiation times up to 90 minutes, monomer conversions of 40% and 30% were obtained in 7 hours for ε-CL and TMC, respectively, whereas δ-VL achieved 70% conversion in 2 hours ($[M]_0/[I]_0$ = 100) (Scheme 1.21). However, although the dispersity values remained low throughout the polymerisation ($Đ_M$ < 1.2), bimodal distributions associated with transesterification were observed.

More interestingly, the relevance of an "on-demand" catalyst generation was demonstrated by exploring the different reactivities of L-LA and δ-VL under acidic and basic conditions and carrying out a "one-pot" copolymerisation. While the PAG investigated in this study can promote the ROP of δ-VL and not of L-LA, DBU has shown high activity for L-LA, but polymerises δ-VL only in the presence of a monomer activator cocatalyst. As a result, a solution containing both monomers, DBU, the PAG salt and an alcohol initiator was shown to initially polymerise L-LA in the absence of irradiation, whereas δ-VL showed no polymerisation. After 3 hours in the dark, the L-LA monomer was fully consumed, and the solution was irradiated at λ = 365 nm for 90 minutes, which induced the release of protons that inactivated the base and further allowed the ROP of δ-VL to proceed and form well-defined block copolymers.

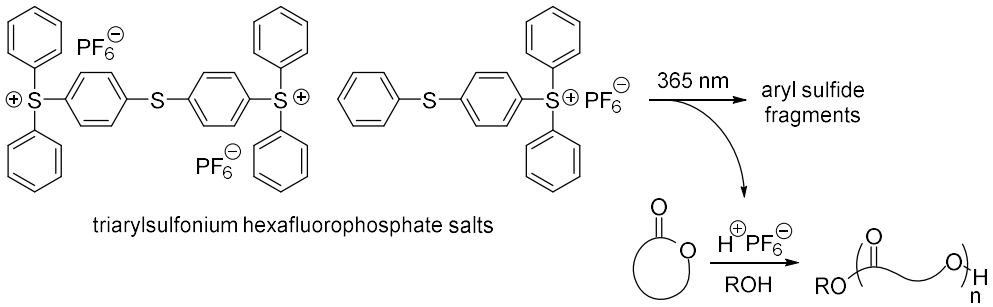

Scheme 1.21. Phototriggered ROP of cyclic monomers catalysed by triarylsulfonium hexafluorophosphate salts upon λ = 365 nm irradiation.

More recently, Placet *et al*. reported the use of ketoprofenate salt of TBD in the photoinitiated ROP of L-LA.[136] This PBG decomposes by photodecarboxylation in high quantum yields (Φ_{313} = 0.73)[137] and deprotonates the base to generate free TBD (Scheme 1.22). The authors carried out the polymerisation in a CH_2Cl_2 solution with 0.7 mol% PBG and 1-butanol as the initiator and observed full monomer conversion ($[M]_0/[I]_0$ = 45) after only 10 minutes irradiation at λ = 254 nm, which provided well-defined polymers with relatively low molecular weight distribution ($Đ_M$ = 1.26). Further investigation in the irradiation times showed complete polymerisation in only 3 minutes, although an increase in the dispersity values was observed ($Đ_M$ = 1.39). This PBG demonstrated a very fast release of a base, combined with high catalyst activity that provided an efficient polymerisation system for L-LA. However, there are several concerns related to the use of high-energy UV light (λ < 290 nm), which can cause damage to biological systems, in addition to present low compatibility with reactants and limited curing depth.[138]

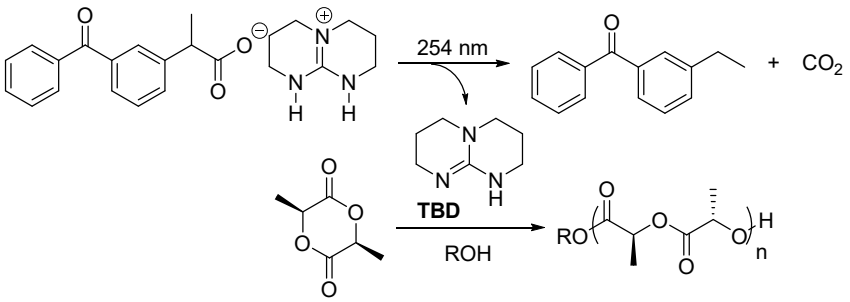

Scheme 1.22. Photoinduced ROP of L-LA using ketoprofenate of TBD upon λ = 254 nm irradiation.

A strategy to overcome the issues caused by the use of high energy light is to utilise photosensitisers in combination with photocaged catalysts in order to modify the wavelength employed.[139] In this biomolecular system, the catalyst is indirectly activated by energy transfer from the excited sensitiser, which allows the use of a wavelength dependent on the absorption of the photosensitiser. For example, isopropylthioxanthone, a compound with a strong absorption between λ = 350 and 390 nm, has been reported in the sensitisation of BPh_4^- salts, which has allowed the photolysis to occur at λ = 365 nm.[140,141] However, it is important to note that the presence of thioxanthone induces the formation of stable radicals. While this is useful to promote concomitant radical thiol-ene reactions, it is undesirable for thiol-Michael additions and requires the use of a radical inhibitor (*i.e.* 2,2,6,6-tetramethyl-1-piperidinyloxy (TEMPO)).[142] In addition, such a bimolecular system can undergo back electron transfer between the excited sensitiser and the photocaged catalyst, which is a disadvantage that has been demonstrated to decrease the initiation efficiency.[143,144]

In this regard, alternative PAGs and PBGs have been investigated in order to obtain increased photolytic efficiency (*i.e.* property that is directly proportional to the quantum yield and the molar absorption coefficient, ε, that represents the ability of a compound to absorb light at a specific wavelength).[145] In addition, compounds with increased photosensitivity at longer wavelengths have been explored in order to avoid issues associated with the use of high-energy UV light. Although PAGs and PBGs have been applied for a series of polymerisation methodologies (*e.g.* amine-epoxy,[146,147] thiol-epoxy,[148,149] thiol-Michael reactions),[150,151] these compounds have been underexplored for ROP. In this regard, considering that base catalysts were mostly investigated in this thesis, an overview of PBGs that have a great potential to be applied for ROP will be presented. A series of review articles have been addressed to PAGs, including the most recent developments on the area.[152-154]

1.4.1 Photobase Generators

PBGs have been demonstrated to photorelease a wide variety of catalysts previously reported for ROP, ranging from amines[155] to stronger bases such as amidines,[156,157] guanidines,[158,159] phosphazenes[157,160] and carbenes.[161] While there a number of classes of PBGs developed to date, many of them release primary or secondary amines that can act as initiators, and therefore, are incompatible as ROP catalysts. As a result, only photolabile carbamates, quaternary ammonium salts and

carboxylate salts are relevant for ROP and, thus, only these classes of compounds will be discussed herein.

The carbamate PBGs comprises the use of a photolabile protecting group (PPG) bonded to an amine *via* a carbamate group that undergoes photodecarboxylation to provide basic species (Scheme 1.23). Although this class of compound has been typically used to generate primary or secondary amines, Bowman and coworkers have demonstrated that a superbase, namely 1,1,3,3-tetramethylguanidine (TMG), can be photocaged *via* a carbamate PPG.[159,162] TMG has been utilised as catalyst in the ROP of *N*-carboxyanhydride[163] and has potential applicability to other cyclic monomers as a consequence of its high p*K*a (TMG.H$^+$: p*K*a = 23.4).[164]

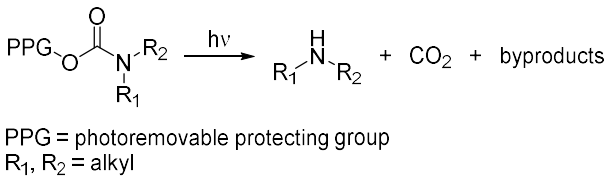

Scheme 1.23. Photolysis of photolabile carbamate PBGs.

The generation of basic amines using carbamate PBGs was introduced in 1990 by Cameron and Fréchet, [165] although the use of photolabile carbonyl groups for the protection of amino acids was established by Barltrop and Schofield in 1962.[166] As the PPGs based on photodecarboxylation have demonstrated great compatibility not only with amines but with other functional groups (*e.g.* alcohols, thiols),[139] extensive structure investigation has been performed in order to obtain improved release efficiency and higher absorptivity at longer wavelengths. In this regard, the *o*-nitrobenzyloxycarbonyl (NBOC, Scheme 1.24) group was proposed as a PPG for amino acids and rapidly became very popular, especially after the development of the dimethoxy analogue, namely *o*-nitroveratryloxycarbonyl (NVOC), which demonstrated absorption above λ = 320 nm, and therefore, was compatible with far-UV-sensitive compounds.[166-168] However, despite its broad applicability, this compound forms nitrosobenzaldehyde after photolysis, which strongly absorbs the incident light and leads to a decreased photocleavage efficiency by acting as an internal filter (Scheme 1.24). In addition, the aldehyde moiety reacts with the released amine to provide a stable imide that reduces the overall yield of free amine generated. Nonetheless, this side reaction has been shown to be avoided by the use of carbonyl

scavengers (*e.g.* hydroxylamine hydrochloride, semicarbazide hydrochloride) or by using an α-substituted nitro compound that leads to the formation of a ketone, compound that is less reactive towards amines than the corresponding aldehyde.[168]

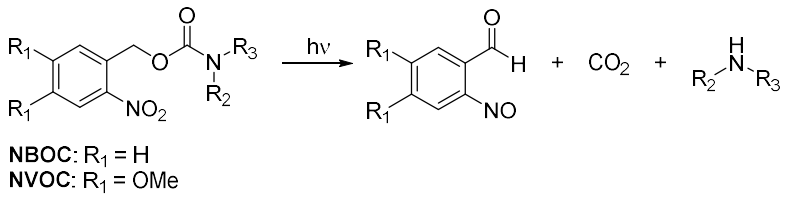

NBOC: R_1 = H
NVOC: R_1 = OMe

Scheme 1.24. Photolysis of *o*-nitrobenzyl group.

Further advances on the *o*-nitrobenzyl structure were reported by Hasan and coworkers with the incorporation of a methylene group between the aromatic and carbonyl groups, producing 2-(*O*-nitrophenyl)ethoxycarbonyl (NPEOC, Scheme 1.25). The authors observed that these compounds decompose *via* a photoinduced β-elimination process that leads to the formation of nitrostyrene as the main byproduct, which is inert to the released amines (Scheme 1.25). In addition, the effect of substituents on the phenyl ring and side chain was investigated, and the compound containing a methyl group in the α position (2-(*o*-nitrophenyl)propoxycarbonyl, NPPOC) presented considerably higher quantum yield when compared to NVOC (NVOC: Φ_{365} = 0.0013, NPPOC: Φ_{365} = 0.35).[169,170] Later on, Somoza and coworkers reported the use of benzoyl (Bz) and thiophenyl (SPh) substituted NPPOC, which presented even higher quantum yields than original NPPOC (Table 1.1).[171] In particular, SPh-NPPOC also showed increased molar absorptivity, which resulted in considerably high photolytic efficiency ($\varepsilon\Phi_{365}$ = 1064 M^{-1} cm^{-1}).

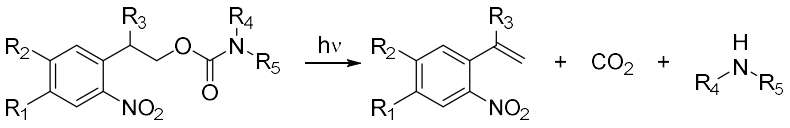

NPEOC: R_1 = R_2 = R_3 = H
NPPOC: R_1 = R_2 = H, R_3 = Me
Bz-NPPOC: R_1 = H, R_2 = (CO)Ph, R_3 = Me
SPh-NPPOC: R_1 = Et, R_2 = SPh, R_3 = Me

Scheme 1.25. Photolysis of NPEOC derivatives.

Table 1.1. Spectroscopic data of NPPOC and derivatives.

Group	ε^a (L mol^{-1} cm^{-1})	$\Phi_{365}{}^b$	$\varepsilon\Phi_{365}{}^c$ (L mol^{-1} cm^{-1})
NPPOC	260	0.40	104
Bz-NPPOC	240	0.84	202
SPh-NPPOC	1560	0.68	1064

[a] ε = molar absorptivity. [b] Φ = quantum yield. [c] $\varepsilon\Phi$ = photolytic efficiency.

Another class of PPG that has received considerable attention is the coumarin-4-ylmethyl group, which has been mostly applied for photocaging biomolecules (*e.g.* peptides, nucleic acid, sugars) for cell studies as a consequence of its fast photocleavage in an aqueous medium.[172,173] Therefore, different substitution in the aromatic ring has been investigated in order to provide increased water solubility and higher sensitivity towards the visible-light region, which minimises the damage of biological systems. While hydroxy or methoxy substituents at the C7 position (R_1) of coumarin-4-ylmethyl presented a maximum absorption at λ = 325 nm, [174-176] insertion of a bromine at C6 (R_2) shifted the absorption maximum to λ = 375 nm (Figure 1.14).[177,178] Further advances were achieved by substituting the C7 position with an amino group, which presented an absorption maximum at λ = 350–400 nm and a quantum yield higher than other analogues (Φ ~ 0.25).[179]

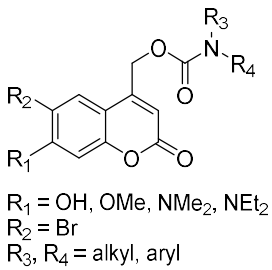

Figure 1.14. Structure of coumarin-4-ylmethyl analogues.

Although coumarin-4-ylmenthyl PPG has been mainly utilised with phosphates, it has also been demonstrated to photocage amines *via* a carbamate bond.[176,178,180] The photolysis of these compounds involves the formation of an anion that decarboxylates to release an amine and a coumarylmethyl cation that is typically stabilised by reacting with a protic nucleophile (usually a solvent, such as H_2O and MeOH) (Scheme 1.26).[181] However, Bowman and coworkers have demonstrated that the photocleavage

could also occur in aprotic solvents (*e.g.* MeCN, $CHCl_3$), which indicated that a different pathway would take place, although this was not further investigated.[162]

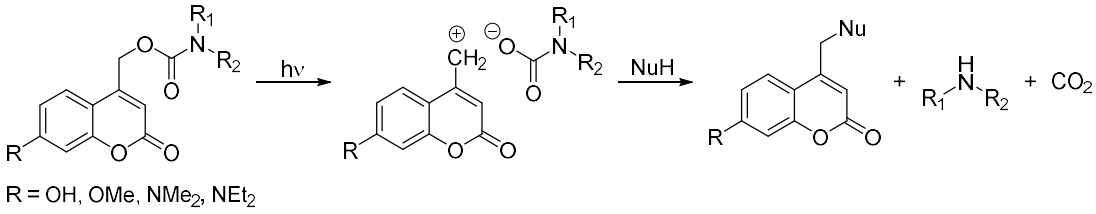

Scheme 1.26. Photolysis of coumarin-4-ylmethyl group in the presence of a nucleophile.

An alternative class of PBG notably relevant to ROP are the photolabile salts, which are able to release tertiary amines and other stronger bases. The first examples of this class of compounds appeared as quaternary ammonium salts (QAs), with a typical structure that consists of a tetrasubstituted ammonium cation directly bonded to a chromophore and a counterion with various structures. In general, QAs undergo a C–N bond cleavage upon irradiation, which generates the corresponding tertiary amine and byproducts originated from the chromophore degradation (Scheme 1.27).[182,183]

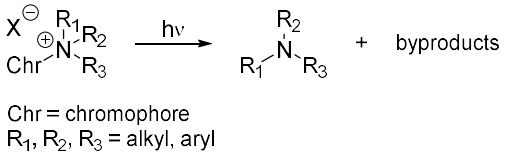

Scheme 1.27. General photolysis of QAs.

In a system developed Neckers and coworkers, borate anions were utilised as electron donors, with different chromophores being investigated as electron acceptors (Figure 1.15).[155] The proposed mechanism for the photolysis involves a single electron transfer (SET) from the borate anion to the excited triplet state of the chromophore (Scheme 1.28). This process generates a radical intermediate that rapidly undergoes C–N bond fragmentation, with a final SET generating free amine and other aromatic byproducts. The quantum yield was shown to be dependent on the electron donating capability of the borate anion, which explains the higher efficiency of triphenylbutylborate over tetraphenylborate, as the former is more easily oxidised. In

addition, the presence of bulky substituents on the nitrogen atom was shown to increase the efficiency by releasing strain energy. However, the dependence of the photolytic performance on the amine structure presents a disadvantage regarding versatility, as this restricts the amines able to be photoreleased.

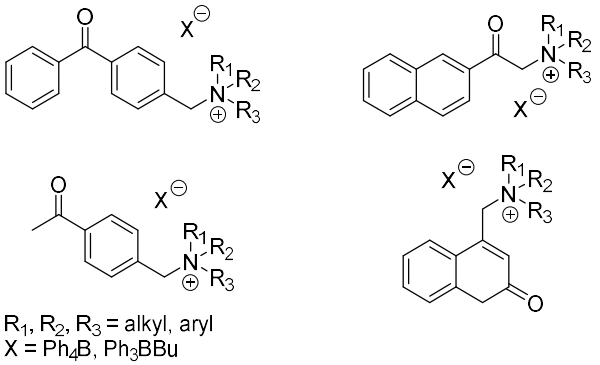

Figure 1.15. QAs developed by Neckers and coworkers.

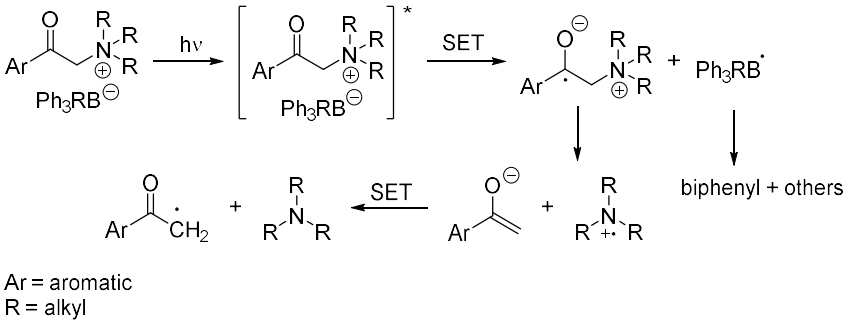

Scheme 1.28. Proposed mechanism for photocleavage of QAs with borate anions.

Alternatively, Tsunooka, Suyama and coworkers have developed QAs from phenacylammonium salts that presented different properties depending on the corresponding anion utilised (Figure 1.16). While QAs containing dithiocarbamate presented high photoreactivity in crosslinking epoxides in PGMA films, a low stability of the salt in the resin or organic solvents was observed.[184-186] The authors then investigated thiocyanate QAs, which presented higher stability, although a low photolysis efficiency was observed.[187,188] Other anions such as phthalimide, benzoate and selenocyanate were studied; however, achieving a balance between an adequate stability and high photoreactivity proved to be challenging.[189] Further investigation using methylbenzophenone as the chromophore for the photoprotection of DBU and phenylglyoxylate as the anion provided a QA with good solubility, thermal resistance

and high reactivity, which demonstrated great potential for the application in photocuring epoxy resins (Figure 1.17).[156]

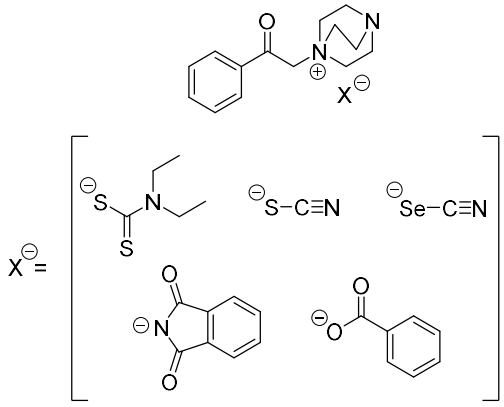

Figure 1.16. Structure of phenylacylammonium salts.

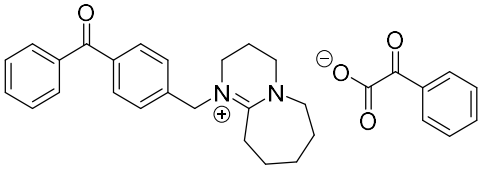

Figure 1.17. Structure of QA salt of benzoylbenzyl-DBU phenylglyoxylate.

The next generation of PBG salts comprised of a protonated base and a photolabile counterion, which releases the active base by deprotonation during photodecomposition. Examples of this class of compounds are the BPh_4^- and ketoprofenate salts, previously introduced in the photoinduced ROP. Specifically, ketoprofenate was the first carboxylate-functional chromophore to photocage bases that decomposes by photodecarboxylation along with deprotonation (Scheme 1.29).[190] Because these PBG salts only require the protonation of a base for deactivation and the quantum yield for photolysis is mainly dependent on the chromophore anion structure, these compounds have shown excellent compatibility with a wide variety of Brønsted bases (*e.g.* amidines, guanidines, phosphazenes and carbenes) (Figure 1.18). In this regard, the simple functionalisation of different chromophores with a carboxylic acid proved to be a versatile strategy to allow tuning the photochemical properties of PBGs.

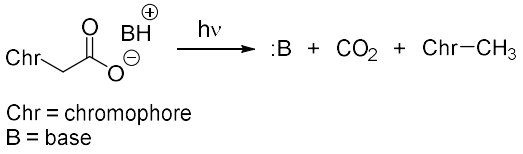

Scheme 1.29. Photolysis of a carboxylate-functional salt.

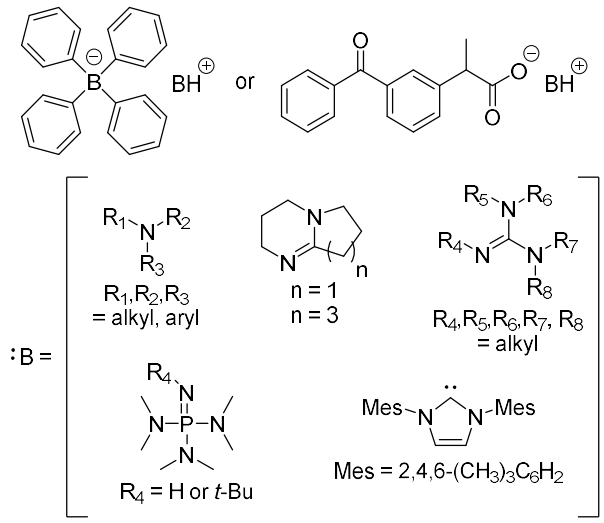

Figure 1.18. Examples of BPh_4^- and ketoprofenate salts.

Later on, a series of ketoprofenate analogues were investigated to comprehend the effect of the chromophore structure on the absorption and quantum yield of PBGs. While the ketoprofenate anion presented an absorption maximum at λ = 255 nm, the incorporation of an oxygen atom between the aromatic groups to form xanthone acetate, shifted the maximum to λ = 345 nm, without compromising considerably the quantum yield (Table 1.2, Entry 1 and 2).[157,191] A further red shift to λ = 382 nm was observed by substituting the oxygen in the ring with a sulphur atom to provide thioxanthone acetate (Entry 3).[192,193] Finally, Yagci, Liu and coworkers investigated the additional insertion of an oxygen atom between the aromatic group and the carboxylate, which increased the maximum absorption to λ = 400 nm (Entry 4).[194,195] Alternative chromophores were investigated and phenylglyoxylate presented high quantum yields at λ = 365 nm (Entry 5),[196,197] whereas phthalimide acetate showed an absorption maximum at $\lambda \sim 290$ nm that could be improved to $\lambda > 300$ nm by incorporating a nitro substituent in the aromatic ring (Entry 6). Further investigation was reported by Jiangwen and coworkers, who described a series of PBG derived from *N*-phthaloyltranexamic acid containing different aromatic substituents (Entry 7).

Again, thioxanthone provided the most significant red shift, and the maximum absorption appeared at λ = 418 nm. More recently, Bouzrati-Zerelli *et al*. reported a bithiophenylcyanoacrylic salt that has a strong absorption up to λ = 450 nm, although a low quantum yield of 0.04 was observed (Entry 8).

Table 1.2. Chemical structure of carboxylate-functional chromophores used for the preparation of PBG salts and the corresponding photochemical properties.

Entry	Carboxylate-functional Anion	Quantum Yield (Wavelength (nm))	Wavelength of Maximum Absorption (nm)	Ref.
1	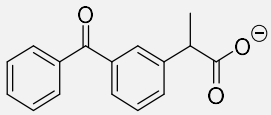	0.75 (313) [a, 137]	255	190
2	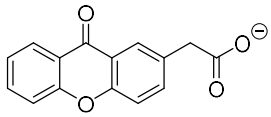	0.64 (350) [a, 191] or 0.38 (365)[b]	345	157
3	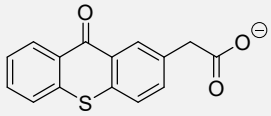	-	382	192
4	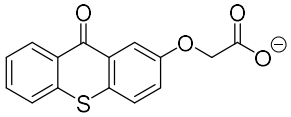	-	400	194
5	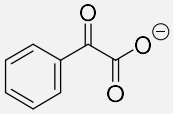	0.72 (365) [c, 198]	254, 366	196,197
6	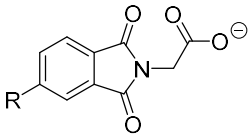 R = H or NO_2	R = H: 0.20 (254)[b]	R = H: ~ 290 R = NO_2: > 300	160
7	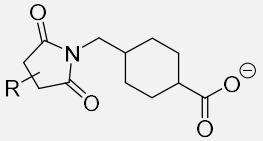 R = aryl, naphthyl, thioxanthone or benzophenone	R = aryl: 0.3 (290)[a, 199]	R = aryl: 295 R = naphthyl: 359 R = thioxanthone: 418 R = benzophenone: 301	200
8	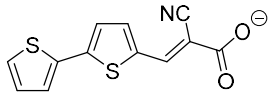	0.04 (405)	386	201

[a] Quantum yield determined for the corresponding carboxylic acid in aqueous solution. [b] Quantum yield determined for the TBD salt in a polystyrene film. [c] Quantum yield determined for the corresponding carboxylic acid in acetonitrile:water (3:1) solution at pH 1.9.

The research in the area of PBGs has favoured the development of ionic derivatives that are more easily tuned than the non-ionic PBG. In fact, the intrinsic structural characteristics of the ionic compounds have allowed the independent modification of the photosensitive moiety to target high quantum yields and absorption at longer wavelengths. In addition, protonated bases can be easily introduced *via* a simple acid-base reaction, which enables the use of a wide variety of ROP catalysts. Nonetheless, the most recent non-ionic PBGs such as carbamate-based derivatives that incorporates highly active catalysts still present great opportunities in the field.

1.5 Post-Polymerisation Modifications of Aliphatic Polyesters and Polycarbonates

The wide variety of catalysts developed to date have allowed the ROP of a range of cyclic monomers, including those containing pendent functionality in the polymer backbone, which is essential to tune the polymer properties (*e.g.* hydrophilicity, degradation rate, thermal and mechanical properties).[202] However, it is noteworthy that not all functional groups are compatible with ROP so that the required functionality needs to be protected or inserted after the polymerisation step.[203] In addition, the presence of different side groups in the monomer results in a particular reactivity towards ROP and therefore, achieving a controlled polymerisation often requires screening of an appropriate catalyst system and reaction conditions for each monomer. In this regard, monomers containing an orthogonal functionality that does not interfere with the polymerisation and are preserved after the polymerisation allows further manipulation by a post-polymerisation methodology. This strategy reduces the optimisation steps for individual monomers and even enables introducing groups incompatible with the polymerisation methodology without the use of protecting groups.

A series pendent functionalities have been utilised for modifying aliphatic polyesters and polycarbonates prepared by ROP, with the majority of examples comprising of alkene, alkyne, and halide.[31,204-206] Among these, the alkene is the most commonly utilised group and has been reported in different types of cyclic monomers, although functionalised cyclic carbonates have been increasingly explored, as a result of their relatively easy synthesis (Figure 1.19). The alkene functionality is very versatile, considering it can undergo a number of chemical transformations (*e.g.* thiol-ene reaction,[207-210] Michael addition,[211-214] epoxidation,[215-218] olefin cross

metathesis,[219,220] etc).[221] For instance, Thomas *et al*. have demonstrated the preparation of thermoresponsive polycarbonates by grafting thiol-terminated poly(ethylene glycol) (PEG) units into a hydrophobic allyl-functionalised polymer (originated from monomer **1.33**) *via* a radical thiol-ene reaction.[222] More interestingly, PEG of different lengths could be easily grafted under the same conditions, which allowed the preparation of a series of polymers presenting lower critical solution temperature (LCST) with varied cloud points depending on the PEG MWt. In another work reported by Zhong and coworkers, vinyl sulfone-functionalised copolymer films were prepared from monomer **1.36**, and ε-CL, LA, or TMC, and the pendent group was further modified *via* a thiol-Michael addition.[214] Notably, the functionalisation was performed in the absence of any catalyst and was shown to be tolerant to other functional groups such as hydroxy, carboxy and amine. This characteristic enabled the surface functionalisation with a series of thiol-containing molecules (*i.e*. 2-mercaptoethanol, cystamine, cysteine, thiolated glycol chitosan, GRGDC and thiolated PEG), which allowed the control over the cell attachment and growth. These examples illustrate the versatility of the alkene pendent group that can be employed to efficiently tune the polymer properties from a single precursor under a particular reaction condition.

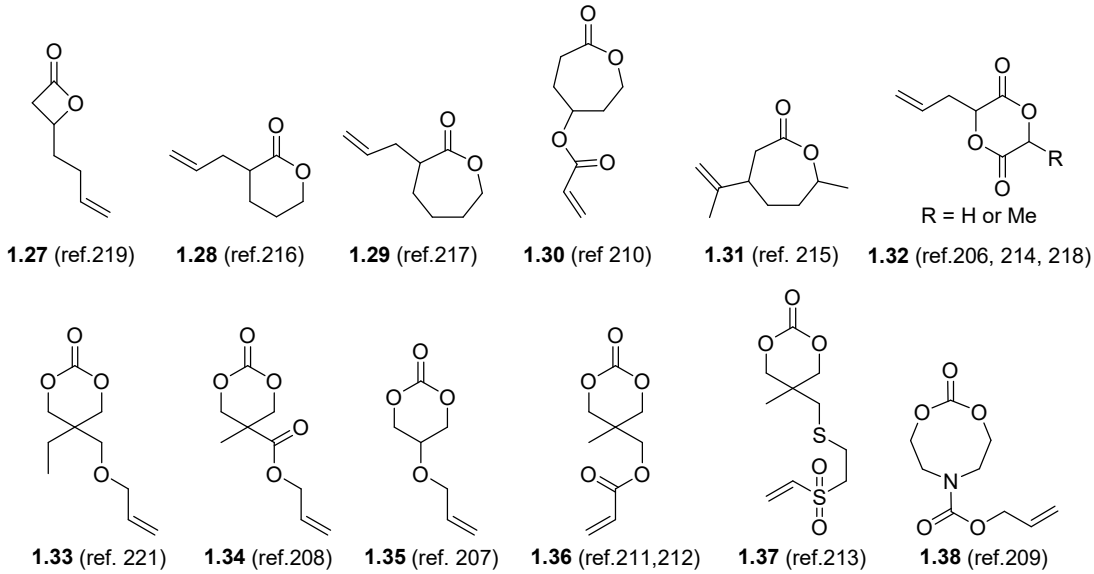

Figure 1.19. Examples of allyl-functionalised cyclic monomers.

Jiang *et al*. utilised the alkene side group of polycarbonates to conjugate the anticancer drug doxorubicin (DOX) utilising consecutive modification reactions.[218]

The authors firstly prepared amphiphilic polycarbonate copolymers from the ROP of monomer **1.35** and an alkyl-functionalised cyclic carbonate, using a PEG initiator. The allyl groups were then epoxidised, which enabled the insertion of hydrazine that was finally utilised to conjugate DOX to the polymer *via* its ketone moiety. The resultant prodrug micelles were shown to release DOX in a pH-responsive manner, as a consequence of the acid sensitivity of the hydrazone linkage. DOX was shown to be effectively delivered and released from the polymer conjugate into the nuclei of HeLa cells, and a good cytotoxicity was also observed, although slightly lower than with free DOX. Despite the large number of modifications required to introduce the desired compound, this strategy demonstrates the applicability of epoxide as a side group to provide a handle to insert additional types of functionalities (*e.g*. amines, alcohols, carboxylic acids) by nucleophilic reactions.

A few halogenated cyclic monomers have also been reported for the preparation of functionalised polymers for post-polymerisation reactions (Figure 1.20). The resultant polymers have been mostly modified by nucleophilic substitution with tertiary amines[223-227] and azides,[228,229] but also utilised for dehydrohalogenation to generate pendent alkene groups and be further functionalised,[224,230] or applied as a macroinitiator to graft acrylate polymers by atom transfer radical polymerisation (ATRP).[231,232] Chin *et al*. utilised the post-polymerisation strategy to prepare a series of antimicrobial cationic polymers by the nucleophilic substitution of chlorine-functionalised polycarbonates with tertiary amines.[226] This methodology allowed easy access to a library of functionalised polymers to evaluate the structure-activity and selectivity relationships on the antimicrobial and nonhemolytic properties. For the polymers functionalised with *N*,*N*-dimethylalkyl amines, the increase in the alkyl chain length was shown to enhance the antimicrobial activity, while maintaining a low hemolysis, up to the butyl group. For longer alkyl chains, the hydrophobicity of the group provided a higher hemolysis and resulted in a lower selectivity of the polymer. This strategy also enabled the insertion of less nucleophilic tertiary amines, such as pyridine and imidazole, although higher temperatures were required to promote an efficient functionalisation.

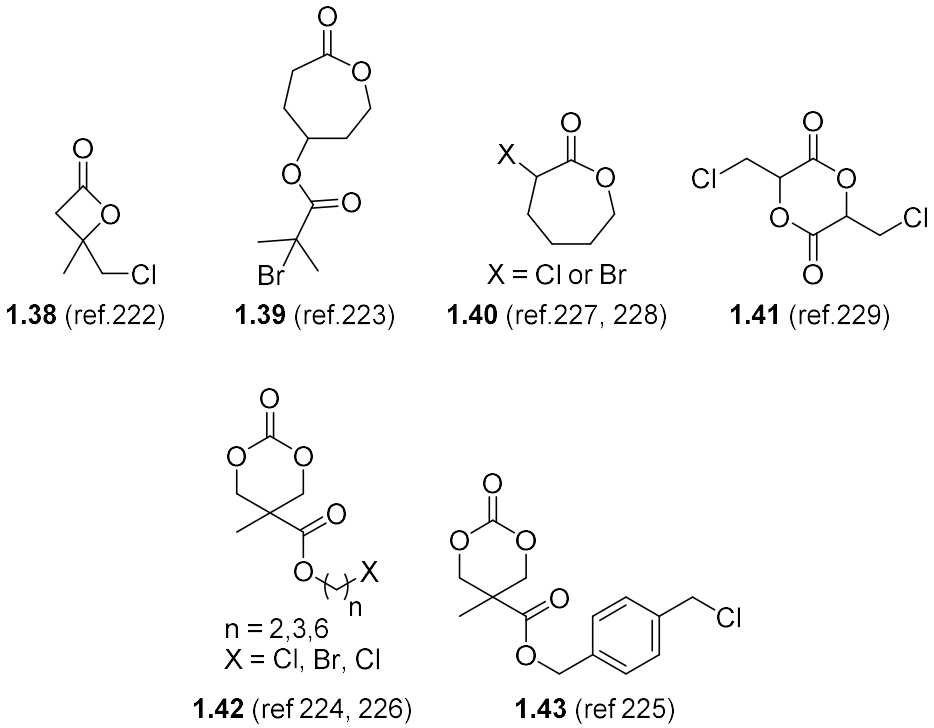

1.38 (ref.222) **1.39** (ref.223) **1.40** (ref.227, 228) **1.41** (ref.229)

1.42 (ref 224, 226) **1.43** (ref 225)

Figure 1.20. Examples of halide-functionalised cyclic monomers.

These examples highlight the advantages in utilising the post-polymerisation modification strategy when a series of functionalised polymers are desired, or to insert functionalities that are incompatible with ROP. However, it is noteworthy that this approach presents some limitations.[202] For instance, the radical thiol-ene reaction typically requires the use of large excess of thiol to avoid crosslinking reactions *via* the alkene group, whereas the nucleophilic substitution of halide-functionalised polymers can promote the degradation of the backbone. In addition, the entanglements in the polymer can prevent complete access to the functionalisable groups, which can restrict a full degree of conversion. Nonetheless, this methodology can be very valuable when the reaction conditions are carefully optimised, allowing for an effective functionalisation with minimum side reactions.

1.6 Conclusions

Biodegradable polycarbonates and polyesters have been playing a crucial role in providing a more sustainable approach in polymer science and have also brought great interest to the application in the biomedical field. The ROP methodology has been preferred for the synthesis of these materials, especially when high MWt polymers are required and/or to obtain good control over the molecular parameters (*i.e.* MWt,

dispersity and end-group fidelity). The remarkable developments achieved in organocatalysis for ROP has provided a range of catalysts that, despite being primarily investigated with traditional monomers, can potentially promote the polymerisation of new cyclic monomers. As a single organocatalyst is unable to provide comparable activities for all monomers, choosing an appropriate catalyst is essential to obtain high levels of control. For instance, acid catalysts polymerise δ-VL, ε-CL, and cyclic carbonates more efficiently than LA, whereas nucleophilic bases and superbase catalysts, such as NHCs and DBU, show high activity for the ROP of LA, although quenching the polymerisation is required to avoid transesterification reactions. On the other hand, while bifunctional catalysts provide significantly low levels of undesirable polymer transesterification, the original thiourea/base catalyst system exhibits poor activity. Remarkably, the development of urea/base and urea anion systems has allowed the polymerisation of a variety of monomers with great activity without compromising the high levels of control.

In addition to the ROP promoted by traditional catalysts, polymerisations externally regulated by photoinduced processes present great opportunities for the preparation of advanced materials. Even though this strategy has been scarcely applied for ROP, the advances in PBGs have contributed to a variety of chromophores that not only release strong bases relevant to ROP but that are also active in a benign UV/visible light (*i.e.* $\lambda > 350$ nm). Hence, these compounds provide alternatives regarding photoinduced ROP with promising applications, such as the synthesis of biodegradable polymers with spatial and temporal control by photolithography.

Finally, the polymers produced by ROP can be further modified to introduce other functionalities, which are essential to tune their final properties. The post-polymerisation modification methodology enables the preparation of a library of functional polymers from a single precursor, and also gives access to functionalities that are incompatible with the polymerisation. The ROP of a number of monomers containing orthogonal groups to polyesters and polycarbonates have been reported, including their applicability in post-polymerisation modifications. However, this methodology presents some limitations depending on the pendent group employed, and optimising the reaction conditions is essential to obtain an efficient functionalisation whilst avoiding any side reactions.

1.7 Aims and Objectives

The aim of this thesis comprises the development of controlled polymerisation strategies for the preparation of well-defined biodegradable polyesters and polycarbonates with potential applications as sustainable polymeric materials and in the biomedical field. In this thesis, we explored two different methodologies: i) the modification of a polymer by the functionalisation of pendent groups and ii) the photochemical control applied in ROP. The first approach explores the development of a biodegradable polymer containing a versatile pendent group that allows the insertion of different functional groups that can modify the polymer properties (*i.e.* thermal, mechanical, hydrophilicity and degradability). Considering the easier access to functional cyclic carbonate monomers than lactones, the synthesis of a functionalised aliphatic polycarbonate was envisioned. Moreover, we anticipated that the high reactivity of the epoxide group derived from the polarisation of the C–O bond, in addition to the strain of the three-membered ring, would provide a versatile handle for functionalisation. The objective of this work is, therefore, to synthesise a polycarbonate from an epoxide-functionalised cyclic carbonate monomer by using a suitable organocatalyst to retain the epoxide group and further use this pendent group to introduce functionalities into the polymer, especially those that are incompatible with the polymerisation methodology.

In the second stage, alternative photopolymerisation systems are explored to overcome the limited efficiency provided by current systems and to avoid the use of harmful high-energy UV light. With the development of a more effective system, the preparation of biodegradable polymers with temporal and spatial control is envisioned. As such, the specific objectives are: i) to develop a polymerisation system that activates a suitable ROP catalyst upon irradiation to provide temporal control (the highly active photobase generators are anticipated to be suitable to achieve this); ii) to synthesise a bifunctional monomer that can act as a crosslinker when polymerised by the same photoinduced catalyst; and iii) to develop an appropriate resin composition by combining the crosslinker and the photocatalyst to prepare self-standing materials with spatial resolution.

1.8 References

1. R. Geyer, J. Jambeck and K. Law, *Sci. Adv.*, 2017, **3**, e1700782.
2. S. R. Forrest, *Nature*, 2004, **428**, 911.
3. M. F. Maitz, *Biosurface and Biotribology*, 2015, **1**, 161.
4. PlasticsEurope, *Plastics - the Facts 2018: An analysis of European plastics production, demand and waste data*, 2018.
5. G. E. Luckachan and C. K. S. Pillai, *J. Polym. Environ.*, 2011, **19**, 637.
6. T. P. Haider, C. Volker, J. Kramm, K. Landfester and F. R. Wurm, *Angew. Chem. Int. Ed.*, 2019, **58**, 50.
7. V. Siracusa, P. Rocculi, S. Romani and M. D. Rosa, *Trends Food Sci. Technol.*, 2008, **19**, 634.
8. L. S. Nair and C. T. Laurencin, *Prog. Polym. Sci.*, 2007, **32**, 762.
9. Y. Ikada and H. Tsuji, *Macromol. Rapid Commun.*, 2000, **21**, 117.
10. J. Xu, E. Feng and J. Song, *J. Appl. Polym. Sci.*, 2014, **131**, 39822.
11. R. P. Brannigan and A. P. Dove, *Biomater. Sci.*, 2017, **5**, 9.
12. I. Manavitehrani, A. Fathi, H. Badr, S. Daly, A. Negahi Shirazi and F. Dehghani, *Polymers*, 2016, **8**.
13. U. Edlund and A.-C. Albertsson, *Adv. Drug Deliv. Rev.*, 2003, **55**, 585.
14. Y. Hu, W. A. Daoud, K. K. L. Cheuk and C. S. K. Lin, *Materials*, 2016, **9**, 133.
15. D. J. Darensbourg and S. J. Wilson, *Green Chem.*, 2012, **14**, 2665.
16. M. R. Kember, A. Buchard and C. K. Williams, *Chem. Commun.*, 2011, **47**, 141.
17. O. Dechy-Cabaret, B. Martin-Vaca and D. Bourissou, in *Handbook of Ring-Opening Polymerization*, eds. P. Dubois, O. Coulembier and J. M. Raquez, WILEY-VCH, Weinheim, 2009, ch. 10, pp. 255.
18. A. C. Albertsson, I. K. Varma and R. K. Srivastava, in *Handbook of Ring-Opening Polymerization*, eds. P. Dubois, O. Coulembier and J. M. Raquez, WILEY-VCH, Weinheim, 2009, ch. 11, pp. 287.
19. H. Keul, in *Handbook of Ring-Opening Polymerization*, eds. P. Dubois, O. Coulembier and J. M. Raquez, WILEY-VCH, Weinheim, 2009, ch. 12, pp. 307.
20. A.-C. Albertsson and I. K. Varma, *Biomacromolecules*, 2003, **4**, 1466.

21. M. Fèvre, J. Vignolle, Y. Gnanou and D. Taton, in *Polymer Science: A Comprehensive Reference*, eds. K. Matyjaszewski and M. Möller, Elsevier, 2012, vol. 4, ch. 4.06.
22. E. Bat, J. A. Plantinga, M. C. Harmsen, M. J. A. van Luyn, Z. Zhang, D. W. Grijpma and J. Feijen, *Biomacromolecules*, 2008, **9**, 3208.
23. P. Gentile, V. Chiono, I. Carmagnola and P. V. Hatton, *Int. J. Mol. Sci.*, 2014, **15**, 3640.
24. D. J. A. Cameron and M. P. Shaver, *Chem. Soc. Rev.*, 2011, **40**, 1761.
25. B. Amsden, S. Wang and U. Wyss, *Biomacromolecules*, 2004, **5**, 1399.
26. D. A. Culkin, W. Jeong, S. Csihony, E. D. Gomez, N. P. Balsara, J. L. Hedrick and R. M. Waymouth, *Angew. Chem. Int. Ed.*, 2007, **46**, 2627.
27. O. Coulembier, J. De Winter, T. Josse, L. Mespouille, P. Gerbaux and P. Dubois, *Polym. Chem.*, 2014, **5**, 2103.
28. F. Jin, S.-H. Hyon, H. Iwata and S. Tsutsumi, *Macromol. Rapid Commun.*, 2002, **23**, 909.
29. S. Corneillie and M. Smet, *Polym. Chem.*, 2015, **6**, 850.
30. X. Lou, C. Detrembleur and R. Jérôme, *Macromol. Rapid Commun.*, 2003, **24**, 161.
31. S. Tempelaar, L. Mespouille, O. Coulembier, P. Dubois and A. P. Dove, *Chem. Soc. Rev.*, 2013, **42**, 1312.
32. R. J. Pounder and A. P. Dove, *Polym. Chem.*, 2010, **1**, 260.
33. X. Jiang, E. B. Vogel, M. R. Smith III and G. L. Baker, *Macromolecules*, 2008, **41**, 1937.
34. X. Jiang, M. R. Smith III and G. L. Baker, *Macromolecules*, 2008, **41**, 318.
35. Y. Kimura, K. Shirotani, H. Yamane and T. Kitao, *Macromolecules*, 1988, **21**, 3338.
36. T. Trimaille, M. Möller and R. Gurny, *J. Polym. Sci., Part A: Polym. Chem.*, 2004, **42**, 4379.
37. S. A. Cairns, A. Schultheiss and M. P. Shaver, *Polym. Chem.*, 2017, **8**, 2990.
38. O. T. du Boullay, E. Marchal, B. Martin-Vaca, F. P. Cossío and D. Bourissou, *J. Am. Chem. Soc.*, 2006, **128**, 16442.
39. J. Feng, R.-X. Zhuo and X.-Z. Zhang, *Prog. Polym. Sci.*, 2012, **37**, 211.
40. R. Wu, T. F. Al-Azemi and K. S. Bisht, *Biomacromolecules*, 2008, **9**, 2921.

41. S. Venkataraman, V. W. L. Ng, D. J. Coady, H. W. Horn, G. O. Jones, T. S. Fung, H. Sardon, R. M. Waymouth, J. L. Hedrick and Y. Y. Yang, *J. Am. Chem. Soc.*, 2015, **137**, 13851.
42. A. Södergård and M. Stolt, in *Poly(lactic acid): Synthesis, Structures, Properties, Processing, and Applications*, eds. R. Auras, L.-T. Lim, S. E. M. Selke and H. Tsuji, John Wiley & Sons, New Jersey, 2010, ch. 3.
43. P. Lecomte and C. Jérôme, in *Synthetic Biodegradable Polymers. Advances in Polymer Science*, eds. B. Rieger, A. Künkel, G. W. Coates, R. Reichardt, E. Dinjus and T. A. Zevaco, Springer, Berlin, Heidelberg 2012, vol. 245.
44. H. R. Kricheldorf, J. Jenssen and I. Kreiser-Saunders, *Makromol. Chem.*, 1991, **192**, 2391.
45. B. Wurm, H. Keul and H. Höcker, *Macromol. Chem. Phys.*, 1994, **195**, 3489.
46. A. P. Dove, *ACS Macro Lett.*, 2012, **1**, 1409.
47. D. W. C. MacMillan, *Nature*, 2008, **455**, 304.
48. A. Nachtergael, O. Coulembier, P. Dubois, M. Helvenstein, P. Duez, B. Blankert and L. Mespouille, *Biomacromolecules*, 2015, **16**, 507.
49. F. Nederberg, E. F. Connor, M. Möller, T. Glauser and J. L. Hedrick, *Angew. Chem. Int. Ed.*, 2001, **40**, 2712.
50. C. Bonduelle, B. Martin-Vaca, F. P. Cossio and D. Bourissou, *Chemistry*, 2008, **14**, 5304.
51. E. F. Connor, G. W. Nyce, M. Myers, A. Möck and J. L. Hedrick, *J. Am. Chem. Soc.*, 2002, **124**, 914.
52. G. W. Nyce, T. Glauser, E. F. Connor, A. Möck, R. M. Waymouth and J. L. Hedrick, *J. Am. Chem. Soc.*, 2003, **125**, 3046.
53. E. J. Shin, H. A. Brown, S. Gonzalez, W. Jeong, J. L. Hedrick and R. M. Waymouth, *Angew. Chem. Int. Ed.*, 2011, **50**, 6388.
54. E. Brulé, V. Guérineau, P. Vermaut, F. Prima, J. Balogh, L. Maron, A. M. Z. Slawin, S. P. Nolan and C. M. Thomas, *Polym. Chem.*, 2013, **4**, 2414.
55. F. Nederberg, B. G. G. Lohmeijer, F. Leibfarth, R. C. Pratt, J. Choi, A. P. Dove, R. M. Waymouth and J. L. Hedrick, *Biomacromolecules*, 2007, **8**, 153.
56. W. Jeong, E. J. Shin, D. A. Culkin, J. L. Hedrick and R. M. Waymouth, *J. Am. Chem. Soc.*, 2009, **131**, 4884.
57. G. O. Jones, Y. A. Chang, H. W. Horn, A. K. Acharya, J. E. Rice, J. L. Hedrick and R. M. Waymouth, *J. Phys. Chem. B*, 2015, **119**, 5728.

58. S. Naumann, A. W. Thomas and A. P. Dove, *ACS Macro Lett.*, 2016, **5**, 134.
59. J. Liu and L. Liu, *Macromolecules*, 2004, **37**, 2674.
60. J. Casas, P. V. Persson, T. Iversen and A. Córdova, *Adv. Synth. Catal.*, 2004, **346**, 1087.
61. F. Zeng, H. Lee, M. Chidiac and C. Allen, *Biomacromolecules*, 2005, **6**, 2140.
62. J. Matsuo, S. Nakano, F. Sanda and T. Endo, *J. Polym. Sci., Part A: Polym. Chem.*, 1998, **36**, 2463.
63. D. Bourissou, B. Martin-vaca, A. Dumitrescu, M. Graullier and F. Lacombe, *Macromolecules*, 2005, **38**, 9993.
64. M. Baśko and P. Kubisa, *J. Polym. Sci., Part A: Polym. Chem.*, 2010, **48**, 2650.
65. D. Delcroix, B. Martín-vaca, D. Bourissou, C. Navarro and S. Magnet, *Macromolecules*, 2008, **41**, 3782.
66. N. Susperregui, D. Delcroix, B. Martin-Vaca, D. Bourissou and L. Maron, *J. Org. Chem.*, 2010, **75**, 6581.
67. D. Delcroix, B. Martín-Vaca, D. Bourissou and C. Navarro, *Macromolecules*, 2010, **43**, 8828.
68. D. J. Coady, H. W. Horn, G. O. Jones, H. Sardon, A. C. Engler, R. M. Waymouth, J. E. Rice, Y. Y. Yang and J. L. Hedrick, *ACS Macro Lett.*, 2013, **2**, 306.
69. R. Kakuchi, Y. Tsuji, K. Chiba, K. Fuchise, R. Sakai, T. Satoh and T. Kakuchi, *Macromolecules*, 2010, **43**, 7090.
70. M. Oshimura, T. Tang and A. Takasu, *J. Polym. Sci., Part A: Polym. Chem.*, 2011, **49**, 1210.
71. Y. Jin, Y. Ji, X. He, S. Kan, H. Xia, B. Liang, J. Chen, H. Wu, K. Guo and Z. Li, *Polym. Chem.*, 2014, **5**, 3098.
72. H. Wu, Y. Ji, Z. Li, X. Wang, Q. Zhang, S. Cui, W. Wu, J. Liu and K. Guo, *J. Polym. Sci., Part A: Polym. Chem.*, 2015, **53**, 729.
73. K. Makiguchi, T. Satoh and T. Kakuchi, *Macromolecules*, 2011, **44**, 1999.
74. K. Makiguchi, Y. Ogasawara, S. Kikuchi, T. Satoh and T. Kakuchi, *Macromolecules*, 2013, **46**, 1772.
75. E. K. Macdonald and M. P. Shaver, *Eur. Polym. J.*, 2017, **95**, 702.
76. B. G. G. Lohmeijer, R. C. Pratt, F. Leibfarth, J. W. Logan, D. A. Long, A. P. Dove, F. Nederberg, J. Choi, C. Wade, R. M. Waymouth and J. L. Hedrick, *Macromolecules*, 2006, **39**, 8574.

77. H. A. Brown, A. G. De Crisci, J. L. Hedrick and R. M. Waymouth, *ACS Macro Lett.*, 2012, **1**, 1113.
78. L. Zhang, F. Nederberg, R. C. Pratt, R. M. Waymouth, J. L. Hedrick and C. G. Wade, *Macromolecules*, 2007, **40**, 4154.
79. L. Zhang, F. Nederberg, J. M. Messman, R. C. Pratt, J. L. Hedrick and C. G. Wade, *J. Am. Chem. Soc.*, 2007, **129**, 12610.
80. S. Liu, H. Li, N. Zhao and Z. Li, *ACS Macro Lett.*, 2018, **7**, 624.
81. H. Alamri, J. Zhao, D. Pahovnik and N. Hadjichristidis, *Polym. Chem.*, 2014, **5**, 5471.
82. H. Li, N. Zhao, C. Ren, S. Liu and Z. Li, *Polym. Chem.*, 2017, **8**, 7369.
83. A. P. Dove, R. C. Pratt, B. G. G. Lohmeijer, R. M. Waymouth and J. L. Hedrick, *J. Am. Chem. Soc.*, 2005, **127**, 13798.
84. R. C. Pratt, B. G. G. Lohmeijer, D. A. Long, P. N. P. Lundberg, A. P. Dove, H. Li, C. G. Wade, R. M. Waymouth and J. L. Hedrick, *Macromolecules*, 2006, **39**, 7863.
85. D. J. Coady, A. C. Engler, H. W. Horn, K. M. Bajjuri, K. Fukushima, G. O. Jones, A. Nelson, J. E. Rice and J. L. Hedrick, *ACS Macro Lett.*, 2012, **1**, 19.
86. S. Tempelaar, I. A. Barker, V. X. Truong, D. J. Hall, L. Mespouille, P. Dubois and A. P. Dove, *Polym. Chem.*, 2013, **4**, 174.
87. S. S. Spink, O. I. Kazakov, E. T. Kiesewetter and M. K. Kiesewetter, *Macromolecules*, 2015, **48**, 6127.
88. K. V. Fastnacht, S. S. Spink, N. U. Dharmaratne, J. U. Pothupitiya, P. P. Datta, E. T. Kiesewetter and M. K. Kiesewetter, *ACS Macro Lett.*, 2016, **5**, 982.
89. N. U. Dharmaratne, J. U. Pothupitiya, T. J. Bannin, O. I. Kazakov and M. K. Kiesewetter, *ACS Macro Lett.*, 2017, **6**, 421.
90. B. Lin and R. M. Waymouth, *Macromolecules*, 2018, **51**, 2932.
91. R. C. Pratt, B. G. G. Lohmeijer, D. A. Long, R. M. Waymouth and J. L. Hedrick, *J. Am. Chem. Soc.*, 2006, **128**, 4556.
92. O. Coulembier, D. P. Sanders, A. Nelson, A. N. Hollenbeck, H. W. Horn, J. E. Rice, M. Fujiwara, P. Dubois and J. L. Hedrick, *Angew. Chem. Int. Ed.*, 2009, **48**, 5170.
93. S. Koeller, J. Kadota, A. Deffieux, F. Peruch, S. Massip, J. M. Léger, J. P. Desvergne and B. Bibal, *J. Am. Chem. Soc.*, 2009, **131**, 15088.

94. S. Koeller, J. Kadota, F. Peruch, A. Deffieux, N. Pinaud, I. Pianet, S. Massip, J. M. Léger, J. P. Desvergne and B. Bibal, *Chemistry*, 2010, **16**, 4196.
95. A. Alba, A. Schopp, A.-P. d. S. Delgado, R. Cherif-Cheikh, B. Martín-Vaca and D. Bourissou, *J. Polym. Sci., Part A: Polym. Chem.*, 2010, **48**, 959.
96. C. Thomas, F. Peruch, A. Deffieux, A. Milet, J.-P. Desvergne and B. Bibal, *Adv. Synth. Catal.*, 2011, **353**, 1049.
97. C. Thomas, F. Peruch and B. Bibal, *RSC Adv.*, 2012, **2**, 12851.
98. J. Liu, C. Chen, Z. Li, W. Wu, X. Zhi, Q. Zhang, H. Wu, X. Wang, S. Cui and K. Guo, *Polym. Chem.*, 2015, **6**, 3754.
99. J. Liu, J. Xu, Z. Li, S. Xu, X. Wang, H. Wang, T. Guo, Y. Gao, L. Zhang and K. Guo, *Polym. Chem.*, 2017, **8**, 7054.
100. D. Specklin, F. Hild, L. Chen, L. Thévenin, M. Munch, F. Dumas, F. Le Bideau and S. Dagorne, *ChemCatChem*, 2017, **9**, 3041.
101. A. Rostami, E. Sadeh and S. Ahmadi, *J. Polym. Sci., Part A: Polym. Chem.*, 2017, **55**, 2483.
102. I. Kaljurand, A. Kütt, L. Sooväli, T. Rodima, V. Mäemets, I. Leito and I. A. Koppel, *J. Org. Chem.*, 2005, **70**, 1019.
103. A. Chuma, H. W. Horn, W. C. Swope, R. C. Pratt, L. Zhang, B. G. G. Lohmeijer, C. G. Wade, R. M. Waymouth, J. L. Hedrick and J. E. Rice, *J. Am. Chem. Soc.*, 2008, **130**, 6749.
104. L. Simón and J. M. Goodman, *J. Org. Chem.*, 2007, **72**, 9656.
105. L. Zhang, R. C. Pratt, F. Nederberg, H. W. Horn, J. E. Rice, R. M. Waymouth, C. G. Wade and J. L. Hedrick, *Macromolecules*, 2010, **43**, 1660.
106. F. Eisenreich, P. Viehmann, F. Müller and S. Hecht, *Macromolecules*, 2015, **48**, 8729.
107. X. Zhang, G. O. Jones, J. L. Hedrick and R. M. Waymouth, *Nat. Chem.*, 2016, **8**, 1047.
108. B. Lin and R. M. Waymouth, *J. Am. Chem. Soc.*, 2017, **139**, 1645.
109. R. R. Walvoord, P. N. Huynh and M. C. Kozlowski, *J. Am. Chem. Soc.*, 2014, **136**, 16055.
110. J. U. Pothupitiya, R. S. Hewawasam and M. K. Kiesewetter, *Macromolecules*, 2018, **51**, 3203.
111. R. S. Stoll and S. Hecht, *Angew. Chem. Int. Ed.*, 2010, **49**, 5054.
112. H. N. Motlagh, J. O. Wrabl, J. Li and V. J. Hilser, *Nature*, 2014, **508**, 331.

113. F. A. Leibfarth, K. M. Mattson, B. P. Fors, H. A. Collins and C. J. Hawker, *Angew. Chem. Int. Ed.*, 2013, **52**, 199.
114. C. K. A. Gregson, V. C. Gibson, N. J. Long, P. J. Oxford and A. J. P. White, *J. Am. Chem. Soc.*, 2006, **128**, 7410.
115. C. Chen, *ACS Catal.*, 2018, **8**, 5506.
116. A. J. D. Magenau, N. C. Strandwitz, A. Gennaro and K. Matyjaszewski, *Science*, 2011, **322**, 81.
117. F. A. Plamper, *Colloid Polym. Sci.*, 2014, **292**, 777.
118. S. Naumann and M. R. Buchmeiser, *Macromol. Rapid Commun.*, 2014, **35**, 682.
119. R. Göstl, A. Senf and S. Hecht, *Chem. Soc. Rev.*, 2014, **43**, 1982.
120. D. Bratton, D. Yang, J. Dai and C. K. Ober, *Polym. Adv. Technol.*, 2006, **17**, 94.
121. R. P. Seisyan, *Tech. Phys.*, 2011, **56**, 1061.
122. D. Wöll, J. Smirnova, M. Galetskaya, T. Prykota, J. Bühler, K.-P. Stengele, W. Pfleiderer and U. E. Steiner, *Chem. Eur. J.*, 2008, **14**, 6490.
123. D. Wöll, S. Walbert, K.-P. Stengele, T. J. Albert, T. Richmond, J. Norton, M. Singer, R. D. Green, W. Pfleiderer and U. E. Steiner, *Helv. Chim. Acta*, 2004, **87**, 28.
124. X. Meng, J. Wei, Y. Wang, H. Zhang and Z. Wang, *Anal. Methods*, 2018, **10**.
125. G. M. Wallraff and W. D. Hinsberg, *Chem. Rev.*, 1999, **99**, 1801.
126. S. A. Skoog, P. L. Goering and R. J. Narayan, *J. Mater. Sci.: Mater. Med.*, 2014, **25**, 845.
127. H. N. Chia and B. M. Wu, *J. Biol. Eng.*, 2015, **9**, 4.
128. S. Yamago and Y. Nakamura, *Polymer*, 2013, **54**, 981.
129. M. Chen, M. Zhong and J. A. Johnson, *Chem. Rev.*, 2016, **116**, 10167.
130. X. Pan, M. A. Tasdelen, J. Laun, T. Junkers, Y. Yagci and K. Matyjaszewski, *Prog. Polym. Sci.*, 2016, **62**, 73.
131. B. P. Harris, J. K. Kutty, E. W. Fritz, C. K. Webb, K. J. L. Burg and A. T. Metters, *Langmuir*, 2006, **22**, 4467.
132. X. Sun, J. P. Gao and Z. Y. Wang, *J. Am. Chem. Soc.*, 2008, **130**, 8130.
133. I. A. Barker and A. P. Dove, *Chem. Commun.*, 2013, **49**, 1205.
134. J. L. Dektar and N. P. Hacker, *J. Am. Chem. Soc.*, 1990, **112**, 6004.

135. S. Peter Pappas, B. C. Pappas, L. R. Gatechair, J. H. Jilek and W. Schnabel, *Polym. Photochem.*, 1984, **5**, 1.
136. E. Placet, J. Pinaud, O. Gimello and P. Lacroix-Desmazes, *ACS Macro Lett.*, 2018, **7**, 688.
137. L. L. Costanzo, G. De Guidi, G. Condorelli, A. Cambria and M. Fama, *Photochem. Photobiol.*, 1989, **60**, 359.
138. K. Suyama and M. Shirai, *Prog. Polym. Sci.*, 2009, **34**, 194.
139. P. Klán, T. Šolomek, C. G. Bochet, A. Blanc, R. Givens, M. Rubina, V. Popik, A. Kostikov and J. Wirz, *Chem. Rev.*, 2013, **113**, 119.
140. J. Shin, H. Matsushima, C. M. Comer, C. N. Bowman and C. E. Hoyle, *Chem. Mater.*, 2010, **22**, 2616.
141. Y. Jian, Y. He, Y. Sun, H. Yang, W. Yang and J. Nie, *J. Mater. Chem. C*, 2013, **1**, 4481.
142. S. Chatani, T. Gong, B. A. Earle, M. Podgórski and C. N. Bowman, *ACS Macro Lett.*, 2014, **3**, 315.
143. E. Andrzejewska, D. Zych-Tomkowiak, M. Andrzejewski, G. L. Hug and B. Marciniak, *Macromolecules*, 2006, **39**, 3777.
144. J. Qiu and J. Wei, *J. Polym. Res.*, 2014, **21**, 559.
145. D. R. Hokanson, K. Li and R. R. Trussell, *Front. Environ. Sci. Eng.*, 2015, **10**, 428.
146. K. Suyama, S. Ozaki and M. Shirai, *React. Funct. Polym.*, 2013, **73**, 518.
147. K. Arimitsu, M. Miyamoto and K. Ichimura, *Angew. Chem. Int. Ed.*, 2000, **39**, 3425.
148. Y. H. Zhao, D. Vuluga, L. Lecamp and F. Burel, *RSC Adv.*, 2016, **6**, 32098.
149. A. O. Konuray, X. Fernández-Francos and X. Ramis, *Polymer*, 2017, **116**, 191.
150. W. Xi, M. Krieger, C. J. Kloxin and C. N. Bowman, *Chem. Commun.*, 2013, **49**, 4504.
151. S. Huang, M. Podgórski, X. Zhang, J. Sinha, M. Claudino, J. W. Stansbury and C. N. Bowman, *J. Dent. Res.*, 2018, **97**, 530.
152. M. Shirai and M. Tsunooka, *Prog. Polym. Sci.*, 1996, **21**, 1.
153. M. Shirai and M. Tsunooka, *Bull. Chem. Soc. Jpn.*, 1998, **71**, 2483.
154. C. J. Martin, G. Rapenne, T. Nakashima and T. Kawai, *J. Photochem. Photobiol., C*, 2018, **34**, 41.

155. A. M. Sarker, Y. Kaneko, A. V. Nikolaitchik and D. C. Neckers, *J. Phys. Chem. A*, 1998, **102**, 5375.

156. K. Suyama, H. Araki and M. Shirai, *J. Photopolym. Sci. Technol.*, 2006, **19**, 81.

157. K. Arimitsu and R. Endo, *Chem. Mater.*, 2013, **25**, 4461.

158. N. Feillée, M. De Fina, A. Ponche, C. Vaulot, S. Rigolet, L. Jacomine, H. Majjad, C. Ley and A. Chemtob, *J. Polym. Sci., Part A: Polym. Chem.*, 2017, **55**, 117.

159. W. Xi, H. Peng, A. Aguirre-Soto, C. J. Kloxin, J. W. Stansbury and C. N. Bowman, *Macromolecules*, 2014, **47**, 6159.

160. K. Arimitsu, K. Fukuda and N. Sakai, *Chem. Lett.*, 2014, **43**, 831.

161. J. Pinaud, T. K. H. Trinh, D. Sauvanier, E. Placet, S. Songsee, P. Lacroix-Desmazes, J.-M. Becht, B. Tarablsi, J. Lalevée, L. Pichavant, V. Heroguez and A. Chemtob, *Chem. Eur. J.*, 2018, **24**, 337.

162. X. Zhang, W. Xi, C. Wang, M. Podgórski and C. N. Bowman, *ACS Macro Lett.*, 2016, **5**, 229.

163. B. A. Chan, S. Xuan, M. Horton and D. Zhang, *Macromolecules*, 2016, **49**, 2002.

164. M. Eckert-Maksić, Z. Glasovac, P. Trošelj, A. Kütt, T. Rodima, I. Koppel and I. A. Koppel, *Eur. J. Org. Chem.*, 2008, **2008**, 5176.

165. J. F. Cameron and J. M. J. Fréchet, *J. Org. Chem.*, 1990, **55**, 5919.

166. J. A. Barltrop and P. Schofield, *Tetrahedron Lett.*, 1962, **3**, 697.

167. J. A. Barltrop, P. J. Plant and P. Schofiel, *Chem. Commun.*, 1966, **0**, 822.

168. A. Patchornik, B. Amit and R. B. Woodward, *J. Am. Chem. Soc.*, 1970, **92**, 6333.

169. A. Hasan, K.-P. Stengele, H. Giegrich, P. Cornwell, K. R. Isham, R. A. Sachleben, W. Pfleiderer and R. S. Foote, *Tetrahedron*, 1997, **53**, 4247.

170. H. Giegrich, S. Eisele-Bühler, C. Hermann, E. Kvasyuk, R. Charubala and W. Pfleiderer, *Nucleosides Nucleotides*, 1998, **17**, 1987.

171. N. Kretschy, A. K. Holik, V. Somoza, K. P. Stengele and M. M. Somoza, *Angew. Chem. Int. Ed.*, 2015, **54**, 8555.

172. T. Furuta, in *Dynamic Studies in Biology: Phototriggers, Photoswitches and Caged Biomolecules*, eds. M. Goeldner and R. Givens, Wiley-VCH, Weinheim, 2005, ch. 1, pp. 29.

173. R. S. Givens, M. Rubina and J. Wirz, *Photochem. Photobiol. Sci.*, 2012, **11**, 472.
174. R. S. Givens and B. Matuszewski, *J. Am. Chem. Soc.*, 1984, **106**, 6860.
175. T. Furuta, H. Torigai, T. Osawa and M. Iwamura, *Chem. Lett.*, 1993, **22**, 1179.
176. A. S. C. Fonseca, M. S. T. Gonçalves and S. P. G. Costa, *Tetrahedron*, 2007, **63**, 1353.
177. T. Furuta, S. S.-H. Wang, J. L. Dantzker, T. M. Dore, W. J. Bybee, E. M. Callaway, W. Denk and R. Y. Tsien, *Proc. Natl. Acad. Sci. U. S. A.*, 1999, **96**, 1193.
178. T. Furuta, T. Watanabe, S. Tanabe, J. Sakyo and C. Matsuba, *Org. Lett.*, 2007, **9**, 4717.
179. V. Hagen, J. Bendig, S. Frings, T. Eckardt, S. Helm, D. Reuter and U. B. Kaupp, *Angew. Chem. Int. Ed.*, 2001, **40**, 1045.
180. R. Subramaniam, Y. Xiao, Y. Li, S. Y. Qian, W. Sun and S. Mallik, *Tetrahedron Lett.*, 2010, **51**, 529.
181. T. Furuta, in *Dynamic Studies in Biology: Phototriggers, Photoswitches and Caged Biomolecules*, eds. M. Goeldner and R. S. Givens, WILEY-VCH, Weinheim, 2005, ch. 1, pp. 29.
182. Y. Kaneko, A. M. Sarker and D. C. Neckers, *Chem. Mater.*, 1999, **11**, 170.
183. H. Tachi, M. Shirai and M. Tsunooka, *J. Photopolym. Sci. Technol.*, 2000, **13**, 153.
184. H. Tachi and M. Tsunooka, *J. Photopolym. Sci. Technol.*, 1999, **12**, 313.
185. H. Tachi, M. Shirai and M. Tsunooka, *J. Photopolym. Sci. Technol.*, 2000, **13**, 153.
186. M. Tsunooka, H. Tachi, T. Yamamoto, K. Akitomo and M. Shirai, *J. Photopolym. Sci. Technol.*, 2001, **14**, 153.
187. M. Tsunooka, T. Yamamoto, Y. Kurokawa, K. Suyama and M. Shirai, *J. Photopolym. Sci. Technol.*, 2002, **15**, 47.
188. K. Suyama, K. Fuke, M. Shirai and M. Tusnooka, *J. Photopolym. Sci. Technol.*, 2003, **16**, 83.
189. K. Suyama, K. Fuke and M. Shirai, *J. Photopolym. Sci. Technol.*, 2004, **17**, 15.
190. K. Arimitsu, A. Kushima and R. Endo, *J. Photopolym. Sci. Technol.*, 2009, **22**, 663.

191. J. A. Blake, E. Gagnon, M. Lukeman and J. C. Scaiano, *Org. Lett.*, 2006, **8**, 1057.
192. X. Dong, P. Hu, G. Zhu, Z. Li, R. Liu and X. Liu, *RSC Adv.*, 2015, **5**, 53342.
193. D. S. Esen, G. Temel, D. K. Balta, X. Allonas and N. Arsu, *Photochem. Photobiol.*, 2014, **90**, 463.
194. Z. Li, W. Shen, X. Liu and R. Liu, *Polym. Chem.*, 2017, **8**, 1579.
195. M. Aydin, N. Arsu and Y. Yagci, *Macromol. Rapid Commun.*, 2003, **24**, 718.
196. H. Salmi, X. Allonas, C. Ley, D. Maréchal and A. Ak., *J. Photopolym. Sci. Technol.*, 2012, **25**, 147.
197. H. Salmi, X. Allonas, C. Ley, A. Defoin and A. Ak, *Polym. Chem.*, 2014, **5**, 6577.
198. A. Defoins, R. Defoin-Straatmann, K. Hildenbrand, E. Bittersmann, D. Kreft and H. J. Kuhn, *J. Photochem.*, 1986, **33**, 237.
199. H. Görner, A. G. Griesbeck, T. Heinrich, W. Kramer and M. Oelgemöller, *Chem. Eur. J.*, 2001, **7**, 1530.
200. M. He, G. Chen, X. Huang, R. Xu, Z. Zeng and J. Yang, *Polym. Chem.*, 2014, **5**, 2951.
201. M. Bouzrati-Zerelli, M. Frigoli, F. Dumur, B. Graff, J. P. Fouassier and J. Lalevée, *Polymer*, 2017, **124**, 151.
202. G. Becker and F. R. Wurm, *Chem. Soc. Rev.*, 2018, **47**, 7739.
203. *Functional Polymers by Post-Polymerization Modification: Concepts, Guidelines, and Applications*, Wiley-VCH, Weinheim, 2013.
204. C. Jérôme and P. Lecomte, *Adv. Drug Deliv. Rev.*, 2008, **60**, 1056.
205. Y. Dai, X. Zhang and F. Xia, *Macromol. Rapid Commun.*, 2017, **38**, 1700357.
206. H. Seyednejad, A. H. Ghassemi, C. F. van Nostrum, T. Vermonden and W. E. Hennink, *J. Control. Release*, 2011, **152**, 168.
207. C. H. Jones, C. K. Chen, M. Chen, A. Ravikrishnan, H. Zhang, A. Gollakota, T. Chung, C. Cheng and B. A. Pfeifer, *Mol. Pharm.*, 2015, **12**, 846.
208. E. M. Pelegri-O'Day, S. J. Paluck and H. D. Maynard, *J. Am. Chem. Soc.*, 2017, **139**, 1145.
209. S. Tempelaar, L. Mespouille, P. Dubois and A. P. Dove, *Macromolecules*, 2011, **44**, 2084.
210. A. Y. Yuen, A. Bossion, A. Veloso, D. Mecerreyes, J. L. Hedrick, A. P. Dove and H. Sardon, *Polym. Chem.*, 2018, **9**, 2458.

211. J. Rieger, K. Van Butsele, P. Lecomte, C. Detrembleur, R. Jérôme and C. Jérôme, *Chem. Commun.*, 2005, **0**, 274.

212. W. Chen, H. Yang, R. Wang, R. Cheng, F. Meng, W. Wei and Z. Zhong, *Macromolecules*, 2010, **43**, 201.

213. S. Li, F. Meng, Z. Wang, Y. Zhong, M. Zheng, H. Liu and Z. Zhong, *Eur. J. Pharm. Biopharm.*, 2012, **82**, 103.

214. R. Wang, W. Chen, F. Meng, R. Cheng, C. Deng, J. Feijen and Z. Zhong, *Macromolecules*, 2011, **44**, 6009.

215. M. Leemhuis, N. Akeroyd, J. A. W. Kruijtzer, C. F. van Nostrum and W. E. Hennink, *Eur. Polym. J.*, 2008, **44**, 308.

216. J. R. Lowe, M. T. Martello, W. B. Tolman and M. A. Hillmyer, *Polym. Chem.*, 2011, **2**, 702.

217. A. E. van der Ende, E. J. Kravitz and E. Harth, *J. Am. Chem. Soc.*, 2008, **130**, 8706.

218. T. Jiang, Y. M. Li, Y. Lv, Y. J. Cheng, F. He and R. X. Zhuo, *Colloids Surf., B*, 2013, **111**, 542.

219. K. R. D. Chiaie, L. M. Yablon, A. B. Biernesser, G. R. Michalowski, A. W. Sudyn and J. A. Byers, *Polym. Chem.*, 2016, **7**, 4675.

220. F. Sinclair, L. Chen, B. W. Greenland and M. P. Shaver, *Macromolecules*, 2016, **49**, 6826.

221. A. W. Thomas and A. P. Dove, *Macromol. Biosci.*, 2016, **16**, 1762.

222. A. W. Thomas, P. K. Kuroishi, M. M. Pérez-Madrigal, A. K. Whittaker and A. P. Dove, *Polymer Chemistry*, 2017, **8**, 5082.

223. X.-Q. Liu, Z.-C. Li, F.-S. Du and F.-M. Li, *Macromol. Rapid Commun.*, 1999, **474**, 470.

224. C. Detrembleur, M. Mazza, X. Lou, O. Halleux, P. Lecomte, D. Mecerreyes, J. L. Hedrick and R. Jérôme, *Macromolecules*, 2000, **33**, 7751.

225. F. Nederberg, Y. Zhang, J. P. K. Tan, K. Xu, H. Wang, C. Yang, S. Gao, X. D. Guo, K. Fukushima, L. Li, J. L. Hedrick and Y.-Y. Yang, *Nat. Chem.*, 2011, **3**, 409.

226. W. Chin, C. Yang, V. W. L. Ng, Y. Huang, J. Cheng, Y. W. Tong, D. J. Coady, W. Fan, J. L. Hedrick and Y. Y. Yang, *Macromolecules*, 2013, **46**, 8797.

227. V. W. L. Ng, J. P. K. Tan, J. Leong, Z. X. Voo, J. L. Hedrick and Y. Y. Yang, *Macromolecules*, 2014, **47**, 1285.

228. R. Riva, S. Schmeits, C. Jérôme, R. Jérôme and P. Lecomte, *Macromolecules*, 2007, **40**, 796.

229. N. Xu, R. Wang, F.-S. Du and Z.-C. Li, *J. Polym. Sci., Part A: Polym. Chem.*, 2009, **47**, 3583.

230. P. P. Kalelkar, G. R. Alas and D. M. Collard, *Macromolecules*, 2016, **49**, 2609.

231. S. Lenoir, R. Riva, X. Lou, C. Detrembleur, R. Jérôme and P. Lecomte, *Macromolecules*, 2004, **37**, 4055.

232. P. Bexis, A. W. Thomas, C. A. Bell and A. P. Dove, *Polym. Chem.*, 2016, **7**, 7126.

Chapter 2

Synthesis and Post-Polymerisation Modification of an Epoxy-Functionalised Polycarbonate

2.1 Introduction

Inserting functional groups on the side chain of polymers is crucial to tune their physicochemical and biological properties, and therefore provide specific interactions with cells or organs.[1] To this end, post-polymerisation modification is a practical method to prepare functional polymers from a single monomer providing that a versatile and reactive side group possesses orthogonal reactivity to the polymerisable group. This approach is advantageous over a pre-polymerisation functionalisation methodology as it no longer requires optimisation of the polymerisation conditions (*e.g.* solvents, catalysts) for each one of the differently substituted monomers.[2] In addition, functionalities that are incompatible with the polymerisation conditions can be incorporated after the polymerisation step, thus avoiding the use of protecting groups that would increase the number of synthetic steps.[3,4]

Regarding the pendent groups, epoxides have been utilised in the post-polymerisation modification of polymers as a consequence of their chemical versatility. Indeed, the high reactivity of this group is originated from the polarisation of the C-O bond and the strain of the three-membered ring that enables ring-opening reactions with a range of nucleophiles.[5] Specifically, reports in this area have mainly focused on the functionalisation of poly(glycidyl(meth)acrylate)s (PG(M)As) *via* epoxy ring-opening by amines,[6,7] thiols,[8,9] and azides[8,10] However, few studies on the modification of biodegradable polymers bearing pendent epoxy groups have been reported thus far.[11-17] Wang *et al.*, for example, prepared an allyl-functionalised aliphatic polycarbonate *via* ring-opening polymerisation (ROP) and further explored the post-polymerisation modification by epoxidising the pendent allyl group.[11] The epoxide groups could then be reacted with low molecular weight polyethylenimines *via* an epoxide-amine reaction, which formed polycations with potential application in gene delivery. This strategy enabled a straightforward insertion of amine groups, which are highly incompatible with the ROP conditions, into the polymer without requiring any protection steps. Similarly, Harth and coworkers introduced epoxide groups in both polyesters and polycarbonates side chains, which allowed the preparation of degradable nanoparticles of controllable size by varying the amount of diamine crosslinker or the percentage of epoxide groups present in the polymer.[14-16]
In addition, Yan and Siegwart described the functionalisation of a polyester (prepared by polycondensation) containing epoxy side groups that were introduced after the

polymerisation step and further opened by a series of amines to provide functional polymers.[17]

Herein, we investigate an alternative strategy to obtain an epoxy-functionalised polycarbonate *via* the selective carbonate ROP of a carbonate monomer bearing an epoxide group. The pendent epoxide functionality is then envisioned to allow further modifications of the polymer through post-polymerisation reactions. This approach would avoid the extensive manipulation of a polymer that contains a labile backbone (*i.e.* polycarbonate) and therefore is expected to be more robust than the epoxidation of the alkene pendent functionality, considering that side reactions were shown to occur when the conditions were not carefully optimised.[18,19] Hence, we aim to expand the library of functional biodegradable polymers with tuneable properties that can potentially incorporate compounds that are incompatible with ROP.

2.2 Results and Discussion

The monomer trimethylenepropane oxirane ether carbonate (TMOC) (**2.1**) was synthesised in 2 steps from the commercially available trimethylolpropane allyl ether (**2.2**), as described previously (Scheme 2.1).[20] Firstly, the allyl-functionalised diol was ring-closed with ethyl chloroformate in the presence of triethylamine to form compound **2.3**, followed by the epoxidation of the allyl group using *meta*-chloroperbenzoic acid (mCPBA). The resultant product was then purified by column chromatography to provide TMOC monomer in 62% overall yield.

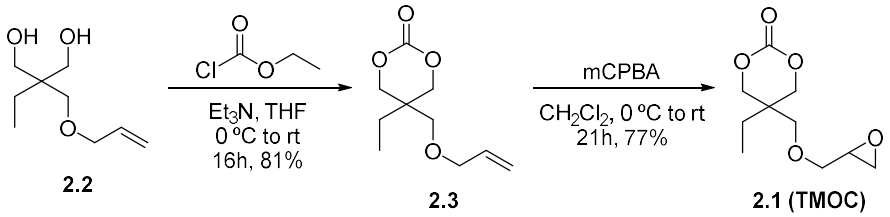

Scheme 2.1. Synthesis of TMOC (**2.1**).

Analysis of the product by ^{1}H NMR spectroscopy showed the characteristic peaks of the epoxide group at δ = 3.09, 2.76 and 2.55 ppm, and the methylene signals of the cyclic carbonate functionality at δ = 4.30 and 4.11 ppm (Figure 2.1a).[20] In addition, the ^{13}C NMR spectrum displayed the signals expected for the desired monomer, including the carbonyl carbon at δ = 148.6 ppm (Figure 2.1b). Then, the monomer was

dried over calcium hydride in CH_2Cl_2 for 2 days. After removing the drying agent by cannula filtration and evaporating the solvent under reduced pressure, the monomer was transferred to a glovebox to carry out the polymerisation studies.

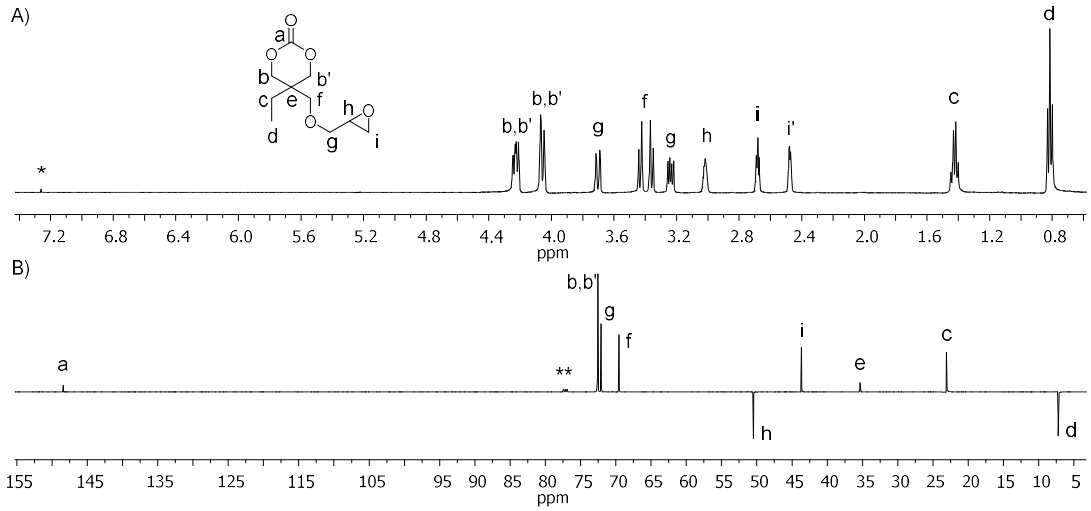

Figure 2.1. A) ^{1}H (500 MHz) and B) ^{13}C APT NMR (125 MHz) spectra of TMOC ($CDCl_3$, 298 K, * = $CHCl_3$, ** = $CDCl_3$).

2.2.2 Ring-Opening Polymerisation of TMOC

The polymerisation conditions for the TMOC monomer had been previously investigated in our group.[21] In those studies, several catalysts were investigated for the ROP of TMOC (Figure 2.2, Table 2.1): i) 1,8-diazabicyclo[5.4.0]undec-7-ene (DBU), ii) a catalyst system composed of DBU and 1-(3,5-bis(trifuoromethyl)phenyl)-3-cyclohexylthiourea (TU), and iii) 1,5,7-triazabicyclo[4.4.0]dec-5-ene (TBD). While DBU and DBU/TU provided a good polymerisation control, TBD was found to be more active, although a 5 mol% catalyst loading resulted in polymers with broad dispersity. The decrease of TBD loading to 1 mol% provided enhanced polymerisation control, producing polymers with low dispersity whilst retaining the epoxy unit. A monomer conversion of around 70% was obtained in less than 20 minutes for an initial monomer-to-initiator concentration ratio ($[M]_0/[I]_0$) of 20, with no substantial changes at prolonged polymerisation times.

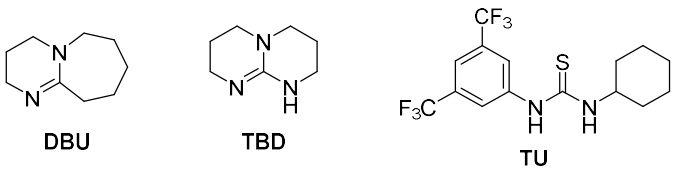

Figure 2.2. Organocatalysts investigated for the ROP of TMOC.

Table 2.1. Catalyst screening for the ROP of TMOC.[21,a]

Entry	Cat. (%)	Time	Monomer conversion[b] (%)	DP[b]	M_n[b] (kg mol^{-1})	M_n[c] (kg mol^{-1})	$Đ_M$[c]
1	DBU (5)	49 h	73	16	3.6	3.0	1.2
2	DBU/ TU (5:5)	22 h	73	17	3.8	2.8	1.3
3	TBD (5)	< 20 min	74	16	3.6	2.9	2.0
4	TBD (1)	< 20 min	72	19	4.2	4.1	1.2

[a] Reactions were carried out in $CDCl_3$ at room temperature with $[M]_0/[I]_0 = 20$ and $[M]_0 = 1.0$ M, using 4-methoxybenzyl alcohol as the initiator. [b] Determined by ^{1}H NMR spectroscopy. [c] Determined by SEC analysis in $CHCl_3$ calibrated against polystyrene standards.

Considering these previous results, our studies towards the polymerisation of TMOC comprised the use of 1 mol% of TBD related to monomer as the catalyst and an initial monomer concentration of 1.0 M in $CDCl_3$ using either 4-methoxybenzyl alcohol or 1,4-benzenedimethanol (1,4-BDM) as initiator (Scheme 2.2). The reaction progress was monitored by ^{1}H NMR spectroscopy, where the monomer conversion was determined by the disappearance of the multiplets that correspond to the methylene resonances of the carbonate monomer at $\delta = 4.33$ and 3.80 ppm, and the appearance of a singlet at $\delta = 4.10$ ppm for the methylene protons resonance on the polycarbonate backbone (Figure 2.3). The polymerisation was quenched by adding benzoic acid in excess since acidic Amberlyst resin, which is more easily removed

from the reaction mixture, decomposed the polymer. Purification by column chromatography using diethyl ether allowed the removal of residual monomer, followed by ethyl acetate as eluent to recover the pure polymer. As determined by size exclusion chromatography (SEC), PTMOC (**2.4**) showed a monomodal distribution with a number-average molecular weight (M_n) of 7.9 kg mol^{-1} and a dispersity value ($Đ_M$) of 1.2 (Figure 2.4).

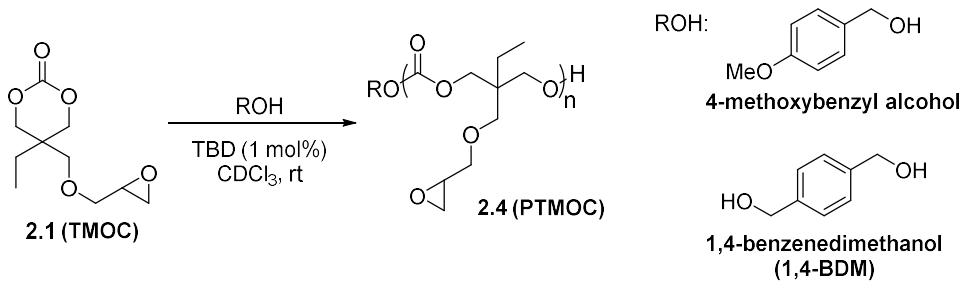

Scheme 2.2. Polymerisation of TMOC (**2.1**).

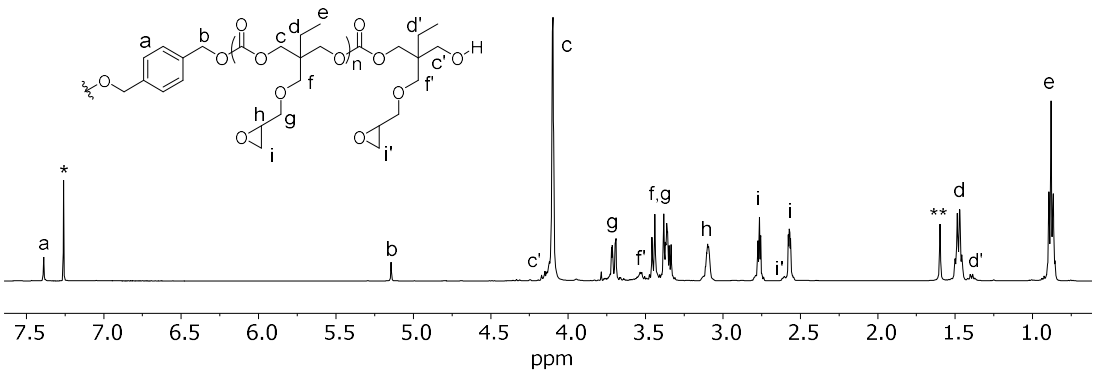

Figure 2.3. ^{1}H NMR spectrum of PTMOC (**2.1**) ($CDCl_3$, 500 MHz, 298 K, * = $CHCl_3$, ** = H_2O). Conditions: $[M]_0$ = 1 M, $[M]_0/[I]_0/[cat]_0$ = 50:1:0.5 using TBD as catalyst and 1,4-BDM as initiator.

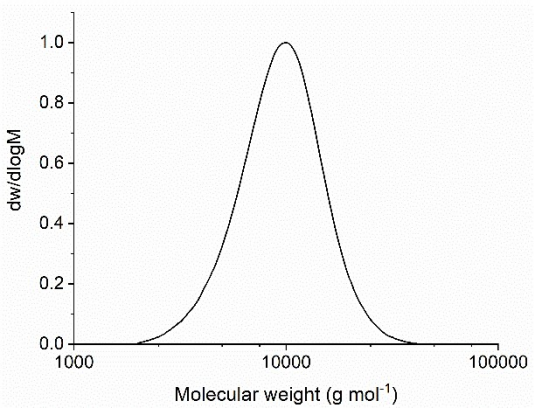

Figure 2.4. Size exclusion chromatogram of PTMOC (M_n = 7.9 kg mol^{-1} and $Đ_M$ = 1.2) ($CHCl_3$, RI, calibrated against polystyrene standards). Conditions: $[M]_0$ = 1 M, $[M]_0/[I]_0/[cat]_0$ = 50:1:0.5 using TBD as catalyst and 1,4-BDM as initiator.

The preservation of the epoxy functionality after the polymerisation of TMOC was confirmed by ^{1}H NMR spectroscopy. The characteristic signals for this group were observed at δ = 3.08, 2.76, and 2.57 ppm, whilst the signals at δ = 7.38 and 5.13 ppm originated from the initiator 1,4-BDM evidenced the end-group fidelity (Figure 2.3). Further analysis by matrix-assisted laser desorption/ionisation time-of-flight mass spectrometry (MALDI-ToF MS) showed the main distribution with a spacing of 216.1 *m*/*z* that corresponds to the monomer unit and a distribution that is assigned to sodium-charged PTMOC initiated from 1,4-BDM (Figure 2.5), which corroborated the results obtained by ^{1}H NMR spectroscopy.

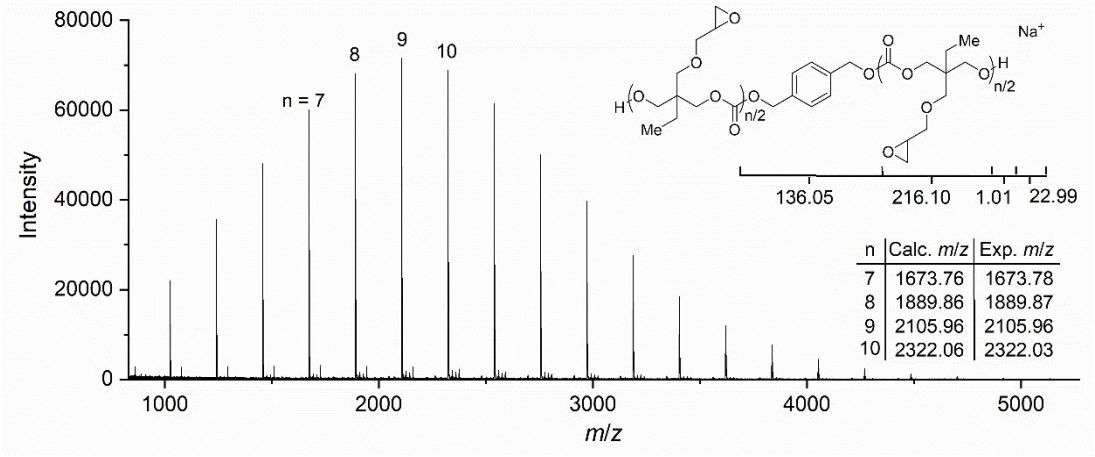

Figure 2.5. MALDI-ToF MS of PTMOC. Conditions: $[M]_0$ = 1 M, $[M]_0/[I]_0/[cat]_0$ = 10:1:0.1, using TBD as catalyst and 1,4-BDM as initiator.

The living characteristics of the polymerisation of TMOC were evidenced by the linear increase of the M_n against monomer conversion while maintaining a narrow and monomodal distribution throughout the polymerisation (Figure 2.6). In addition, a linear relationship between M_n and the degree of polymerisation was observed, which allowed the preparation of polymers with predictable molecular weights according to $[M]_0/[I]_0$ (Figure 2.7). Overall, these data demonstrate the controlled nature of this polymerisation system.

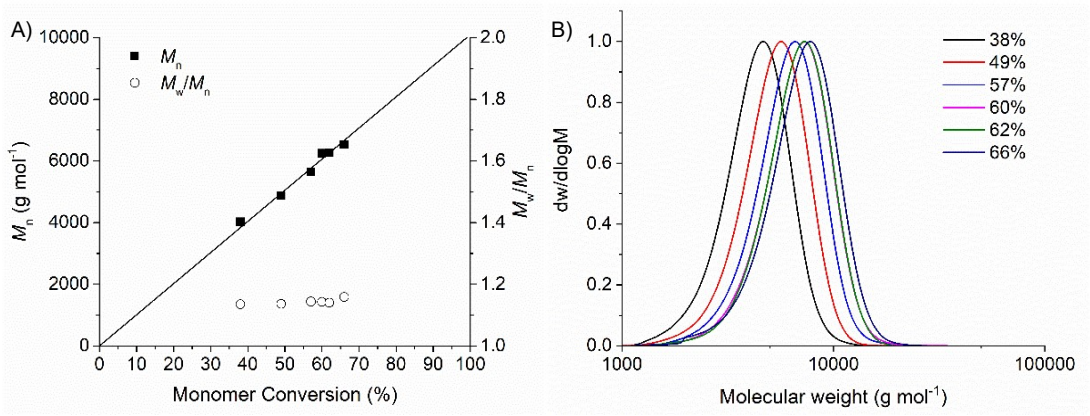

Figure 2.6. A) Number-average molecular weight (M_n; ■) and dispersity ($Đ_M$ = M_w/M_n; ○) against monomer conversion and B) evolution of size exclusion chromatograms of PMTOC with the monomer conversion ($CHCl_3$, RI, calibrated against polystyrene standards). Conditions: $[M]_0$ = 1 M, $[M]_0/[I]_0/[cat]_0$ = 140:1:1.4 using TBD as catalyst and 1,4-BDM as initiator.

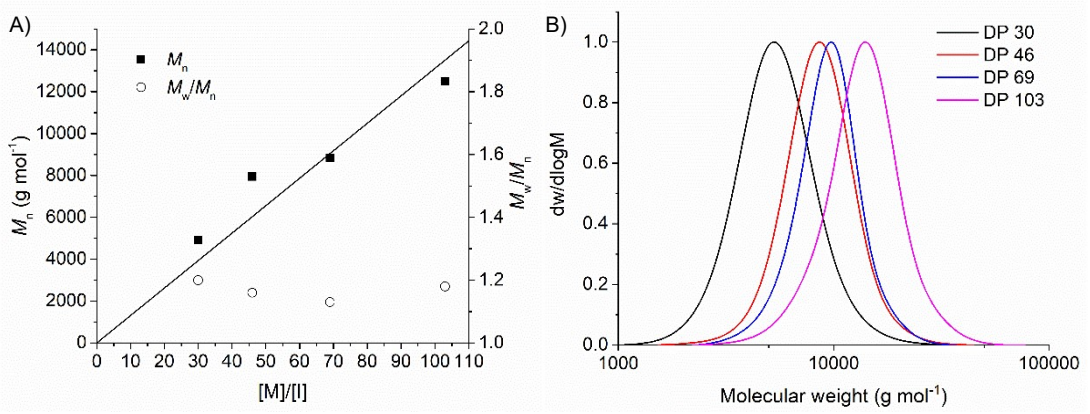

Figure 2.7. A) Number-average molecular weight (M_n; ■) and dispersity ($Đ_M$ = M_w/M_n; ○) against monomer-to-initiator concentration ratio ([M]/[I]) and B) evolution of size exclusion chromatograms of PTMOC with DPs varying from 30 to 103 (DMF, LS). Conditions: $[M]_0$ = 1 M, using 1 mol% TBD and 1,4-BDM as initiator.

2.2.3 Post-Polymerisation Functionalisation of PTMOC with Amines

After demonstrating the preparation of well-defined epoxy-functionalised polycarbonates, the post-polymerisation modification of PTMOC with amines was investigated as a route to incorporate functional groups incompatible with the polymerisation methodology. The aminolysis of epoxides in small molecules typically involves the use of high temperatures or pressure.[22-24] As an alternative, several Lewis acids have been previously investigated in order to activate the epoxide ring and, therefore, promote the reaction under mild conditions.[25,26]

In our preliminary studies, a range of Lewis acid catalysts (lithium bromide, calcium triflate, montmorillonite, scandium(III) triflate, silica gel) previously applied for non-polymeric systems was investigated in the post-polymerisation functionalisation of PTMOC with benzylamine as a model compound to form PTMOC-amine (**2.5**) (Scheme 2.3).[27-30] Most of these reactions reported were carried out under solvent-free conditions; however, acetonitrile was used as a solvent in our studies as a consequence of the high viscosity of PTMOC. In addition, an excess amine (5 equivalents) was utilised, which has been shown to avoid the incidence of crosslinking that is caused when the secondary amine formed after ring-opening the epoxide reacts with a further epoxy ring to create a polymer network (Scheme 2.4).[7]

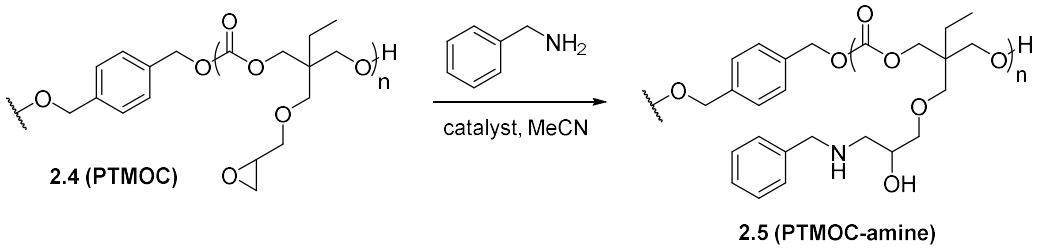

Scheme 2.3. Functionalisation of PTMOC with benzylamine.

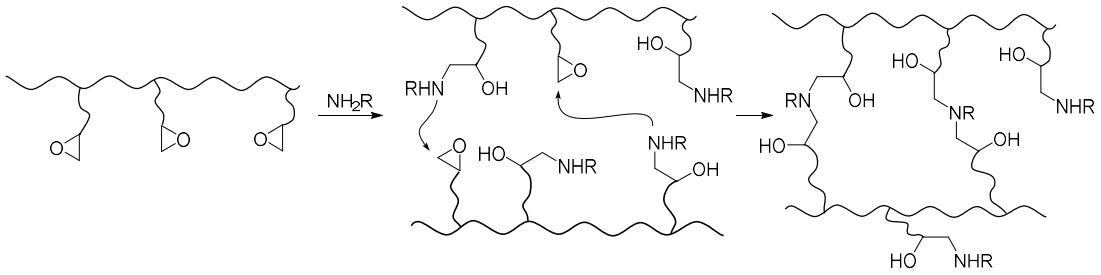

Scheme 2.4. Possible formation of a network during the modification of an epoxy-functionalised polymer with primary amines.

Firstly, the functionalisation was carried out with benzylamine as a model over 24 hours at room temperature varying the type and amount of catalyst (LiBr (20 mol%), $Ca(OTf)_2$ (50 mol%), montmorillonite K10 (10 wt%), $Sc(OTf)_3$ (5 mol%)). For all catalysts, over 95% conversion was achieved as evidenced by the disappearance of the epoxide signals at δ = 2.57, 2.76 and 3.09 ppm in the ^{1}H NMR spectra (Figure 2.8). However, the appearance of signals at δ = 4.3 ppm, as well as the broadening of the peaks corresponding to the polymer, indicated that side reactions were occurring during the functionalisation. Further analysis of the resultant polymers by SEC showed distributions with molecular weight lower than the initial polymer (Figure 2.9). These data indicated a degradation of the polymer, which was promoted by the presence of Lewis acid catalyst that not only was activating the epoxide but also interacting with the carbonyl in the polymer backbone and, therefore, facilitating the attack of the amine on that carbon. Furthermore, the attempt to functionalise PTMOC with benzylamine using silica gel as catalyst resulted in an insoluble solid, which suggests that the polymer had undergone a significant degree of crosslinking.

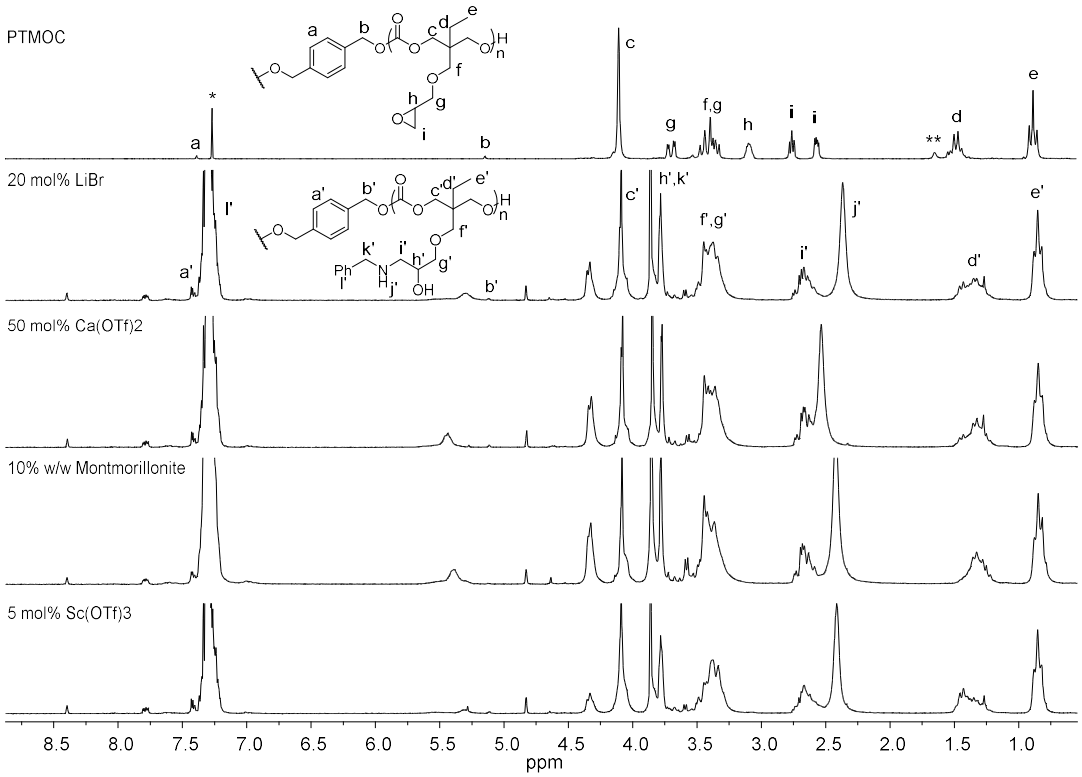

Figure 2.8. ^{1}H NMR spectra of PTMOC modified with benzylamine applying different catalysts ($CDCl_3$, 250 MHz, 298 K, * = $CHCl_3$, ** = H_2O).

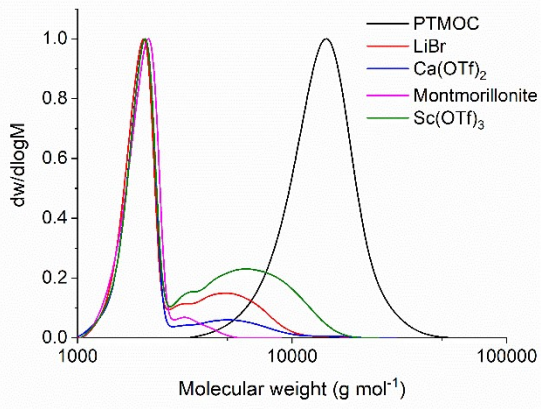

Figure 2.9. Size exclusion chromatograms of PTMOC before and after post-polymerisation functionalisation with benzylamine using different catalysts (LiBr: M_n = 2.2 kg mol^{-1}, $Đ_M$ = 1.3; $Ca(OTf)_2$: M_n = 2.1 kg mol^{-1}, $Đ_M$ = 1.2; montmorillonite: M_n = 2.0 kg mol^{-1}, $Đ_M$ = 1.1; $Sc(OTf)_3$: M_n = 2.6 kg mol^{-1}, $Đ_M$ = 1.5) (DMF, RI, calibrated against poly(methyl methacrylate) standards).

Alternatively, the functionalisation of PTMOC was performed at elevated temperatures in the absence of a catalyst. However, after heating a solution of PTMOC

and benzylamine (or hexylamine) in acetonitrile at 50 °C for 6 hours, a solid that was insoluble in several organic solvents and water was obtained. Less basic or bulkier amines, such as aniline or diisopropylamine, were tested under these conditions but no conversion was observed during the same period. Finally, the use of DMSO as a solvent was investigated for the functionalisation with benzylamine with the reaction being performed for 24 hours at 70 °C. Analysis by ^{1}H NMR spectroscopy showed > 95% conversion, with the appearance of signals at δ = 7.2-7.3 ppm that correspond to the aromatic group of benzylamine and the carbinolic proton resonance at δ = 3.91 ppm, which indicates a successful functionalisation (Figure 2.10).

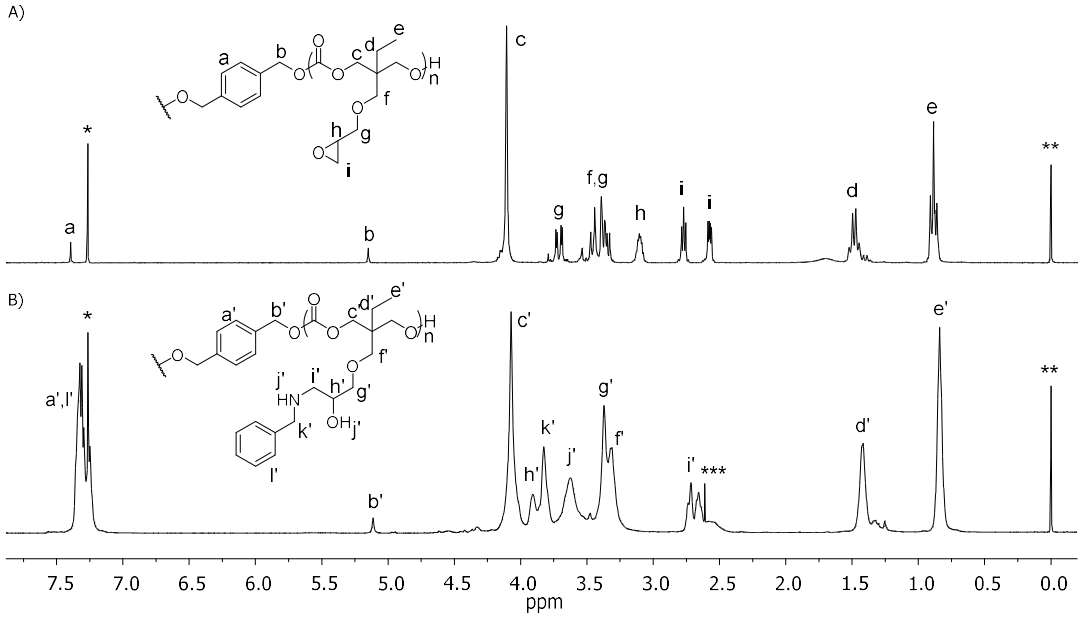

Figure 2.10. ^{1}H NMR spectra of PTMOC A) before and B) after post-polymerisation functionalisation with benzylamine ($CDCl_3$, 500 MHz, 298 K, * = $CHCl_3$, ** = TMS, *** = DMSO).

In addition, SEC analysis exhibited a shift to higher molecular weight (pre: M_n = 9.7 kg mol^{-1}, $Đ_M$ = 1.2, post: M_n = 11.4 kg mol^{-1}, $Đ_M$ = 1.18) although the low intensity recorded may also support the formation of crosslinked material that could be trapped in the filter used for the sample preparation (Figure 2.11). These reaction conditions were also applied for butylamine; however, the degradation of the polymer backbone was demonstrated by SEC analysis (Figure 2.11, M_n = 0.9 kg mol^{-1}; $Đ_M$ = 1.2)), whilst the reaction with diisopropylamine showed very low conversion (< 37%). Therefore, these results indicate that for less hindered aliphatic amines, the reaction takes place

in the carbonate moiety present in the polymer backbone, whereas the reaction rate decreases significantly by using bulkier amines as a consequence of the lower nucleophilicity caused by the high steric hindrance.

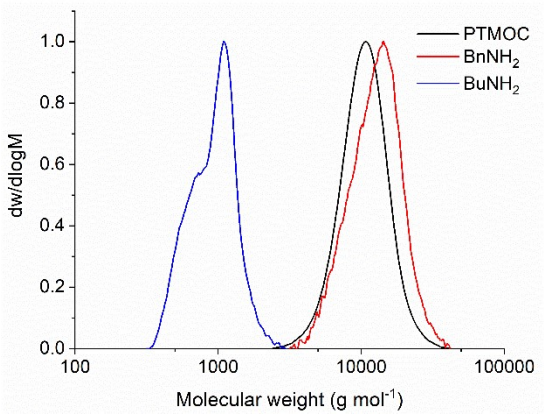

Figure 2.11. Size exclusion chromatograms of $PTMOC_{34}$ before and after post-polymerisation modification with benzylamine (M_n = 11.4 kg mol^{-1}, $Đ_M$ = 1.18) and with butylamine (M_n = 0.9 kg mol^{-1}; $Đ_M$ = 1.1) (DMF, RI, calibrated against poly(methyl methacrylate) standards).

2.2.3.1 Studies Towards the Functionalisation of PTMOC with Amino Acid Derivatives

The next studies comprised the modification of PTMOC with amino acid derivatives to broaden the library of functional groups that could lead to more complex compounds such as peptides. L-Phenylalanine was initially used as a model, with the acid group protected with methyl ester to avoid side reactions. As commercially available aminoesters are found as hydrochlorides, the amine was obtained after neutralisation with a saturated aqueous solution of $NaHCO_3$ prior to use. The functionalisation of PTMOC was attempted using freshly isolated aminoester; however, no disappearance of the epoxide group in the ^{1}H NMR spectrum was observed (data not shown). However, it must be noted that the isolated amine was not fully purified and characterised, which could be the reason of this negative outcome.

Previous studies by Jiang and coworkers described the synthesis of a hyperbranched polymer *via* the aminolysis of epoxides using a compound containing both functionalities of amine and epoxide.[31] The authors carried out the reaction starting from a hydrochloride amine, and the free amine was released in the reaction

medium by reacting with Et_3N (Scheme 2.5). Based on these studies, the functionalisation of PTMOC was investigated using L-phenylalanine methyl ester hydrochloride in the presence of Et_3N. Initially, the reaction was carried out using 2 equivalents of aminoester and 2.4 equivalents of Et_3N related to epoxide groups in DMSO at 70 °C. After 24 hours under these conditions, the reaction medium was diluted with EtOAc and washed with saturated aqueous solution of NH_4Cl to remove the excess amine and DMSO. Analysis of the resultant polymer by ^1H and ^{13}C NMR spectroscopy showed the disappearance of signals corresponding to the epoxide proton resonances, although no signals corresponding to the aminoester were observed (Figure 2.12 and Figure 2.13). The ^{13}C NMR spectrum displayed a shift of the signal corresponding to the methine carbon in the epoxide in PTMOC from δ = 50.9 to 70.3 ppm, which is in agreement with a chemical shift for the carbon after being ring-opened. In addition, the methylene carbon in the epoxy group shifted from δ = 44.1 to 45.9 ppm, signal that is compatible with a chemical shift of a carbon bonded to a nitrogen, although the absence of signals from the side chain of the aminoester was inconsistent with the desirable functionalisation.

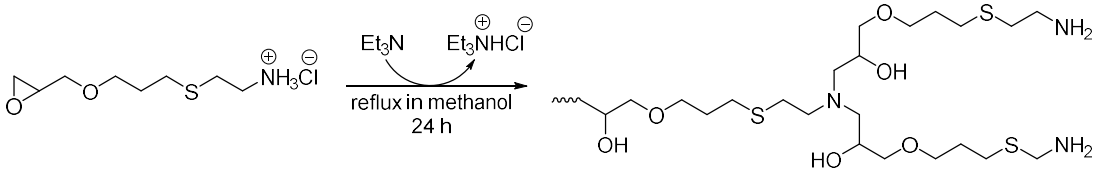

Scheme 2.5. Strategy for the synthesis of hyperbranched poly(thiol-ether amine) reported by Jiang and coworkers.[31]

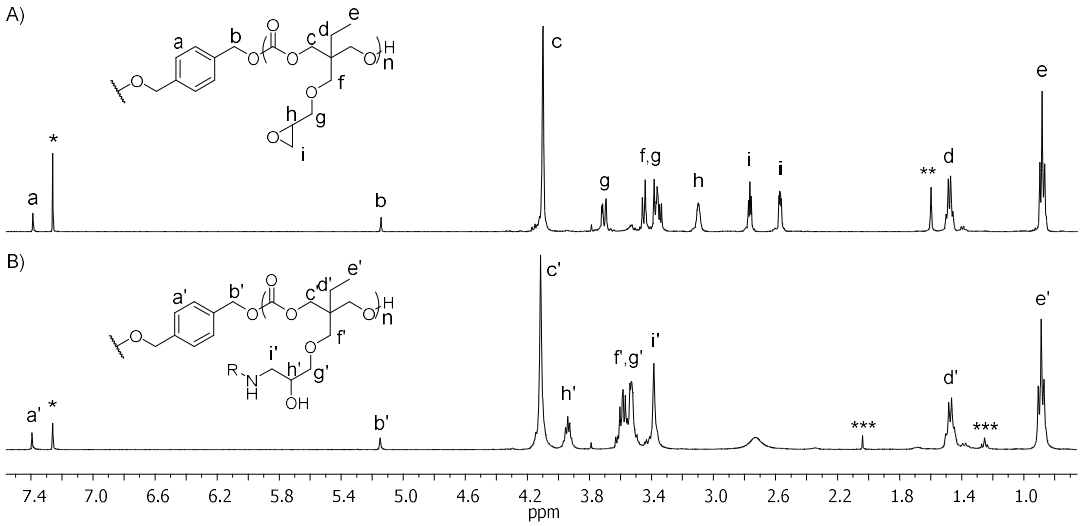

Figure 2.12. ^{1}H NMR spectra of PTMOC A) before (500 MHz) and B) after (400 MHz) functionalisation of PTMOC with L-phenylalanine methyl ester hydrochloride in the presence of Et_3N ($CDCl_3$, 298 K, * = $CHCl_3$, ** = H_2O, *** = EtOAc).

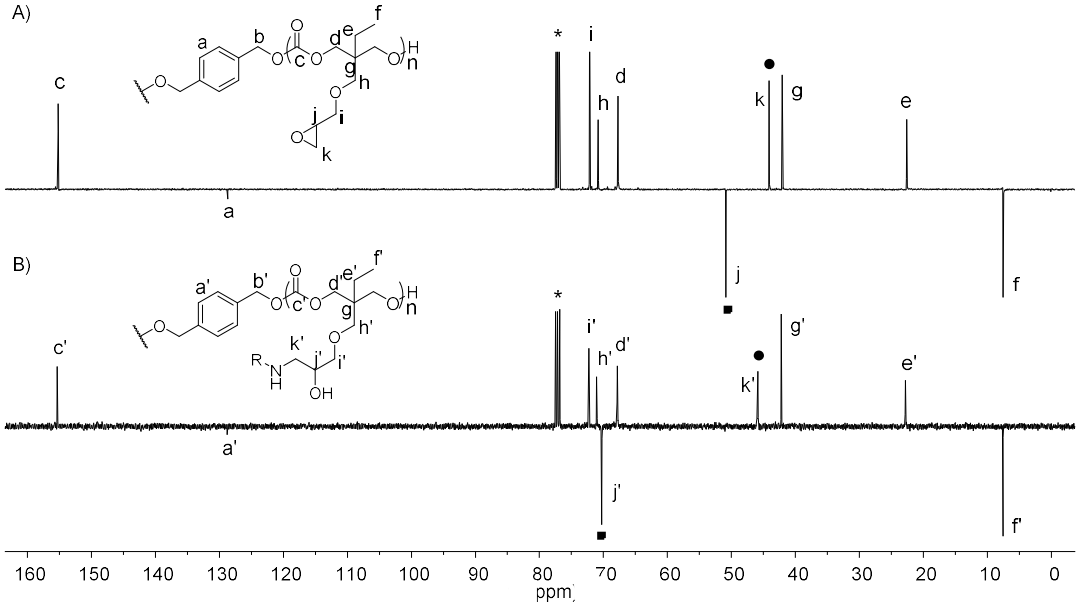

Figure 2.13. ^{13}C APT NMR spectra of PTMOC A) before (125 MHz) and B) after (100 MHz) functionalisation of PTMOC with L-phenylalanine methyl ester hydrochloride in the presence of Et_3N ($CDCl_3$, 298 K, * = $CDCl_3$).

Further analysis of the product by Fourier-transform infrared (FT-IR) spectroscopy showed the presence of a band at 729 cm^{-1} that corresponds to a C-Cl stretching, which indicated the functionalisation of PTMOC with chlorine (Figure 2.14). Elemental analysis showed a composition of 42.5% of carbon, 5.9% of

hydrogen and 16.3% chlorine (calculated for PTMOC-Cl, DP = 71, $C_{718}H_{1217}Cl_{71}O_{357}$: C, 47.7; H, 6.8; Cl, 13.9), which further confirmed the presence of chlorine in the polymer structure. The difference between the obtained values and the expected could be a consequence of the presence of trapped solvent in the viscous polymer that could not be removed. After identifying the presence of chlorine in the polymer structure, the signals in the ^{1}H and ^{13}C NMR spectra could be assigned (Figure 2.15). Further characterisation of PTMOC-Cl (**2.6**) by SEC showed an increase in the molecular weight, while the dispersity remained low (pre: M_n = 9.7 kg mol^{-1}, $Đ_M$ = 1.2; post: M_n = 12.5 kg mol^{-1}, $Đ_M$ = 1.16) (Figure 2.16).

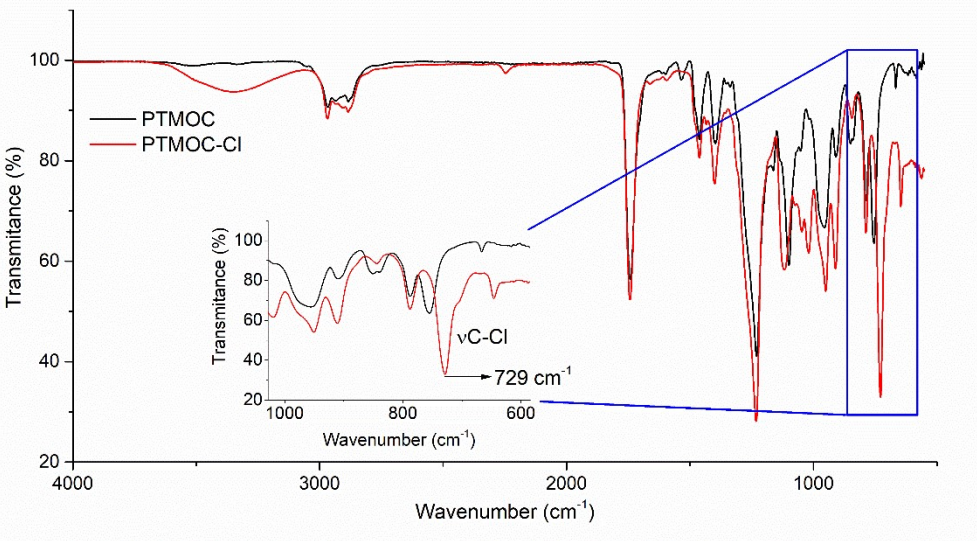

Figure 2.14. FT-IR spectrum of PTMOC (black) and PTMOC functionalised with L-phenylalanine methyl ester hydrochloride (PTMOC-Cl, **2.6**) in the presence of Et_3N (red).

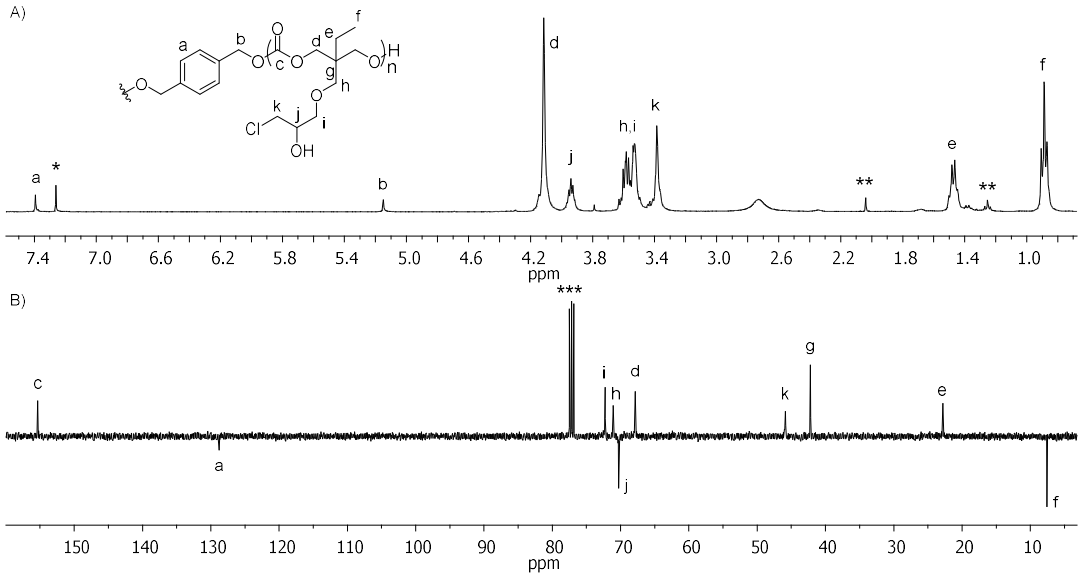

Figure 2.15. A) ^{1}H (400 MHz) and B) ^{13}C APT NMR (100 MHz) spectra of PTMOC-Cl (**2.6**) ($CDCl_3$, 298 K, *, $CHCl_3$, ** = EtOAc, *** = $CDCl_3$).

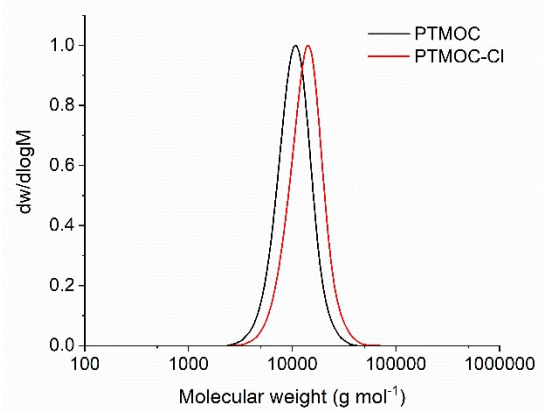

Figure 2.16. Size exclusion chromatograms of PTMOC before (M_n = 9.7 kg mol^{-1}, $Đ_M$ = 1.2) and after functionalisation with chorine (M_n = 12.5 kg mol^{-1}, $Đ_M$ = 1.16) (DMF, RI, calibrated against polystyrene standards).

The unexpected functionalisation of PTMOC with chlorine indicates the higher nucleophilicity of the chloride anion when compared to the amino acid derivatives under the conditions applied in these studies. In order to avoid this undesirable reaction, a more thorough neutralisation of the amines would be necessary, so that the presence of other nucleophiles would be eliminated. In addition, more nucleophilic amino acid derivatives (*e.g.* proline methyl ester) should be investigated to allow for a more efficient amine-epoxy reaction.[32]

2.2.3.2 Studies Towards the Quarternisation of PTMOC *via* Nucleophilic Substitution of PTMOC-halide

Although the use of a aminoester hydrochloride in the presence of Et_3N led to undesirable results, we considered using the chlorine-functionalised PTMOC to prepare quaternary ammonium derivatives by nucleophilic substitutions for antimicrobial applications.[33] Antimicrobial polymers consist of an amphiphilic structure, with the hydrophilic portion being composed of cationic functional groups that interact with the negatively charged microbial cell membrane.[34] The hydrophobic groups are then able to insert into the lipid layers, which leads to the disintegration of the cell membrane. This mechanism, which involves the disruption of the membrane, has no action in specific targets in the biosynthetic pathway of the microorganism; consequently, bacteria are less likely to develop resistance, which makes these polymers very promising antibiotic candidates.[35]

In our work, the quarternisation of PTMOC-Cl with a series of tertiary amines (*i.e.* pyridine, 4-dimethylaminopyridine (DMAP), 1-methylimidazole, 1-butylimidazole, and *N*,*N*-dimethylbutylamine) was investigated. Following a previously described procedure,[36] acetonitrile was used as a solvent, and the reaction was performed at 40 °C for 24 hours; however, no functionalisation was observed for any of these amines. Hedrick and coworkers have studied the quarternisation of haloalkyl-functionalised polycarbonates using aliphatic amines, pyridine and imidazole derivatives.[37] The reactions using the chloroalkyl-functionalised polymers were reported to be inefficient, yielding low functionalisation even at elevated temperatures (80 °C). Nevertheless, the authors observed higher activity for the bromoalkyl-functionalised polycarbonates, which were able to provide quarternisation at room temperature with more nucleophilic amines (*i.e.* trimethylamine and DMAP), whereas the less reactive ones (*i.e.* pyridine and imidazole derivatives) required higher temperatures (50 °C), which led to an undesirable fragmentation of the polymer.

Following these studies, the preparation of a bromine or iodine-functionalised PTMOC was investigated to insert better leaving groups into the polymer and, therefore, facilitate the functionalisation with tertiary amines. Firstly, either potassium iodide or tetrabutylammonium iodide (TBAI) was used to promote the epoxide ring-opening in PTMOC using DMSO as solvent at 70 °C. Both reactions showed low degrees of functionalisation after 24 hours, as evidenced by comparing the integration of the methylene signal of the polymer backbone at δ = 4.10 ppm and the epoxide signal at δ = 3.10 ppm (Figure 2.17). In addition, the appearance of a series of signals indicated the degradation of the polymer, which resulted from the competitive reactions between the nucleophilic attack of the iodide at the epoxide ring or the carbonyl group of the polycarbonate backbone.[37] Attempts to functionalise PTMOC with bromine using potassium bromide or tetrabutylammonium bromide (TBAB) provided similar results to those obtained for the iodide derivative, thus preventing the preparation of halide-functionalised polycarbonates using this strategy.

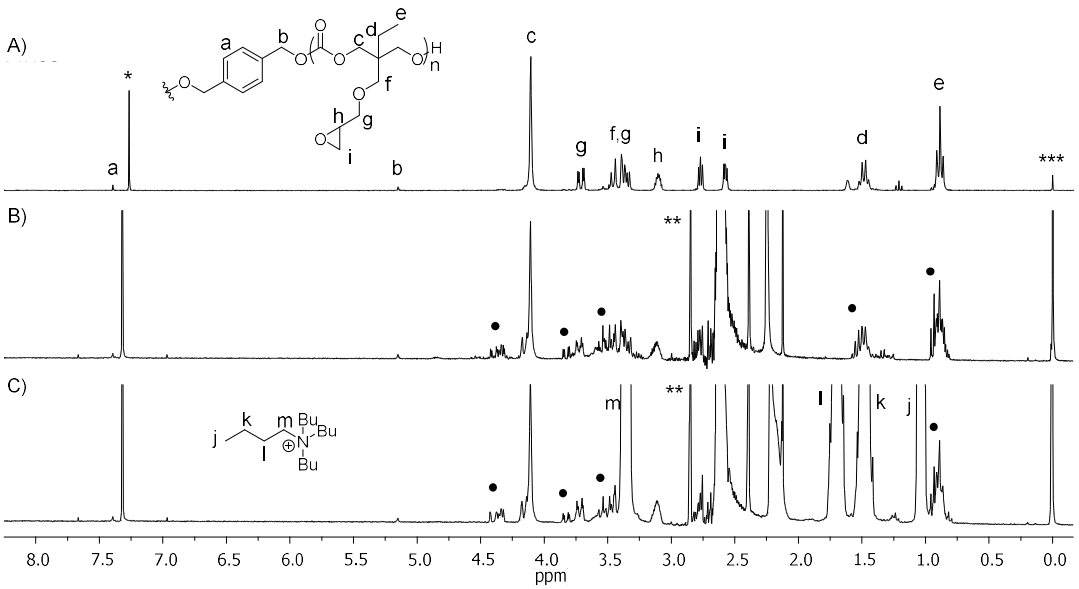

Figure 2.17. ^{1}H NMR spectra of A) PTMOC and crude reaction mixture of the functionalisation of PTMOC with B) KI and C) TBAI ($CDCl_3$, 300 MHz, 298 K, * = $CHCl_3$, ** = DMSO, *** = TMS, ● = degradation signals).

As the functionalisation of PTMOC with chlorine was achieved successfully by using Et_3NHCl, the corresponding hydroiodide, Et_3NHI, was applied to prepare the iodine-functionalised polycarbonate. The ^{1}H NMR spectrum of the resultant polymer

showed the disappearance of the epoxide signals at δ = 3.10, 2.77, and 1.57 ppm and the appearance of the signal at δ = 3.73 ppm corresponding to a proton resonance neighbouring a hydroxy group, which indicates that the epoxide ring was opened (Figure 2.18a). In addition, the ^{13}C NMR spectrum was consistent with the formation of the iodine-functionalised PTMOC, with the signal expected for a methylene carbon next to iodine at δ = 9.1 ppm (Figure 2.18b). SEC analysis of the product revealed a slight increase in the molecular weight when compared to original PTMOC, yet, with a high molecular weight shoulder (Figure 2.19, pre: M_n = 9.7 kg mol^{-1}, $Đ_M$ = 1.2; post: M_n = 11.1 kg mol^{-1}, $Đ_M$ = 1.32). In fact, an insoluble solid was obtained after the sample was maintained at room temperature for one day, which indicated that some crosslinking had occurred within the product. As iodide is a better leaving group than chloride, the hydroxyl group formed after opening the epoxide ring can react with the C-I bond from another polymer chain by nucleophilic substitution, which forms a crosslinked material (Scheme 2.6).

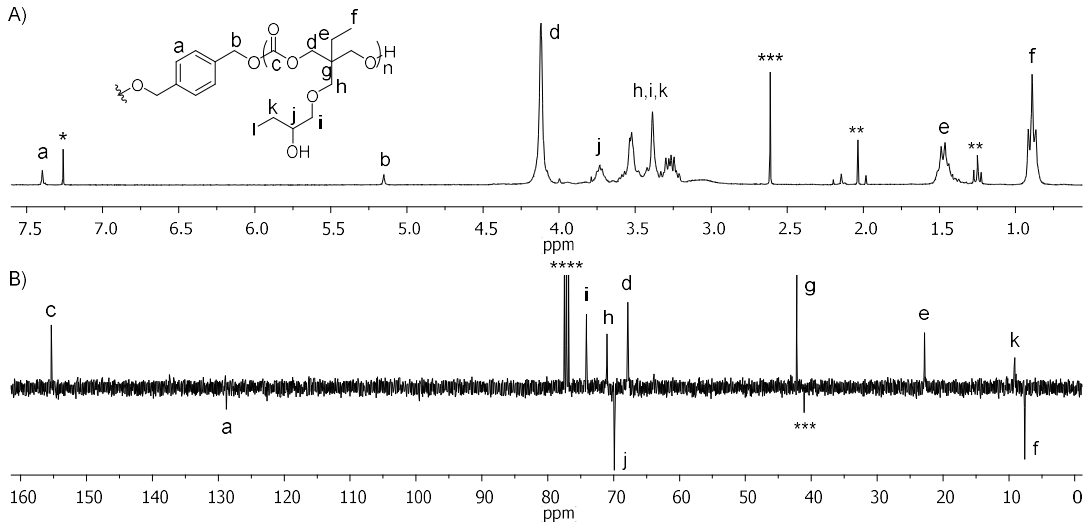

Figure 2.18. A) ^{1}H (300 MHz) and B) ^{13}C APT NMR (100 MHz) spectra of PTMOC functionalised with iodine ($CDCl_3$, 298 K, * = $CHCl_3$, ** = EtOAc, *** = DMSO, **** = $CDCl_3$).

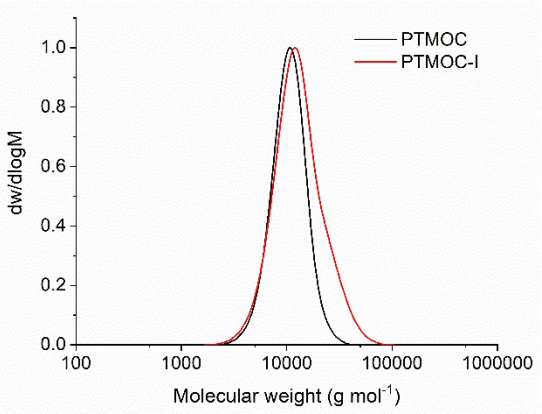

Figure 2.19. Size exclusion chromatogram of PTMOC before (M_n = 9.7 kg mol^{-1}, $Đ_M$ = 1.2) and after functionalisation using Et_3NHI (M_n = 11.1 kg mol^{-1}, $Đ_M$ = 1.32) (DMF, RI, calibrated against poly(methyl methacrylate) standards).

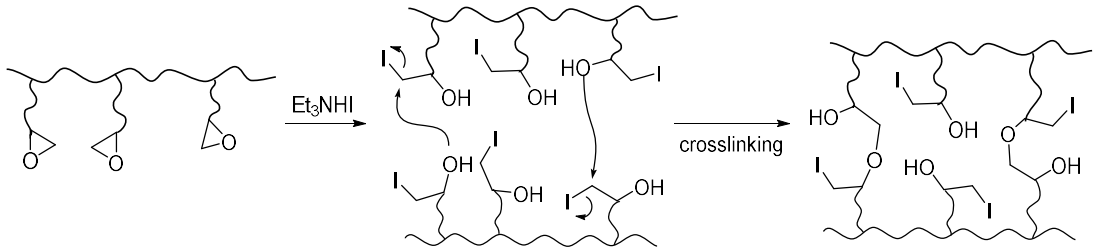

Scheme 2.6. Proposed formation of a network from the modification of the epoxide groups in PTMOC with iodine.

To avoid this undesirable crosslinking reaction, the quarternisation reaction was carried out by adding *N*,*N*-dimethylbutylamine immediately after the preparation of PTMOC-I. In addition, a second strategy was attempted, which comprised of a one-pot, two steps reaction where Et_3NHI and *N*,*N*-dimethylbutylamine were added at once into the reaction mixture with PTMOC. However, regardless of the approach followed, the ^{1}H NMR spectra of the resultant crude polymer showed a broadening in the signal at 4.1 ppm, which indicated a decomposition of the polymer backbone (Figure 2.20). This observation was confirmed by SEC analysis since the molecular weight distributions of the polymers were considerably lower than that displayed by the original PTMOC (Figure 2.21). Therefore, competitive nucleophilic reactions between the alkyl iodide and the carbonyl in the polymer backbone demonstrated the impracticality of this strategy to obtain quarternised polycarbonates. In addition, the presence of undesirable crosslinking reactions when using PTMOC-I, as well as the

complete inactivity of the corresponding chlorine-functionalised polymer evidenced the challenges in finding a suitable leaving group in terms of reactivity.

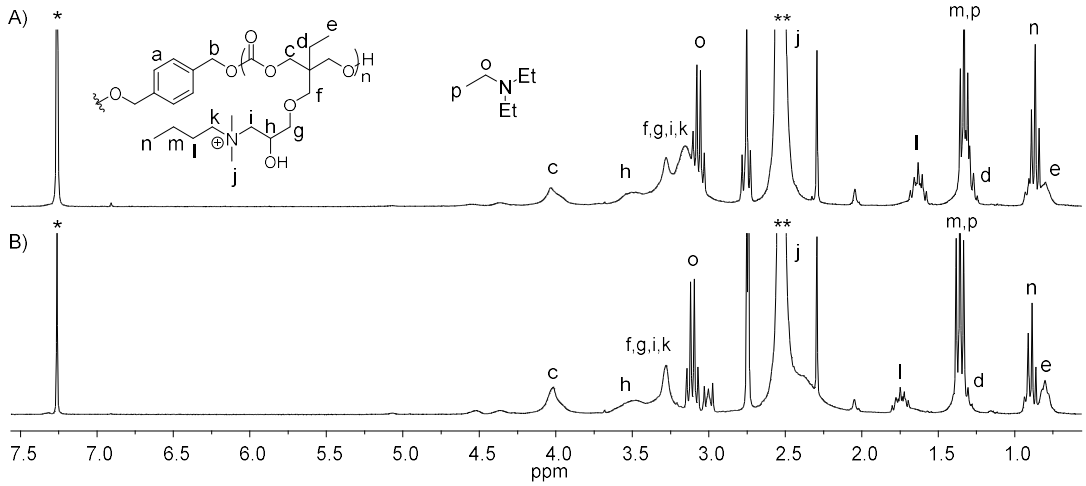

Figure 2.20. ^{1}H NMR spectra of crude reaction mixture of functionalisation of PTMOC with A) Et_3NHI followed by N,N-dimethylbutylamine and B) Et_3NHI and N,N-dimethylbutylamine in one-pot synthesis ($CDCl_3$, 300 MHz, 298 K, * = $CHCl_3$, ** = DMSO).

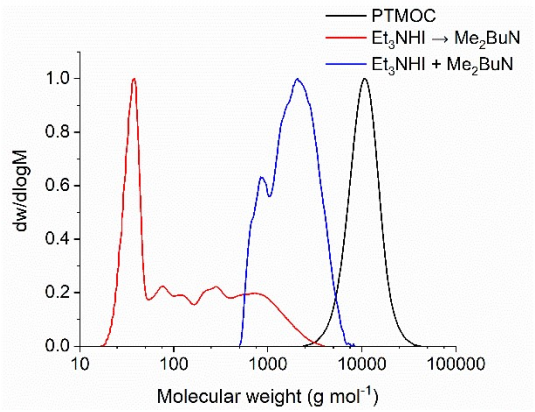

Figure 2.21. Size exclusion chromatogram of PTMOC before (M_n = 9.7 kg mol^{-1}, $Đ_M$ = 1.2) and after functionalisation using Et_3NHI, followed by *N*,*N*-dimethylbutylamine (M_n = 0.07 kg mol^{-1}, $Đ_M$ = 5), and using Et_3NHI and *N*,*N*-dimethylbutylamine in one-pot (M_n = 1.6 kg mol^{-1}, $Đ_M$ = 1.4) (DMF, RI, calibrated against polystyrene standards).

2.2.4 Post-Polymerisation Functionalisation of PTMOC with Thiols

To further expand the scope of functional groups able to modify PTMOC, thiols were investigated for this system. Although the thiol-epoxy click reaction has been

widely studied for small molecules,[38-42] only a few examples of the functionalisation of epoxy-functionalised polymers with thiols have been reported.[43,44] In this case, most studies have focused on the modification of the non-biodegradable PG(M)A.[45-47] Gadwal *et al*. had previously investigated the use of Et_3N, tributylammonium fluoride (TBAF) or LiOH as catalyst for the functionalisation of PGMA with aromatic and aliphatic thiols (Scheme 2.7).[9] Comparing the three catalysts, the authors observed that LiOH provided higher degrees of functionalisation using minimum catalyst loading with shorter reaction times as a consequence of its higher basicity.

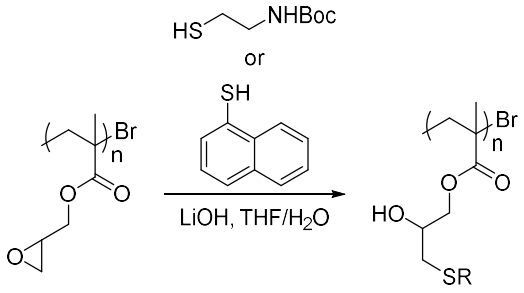

Scheme 2.7. Functionalisation of PGMA with thiols reported by Gadwal *et al.*[9]

In order to understand the effect of the substituent in the thiol used to functionalise PTMOC, 1-dodecanethiol, benzyl mercaptan and thiophenol were investigated in our studies (Scheme 2.8). Firstly, 1-dodecanethiol was initially applied using similar conditions to those applied by Gadwal *et al*.[9] (*i.e.* 1.25 equivalents of thiol and 1 mol% of LiOH (relative to thiol) using THF/H_2O (10:1) as solvent). The reaction mixture was stirred for 3 hours at room temperature and quenched by diluting with CH_2Cl_2 and washing with water to remove the catalyst. After concentration, the resultant polymer was analysed by ^{1}H NMR spectroscopy, which showed no modification in the initial polymer, with similar results being observed when 5 mol% of catalyst was used (Table 2.2). Increasing the amount of catalyst to 12 mol% resulted in 39% functionalisation, which was evidenced by a decrease in the integration of the signals corresponding to the epoxide group at δ = 2.57, 2.76, and 3.09 ppm in the ^{1}H NMR spectrum (Figure 2.22). Besides, the appearance of a signal at δ = 3.83 ppm is also consistent with the carbinolic proton resonance after ring-opening the epoxide. Further analysis by SEC revealed two distributions: the main one presented a molecular weight higher than that showed by the original PTMOC (pre: DP = 63, M_n = 7.5 kg mol^{-1}, $Đ_M$ = 1.2; post: M_n = 8.3 kg mol^{-1}, $Đ_M$ = 1.3), whereas the minor distribution displayed a molecular weight

considerably lower (M_n = 0.5 kg mol^{-1}, $Đ_M$ = 1), which suggested a decomposition of the polymer backbone (Figure 2.23).

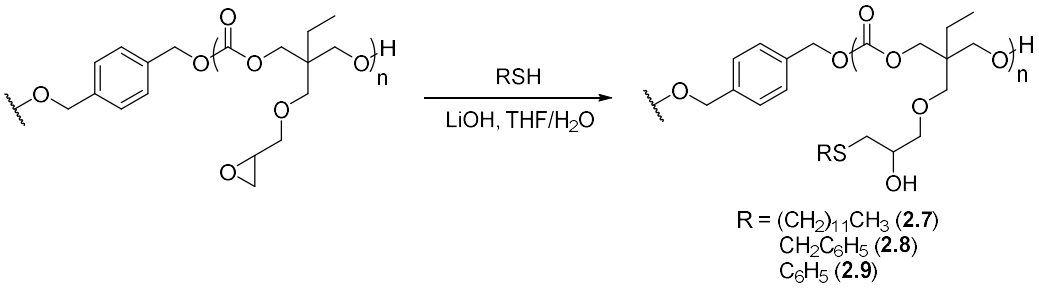

Scheme 2.8. Functionalisation of PTMOC with thiols.

Table 2.2. Post-polymerisation functionalisation of PTMOC with 1-dodecanethiol.[a]

Entry	Catalyst Loading (mol%)	Degree of Functionalisation[b] (%)	M_n[c] (kg mol^{-1})	$Đ_M$[c]
1	2	< 5	-	-
2	5	< 5	-	-
3	12	39	8.3 (0.5)[d]	1.3 (1.04)[d]

[a] Reactions were carried out using 1.25 equivalents of thiol in THF:H_2O (10:1) for 3 hours at room temperature with LiOH as catalyst (PTMOC: DP = 63, M_n = 7.5 kg mol^{-1}, $Đ_M$ = 1.2). [b] Determined by ^{1}H NMR spectroscopy. [c] Determined by SEC analysis in $CHCl_3$ using RI detector, calibrated against polystyrene. [d] (Value) corresponds to minor distribution.

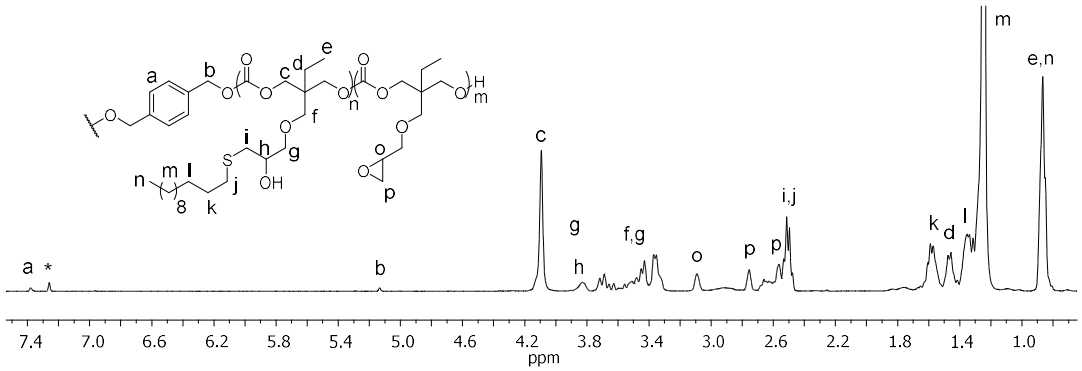

Figure 2.22. ^{1}H NMR spectrum of PTMOC after partial post-polymerisation functionalisation with 1-dodecanethiol ($CDCl_3$, 500 MHz, 298 K, * = $CHCl_3$).

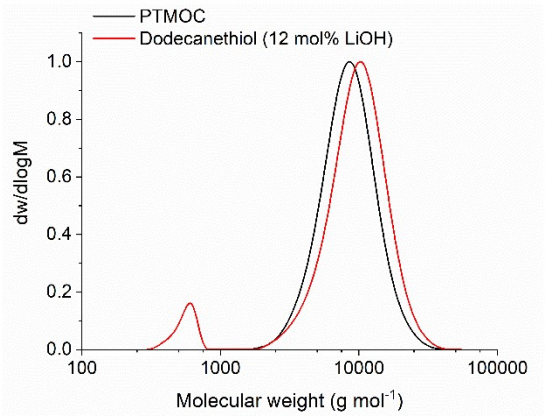

Figure 2.23. Size exclusion chromatograms of PTMOC before (M_n = 7.5 kg mol^{-1}, $Đ_M$ = 1.2) and after post-polymerisation functionalisation with 1-dodecanethiol catalysed by 12 mol% of LiOH (M_n = 8.3 kg mol^{-1}, $Đ_M$ = 1.3) ($CHCl_3$, RI, calibrated against polystyrene standards).

Because of the low reactivity displayed by 1-dodecanethiol, the modification of PTMOC with benzyl mercaptan using 2 mol% of LiOH was investigated. These conditions led to only 29% functionalisation, whilst utilising 5 mol% of the same catalyst yielded 49% conversion (Table 2.3). Besides the improved conversions, the size exclusion chromatogram of the resultant polymer presented a low molecular weight distribution, similar to that observed for the reaction with 1-dodecanethiol (Figure 2.24). The degradation of the polymer backbone was avoided by increasing the amount of thiol to 2 equivalents while maintaining the catalyst loading at 2 mol%. Under these conditions, a degree of functionalisation of 56% was obtained, with SEC analysis showing a single molecular weight distribution (Figure 2.25).

Table 2.3. Post-polymerisation functionalisation of PTMOC with benzyl mercaptan.[a]

Entry	Equivalents of Thiol	Catalyst Loading (mol%)	Degree of Functionalisation[b] (%)	M_n[c] (kg mol^{-1})	$Đ_M$[c]
1	1.25	2	29	9.6	1.2
2	1.25	5	41	9.6 (0.6)[d]	1.5 (1.1)[d]
3	2.0	2	56	13.9[e]	1.26[e]

[a] Reactions were carried out in THF:H_2O (10:1) for 3 hours at room temperature with LiOH as catalyst (PTMOC: DP = 63, M_n = 7.5 kg mol^{-1}, $Đ_M$ = 1.2). [b] Determined by ^{1}H NMR

spectroscopy. [c] Determined by SEC analysis in $CHCl_3$ using RI detector, calibrated against polystyrene standards. [d] (Value) corresponds to minor distribution. [e] PTMOC: DP = 73, M_n = 12.1 kg mol^{-1}, $Đ_M$ = 1.28 ($CHCl_3$, RI).

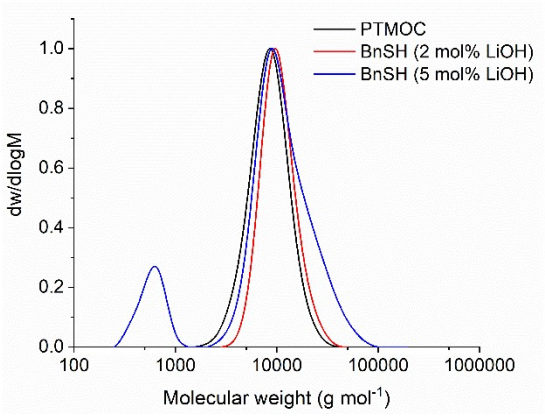

Figure 2.24. Size exclusion chromatograms of PTMOC before (M_n = 7.5 kg mol^{-1}, $Đ_M$ = 1.2) and after post-polymerisation functionalisation with 1.25 equivalents of benzylmercaptan catalysed by 2 (M_n = 9.6 kg mol^{-1}, $Đ_M$ = 1.2) and 5 mol% of LiOH (M_n = 9.6 kg mol^{-1}, $Đ_M$ = 1.5) ($CHCl_3$, RI, calibrated against polystyrene standards).

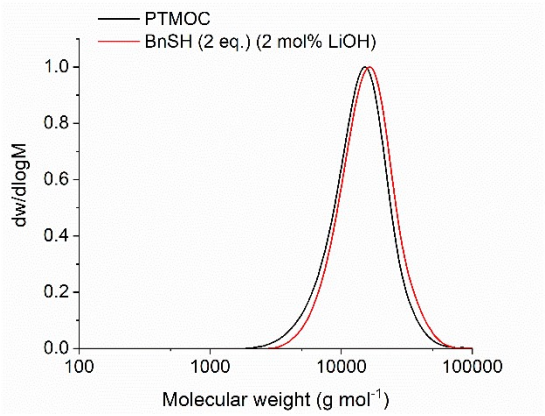

Figure 2.25. Size exclusion chromatograms of PTMOC before (M_n = 12.1 kg mol^{-1}, $Đ_M$ = 1.28) and after post-polymerisation functionalisation with 2.0 equivalents of benzylmercaptan catalysed by 2 mol% of LiOH (M_n = 13.9 kg mol^{-1}, $Đ_M$ = 1.26) ($CHCl_3$, RI, calibrated against polystyrene standards).

Finally, thiophenol was investigated in the thiol-epoxy reaction of PTMOC utilising 2 mol% of LiOH. The degrees of functionalisation obtained were 88% and 94% when 1.25 and 2.0 equivalents of thiol were utilised, respectively, which was considerably higher than the thiols previously studied. The ^{1}H NMR spectrum was

consistent with the functionalised polymer, with signals at δ = 7.17, 7.26, and 7.35 ppm corresponding to the aromatic group of thiophenol, while the presence of the carbinolic group at δ = 3.84 ppm indicated that the epoxide had been opened to provide PTMOC-thiophenol (**2.9**) (Figure 2.26). In addition, SEC analysis showed a single molecular weight distribution, which confirmed the absence of decomposition of the polymer backbone (Figure 2.27).

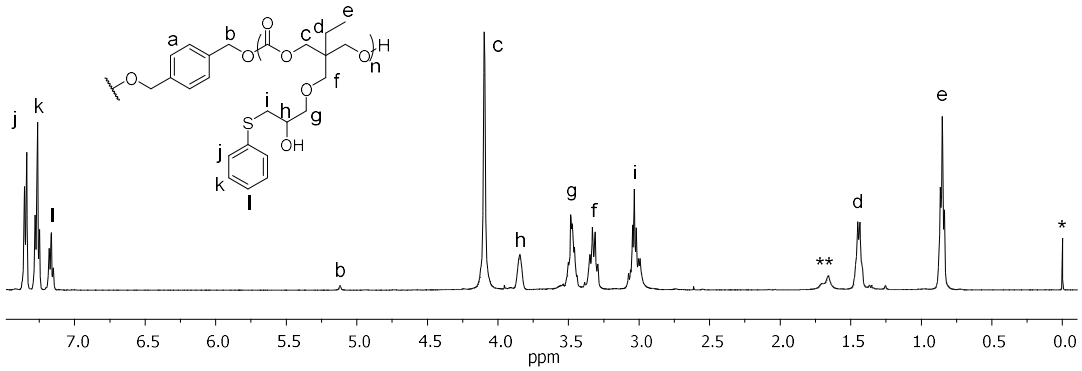

Figure 2.26. ^{1}H NMR spectrum of PTMOC-thiophenol (**2.9**) ($CDCl_3$, 500 MHz, 298 K, * = TMS, ** = H_2O).

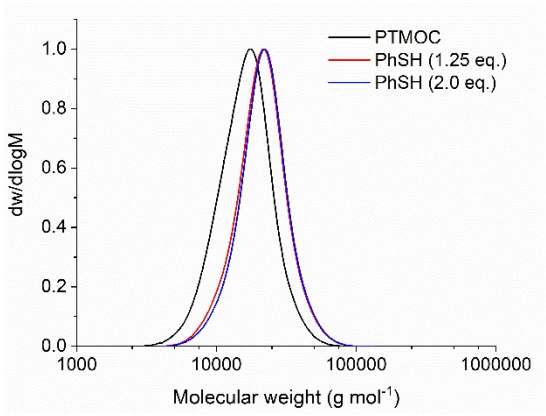

Figure 2.27. Size exclusion chromatograms of PTMOC before (M_n = 14.2 kg mol^{-1}, $Đ_M$ = 1.21) and after functionalisation using 1.25 equivalents (M_n = 18.8 kg mol^{-1}, $Đ_M$ = 1.19) or 2.0 equivalents (M_n = 18.4 kg mol^{-1}, $Đ_M$ = 1.19) of thiophenol (DMF, IR, calibrated against poly(methyl methacrylate) standards).

The mechanism of the thiol-epoxy reaction under basic conditions involves the initial abstraction of the proton from the thiol (Scheme 2.9).[44] The resulting thiolate then attacks the least hindered carbon in the epoxide *via* a S_N2 mechanism. The

resultant alkoxide is highly basic and, therefore, is protonated by another thiol molecule or protic species present in the reaction medium to form the final product. The difference in reactivity of the thiols utilised herein is explained by the higher nucleophilicity of more acidic thiols (in this case thiophenol (pKa = 6.9), followed by benzyl mercaptan (p*K*a = 9.4) and 1-dodecanethiol (p*K*a ~10)) that provide faster reaction rates.[48] These results were in agreement with other reports in literature involving nucleophilic reactions with thiols, such as thiol-epoxy and thiol-Michaels additions.[9,49]

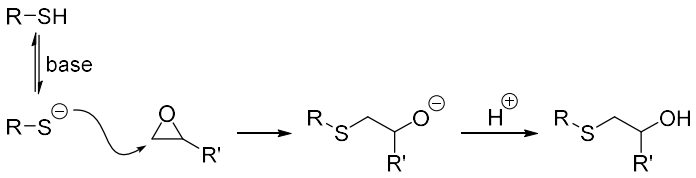

Scheme 2.9. Mechanism for the thiol-epoxy reaction under basic conditions.[44]

Finally, to investigate the efficacy of organocatalysts (*i.e*. DMAP, TBD and DBU) in the post-polymerisation modification of PTMOC, thiophenol was used as the nucleophile, as it was shown to be the most active compound under investigation. As previously performed with LiOH, the functionalisation was carried out with 2 mol% organocatalyst but without the addition of H_2O as a solvent. DMAP was shown to provide 16% functionalisation, whereas 43% conversion was obtained with TBD (Table 2.4). However, the size exclusion chromatograms of the polymer functionalised using the guanidine catalyst showed the presence of a broad low molecular weight distribution, which indicated that decomposition had occurred during the reaction (Figure 2.28). The modification catalysed by DBU yielded 79% conversion after 3 hours, while optimisation demonstrated 90% functionalisation in 7 hours. However, no further reaction was observed after this period, which could be a consequence of the increased steric effects around the polymer backbone. Size exclusion chromatograms showed an increase in the molecular weight, whilst maintaining a unimodal and narrow distribution (Figure 2.29). Hence, these optimised conditions were applied to other 4-substituted thiophenols. The chlorine analogue achieved 90% conversion and, surprisingly, only 49% conversion was observed for 4-methoxythiophenol (Figure 2.29). This low functionalisation is probably a consequence of the air sensitivity presented by the 4-methoxy substituted thiol, which

could have undergone decomposition despite the additional care taken by carrying out the reaction under a N_2 atmosphere. Finally, DBU was utilised as a catalyst in order to functionalise PTMOC with other classes of thiol (*i.e.* dodecanethiol, benzyl mercaptan and thioglycerol); however, no changes were observed in the initial polymer, which demonstrated that DBU was efficient only for thiophenol derivatives.

Table 2.4. Post-polymerisation functionalisation of PTMOC with aromatic thiol using organocatalysts.[a]

Entry	Thiol	Catalyst	Time (h)	Degree of Function.[b] (%)	M_n[c] (kg mol^{-1})	$Đ_M$[c]
1	Thiophenol	-	7	< 5%	16.4[d]	1.10[d]
2	Thiophenol	TBD	3	16	6.5[d]	2.3[d]
3	Thiophenol	DMAP	3	43	16.8[d]	1.10[d]
4	Thiophenol	DBU	3	79	19.0[d]	1.16[d]
5	Thiophenol	DBU	7	90	20.2[e]	1.19[e]
6	4-Chloro thiophenol	DBU	7	90	19.5[e]	1.18[e]
7	4-Methoxy thiophenol	DBU	7	49	19.4[e]	1.19[e]

[a] Reactions were carried out in THF with 2 mol% of catalyst at room temperature. [b] Determined by ^{1}H NMR spectroscopy. [c] Determined by SEC analysis in DMF using RI detector, calibrated against poly(methyl methacrylate) standards. [d] PTMOC: DP = 78, M_n = 14.7 kg mol^{-1}, $Đ_M$ = 1.15 (DMF, IR). [e] PTMOC: DP = 73, M_n = 14.2 kg mol^{-1}, $Đ_M$ = 1.21 (DMF, IR).

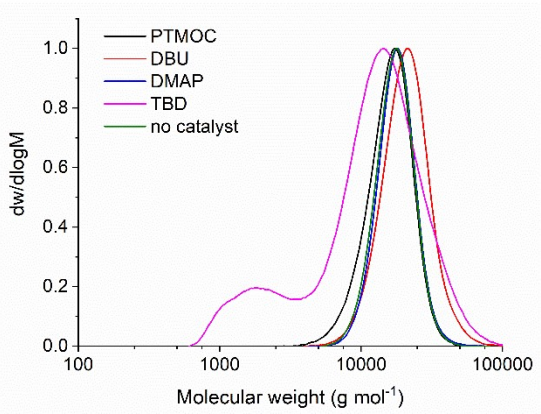

Figure 2.28. Size exclusion chromatograms of PTMOC before (M_n = 14.7 kg mol^{-1}, $Đ_M$ = 1.15), and after post-polymerisation functionalisation with thiophenol catalysed by 2 mol% of DBU (M_n = 19.0 kg mol^{-1}, $Đ_M$ = 1.16), DMAP (M_n = 16.8 kg mol^{-1}, $Đ_M$ = 1.15), TBD (M_n = 6.5 kg mol^{-1}, $Đ_M$ = 2.3) and in the absence of catalyst (M_n = 16.4 kg mol^{-1}, $Đ_M$ = 1.10) (DMF, RI, calibrated against poly(methyl methacrylate) standards).

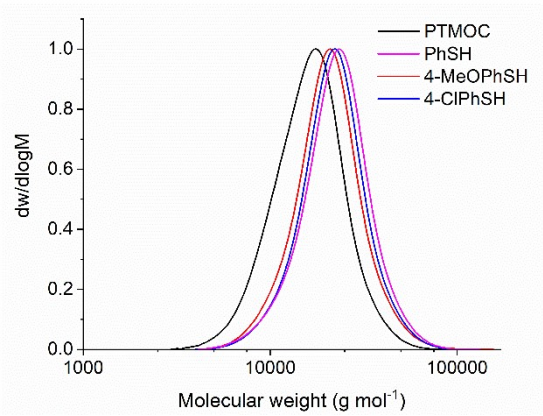

Figure 2.29. Size exclusion chromatograms of PTMOC before (M_n = 14.2 kg mol^{-1}, $Đ_M$ = 1.21) and after post-polymerisation functionalisation with thiophenol (M_n = 20.2 kg mol^{-1}, $Đ_M$ = 1.19), 4-methoxythiophenol (M_n = 19.5 kg mol^{-1}, $Đ_M$ = 1.18), and 4-chlorothiophenol (M_n = 19.4 kg mol^{-1}, $Đ_M$ = 1.19) (DMF, RI, calibrated against poly(methyl methacrylate) standards).

While most of post-polymerisation methodologies that inserts thioether functionalities into polycarbonates typically involves thiol-ene and thiol-Michael additions,[2,50-52] the thiol-epoxy reactions reported herein represents a unique and versatile strategy, which provides an additional hydroxyl group that can be utilised in further modifications. Rather similar approach was reported by Hedrick and

coworkers in the functionalisation of thioether-functionalised polycarbonates with different epoxides to form sulfonium groups.[53] Although the reactions were carried out under acidic conditions, the degrees of functionalisation were comparable to our approach (*i.e.* 58 to 90%).

2.3 Conclusions

The organocatalytic ROP of the epoxy-functionalised cyclic carbonate TMOC was demonstrated to be selective for the carbonate ring by using TBD as catalyst, which preserved the epoxy side chain group. In addition, this catalyst provided good control over the molecular weight, with the resultant polymers presenting low dispersities, which allowed the synthesis of polymers with predictable molecular weight values based on the monomer-to-initiator ratio. This approach showed to be an attractive alternative over the functionalisation of pendent alkene group of polycarbonates, as well-defined polymers could be easily obtained in the absence of side reactions.

The following studies on the post-polymerisation modification of the pendent epoxide with primary amines proved to be challenging as the presence of Lewis acids promoted the degradation of the polymer backbone in a competitive manner. When high temperatures were employed instead of catalysts, > 95% conversion was obtained with benzylamine, yet low levels of crosslinking occurred. However, attempts to functionalise PTMOC with other classes of amine (*i.e.* aryl or aliphatic amines) under the same conditions were impractical as a consequence of their low nucleophilicity. In addition, when L-phenylalanine methyl ester hydrochloride was utilised, an unexpected functionalisation with chlorine was observed.

As the preparation of a chlorine-functionalised polycarbonate was shown to be straightforward using triethylamine hydrochloride, the further quarternisation of the polymer was investigated *via* the nucleophilic substitution using tertiary amines. However, the poor leaving group characteristic of chlorine resulted in the absence of any modification when utilising different amines. The iodine-functionalised polycarbonate was then prepared in order to insert a better leaving group into the polymer. However, the resultant functional polymer underwent self-crosslinking, which suggested that the iodine was being easily displaced by the hydroxyl groups formed after ring-opening the epoxide. At this point, achieving a balance between a good and a poor leaving group had shown to be challenging.

The post-polymerisation modification of PTMOC by thiol-epoxy reactions using LiOH as catalyst showed a higher degree of functionalisation for arylthiols than for benzylic, followed by the aliphatic ones. This could be rationalised based on the different nucleophilicity of the corresponding thiolates, which increases from the arylthiols to the aliphatic thiols.[54] Finally, some organocatalysts were applied to functionalise PTMOC with thiols. Specifically, even though DBU was active exclusively for arylthiols, it afforded comparable conversion values to those obtained using LiOH.

In some occasions, the carbonate moiety of PTMOC was shown to be susceptible to nucleophilic attack during the modifications of the pendent epoxide group in the polymer. Nonetheless, after optimising the reaction conditions, we demonstrated that the epoxide-functionalised polycarbonate, PTMOC, could be used as a means to the insertion of amines that are typically incompatible with ROP and thiols with varied structures.

2.3 References

1. J. Feng, R.-X. Zhuo and X.-Z. Zhang, *Prog. Polym. Sci.*, 2012, **37**, 211.
2. S. Tempelaar, L. Mespouille, O. Coulembier, P. Dubois and A. P. Dove, *Chem. Soc. Rev.*, 2013, **42**, 1312.
3. D. J. Hall, H. M. Van Den Berghe and A. P. Dove, *Polym. Int.*, 2011, **60**, 1149.
4. A. C. Engler, J. M. W. Chan, D. J. Coady, J. M. O'Brien, H. Sardon, A. Nelson, D. P. Sanders, Y. Y. Yang and J. L. Hedrick, *Macromolecules*, 2013, **46**, 1283.
5. H. C. Kolb, M. G. Finn and K. B. Sharpless, *Angew. Chem. Int. Ed.*, 2001, **40**, 2004.
6. C. Shanthi and K. P. Rao, *Carbohydr. Polym.*, 2001, **44**, 123.
7. K. A. McEwan, S. Slavin, E. Tunnah and D. M. Haddleton, *Polym. Chem.*, 2013, **4**, 2608.
8. S. Li, J. Han and C. Gao, *Polym. Chem.*, 2013, **4**, 1774.
9. I. Gadwal, M. C. Stuparu and A. Khan, *Polym. Chem.*, 2015, **6**, 1393.
10. J. S. Basuki, L. Esser, H. T. T. Duong, Q. Zhang, P. Wilson, M. R. Whittaker, D. M. Haddleton, C. Boyer and T. P. Davis, *Chem. Sci.*, 2014, **5**, 715.
11. C.-F. Wang, Y.-X. Lin, T. Jiang, F. He and R.-X. Zhuo, *Biomaterials*, 2009, **30**, 4824.

12. T. Jiang, Y. M. Li, Y. Lv, Y. J. Cheng, F. He and R. X. Zhuo, *Colloids Surf., B*, 2013, **111**, 542.
13. T. Jiang, Y. Li, Y. Lv, Y. Cheng, F. He and R. Zhuo, *J. Mater. Sci.: Mater. Med.*, 2014, **25**, 131.
14. A. E. van der Ende, E. J. Kravitz and E. Harth, *J. Am. Chem. Soc.*, 2008, **130**, 8706.
15. A. van der Ende, T. Croce, S. Hamilton, V. Sathiyakumar and E. Harth, *Soft Matter*, 2009, **5**, 1417.
16. D. M. Stevens, S. Tempelaar, A. P. Dove and E. Harth, *ACS Macro Lett.*, 2012, **1**, 915.
17. Y. Yan and D. J. Siegwart, *Polym. Chem.*, 2014, **5**, 1362.
18. B. D. Mullen, C. N. Tang and R. F. Storey, *J. Polym. Sci., Part A: Polym. Chem.*, 2003, **41**, 1978.
19. J. R. Lowe, M. T. Martello, W. B. Tolman and M. A. Hillmyer, *Polym. Chem.*, 2011, **2**, 702.
20. Y. He, H. Keul and M. Möller, *React. Funct. Polym.*, 2011, **71**, 175.
21. M. J. Bennison, PhD thesis, University of Warwick, 2013.
22. C. Weng, H. Zhang, X. Xiong, X. Lu and Y. Zhou, *Asian J. Chem.*, 2014, **26**, 3761.
23. J. A. Deyrup and C. L. Moyer, *J. Org. Chem.*, 1969, **34**, 175.
24. M. Meguro, N. Asao and Y. Yamamoto, *J. Chem. Soc., Perkin Trans. 1*, 1994, **0**, 2597.
25. M. Chini, P. Crotti and F. Macohiat, *Tetrahedron Lett.*, 1990, **31**, 4661.
26. F. A. Saddique, A. F. Zahoor, S. Faiz, S. A. R. Naqvi, M. Usman and M. Ahmad, *Synth. Commun.*, 2016, **46**, 831.
27. I. Cepanec, M. Litvić, H. Mikuldaš, A. Bartolinčić and V. Vinković, *Tetrahedron*, 2003, **59**, 2435.
28. A. K. Chakraborti, S. Rudrawar and A. Kondaskar, *Eur. J. Org. Chem.*, 2004, **2004**, 3597.
29. A. K. Chakraborti, A. Kondaskar and S. Rudrawar, *Tetrahedron*, 2004, **60**, 9085.
30. A. T. Placzek, J. L. Donelson, R. Trivedi, R. A. Gibbs and S. K. De, *Tetrahedron Lett.*, 2005, **46**, 9029.
31. J. Yu, Z. Su, H. Xu, X. Ma, J. Yin and X. Jiang, *Polym. Chem.*, 2015, **6**, 6946.

32. F. Brotzel and H. Mayr, *Org. Biomol. Chem.*, 2007, **5**, 3814.
33. E.-R. Kenawy, S. D. Worley and R. Broughton, *Biomacromolecules*, 2007, **8**, 1359.
34. Z. Y. Ong, D. J. Coady, J. P. K. Tan, Y. Li, J. M. W. Chan, Y. Y. Yang and J. L. Hedrick, *J. Polym. Sci., Part A: Polym. Chem.*, 2016, **54**, 1029.
35. F. Nederberg, Y. Zhang, J. P. K. Tan, K. Xu, H. Wang, C. Yang, S. Gao, X. D. Guo, K. Fukushima, L. Li, J. L. Hedrick and Y.-Y. Yang, *Nat. Chem.*, 2011, **3**, 409.
36. W. Chin, C. Yang, V. W. L. Ng, Y. Huang, J. Cheng, Y. W. Tong, D. J. Coady, W. Fan, J. L. Hedrick and Y. Y. Yang, *Macromolecules*, 2013, **46**, 8797.
37. V. W. L. Ng, J. P. K. Tan, J. Leong, Z. X. Voo, J. L. Hedrick and Y. Y. Yang, *Macromolecules*, 2014, **47**, 1285.
38. N. Azizi, A. Khajeh-Amiri, H. Ghafuri and M. Bolourtchian, *Phosphorus, Sulfur Silicon Relat. Elem.*, 2010, **185**, 1550.
39. J. Wu and H.-G. Xia, *Green Chem.*, 2005, **7**.
40. V. Polshettiwar and M. P. Kaushik, *Catal. Commun.*, 2004, **5**, 515.
41. G. H. Posner and D. Z. Rogers, *J. Am. Chem. Soc.*, 1977, **99**, 8208.
42. F. Fringuelli, F. Pizzo, S. Tortoioli and L. Vaccaro, *Tetrahedron Lett.*, 2003, **44**, 6785.
43. U. S. Gunay, E. Demirel, G. Hizal, U. Tunca and H. Durmaz, *React. Funct. Polym.*, 2015, **94**, 35.
44. M. C. Stuparu and A. Khan, *J. Polym. Sci., Part A: Polym. Chem.*, 2016, **54**, 3057.
45. M. Benaglia, A. Alberti, L. Giorgini, F. Magnoni and S. Tozzi, *Polym. Chem.*, 2013, **4**, 124.
46. Q. Zhang, A. Anastasaki, G.-Z. Li, A. J. Haddleton, P. Wilson and D. M. Haddleton, *Polym. Chem.*, 2014, **5**, 3876.
47. E. M. Muzammil, A. Khan and M. C. Stuparu, *RSC Adv.*, 2017, **7**, 55874.
48. C. E. Hoyle, A. B. Lowe and C. N. Bowman, *Chem. Soc. Rev.*, 2010, **39**, 1355.
49. J. W. Chan, C. E. Hoyle, A. B. Lowe and M. Bowman, *Macromolecules*, 2010, **43**, 6381.
50. R. J. Williams, I. A. Barker, R. K. O'Reilly and A. P. Dove, *ACS Macro Lett.*, 2012, **1**, 1285.

51. B. B. Uysal, U. S. Gunay, G. Hizal and U. Tunca, *J. Polym. Sci., Part A: Polym. Chem.*, 2014, **52**, 1581.
52. Y. Dai, X. Zhang and F. Xia, *Macromol. Rapid Commun.*, 2017, **38**, 1700357.
53. N. H. Park, M. Fevre, Z. X. Voo, R. J. Ono, Y. Y. Yang and J. L. Hedrick, *ACS Macro Lett.*, 2016, **5**, 1247.
54. M. M. Kreevoy, E. T. Harper, R. E. Duvall, H. S. Wilgus III and L. T. Ditsch, *J. Am. Chem. Soc.*, 1960, **82**, 4899.

Chapter 3

(Photoinduced) Ring-Opening Polymerisation of Cyclic (Di)esters Using 1,1,3,3-Tetramethylguanidine as a Catalyst

3.1 Introduction

The use of external regulations for controlling polymerisations is a powerful strategy that has the potential to define the polymer structure and properties of materials.[1] Light is a stimulus that has a series of properties for an ideal system that provides temporal and spatial resolution by inducing chemical reactions in an appropriate wavelength.[2] These reactions can be promoted by i) photocatalysts that are only active in the photoexcited state, ii) photocaged or photoactivated catalysts, which generates ground state active species by an irreversible photochemical reaction, or iii) photoswitchable catalysts, which are compounds containing photochromic moieties that allows the catalytic centre to be reversibly altered between active and inactive form (Figure 3.1).[3] In particular, the photoactivated catalysts offer the advantage of controling the polymerisation initiation by releasing the active species upon irradiation, while the photoswitchable catalysts are able to modify the catalyst activity during the reaction, which has been proved useful for controlling the polymer microstructure.[4,5]

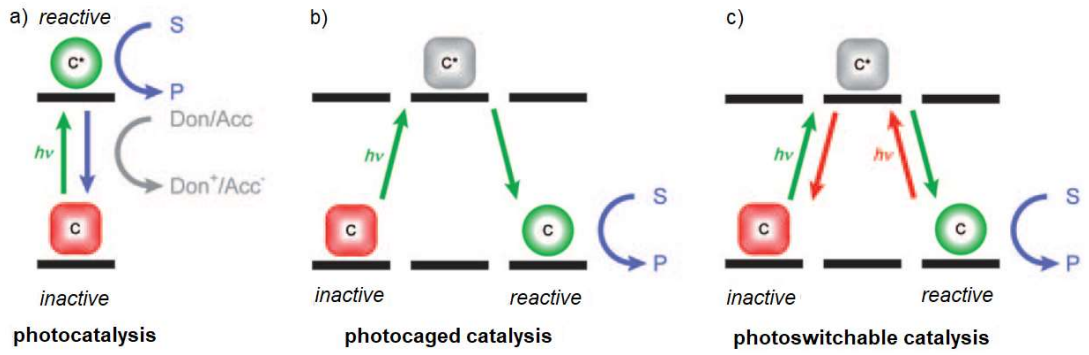

Figure 3.1. Representation of approaches for the photocontrol of catalytic activity by a) photocatalysis, b) photocaged catlysis and c) photoswitchable catalysis (c = catalyst, S = substrate, and P = product). Reproduced from ref. 3 with permission from John Wiley and Sons.

Regarding the preparation of biodegradable polymer by ring-opening polymerisation (ROP), only a few studies have been reported utilising photoswitchable catalysts.[6-9] For instance, Hecht and coworkers recently reported a bifunctional catalyst system that is composed of a base that activates the alcohol initiator/chain end, and an electron deficient phenol group for monomer activation.[9] In addition, a diarylethene switch group was introduced to allow interconversion

between an open form that contains the phenol moiety, and a closed form where an inactive keto tautomer is formed under UV light in the presence of a base (Scheme 3.1). The performance of this photoswitchable catalyst was initially demonstrated in the ROP of L-LA using *N*,*N*-dimethylcyclohexylamine and, by starting with the catalyst in the inactive form, the polymerisation rate could be controlled by increasing the amount of active catalyst when exposing the solution to visible light. Further investigation on the polymerisation of TMC and δ-VL using 1,8-diazabicyclo[5.4.0]undec-7-ene (DBU) revealed different reactivities of the monomers in the open and closed form of the photoswitchable catalyst. This allowed the copolymerisation of these monomers to occur with higher incorporation of TMC in the closed form, whereas higher δ-VL incorporation was obtained in the open form of the catalyst, thus providing a fine control over the polymer microstructure. This methodology allowed for a great regulation on the catalytic activity, although the requirement for an external base resulted in a system that was still active in the absence of the photoswitchable catalyst.

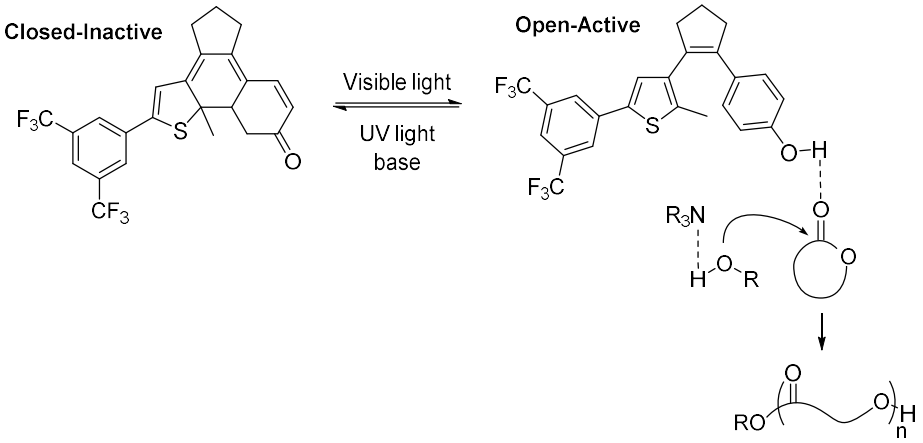

Scheme 3.1. Photoswitchable ROP of cyclic monomers catalysed by a diarylethene photoswitch group containing phenol hydrogen-bond donor in the active form.

Despite the advantages of photoswitchable catalysts in controlling the polymer structure, the systems developed to date have shown a slow formation of active species and/or low catalytic activity. These characteristics compromise the spatial control of the system, once this methodology requires fast polymerisation reactions to avoid difusion of reactive species that can decrease the overall resolution.[10] However, for applications in areas such as microelectronics [11] and stereolithography[12] where the

precise control of space is essential, the fine regulation on the polymerisation initiation is a more relevant requirement.

In this context, photoinduced catalysts have been reported for controlling the polymerisation initiation in ROP.[13-15] As discussed in Chapter 1, the works reported to date present limitations, such as the use of high-energy UV light sources that can cause damage to biological systems, present low compatibility with reactants, and show limited curing depth.[16] In this regard, photoinduced catalysts that release bases as the active species, namely photobase generators (PBG), can provide more efficient alternatives for ROP. Specifically, 7-diethylamino-4-methylcoumarin and 2-(2-nitrophenyl)propoxycarbonyl (NPPOC) are chromophores that are active at $\lambda > 350$ nm and have been demonstrated to photocage the superbase 1,1,3,3-tetramethylguanidine (TMG, p*K*a = 23.4 in MeCN)[17] (Figure 3.2).[10,18]

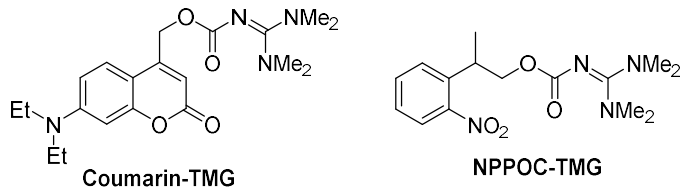

Figure 3.2. Chemical structures of TMG PBGs based on the carbamate group.

Herein, we investigate PBGs that releases TMG upon irradiation as potential candidates to photoinduce the ROP of cyclic monomers. Although the use of TMG as a ROP catalyst has been only reported for the *N*-butyl *N*-carboxyanhydride monomer using alcohol initiators,[19] we envisioned that TMG would be able to catalyse the ROP of other cyclic monomers in a similar manner as DBU (p*K*a = 24.3 in MeCN)[20] and acyclic guanidines[21] as a consequence of its high basicity. Therefore, we firstly investigate the use of free TMG as an organocatalyst for the ROP of cyclic (di)esters and, subsequently, TMG is photocaged with a chromophore to explore the photoinduced polymerisation.

3.2 Results and Discussion

3.2.1 Ring-Opening Polymerisation of Cyclic (Di)esters Catalysed by 1,1,3,3-Tetramethylguanidine

Initial investigation on the activity of TMG as a ROP catalyst was performed with L-LA in $CDCl_3$ ($[M]_0$ = 2 M) at room temperature using benzyl alcohol as initiator

(Scheme 3.2). The polymerisation was monitored by ^{1}H NMR spectroscopy, which revealed a decrease in the signals at δ = 5.07 and 1.56 ppm corresponding to the methine and methyl group in the monomer, respectively, and the increase in the corresponding proton resonances in the polymer at δ = 5.12 and 1.51 ppm. With an initial monomer-to-initiator concentration ratio ($[M]_0/[I]_0$) of 50 and utilising 1 mol% TMG, the polymerisation achieved 92% monomer conversion in 2 hours. After purification by precipitation in hexane and methanol, the resultant polymer was analysed by size exclusion chromatography (SEC), which presented a monomodal distribution and narrow dispersity (M_n = 10.6 kg mol^{-1}, $Đ_M$ = 1.05) (Figure 3.3). Further analysis of the purified polymer by ^{1}H NMR spectroscopy showed a PLLA (**3.1**) with a DP of 49 as calculated from the comparison of integration of the end-group aromatic signals at δ = 7.35 ppm and the methyl proton resonances of the polymer at δ = 5.17 ppm (Figure 3.4).

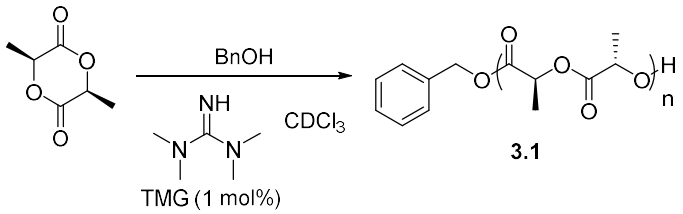

Scheme 3.2. ROP of L-LA catalysed by TMG.

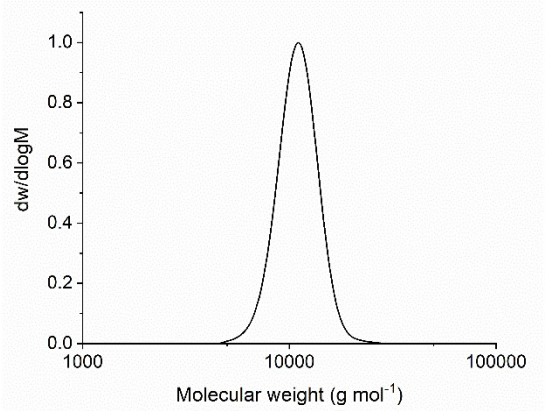

Figure 3.3. Size exclusion chromatogram of PLLA (**3.1**) (M_n = 10.6 kg mol^{-1}, $Đ_M$ = 1.05) ($CHCl_3$, RI, calibrated against polystyrene standards). Conditions: $[M]_0$ = 2 M in CH_2Cl_2, $[M]_0/[I]_0/[cat]_0$= 50:1:0.5, using TMG as catalyst and benzyl alcohol as initiator.

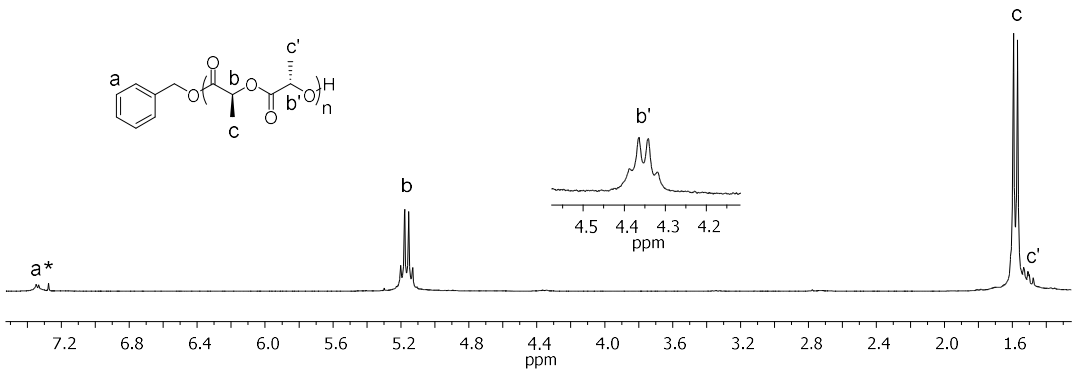

Figure 3.4. ^{1}H NMR spectrum of PLLA (**3.1**) ($CDCl_3$, 300 MHz, 298 K, * = $CHCl_3$). Conditions: $[M]_0$ = 2 M in CH_2Cl_2, $[M]_0/[I]_0$ = 50, using 1 mol% TMG and benzyl alcohol as initiator.

Investigation of the polymerisation control of L-LA catalysed by TMG showed a first-order dependence on the monomer in the semilogarithmic plot (Figure 3.5a), as well as a linear increase of the molecular weight with the monomer conversion and with [M]/[I] (Figure 3.5b and Figure 3.6). The dispersity values remained low throughout the polymerisations, although for higher DPs, a high molecular weight shoulder indicated that transesterification was occurring in a small extent (Figure 3.7). Finally, analysis by matrix-assisted laser desorption/ionization time-of-flight mass spectrometry (MALDI-ToF MS) spectroscopy revealed a single distribution with a spacing of 144 *m*/*z* that corresponds to the L-LA unit and a peak at 4600 *m*/*z* that is assigned to a sodium cationised PLLA initiated from benzyl alcohol containing 31 repeating units (Figure 3.8). These characteristics demonstrated the high end-group fidelity, as well as the controlled nature of this polymerisation system.

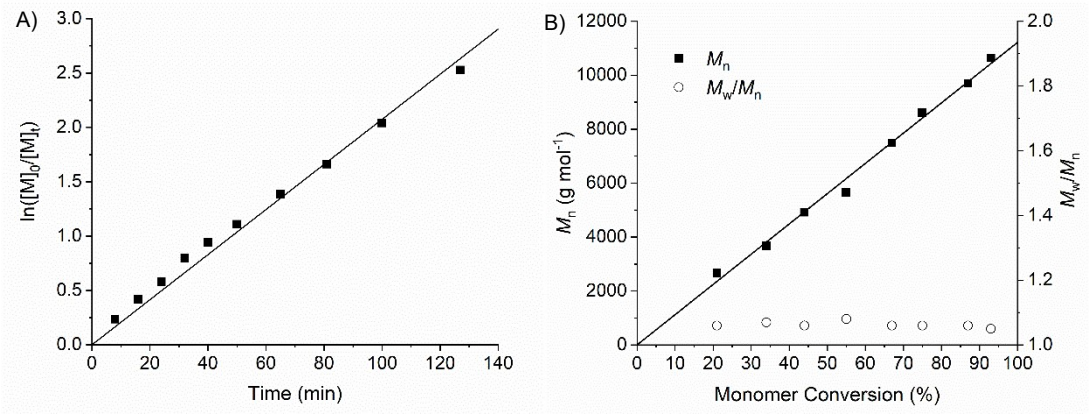

Figure 3.5. Plots of A) ln of initial monomer concentration by monomer concentration ($\ln([M]_0/[M]_t)$) against time and B) number-average molecular weight (M_n; ■) and dispersity ($Đ_M = M_w/M_n$; ○) against monomer conversion for the ROP of L-LA. Conditions: $[M]_0$ = 2 M in CH_2Cl_2, $[M]_0/[I]_0$ = 50, using 1 mol% TMG and benzyl alcohol as initiator.

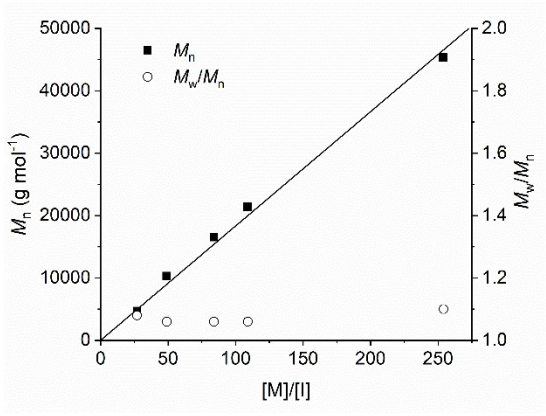

Figure 3.6. Plot of number-average molecular weight (M_n; ■) and dispersity ($Đ_M = M_w/M_n$; ○) against monomer-to-initiator concentration ([M]/[I]) for the ROP of L-LA. Conditions: $[M]_0$ = 2 M in CH_2Cl_2, using 1 mol% TMG and benzyl alcohol as initiator.

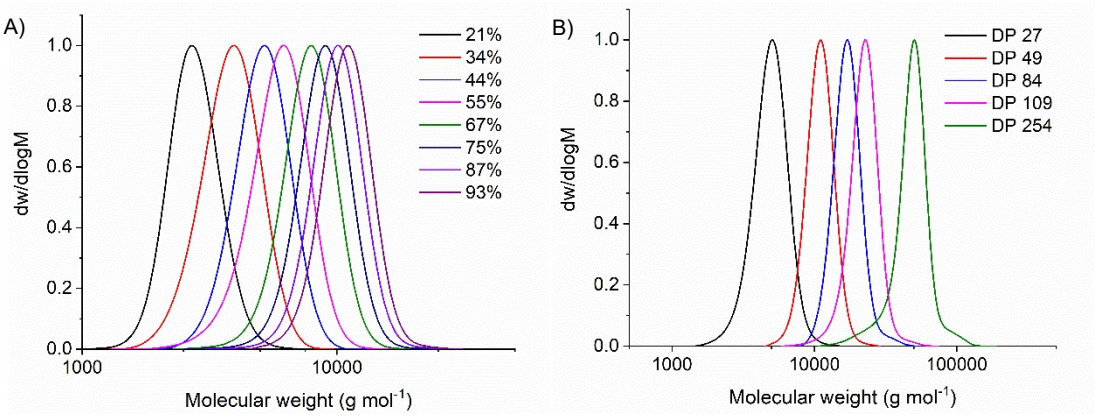

Figure 3.7. Evolution of size exclusion chromatograms of PLLA A) with the monomer conversion ($[M]_0/[I]_0$ = 50) and B) with different DPs varying from 27 to 254 ($CHCl_3$, RI, calibrated against polystyrene standards). Conditions: $[M]_0$ = 2 M in CH_2Cl_2, using 1 mol% TMG and benzyl alcohol as initiator.

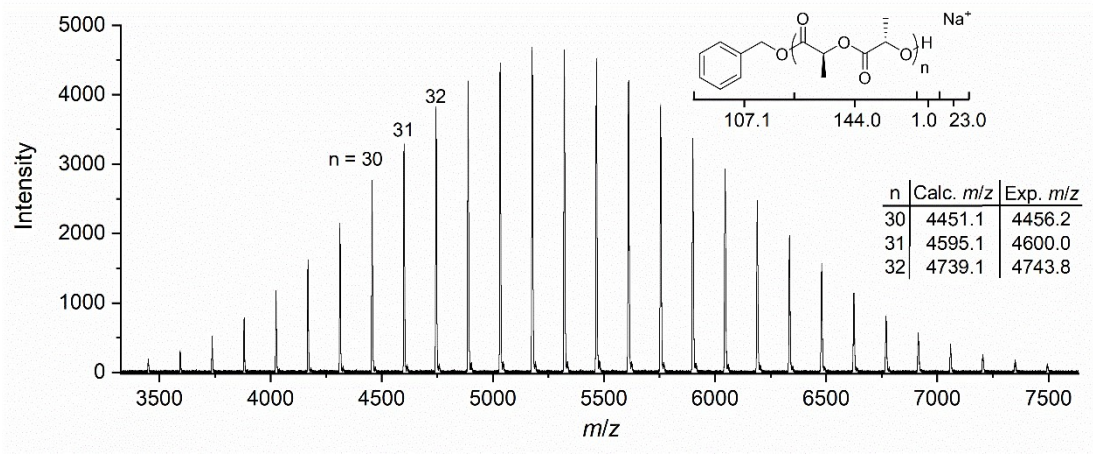

Figure 3.8. MALDI-ToF MS spectrum of PLLA (**3.1**). Conditions: $[M]_0$ = 2 M in CH_2Cl_2, $[M]_0/[I]_0$ = 40, using 1 mol% TMG and benzyl alcohol as initiator.

As with L-LA, the ROP of δ-VL and ε-CL catalysed by TMG was investigated and monitored by ^{1}H NMR spectroscopy. While using 1 mol% of catalyst, no polymerisation occurred for both monomers, increasing the catalyst loading to 5 mol%, only an incomplete initiation was observed in 20 hours for δ-VL (57%) and ε-CL (< 5%) ($[M]_0$ = 2 M in C_6D_6, $[M]_0/[I]_0$ = 60). This was evidenced by the shift in the methylene signal from benzyl alcohol in the ^{1}H NMR spectra before (δ = 4.72 ppm) and after (δ = 4.99 ppm) initiating the polymerisation, which proved the low efficiency of this catalyst for the polymerisation of these lactones (Figure 3.9).

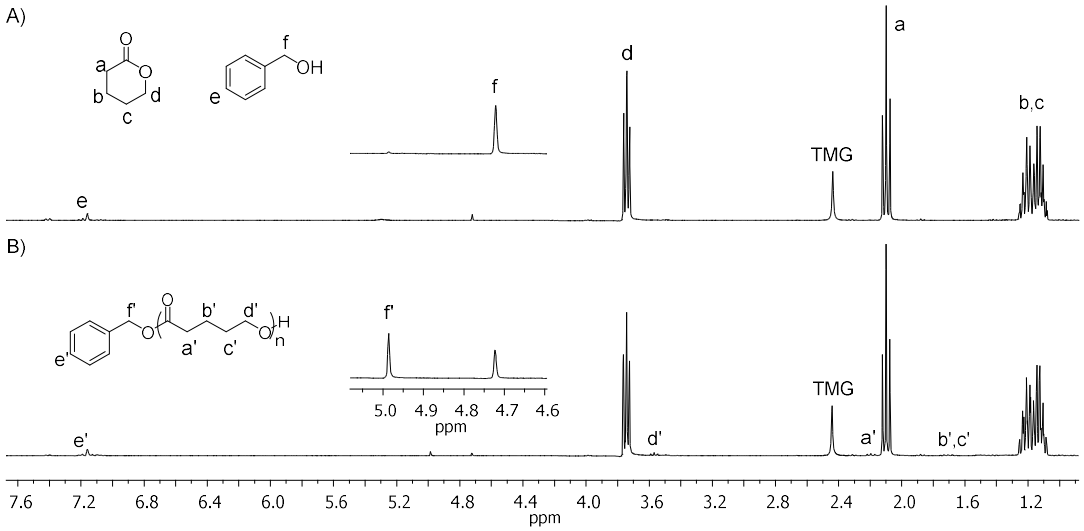

Figure 3.9. ^{1}H NMR spectra during of ROP of δ-VL after A) 30 minutes and B) 20 hours ($CDCl_3$, 300 MHz, 298 K). Conditions: $[M]_0$ = 2 M in C_6D_6, $[M]_0/[I]_0$ = 60, using 5 mol% TMG and benzyl alcohol as initiator.

Similar results were previously reported by Lohmeijer *et al*. that observed the high activity of the superbase DBU as a catalyst for the ROP of L-LA, although it was not effective in the polymerisation of δ-VL even using a catalyst loading of 20 mol%.[22] To enable the use of this catalyst for the polymerisation of δ-VL, the authors utilised a thiourea as a cocatalyst in the presence of DBU, as it had previously demonstrated to decrease the polymerisation times by activating the carbonyl in the monomer.[23] Under these conditions, the polymerisation of δ-VL proceeded to full conversion in 3 hours for a $[M]_0/[I]_0$ of 50. Based on these previous results, our catalyst system comprised of 1-(3,5-bis(trifluoromethyl)phenyl)-3-cyclohexylthiourea (TU) cocatalyst in combination with TMG (TMG/TU (5 mol% each)) (Scheme 3.3). Under these conditions, the polymerisation rate of δ-VL increased significantly, affording a monomer conversion of 93% in 23 hours for a $[M]_0/[I]_0$ of 30. The ^{1}H NMR spectrum of the purified PVL (**3.2**) showed a DP of 24, demonstrated by comparison of the integration of the methylene signals from the benzyl ester end-group at δ = 5.12 ppm and the methylene signals of the polymer backbone at δ = 4.08, 2.34 and 1.68 ppm (Figure 3.10). This catalyst system was also applied for ε-CL; however, the formation of PCL (**3.3**) was still considerably slow, with a $[M]_0/[I]_0$ of 25 requiring 15 days to provide a monomer conversion of 96% (Figure 3.11).

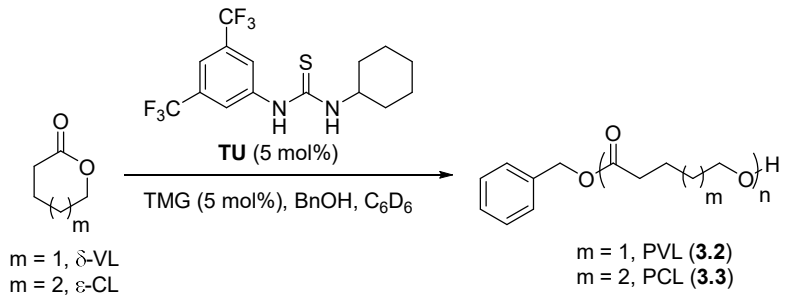

Scheme 3.3. ROP of δ-VL or ε-CL catalysed by the system of TMG and TU.

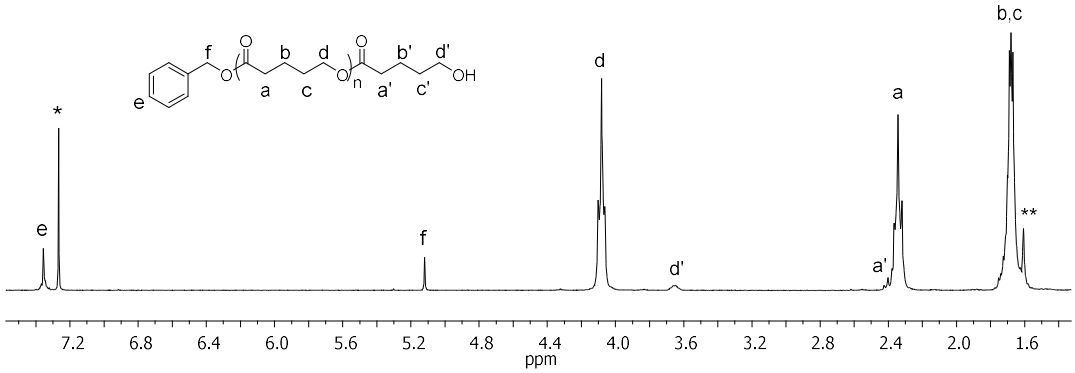

Figure 3.10. ^{1}H NMR spectrum of PVL (**3.2**) ($CDCl_3$, 300 MHz, 298 K, * = $CHCl_3$, ** = H_2O). Conditions: $[M]_0$ = 2 M in C_6D_6, $[M]_0/[I]_0$ = 30, using 5 mol% TMG, 5 mol% TU and benzyl alcohol as initiator.

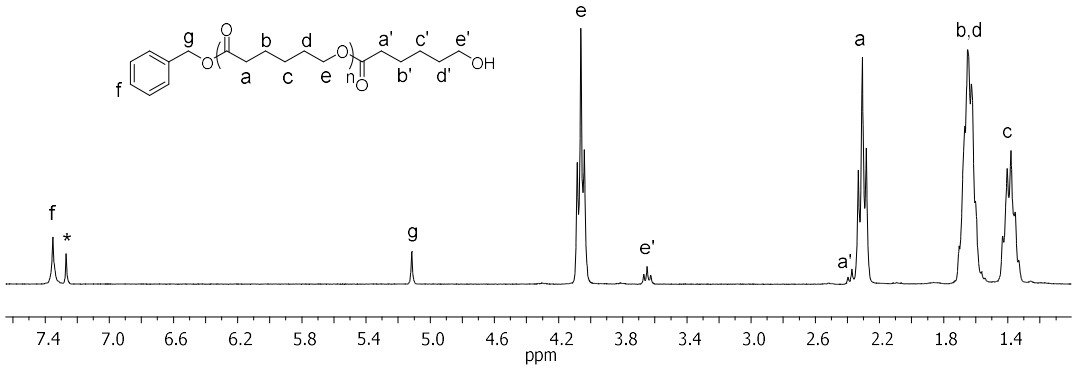

Figure 3.11. ^{1}H NMR spectrum of PCL (**3.3**) ($CDCl_3$, 300 MHz, 298 K, * = $CHCl_3$). Conditions: $[M]_0$ = 2 M in C_6D_6, $[M]_0/[I]_0$ = 25, using 5 mol% TMG, 5 mol% TU and benzyl alcohol as initiator.

The polymerisation of both monomers was shown to proceed in a controlled manner, providing a linear relationship between $\ln([M]_0/[M]_t)$ and time (Figure 3.12). In particular, the polymerisation of δ-VL showed a linear increase of the molecular

weight with the monomer conversion along with low dispersity values and monomodal distributions, which demonstrated the controlled nature of the system (Figure 3.13). Similar results were observed for the ROP of ε-CL, although high molecular weight shoulders were obtained at monomer conversions above 90%, which indicated that undesirable transesterification was occurring (Figure 3.14). Finally, the MALDI-ToF MS spectra revealed a single distribution for both polymers, with a spacing of 100 *m*/*z* for the δ-VL unit and 114 *m*/*z* for ε-CL and peaks that correspond to the sodium cationised species initiated from benzyl alcohol, which confirmed a high end-group fidelity (Figure 3.15).

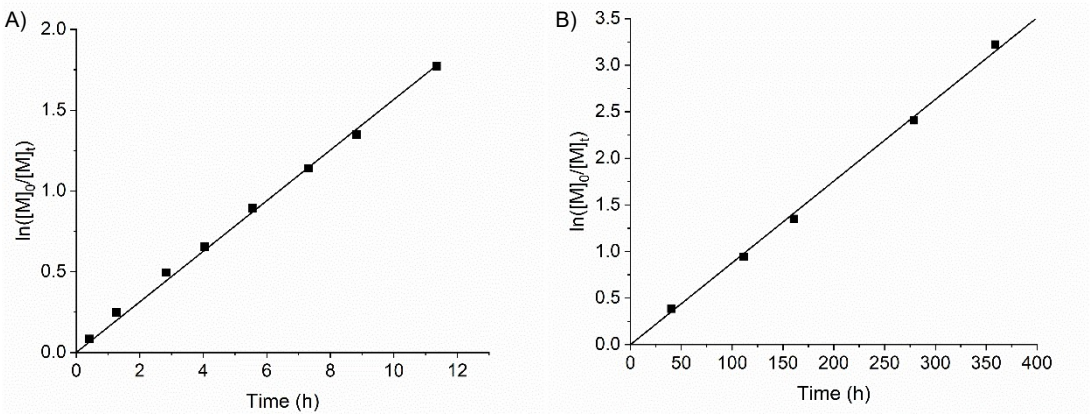

Figure 3.12. Kinetic plot of ln of initial monomer concentration by monomer concentration ($\ln([M]_0/[M]_t)$) against time for the ROP of A) δ-VL and B) ε-CL. Conditions: $[M]_0$ = 2 M in C_6D_6, using 5 mol% TMG, 5 mol% TU, and benzyl alcohol as initiator; δ-VL: $[M]_0/[I]_0$ = 30, ε-CL $[M]_0/[I]_0$ = 25.

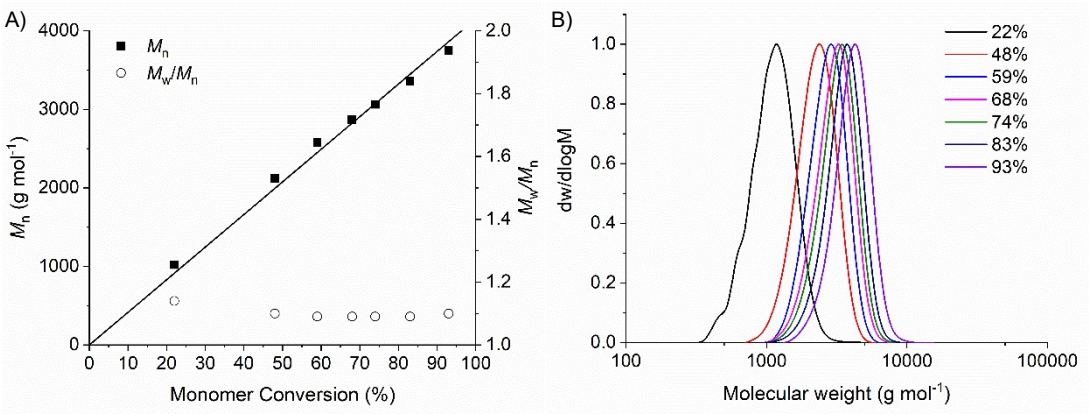

Figure 3.13. A) Number-average molecular weight (M_n; ■) and dispersity ($Đ_M$ = M_w/M_n; ○) against monomer conversion for the ROP of δ-VL and B) evolution of size exclusion chromatograms of PVL with the monomer conversion ($CHCl_3$, RI, calibrated against polystyrene standards). Conditions: $[M]_0$ = 2 M in C_6D_6, $[M]_0/[I]_0$ = 30, using 5 mol% TMG, 5 mol% TU, and benzyl alcohol as initiator.

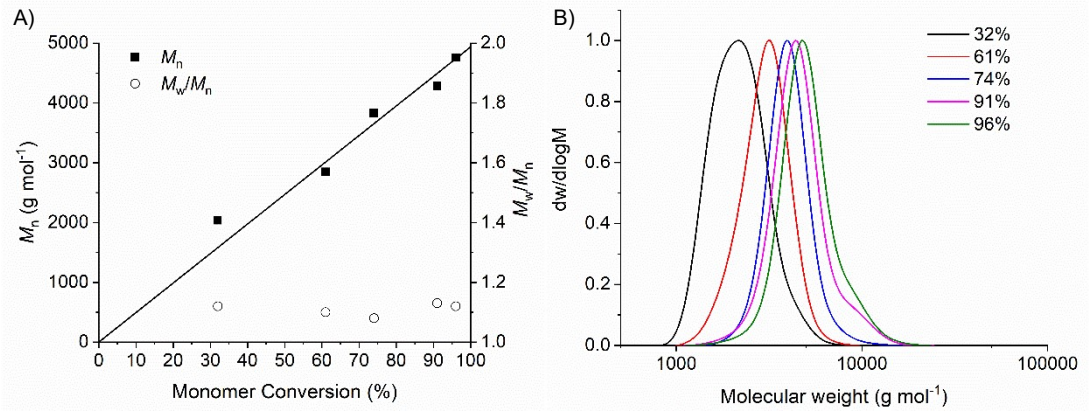

Figure 3.14. A) Number-average molecular weight (M_n; ■) and dispersity ($Đ_M$ = M_w/M_n; ○) against monomer conversion for the ROP of ε-CL and B) evolution of size exclusion chromatograms of PCL with the monomer conversion ($CHCl_3$, RI, calibrated against polystyrene standards). Conditions: $[M]_0$ = 2 M in C_6D_6, $[M]_0/[I]_0$ = 25, using 5 mol% TMG, 5 mol% TU, and benzyl alcohol as initiator.

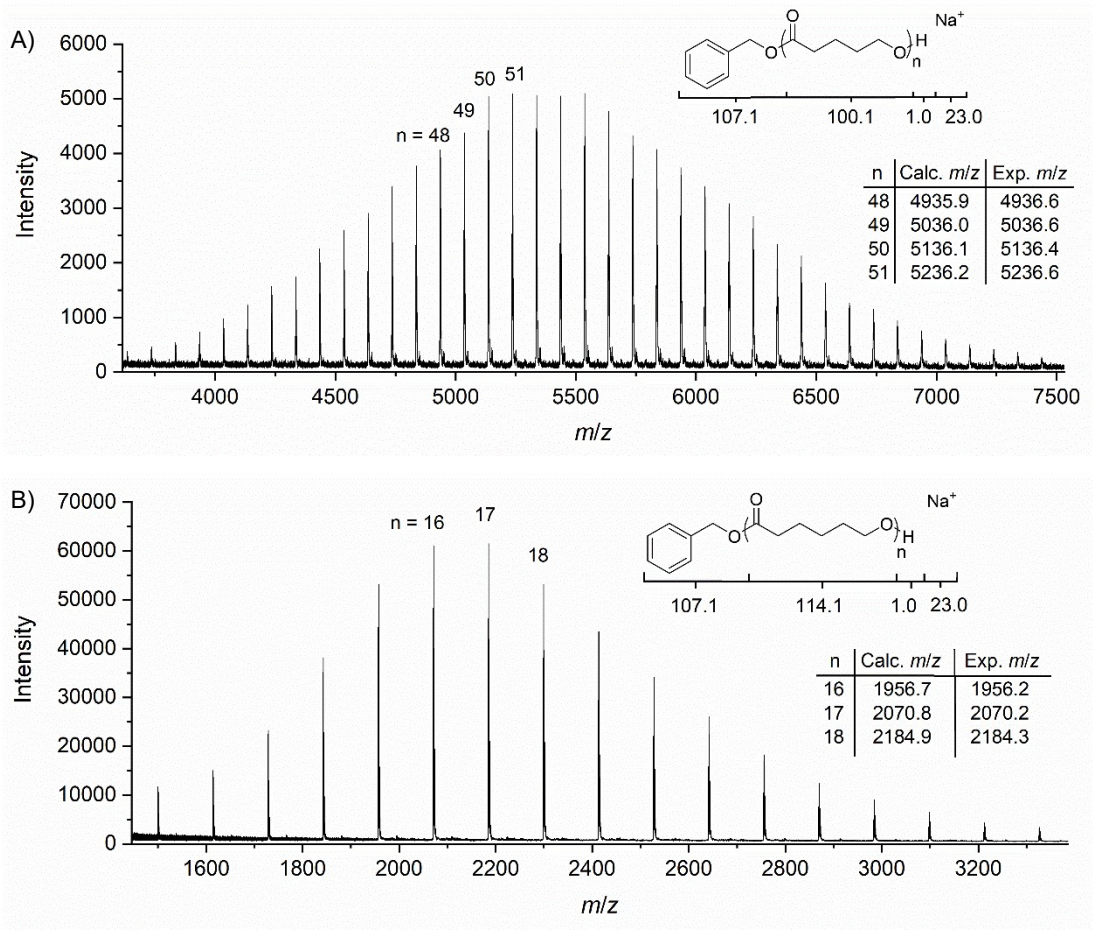

Figure 3.15. MALDI-ToF MS spectra of A) PVL (**3.2**) ($[M]_0/[I]_0$ = 55) and B) PCL (**3.3**) ($[M]_0/[I]_0$ = 20). Conditions: $[M]_0$ = 2 M in C_6D_6, using 5 mol% TMG, 5 mol% TU, and benzyl alcohol as initiator.

3.2.2 Synthesis of Photobase Generators and Photocleavage Studies

Following the demonstration that the polymerisation of L-LA, δ-VL and ε-CL catalysed by TMG(/TU) was well controlled, we turned our attention to the investigation of PBGs based on coumarin and NPPOC groups. Initially, we focused on the preparation of coumarin-TMG (**3.4**), which was synthesised from the oxidation of 7-diethylamino-4-methylcoumarin (**3.5**) with selenium dioxide, followed by reduction with sodium borohydride to provide the corresponding alcohol **3.6** (Scheme 3.4).[18] The alcohol was then treated with carbonyldiimidazole and subsequently with 4-dimethylaminopyridine (DMAP) and TMG to provide coumarin-TMG (**3.4**) in 12% overall yield. The ^{1}H NMR spectrum of the product was in agreement with the data

reported in the literature, which confirmed the formation of coumarin-TMG (Figure 3.16).

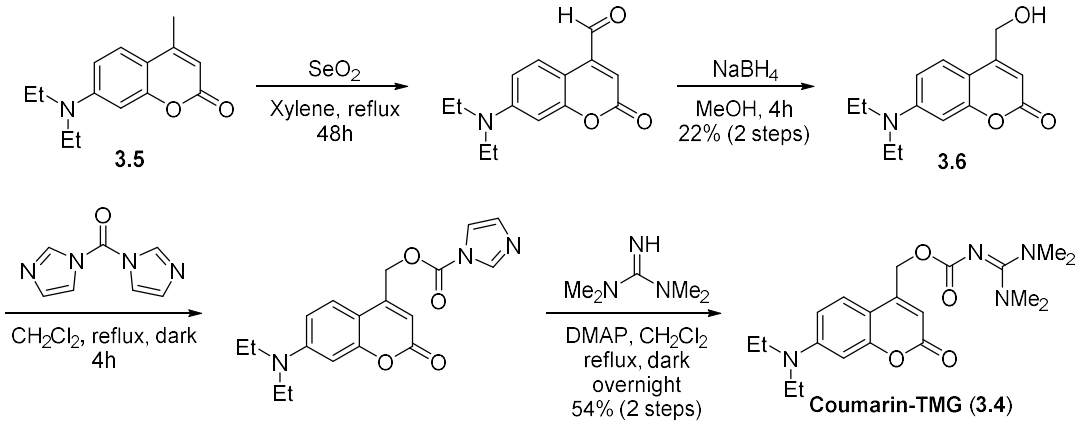

Scheme 3.4. Synthesis of coumarin-TMG (**3.4**).

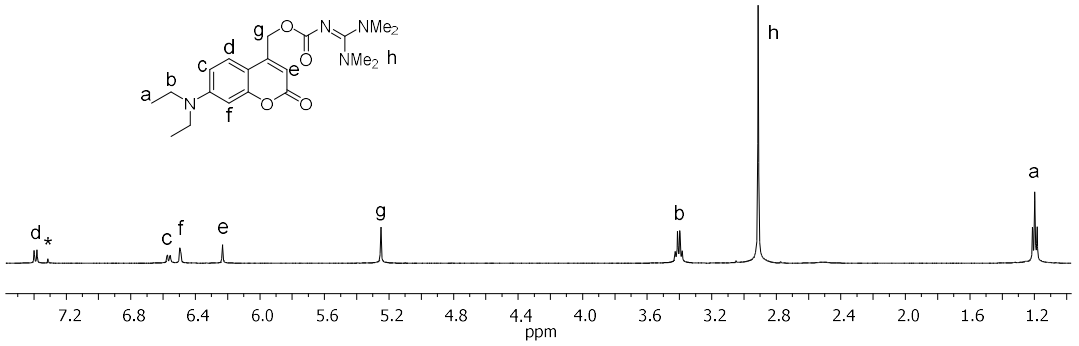

Figure 3.16. ^{1}H NMR spectrum of coumarin-TMG (**3.4**) ($CDCl_3$, 500 MHz 298 K, * = $CHCl_3$).

The photolysis of coumarin-TMG (**3.4**) in protic solvents occurs through a proposed mechanism (Scheme 3.5).[18] The lowest excited singlet state can be achieved upon visible-light irradiation, which can undergo non-radiative decay or fluorescence or a productive heterolysis process. In the second case, a heterolytic C–O bond cleavage forms an ion pair of coumarinylmethyl cation and the carbamate anion. While the cation reacts with nucleophiles or solvent to form a stable coumarin methyl product, the carbamate anion decarboxylates to release CO_2 and free TMG. In the presence of aprotic solvents, the photolysis process takes a non-stablished pathway that has shown a slower degradation rate.

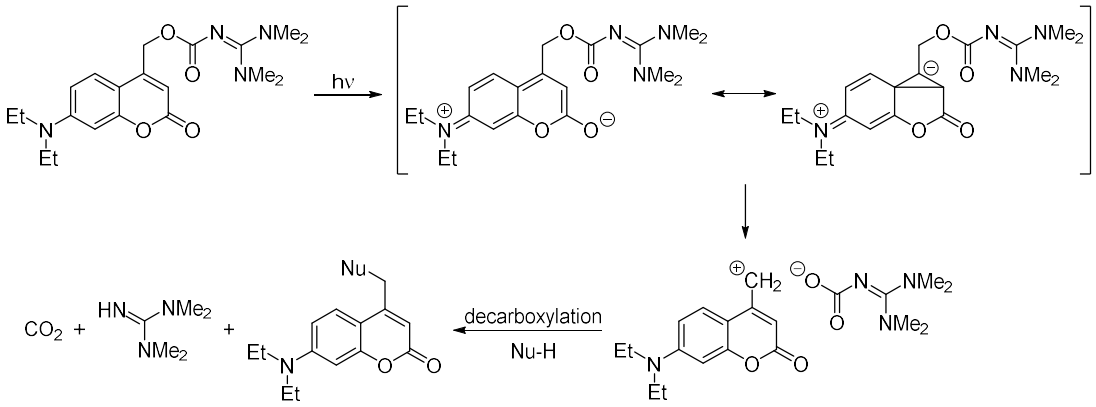

Scheme 3.5. Proposed mechanism for coumarin-TMG (**3.4**) photolysis in the presence of a nucleophile.

As the maximum absorption for coumarin-TMG (**3.4**) in MeCN is at λ = 380 nm (Figure 3.17), the photolysis was then investigated using a commercial curing chamber containing a light source of λ = 320–400 nm (Figure 3.18a). NMR tubes containing the solutions of coumarin-TMG were typically placed in the centre of the chamber, 10 cm away from the source (Figure 3.18b). Considering that protic solvents can affect the degradation rate of TMG, solutions of coumarin-TMG in $CDCl_3$ and CD_3OD (20 mM) were exposed to irradiation and monitored by ^{1}H NMR spectroscopy. A decrease in the integration of the signal at $\delta \sim 2.9$ ppm corresponding to the protected TMG and increase of the free TMG signal at $\delta \sim 3.0$ ppm was observed, which evidenced a photocleavage of 7% in $CDCl_3$ and 9% in CD_3OD after 3 hours (Figure 3.19 and Figure 3.20).

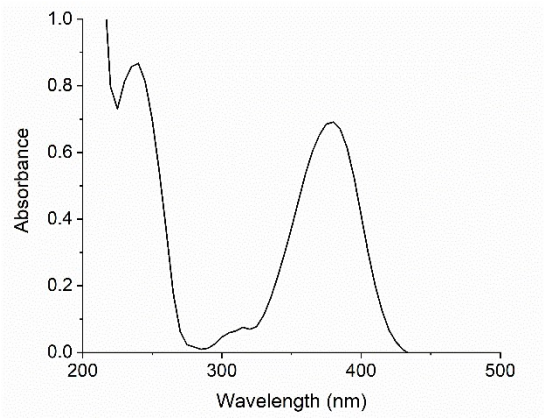

Figure 3.17. UV-Vis spectrum of Coumarin-TMG (**3.4**) (0.04 mM in MeCN).

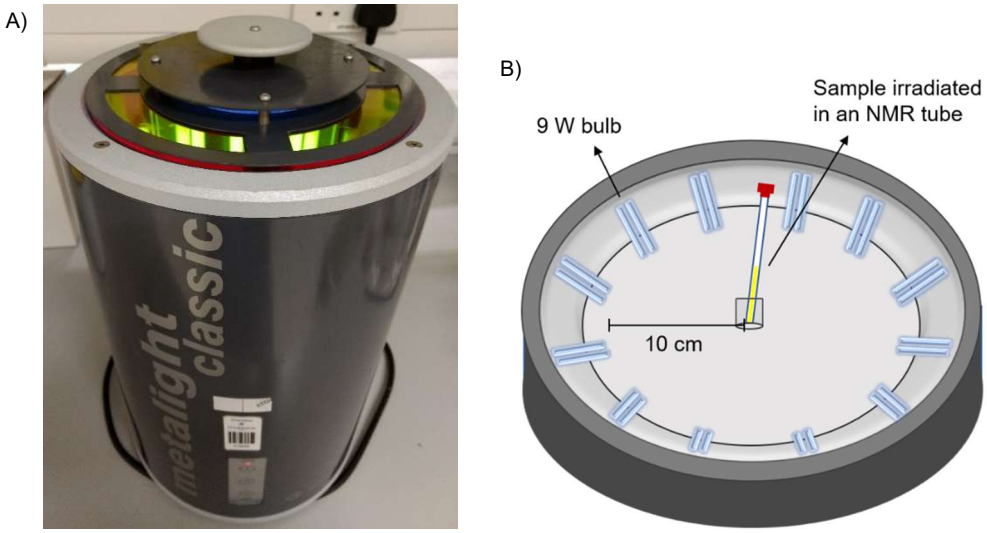

Figure 3.18. A) Photograph of Metalight Classic light chamber and B) Schematic representation of photoreaction setup.

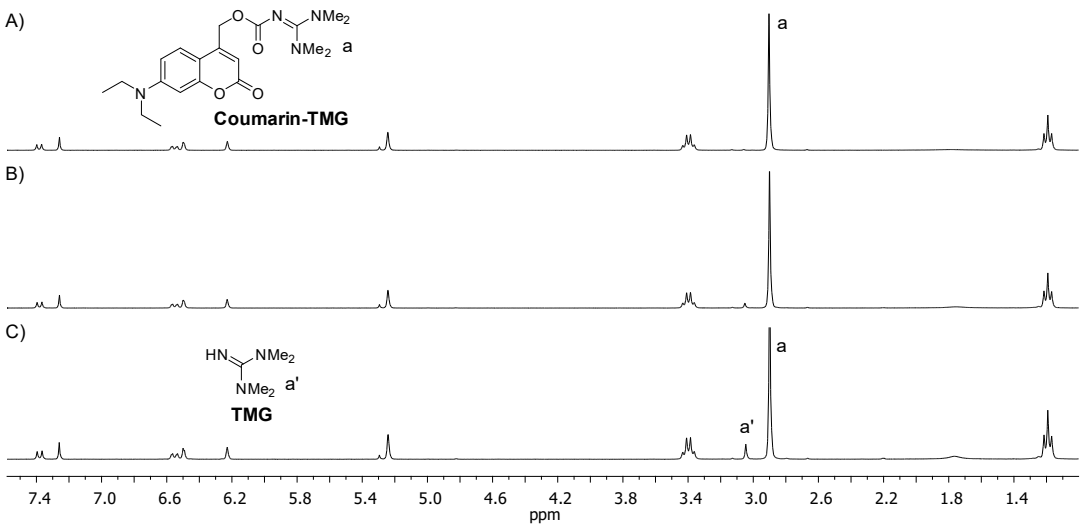

Figure 3.19. ^{1}H NMR spectra of coumarin-TMG (**3.4**) solution in $CDCl_3$ (20 mM) A) before, and after λ = 320–400 nm irradiation for B) 1 hour and C) 3 hours ($CDCl_3$, 300 MHz, 298 K).

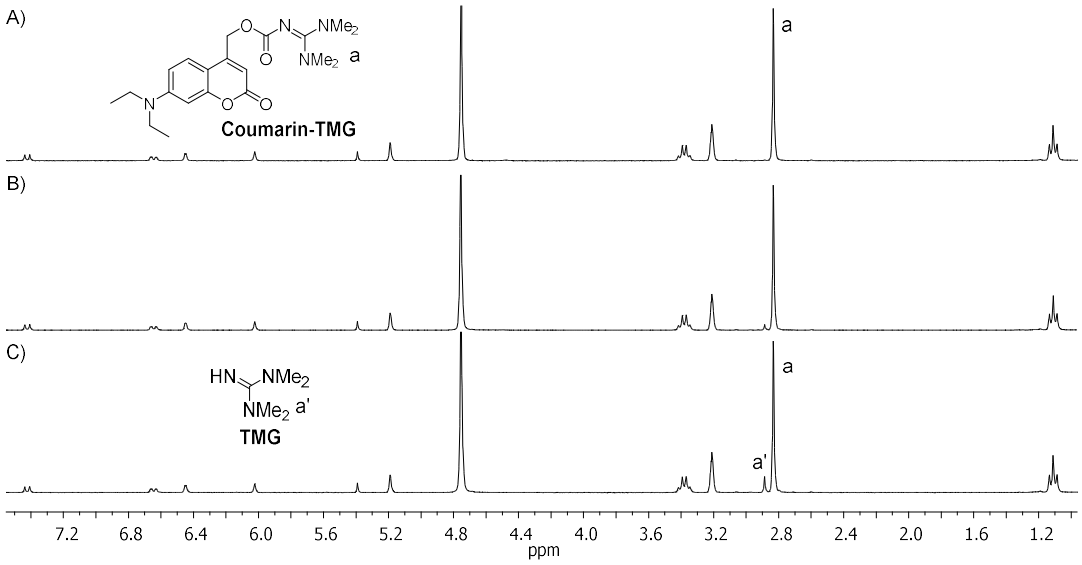

Figure 3.20. ^{1}H NMR spectra of a coumarin-TMG (**3.4**) solution in CD_3OD (20 mM) A) before, and after λ = 320–400 nm irradiation for B) 1 hour and C) 3 hours (CD_3OD, 300 MHz, 298 K).

As we aimed to obtain a temporal control over the polymerisation initiation, the release of TMG should occur as quickly as possible, ideally within minutes. We, therefore, focused on the synthesis of a NPPOC-TMG (**3.7**), as its photolysis has shown to present a higher quantum yield (NPPOC-TMG: Φ = 0.15,[10] coumarin-TMG: Φ = 0.044).[18] Regarding the synthesis, this catalyst is also more advantageous as it can be prepared in a single step from 2-(2-nitrophenyl)propyl chloroformate (**3.8**) in reasonable yields (Scheme 3.6). The ^{1}H NMR spectrum was in agreement with the one reported in the literature, which confirmed the synthesis of the desired PBG (Figure 3.21).[10]

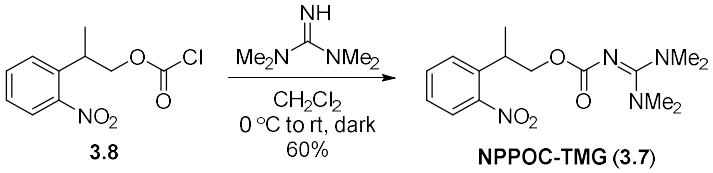

Scheme 3.6. Synthesis of NPPOC-TMG (**3.7**).

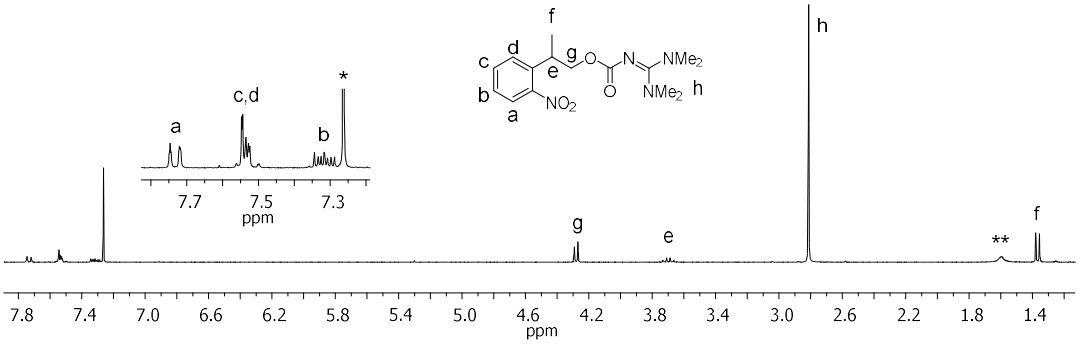

Figure 3.21. ^{1}H NMR spectrum of NPPOC-TMG (**3.7**) ($CDCl_3$, 300 MHz, 298 K, * = $CHCl_3$, ** = H_2O).

The photolysis of NPPOC-TMG (**3.7**) can occur *via* two main pathways, depending if the reaction takes place from the protonated or deprotonated aci-nitro form (Scheme 3.7).[24,25] The protonated aci-nitro decomposes to form the nitro product **1**, which undergoes cyclisation to free TMG. On the other hand, the anion form is cleaved by *β*-elimination, forming nitrostyrene and releasing CO_2 and TMG. The second pathway becomes favoured over time, once the amines are being released and are able to deprotonate the aci-nitro intermediate.

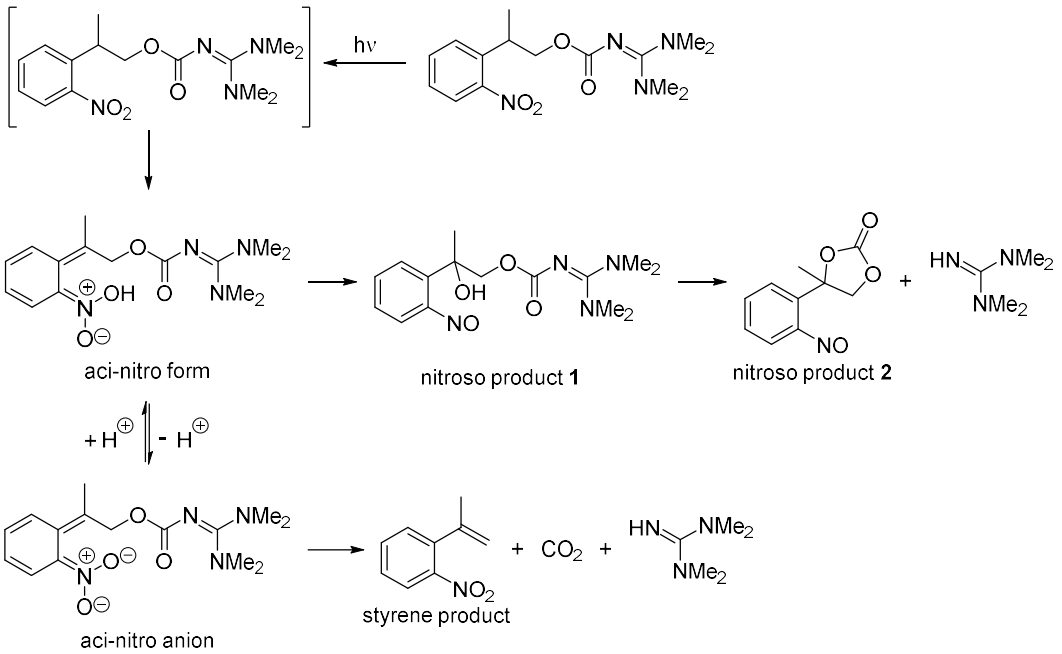

Scheme 3.7. Main photocleavage pathways of NPPOC-TMG (**3.7**).

The photolysis studies were carried out under λ = 320–400 nm irradiation as the UV-Vis spectrum of NPPOC-TMG (**3.7**) showed absorptions up to 380 nm (Figure 3.22). In addition, as the polymerisations of L-LA and δ-VL were carried out in $CDCl_3$ and C_6D_6, respectively, both solvents were investigated herein. Accordingly, a 20 mM solution of NPPOC-TMG (**3.7**) in $CDCl_3$ (equivalent to 1 mol% catalyst and $[M]_0$ = 2 M in the ROP of L-LA), showed 86% release of TMG after 60 minutes UV irradiation, as evidenced by ^{1}H NMR spectroscopy. The spectrum showed a decrease in the integration of the methyl signal in the photoprotected TMG at δ = 2.81 ppm and an increase of the corresponding signal for the free base at δ = 2.74 ppm (Figure 3.23). In addition, the signals from the NPPOC protecting group decreased as the sample was irradiated, while the appearance of signals at δ = 7.85, 5.15, 4.94 and 2.09 pm indicated the formation of the main byproduct nitrostyrene (Figure 3.23c). Similarly, the photolysis of a 100 mM solution of NPPOC-TMG (**3.7**) in C_6D_6 (equivalent to 5 mol% catalyst and $[M]_0$ = 2 M in the ROP of δ-VL) was monitored by ^{1}H NMR spectroscopy, which showed 81% TMG release after 3 hours irradiation. In this solvent, the ^{1}H NMR spectrum displayed a decrease in the methyl signal of NPPOC-TMG (**3.7**) at δ = 2.32 ppm and an increase of the signal at δ = 2.44 ppm corresponding to the free guanidine (Figure 3.24).

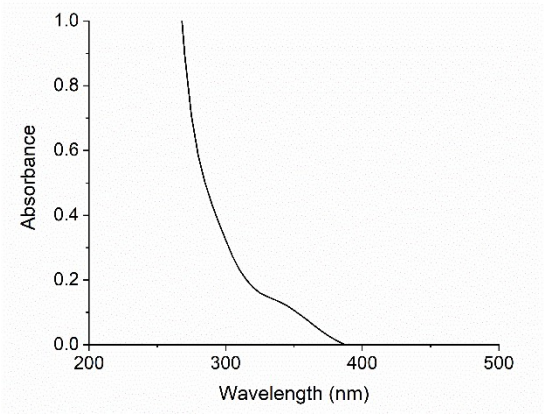

Figure 3.22. UV-Vis spectrum of NPPOC-TMG (**3.7**) (0.3 mM in MeCN).

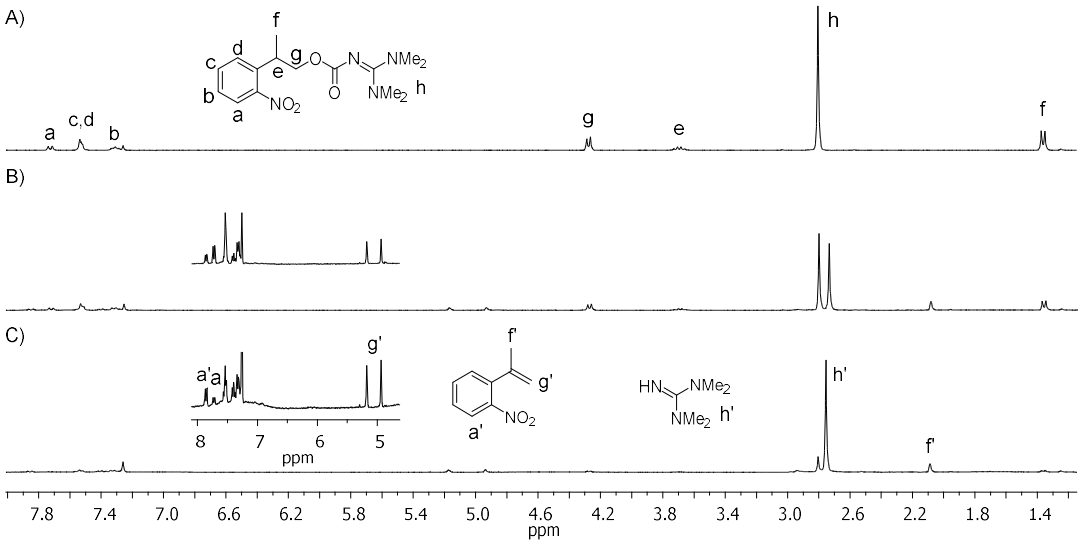

Figure 3.23. ^{1}H NMR spectra of NPPOC-TMG (**3.7**) solution in $CDCl_3$ (20 mM) A) before, and after λ = 320–400 nm irradiation for B) 15 minutes and C) 60 minutes ($CDCl_3$, 300 MHz, 298 K).

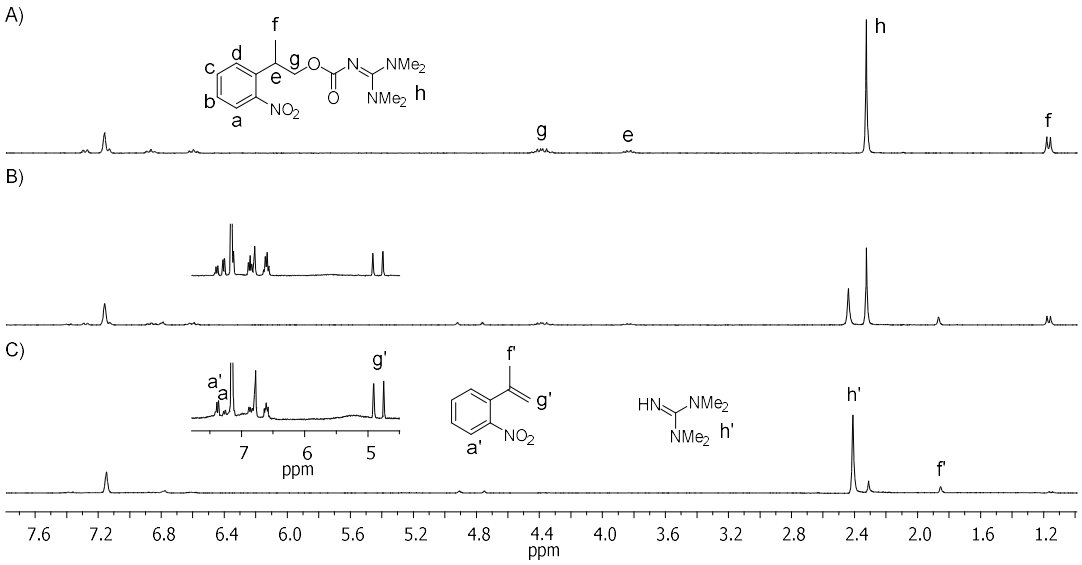

Figure 3.24. ^{1}H NMR spectra of NPPOC-TMG (**3.7**) solution in C_6D_6 (20 mM) A) before, and after λ = 320–400 nm irradiation for B) 15 minutes and C) 60 minutes (C_6D_6, 300 MHz, 298 K).

In order to verify that the difference in the photodegradation times was not caused by the use of different solvents, the photolysis of a 20 mM solution of NPPOC-TMG (**3.7**) in C_6D_6 and a 100 mM solution in $CDCl_3$ were investigated. In this case, the low concentration solution in C_6D_6 showed similar release profile as the 20 mM solution

in $CDCl_3$, with both high concentration solutions also demonstrating comparable results (Figure 3.25). Although the data was acquired only once for each sample, the release profile evidence that the solvents presented no effect on the photolysis rate, although a high dependency on the concentration of the PBG was observed. These results can be explained by the presence of undesirable effects such as scattering and absorption that decreases the efficiency of the photochemical process when high concentrations of the chromophore are used.[2,26]

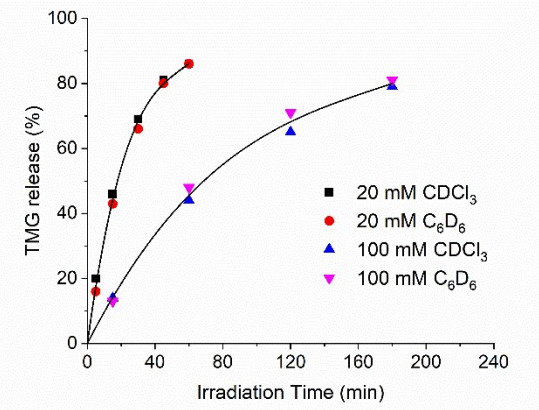

Figure 3.25. Plot of TMG release against irradiation time for NPPOC-TMG (**3.7**) solutions of 20 and 100 mM in both $CDCl_3$ and C_6D_6.

3.2.3 Photoinduced Ring-Opening Polymerisation of Cyclic (Di)esters

Having determined the release rate of TMG by using the NPPOC group, initial investigation of the photoinduced ROP of L-LA comprised on preparing a solution of L-LA, benzyl alcohol and NPPOC-TMG (**3.7**) in $CDCl_3$ ($[M]_0$ = 2 M, $[M]_0/[I]_0/[cat]_0$ = 50:1:0.5, using benzyl alcohol as initiator) and monitoring by ^1H NMR spectroscopy. The spectrum showed no modification of the monomer signals, as well as the presence of the methylene proton resonances of benzyl alcohol at δ = 4.58 ppm, which indicated that no polymerisation had occurred after 24 hours in the absence of light (Figure 3.26a). The polymerisation solution was then exposed to λ = 320–400 nm light for 15 minutes, enough to release the superbase and trigger the ROP of L-LA, which then proceeded in the dark to reach 90% monomer conversion in 3 hours (Figure 3.26). The obtained poly(L-lactic acid) (PLLA) (**3.1**) showed a M_n of 9.9 kg mol^{-1} with a narrow dispersity ($Đ_M$ = 1.1), which was in agreement with the polymerisation catalysed by free TMG (Figure 3.27). However, the polymerisation rate was lower than when the guanidine was used alone, probably as a result of the incomplete release

of the active catalyst into the solution. The signals of the photoprotected and free TMG in the ^{1}H NMR spectrum of the polymerisation solution after irradiation were overlapped, which prevented the calculation of the amount of TMG released (Figure 3.26). The influence of irradiation time was then investigated by preparing polymerisation solutions containing the same concentration of L-LA, benzyl alcohol and catalyst **3.7**. Each sample was individually irradiated for 15, 30 and 45 minutes and quenched after 3 hours from the start of the irradiation. Analysis by ^{1}H NMR spectroscopy revealed monomer conversions of 90%, 94% and 95%, respectively. Considering that the difference in conversions was minimal, the irradiation time of 15 minutes was selected for further experiments.

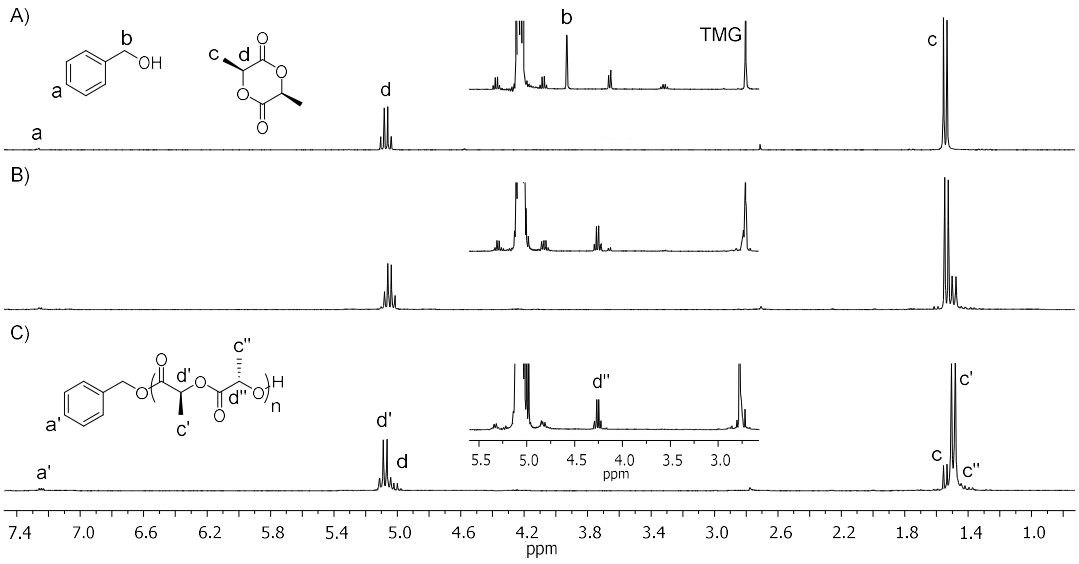

Figure 3.26. ^{1}H NMR spectra of polymerisation of L-LA catalysed by NPPOC-TMG (**3.7**) A) before and B) after λ = 320−400 nm irradiation for 15 minutes and C) after 180 minutes from the start of irradiation ($CDCl_3$, 300 MHz, 298 K). Conditions: $[M]_0$ = 2 M in $CDCl_3$, $[M]_0/[I]_0/[cat]_0$ = 50:1:0.5, using benzyl alcohol as initiator.

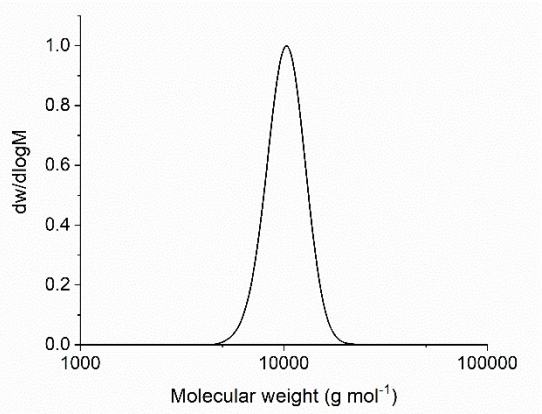

Figure 3.27. Size exclusion chromatogram of PLLA (**3.1**) (M_n = 9.9 kg mol^{-1}, $Đ_M$ = 1.1) ($CHCl_3$, RI, calibrated against polystyrene standards). Conditions: $[M]_0$ = 2 M in $CDCl_3$, $[M]_0/[I]_0/[cat]_0$ = 50:1:0.5, using NPPOC-TMG (**3.7**) as catalyst and benzyl alcohol as initiator, 15 minutes under λ = 320–400 nm irradiation.

To further demonstrate that the reaction occurred only upon UV irradiation, four polymeric solutions containing the same ratio of $[M]_0/[I]_0/[cat]_0$ of 50:1:0.5 were maintained in dark conditions for a determined number of days (*i.e.* 1, 2, 5 or 9 days), and then individually irradiated with UV light for 15 minutes and quenched after 3 hours. In all cases, the monomer conversion, and M_n and $Đ_M$ values were analogous, which confirmed that no polymerisation occurred even after 9 days in the dark (Figure 3.28 and Table 3.1). In addition, almost no initiation was observed when the sample was kept under ambient light for over 24 hours, which indicated that UV irradiation was essential to trigger the ROP of L-LA using our catalyst system. Moreover, no polymerisation took place after irradiation in the absence of NPPOC-TMG (**3.7**), which demonstrated the requirement of PBG to induce the polymerisation.

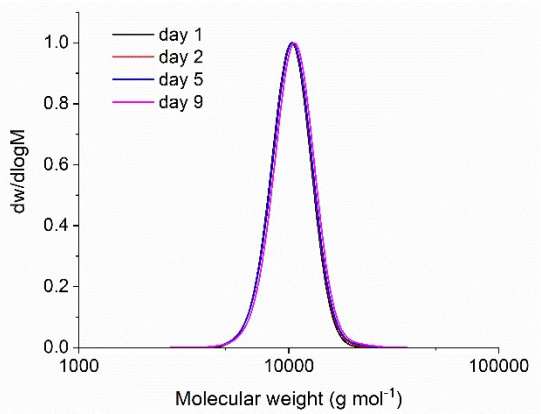

Figure 3.28. Size exclusion chromatograms of PLLA (**3.1**) prepared by maintaining polymerisation solutions in the presence of NPPOC-TMG (**3.7**) in the dark over 1, 2, 5 and 9 days and then irradiating the solutions to photoinduce the ROP of L-LA ($CHCl_3$, RI, calibrated against polystyrene standards). Conditions: $[M]_0$ = 2 M in $CDCl_3$, $[M]_0/[I]_0/[cat]_0$ = 50:1:0.5, using benzyl alcohol as initiator, 15 minutes under λ = 320–400 nm irradiation.

Table 3.1. Monomer conversion and SEC data from the polymerisation of L-LA catalysed by NPPOC-TMG (**3.7**) after leaving 1, 2, 5 and 9 days in the dark and then irradiating with λ = 320–400 nm light.[a]

Days in the dark	Monomer Conversion[b] (%)	M_n[c] (kg mol^{-1})	$Đ_M$[c]
1	90	9.9	1.05
2	90	10.0	1.05
5	91	10.0	1.05
9	91	10.3	1.06

[a] Conditions: $[M]_0$ = 2 M in $CDCl_3$, $[M]_0/[I]_0/[cat]_0$ = 50:1:0.5, using NPPOC-TMG as catalyst and benzyl alcohol as initiator. [b] Determined by ^{1}H NMR spectroscopy. [c] Obtained from SEC analysis in $CHCl_3$, calibrated against polystyrene standards.

The kinetics of the photoinduced ROP of L-LA were investigated, which showed a linear increase of $\ln([M]_0/[M]_t)$ over time, and further linear evolution of M_n with the monomer conversion (Figure 3.29). In addition, a high end-group fidelity was evidenced by MALDI-ToF MS analysis, which revealed a single distribution attributed to the sodium cationised PLLA initiated from benzyl alcohol (Figure 3.30). These data indicated that no side reactions occurred and demonstrated that the

polymerisation was well controlled in a similar fashion as the ROP catalysed by the free TMG.

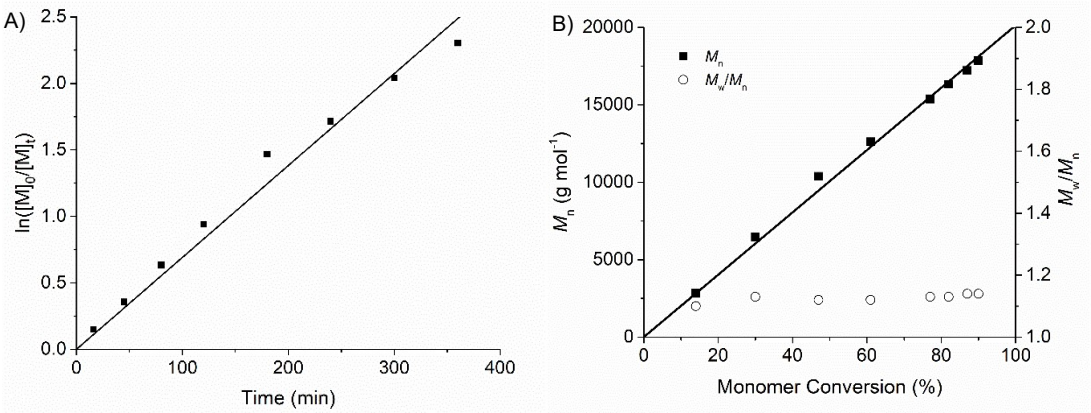

Figure 3.29. Plots of A) ln of initial monomer concentration by monomer concentration ($\ln([M]_0/[M]_t)$) against time for the ROP of L-LA and B) number-average molecular weight (M_n; ■) and dispersity ($Đ_M = M_w/M_n$; ○) against monomer conversion for the ROP of L-LA. Conditions: $[M]_0 = 2$ M, $[M]_0/[I]_0/[cat]_0 = 100:1:1$, using NPPOC-TMG (**3.7**) as catalyst and benzyl alcohol as initiator, 15 minutes of λ = 320–400 nm irradiation.

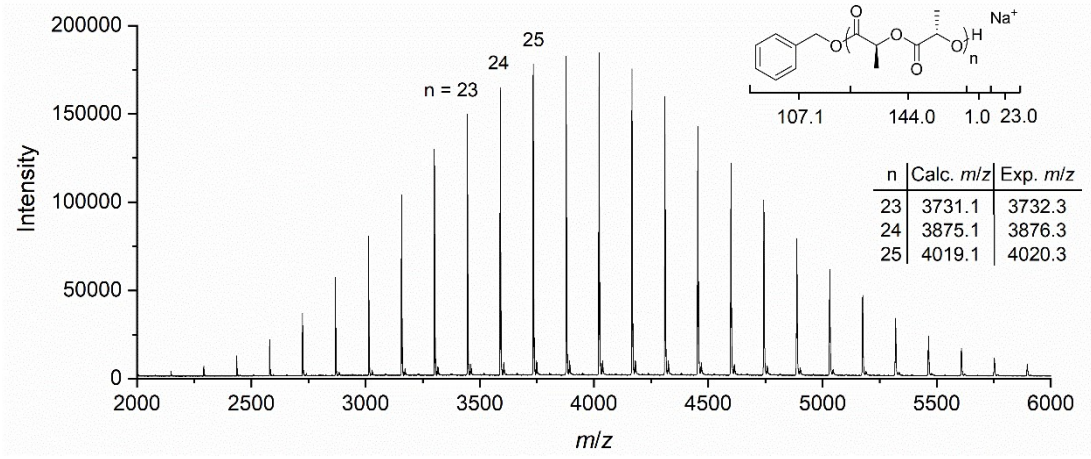

Figure 3.30. MALDI-ToF MS spectrum of PLLA (**3.1**). Conditions: $[M]_0 = 2$ M, $[M]_0/[I]_0/[cat]_0 = 25:1:0.25$, using NPPOC-TMG (**3.7**) as catalyst and benzyl alcohol as initiator, 15 minutes of λ = 320–400 nm irradiation.

Finally, although the irradiation time necessary to release TMG was relatively high for a 100 mM solution of NPPOC-TMG (**3.7**), the photoinduced ROP of δ-VL was investigated under similar conditions to those described for L-LA. Accordingly, a

polymeric solution of δ-VL, benzyl alcohol and NPPOC-TMG (**3.7**) in C_6D_6 ($[M]_0$ = 2 M, $[M]_0/[I]_0/[NPPOC\text{-}TMG]_0/[TU]_0$ = 22:1:1.1:1.1) was monitored by ^{1}H NMR spectroscopy, which revealed the absence of polymerisation after 24 hours in the dark (Figure 3.31a). The polymeric solution was then irradiated with UV light for 3 hours, which induced the ROP of δ-VL. However, the polymerisation occurred at a considerably lower rate than that observed with free TMG, which resulted in a 34% monomer conversion after 76 hours. In addition, TU was shown to be stable when exposed to UV light for 3 hours, which indicated that the slower polymerisation was caused by the incomplete release of TMG.

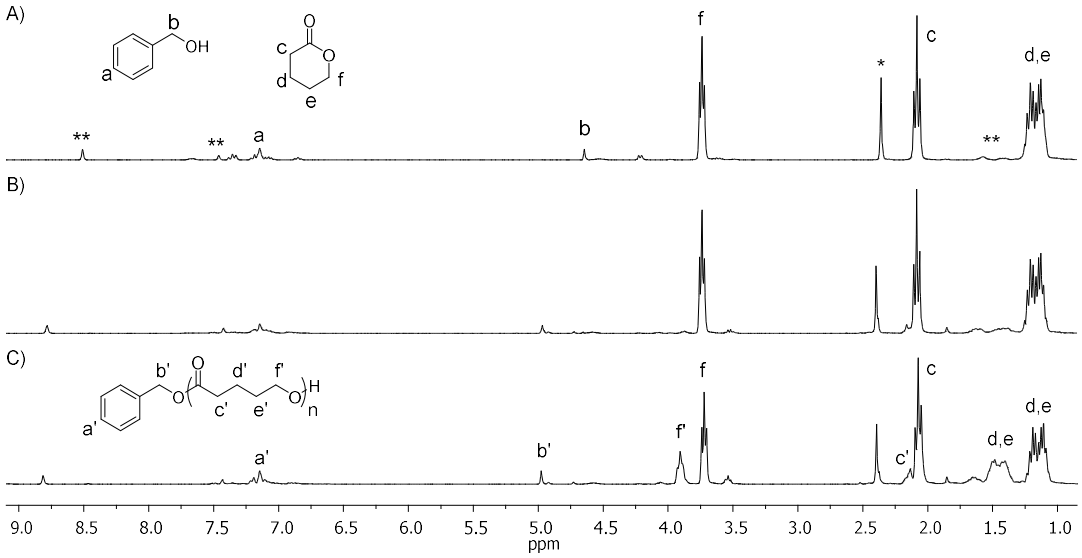

Figure 3.31. ^{1}H NMR spectra of polymerisation of δ-VL catalysed by NPPOC-TMG (**3.7**) and TU A) before and B) after λ = 320−400 nm irradiation for 3 hours and C) after 76 hours from the start of irradiation (C_6D_6, 300 MHz, 298 K, * = (NPPOC-)TMG, ** = TU). Conditions: ($[M]_0$ = 2 M, $[M]_0/[I]_0/[NPPOC\text{-}TMG]_0/[TU]_0$ = 22:1:1.1:1.1, using benzyl alcohol as initiator.

This photoinduced catalyst system, although provided slow polymerisation for δ-VL, was shown to be very efficient in producing well-defined PLLA with short irradiation times (15 minutes) and using low-energy UV light (λ > 300 nm). However, this methodology presented slower polymerisation rates than that applied by Placet *et al.*,[15] who demonstrated the ROP of L-LA ($[M]_0/[I]_0/[cat]_0$ = 134:1.9:1) achieving full monomer conversions in 10 minutes *vs* 3 hours (($[M]_0/[I]_0/[cat]_0$ = 50:1:0.5) for our catalyst system. Still, the strategy presented in this thesis showed to be more efficient

in terms of the light source employed when compared to the methodologies applied by Wang and coworkers and Placet *et at*., who utilised irradiation at λ = 254 nm.[13]

3.3 Conclusions

In this work, the use of TMG, a commercially available superbase, was demonstrated for the first time in the organocatalysed ROP of cyclic (di)esters. The ROP of L-LA catalysed by 1 mol% of TMG was shown to be well controlled, providing polymers with low dispersity values and predictable molecular weights based on $[M]_0/[I]_0$. TMG demonstrated low activity for δ-VL, which was shown to be enhanced by the use of a TU cocatalyst. Under these conditions, polymers with controlled molecular weight and narrow dispersity values were obtained. The same catalyst system was employed in the ROP of ε-CL and, although the polymerisation rate was considerably lower, it was able to afford well-defined polyesters. Overall, TMG displayed comparable reactivity to amidines such as DBU, which demonstrated an excellent addition to the highly active catalyst group for ROP.

In a second stage, the activity of TMG was inhibited by the incorporation of photocaging groups (*i.e*. coumarin or NPPOC) to allow the controlled release of active TMG upon irradiation. Unfortunately, a 20 mM solution of coumarin-TMG provided very slow photolysis, generating only 7% of guanidine in 3 hours. In contrast, a solution of the same concentration of NPPOC-TMG showed a TMG release of 86% within 60 minutes irradiation. Notably, the photolysis of NPPOC-TMG appeared to be very concentration-dependent, with a solution containing 5 times more catalyst requiring 3 hours to produce similar quantities of TMG.

Once the photodegradation profile was investigated, the photocaged catalyst was applied in the photoinduced ROP of L-LA, which showed no polymerisation occurring up to 9 days in the absence of light, whereas upon 15 minutes under λ = 320–400 nm irradiation, the polymerisation of L-LA was triggered and proceeded in the dark, reaching 90% monomer conversion in 3 hours. Furthermore, this polymerisation system was able to provide well-defined polyesters in a similar way as that employing free TMG, which indicated the absence of side reactions occurring by the presence of byproducts. This work demonstrated the precise temporal control over the polymerisation initiation, which opens new routes to the investigation of a system comprising NPPOC-TMG and L-LA in the spatial resolution for advanced applications such as photopatterning.

3.4 References

1. F. A. Leibfarth, K. M. Mattson, B. P. Fors, H. A. Collins and C. J. Hawker, *Angew. Chem. Int. Ed.*, 2013, **52**, 199.
2. R. Göstl, A. Senf and S. Hecht, *Chem. Soc. Rev.*, 2014, **43**, 1982.
3. R. S. Stoll and S. Hecht, *Angew. Chem. Int. Ed.*, 2010, **49**, 5054.
4. A. J. Teator, D. N. Lastovickova and C. W. Bielawski, *Chem. Rev.*, 2016, **116**, 1969.
5. S. P. Ihrig, F. Eisenreich and S. Hecht, *Chem. Commun.*, 2019, **55**, 4290.
6. B. M. Neilson and C. W. Bielawski, *Chem. Commun.*, 2013, **49**, 5453.
7. C. Fu, J. Xu and C. Boyer, *Chem. Commun.*, 2016, **52**, 7126.
8. Z. Dai, Y. Cui, C. Chen and J. Wu, *Chem. Commun.*, 2016, **52**, 8826.
9. F. Eisenreich, M. Kathan, A. Dallmann, S. P. Ihrig, T. Schwaar, B. M. Schmidt and S. Hecht, *Nature Catalysis*, 2018.
10. W. Xi, H. Peng, A. Aguirre-Soto, C. J. Kloxin, J. W. Stansbury and C. N. Bowman, *Macromolecules*, 2014, **47**, 6159.
11. D. Bratton, D. Yang, J. Dai and C. K. Ober, *Polym. Adv. Technol.*, 2006, **17**, 94.
12. J. V. Crivello and E. Reichmanis, *Chem. Mater.*, 2014, **26**, 533.
13. X. Sun, J. P. Gao and Z. Y. Wang, *J. Am. Chem. Soc.*, 2008, **130**, 8130.
14. I. A. Barker and A. P. Dove, *Chem. Commun.*, 2013, **49**, 1205.
15. E. Placet, J. Pinaud, O. Gimello and P. Lacroix-Desmazes, *ACS Macro Lett.*, 2018, **7**, 688.
16. K. Suyama and M. Shirai, *Prog. Polym. Sci.*, 2009, **34**, 194.
17. M. Eckert-Maksić, Z. Glasovac, P. Trošelj, A. Kütt, T. Rodima, I. Koppel and I. A. Koppel, *Eur. J. Org. Chem.*, 2008, **2008**, 5176.
18. X. Zhang, W. Xi, C. Wang, M. Podgórski and C. N. Bowman, *ACS Macro Lett.*, 2016, **5**, 229.
19. B. A. Chan, S. Xuan, M. Horton and D. Zhang, *Macromolecules*, 2016, **49**, 2002.
20. I. Kaljurand, A. Kütt, L. Sooväli, T. Rodima, V. Mäemets, I. Leito and I. A. Koppel, *J. Org. Chem.*, 2005, **70**, 1019.
21. L. Zhang, R. C. Pratt, F. Nederberg, H. W. Horn, J. E. Rice, R. M. Waymouth, C. G. Wade and J. L. Hedrick, *Macromolecules*, 2010, **43**, 1660.

22. B. G. G. Lohmeijer, R. C. Pratt, F. Leibfarth, J. W. Logan, D. A. Long, A. P. Dove, F. Nederberg, J. Choi, C. Wade, R. M. Waymouth and J. L. Hedrick, *Macromolecules*, 2006, **39**, 8574.
23. R. C. Pratt, B. G. G. Lohmeijer, D. A. Long, P. N. P. Lundberg, A. P. Dove, H. Li, C. G. Wade, R. M. Waymouth and J. L. Hedrick, *Macromolecules*, 2006, **39**, 7863.
24. A. Hasan, K.-P. Stengele, H. Giegrich, P. Cornwell, K. R. Isham, R. A. Sachleben, W. Pfleiderer and R. S. Foote, *Tetrahedron*, 1997, **53**, 4247.
25. D. Wöll, J. Smirnova, M. Galetskaya, T. Prykota, J. Bühler, K.-P. Stengele, W. Pfleiderer and U. E. Steiner, *Chem. Eur. J.*, 2008, **14**, 6490.
26. S. C. Ligon, R. Liska, J. Stampfl, M. Gurr and R. Mülhaupt, *Chem. Rev.*, 2017, **117**, 10212.

Chapter 4

Synthesis of a Bis(Cyclic Diester) as a Crosslinker in Ring-Opening Polymerisation

4.1 Introduction

Temporal and spatial control over polymerisations using light as an external stimulus has found high-value applications, such as in the preparation of microelectronic devices[1] and DNA microarrays.[2,3] While temporal control can be achieved by irradiating a particular wavelength to induce photochemical reactions, spatial resolution concerns the focussing of light in defined areas so that the reaction occurs only in the irradiated space. Photopatterning is a prime example of a spatial control technique where a resin is selectively polymerised using a photomask that allows light to penetrate through a defined pattern (Figure 4.1).[4] In addition, the fast crosslinking of the resin is essential to avoid the diffusion of active species that compromises the resolution of the final material.[5] Finally, the process is completed by removing unreacted resin with simple washes to furnish a crosslinked material with a defined pattern provided by the photomask.

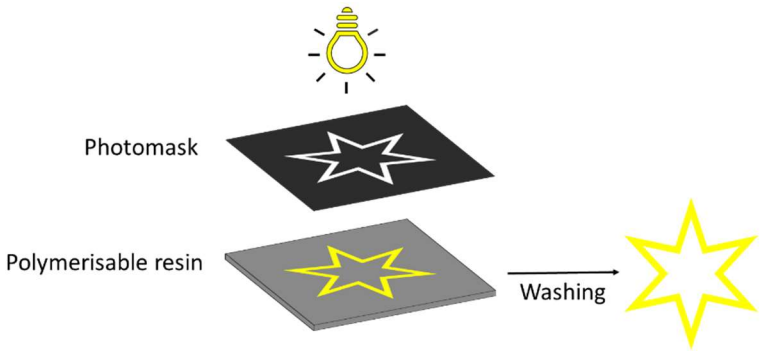

Figure 4.1. Illustration of a photopatterning process.

Resins that are commonly used in photopatterning processes are typically composed of epoxides or acrylates that are suitable for ring-opening or radical photopolymerisation, respectively. Although these crosslinking processes are robust, the resultant materials often possess poor biodegradability and/or biocompatibility.[4] Alternatively, thiol-ene and thiol-Michael reactions of small multi-functional molecules have been investigated in the preparation of polymeric networks.[5-8] The most commonly utilised thiols contain ester moieties that provides degradability to the materials; however the potential toxicity of the resulting degradation products present concerns regarding their biocompatibility.[9,10] Nevertheless, materials prepared from aliphatic polyesters or polycarbonates have the advantage of applying stablished biodegradable and biocompatible polymers.[11,12] They have been utilised in

photopolymerisation strategies by functionalising the end-groups with acrylate to promote the crosslinking *via* a radical photopolymerisation.[13-15] However, unreacted acrylates in the resin can present toxicity issues, and the formation of non-degradable moieties in the material can decrease their overall biodegradability and biocompatibility.[13,16]

In order to obtain more efficient photopolymerisation systems, we demonstrated in Chapter 3 the excellent temporal control of 2-(2-nitrophenyl)propoxycarbonyl 1,1,3,3-tetramethylguanidine (NPPOC-TMG), a photo-responsive base, for the ring-opening polymerisation (ROP) of L-lactide (L-LA). However, to apply this system to further obtain spatial control, the use of a bicyclic monomer that can be polymerised *via* ROP is essential to enable the formation of a network. The synthesis of such crosslinkers based on ε-caprolactone (ε-CL)[17] and trimethylene carbonate (TMC)[18] have been reported in the literature; however, TMG showed low activity for these monomers and was only effective for the polymerisation of L-LA (refer to Chapter 3). As such, we envisioned that a bis(cyclic diester) possessing a reactivity profile similar to L-LA would be an ideal crosslinker for this system.

In this regard, the synthesis of functional cyclic diesters typically involves the cyclisation of α-hydroxy acids *via* two different approaches. The first one comprises the dimerisation of α-hydroxy acids in the presence of *p*-toluenesulfonic acid (PTSA) to furnish a homobifunctional lactide (Scheme 4.1a).[19,20] While this strategy utilises highly diluted conditions to minimise the undesirable formation of oligomers *via* intermolecular condensation, this side reaction cannot be prevented entirely, and it often results in decreased product yields (< 40% yield in most cases).[21] Alternatively, the condensation of α-hydroxy acids with α-haloacyl halides followed by a base-mediated cyclisation can yield heterobifunctional cyclic diesters (Scheme 4.1b).[22,23] Although this reaction can also produce undesirable oligomers, the product yields can be increased to near 60% by employing *pseudo*-high dilution conditions (*i.e.* slow addition of a prediluted solution of haloacyl ester into a diluted solution of a base).[24] Moreover, this strategy is more versatile, as it allows the incorporation of two different functionalities into a single monomer.

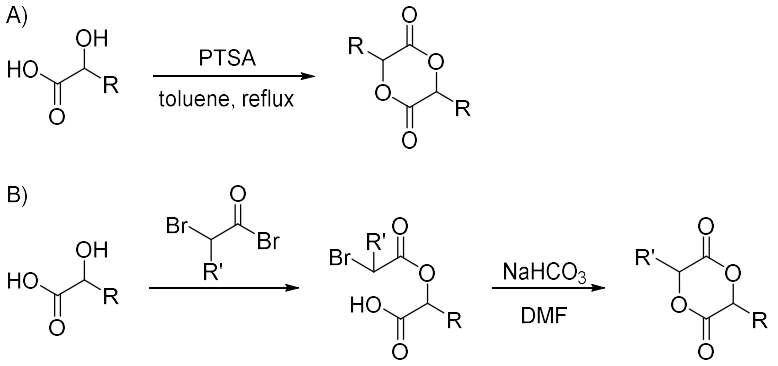

Scheme 4.1. Synthesis of functional cyclic diesters *via* A) dimerisation of α-hydroxy acids or B) condensation of α-haloacyl halide and subsequent cyclisation.

The installation of a reactive group in the side chain of α-hydroxy acids is essential to prepare functional cyclic diesters. In this regard, α-amino acids containing additional functionality (*i.e.* hydroxy, amino, carboxylic acid) can be converted into the corresponding α-hydroxy acids *via* diazotisation in an acidic aqueous medium (Scheme 4.2).[25] Since the side groups can interfere in the diazotisation and/or cyclisation reactions, protecting groups were utilised, and resulted in the synthesis of a series of functional cyclic diesters *via* coupling with α-haloacyl halides (Scheme 4.2b).[22,26] Alternatively, our group demonstrated that commercially available functional α-hydroxy acids such as L-malic acid could be a useful starting material to prepare cyclic diesters.[24] However, an acetal protecting group was required to allow the installation of the benzyl group in a single carboxylic acid (Scheme 4.3). Nevertheless, this synthetic route proved to be very efficient, as the cyclic diester was obtained in higher yields than previous routes starting from aspartic acid.[22]

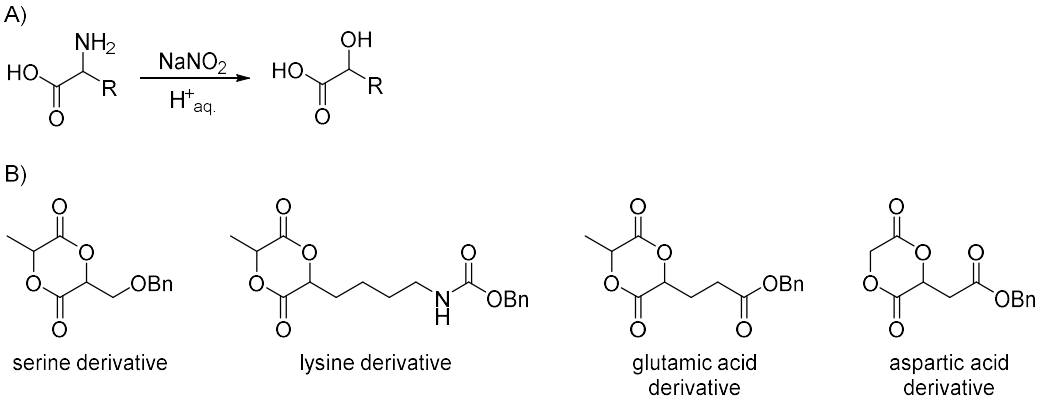

Scheme 4.2. A) Synthesis of α-hydroxy acids *via* the diazotisation of amino acids in acidic aqueous solution and B) cyclic diesters prepared from α-amino acids.

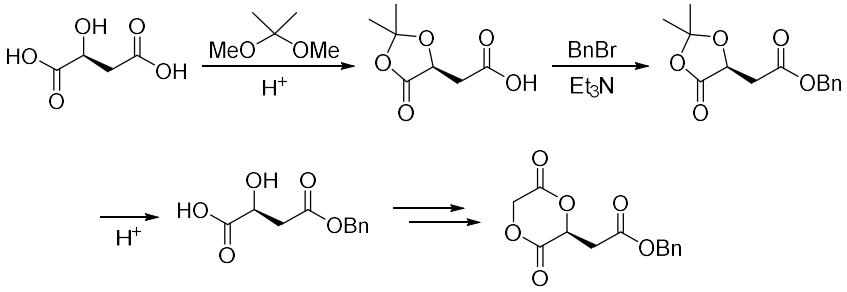

Scheme 4.3. Synthesis of a cyclic diester from L-malic acid.

The synthesis of cyclic diesters containing other reactive moieties, such as an alkene or alkyne, has also been reported. Jiang *et al*. described the preparation of a propargyl-functional cyclic diester *via* a Barbier-type propargylation of ethyl glyoxylate with subsequent hydrolysis. (Scheme 4.4a).[19] The resultant hydroxy acid was cyclised by dimerisation with PTSA or by condensation with an α-haloacyl halide.[27,28] Utilising a similar strategy, Leemhuis *et al*. synthesised an allyl-functional glycolide using a Barbier-type addition of allyl bromide to glyoxylic acid to furnish the corresponding allyl-glyoxylic acid (Scheme 4.4b).[29] The cyclisation step was accomplished by condensation with an α-haloacyl halide to form the glycolide or lactide functional monomer.[30]

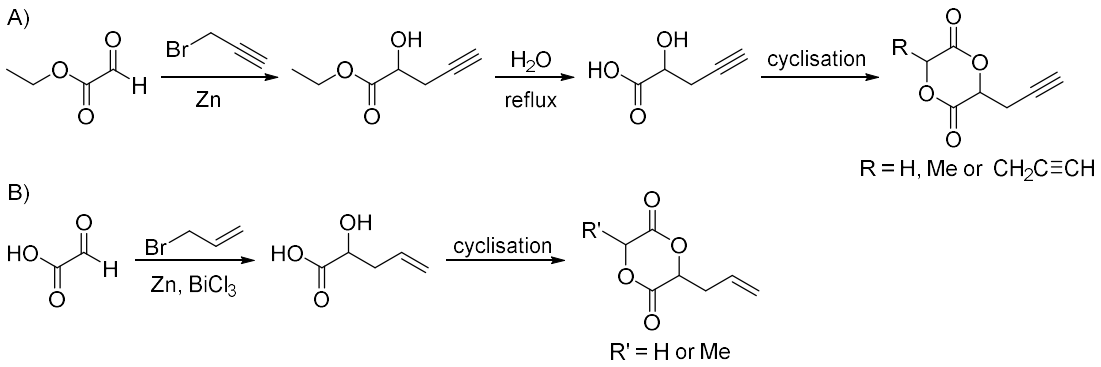

Scheme 4.4. Synthesis of a A) propargyl and B) allyl-functional cyclic diesters using Barbier-type additions.

Functional cyclic diesters prepared from the direct modification of lactide have been known for some time. In 1969, Scheibelhoffer *et al*. demonstrated the synthesis of a methylene-functional lactide (MLA) from the monobromination of lactide using *N*-bromosuccinimide (NBS) followed by base-catalysed dehydrobromination (Scheme 4.5).[31] MLA could be polymerised by a radical vinyl addition pathway; however, attempts to polymerise it *via* ROP resulted in monomer decomposition to produce nonpolymerizable byproducts.[32] Nonetheless, Jiang and Hillmyer demonstrated that further derivatisation of MLA could provide functional monomers for ROP (Scheme 4.5).[33] In that work, the authors utilised MLA as a dienophile in a Diels-Alder reaction with cyclopentadiene. The resultant tricyclic product could be polymerised by either ROP of the lactide ring or *via* ring-opening metathesis polymerisation (ROMP). Later on, Hillmyer and coworkers explored other dienes to expand the library of functional lactide monomers, and further polymerisation provided new polyesters with diverse thermal properties.[34]

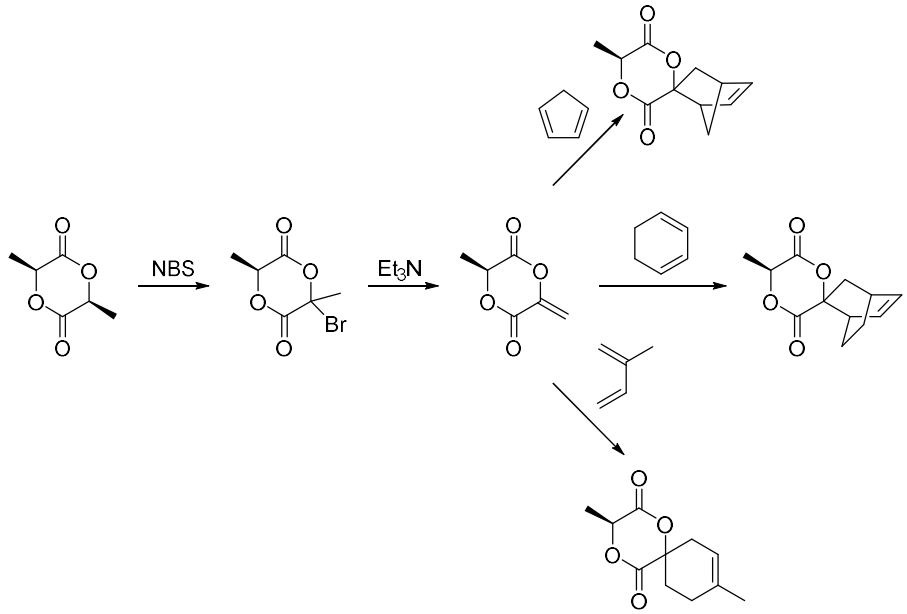

Scheme 4.5. Synthesis of MLA and Diels-Alder reactions with various dienes.

After the successful derivatisation of MLA, other strategies emerged to modify MLA. Fuoco *et al*. described the synthesis of a thioether lactide by the thiol-Michael addition of triphenylmethanethiol to MLA (Scheme 4.6a).[35] This strategy was shown to be more efficient than the traditional cyclisation of the corresponding functional α-hydroxy acid (68% *vs* 30% yield, respectively). More recently, Sinclair and Shaver reported the olefin cross-metathesis of MLA with 1-hexene (Scheme 4.6b).[36] Although the resultant compound was susceptible to decomposition (similarly to MLA),[32] the sensitivity could be mitigated by hydrogenation of the alkene. As a result, the hydrogenated compound was active for ROP when employing either metal- or organo-based catalysts.

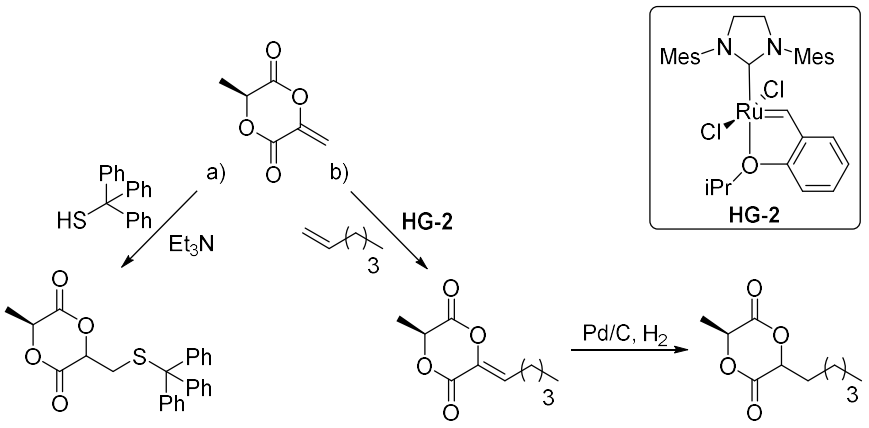

Scheme 4.6. Modification of MLA to prepare functional monomers *via* A) thiol-Michael addition or B) olefin cross-metathesis.

Herein, we explored several methodologies to synthesise functional cyclic diesters suitable for ROP to serve as crosslinkers for preparing biodegradable networks. The synthesis of a monomer precursor containing a reactive functional group is desirable to allow further modification through different routes. As such, the synthesis of a bis(cyclic diester) using the methods involving the ring-closure of α-hydroxy acids was investigated. In addition, using a key intermediate containing a reactive group such as MLA to introduce a bifunctional group was explored.

4.2 Results and Discussion

4.2.1 Synthesis of a Bis(cyclic diester) from L-Malic Acid

Initial investigation on the preparation of a bis(cyclic diester) involved a strategy previously investigated in our group, in which L-malic acid was functionalised with a benzyl moiety and subsequently ring-closed to provide a functional cyclic diester (Scheme 4.3).[24] We envisioned that a similar synthetic route using a bifunctional group would lead to a bis(α-hydroxy acid) that could be suitable for a ring-closing reaction to form a bicyclic monomer (Scheme 4.7).

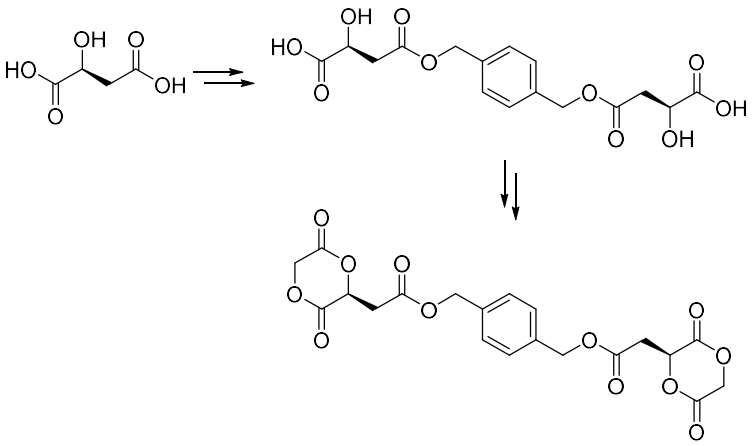

Scheme 4.7. Proposed synthetic route to prepare a bicyclic monomer from L-malic acid.

L-Malic acid (**4.1**) was initially protected using 2,2-dimethoxypropane in the presence of PTSA (Scheme 4.8). The crude product could be purified by recrystallisation in Et_2O to provide the acetonide **4.2** in 62% yield. The ^1H NMR spectrum of the purified product showed the methyl signals from the acetonide group at δ = 1.57 and 1.62 ppm, the methine group resonance at δ = 4.72 ppm, and the methylene signals at δ = 3.00 and 2.86 ppm (Figure 4.2). This spectrum was consistent with previous literature reports, which confirmed the selective α-hydroxy acid protection of L-malic acid.[24]

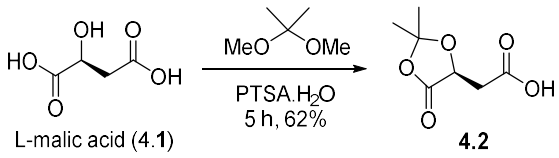

Scheme 4.8. Protection of L-malic acid (**4.1**) with 2,2-dimethoxypropane.

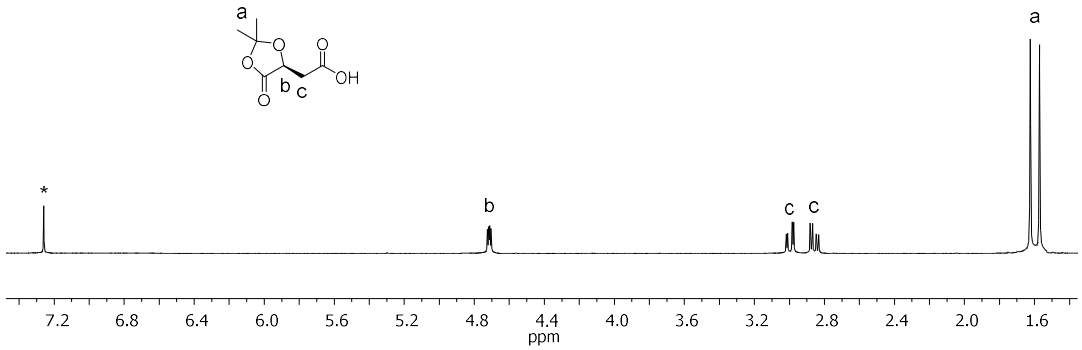

Figure 4.2. ^{1}H NMR spectrum of acetonide-protected L-malic acid **4.2** ($CDCl_3$, 500 MHz 298 K, * = $CHCl_3$).

The benzylation of acid **4.2** with α,α'-dibromo-*p*-xylene was accomplished by refluxing in acetone with excess Et_3N to produce compound **4.3** (Scheme 4.9). The product was purified by column chromatography and analysed by ^{1}H NMR spectroscopy. The resultant spectrum indicated new signals at δ = 7.35 and 5.17 ppm corresponding to the aromatic ring and benzylic proton resonances, respectively, and two carbinolic proton resonances at δ = 4.73 ppm (Figure 4.3). In addition, the ^{13}C NMR spectrum displayed the characteristic signals of the acetonide-protected malic acid (δ = 26.0 and 26.9 ppm) and the benzylic group (δ = 66.7, 128.7 and 135.7 ppm). The acetonide groups of **4.3** were quantitatively removed by hydrolysis in a mixture of AcOH/THF/H_2O (1:1:1) at 40 °C to furnish the bis(α-hydroxy acid) **4.4**. Analysis by ^{1}H and ^{13}C NMR spectroscopy revealed the disappearance of the acetonide signals, which confirmed the complete removal of the protecting group (Figure 4.4).

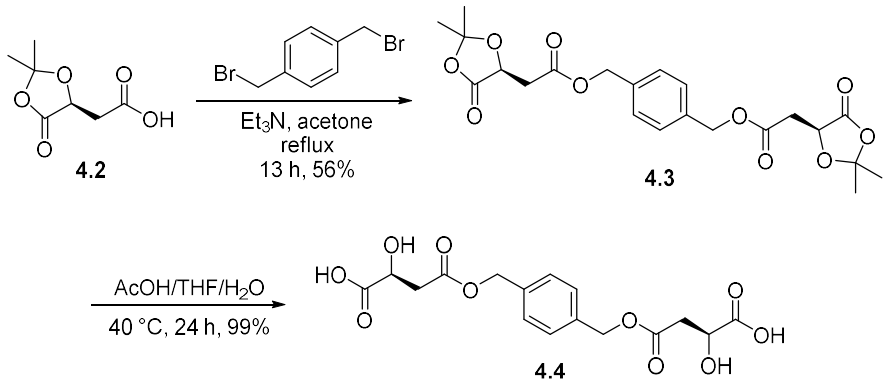

Scheme 4.9. Preparation of bis(α-hydroxy acid) **4.4**.

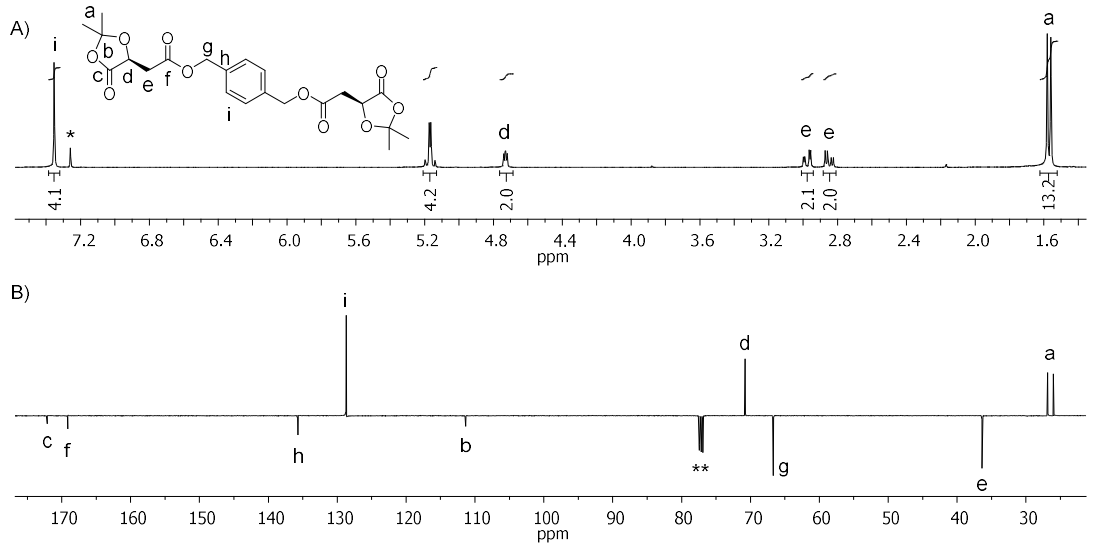

Figure 4.3. A) ^{1}H (500 MHz) and B) ^{13}C APT (125 MHz) NMR spectra of compound **4.3** ($CDCl_3$, 298 K, * = $CHCl_3$, ** = $CDCl_3$).

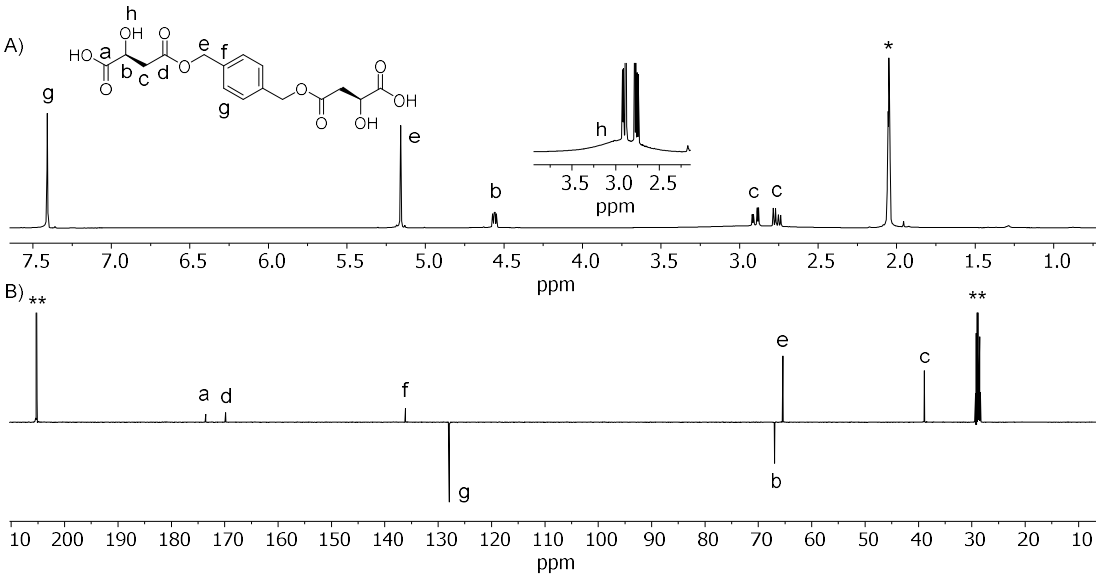

Figure 4.4. A) ^{1}H (500 MHz) and B) ^{13}C APT (125 MHz) NMR spectra of bis(α-hydroxy acid **4.4** ($(CD_3)_2CO$, 298 K, * = $(CH_3)_2CO$, ** = $(CD_3)_2CO$).

The bis(α-hydroxy acid) **4.4** was then treated with bromoacetyl bromide in the presence of Et_3N and the resultant Et_3N.HBr salt was removed by filtration (Scheme 4.10). The crude product was isolated by an aqueous work-up and was used directly in the next step. The ring-closing reaction was carried out in *pseudo*-high dilution conditions to avoid undesirable oligomer formation. Specifically, a solution of compound **4.5** in DMF (0.12 M) was added slowly (1.2 mL h^{-1}) into a suspension of

$NaHCO_3$ in DMF (final concentration of 0.02 M). The resultant product displayed limited solubility in most organic solvents and water, which prevented its purification by column chromatography. However, the crude product was analysed by ^{1}H and ^{13}C NMR spectroscopy in DMSO-d_6. According to the ^{1}H NMR spectrum, the signals corresponding to methine group at $\delta = 5.65$, and the methylene protons at $\delta = 5.31$ and 4.99 ppm were present and indicative of a cyclic structure (Figure 4.5). However, SEC analysis revealed the presence of oligomers with M_n of 2.0 kg mol^{-1} (Figure 4.6). To suppress intermolecular reactions, a slower addition of reactant and the use of more diluted conditions were implemented, but the oligomerisation reactions still occurred.

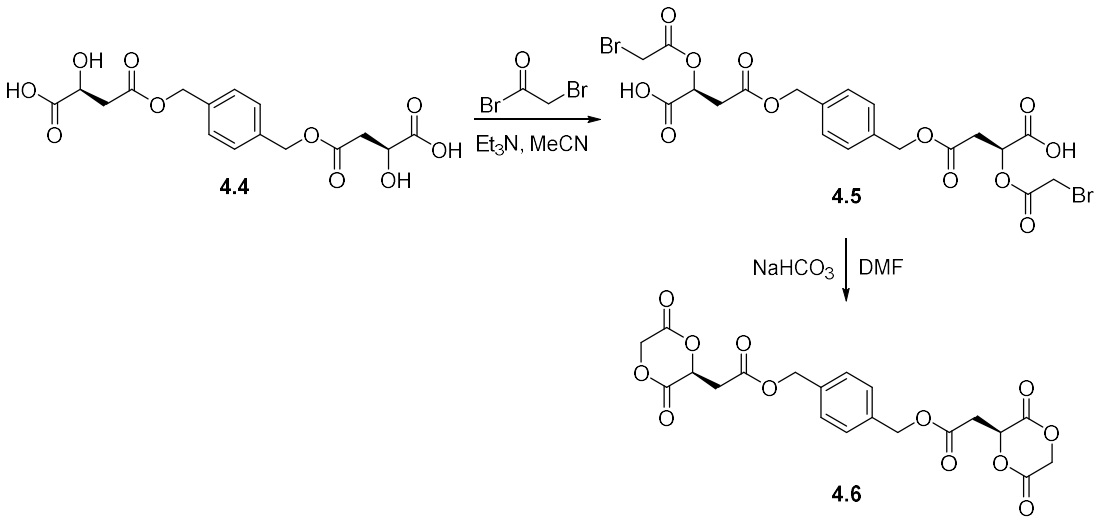

Scheme 4.10. Synthesis of bis(cyclic diester) **4.6**.

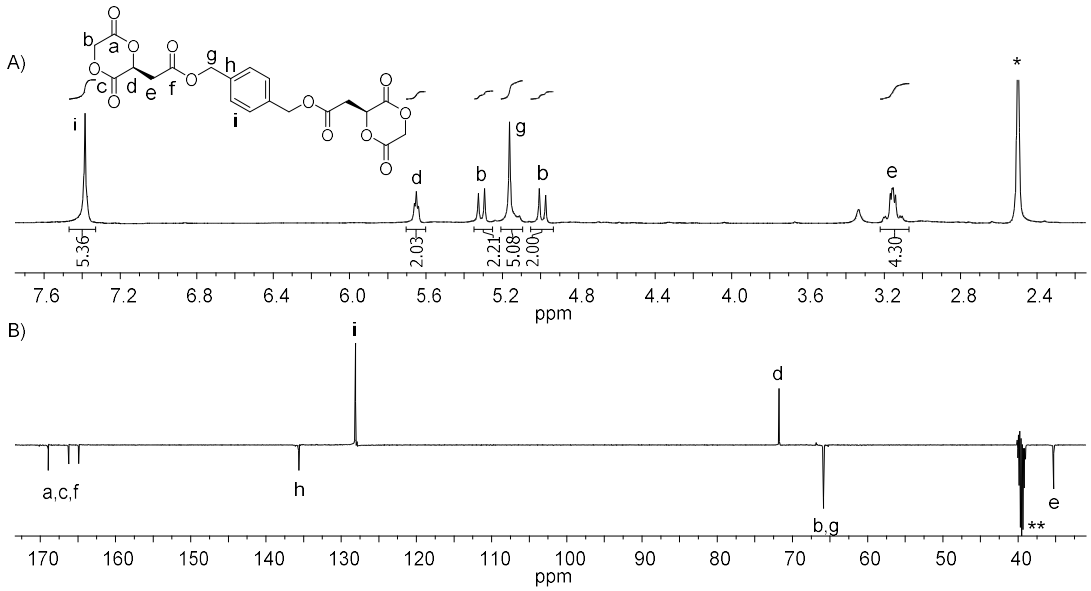

Figure 4.5. ^{1}H (500 MHz) and ^{13}C APT (125 MHz) NMR spectra of bis(cyclic diester) **4.6** ($(CD_3)_2SO$, 298 K, * = $(CH_3)_2SO$, ** = $(CD_3)_2SO$).

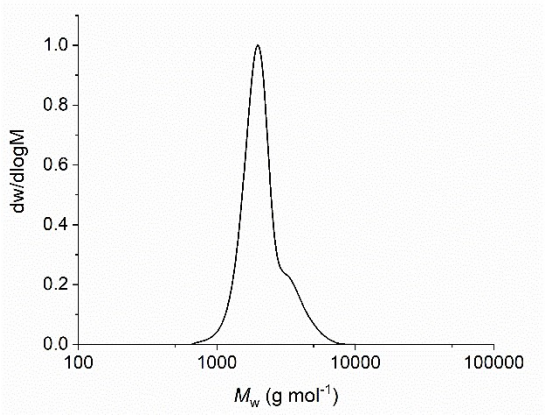

Figure 4.6. Size exclusion chromatogram of compound **4.6** (M_n = 2.0 kg mol^{-1}, $Đ_M$ = 1.1) (DMF, RI, calibrated against poly(methyl methacrylate) standards).

4.2.2 Synthesis of a Bis(cyclic diester) *via* the Functionalisation of L-Lactide

Since the ring-closing reaction of a bis(α-hydroxy acid) led to significant intermolecular side reactions, a strategy to apply a ring-closed intermediate containing a reactive side group was investigated. In this regard, MLA was envisioned to be a suitable compound for the desired functionalisations by coupling with a bifunctional compound (Scheme 4.11). As such, MLA was synthesised as reported previously from the bromination of L-LA with NBS (Scheme 4.12).[31,33] The crude product was purified by recrystallisation in ethyl acetate and hexane to provide bromo-lactide (**4.7**) in 47%

yield. The ^{1}H NMR spectroscopic analysis of this compound indicated a new signal at δ = 2.34 ppm that is attributed to the methyl group adjacent to the bromine, which is in accordance with previously reported values (Figure 4.7a).[33] Compound **4.7** was treated with NEt_3 to undergo dehydrobromination and afford MLA (**4.8**) in 30% overall yield after purification of the crude product by sublimation. The ^{1}H NMR spectrum of the resultant product showed the disappearance of the signal attributed to the methyl group in bromo-lactide (**4.7**) (δ = 2.34 ppm) and the appearance of methylene signals at δ =5.55 and 5.95 ppm, which is in agreement with previous data (Figure 4.7b).[33]

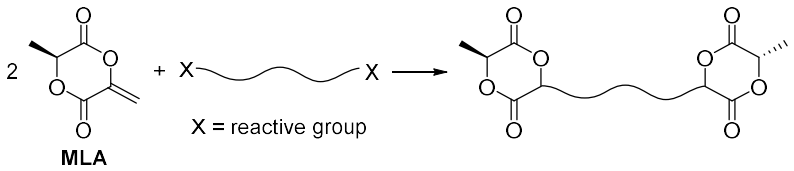

Scheme 4.11. Preparation of a bicyclic lactide monomer from MLA and a bifunctional reactive group.

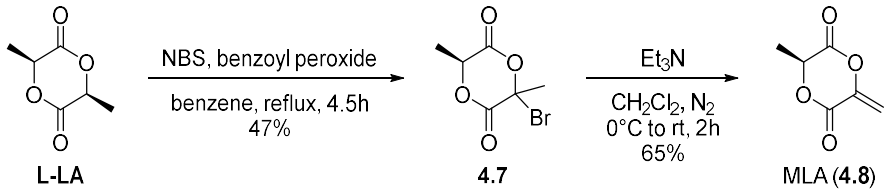

Scheme 4.12. Synthesis of MLA (**4.8**).

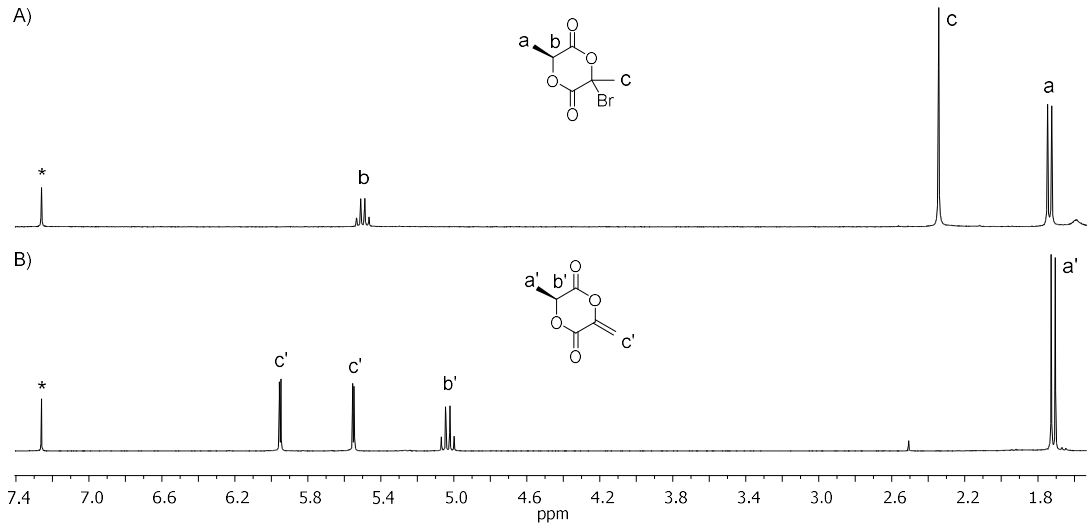

Figure 4.7. ^{1}H NMR spectra of A) bromo-lactide (**4.7**) and B) MLA (**4.8**) ($CDCl_3$, 298 K, 500 MHz, * = $CHCl_3$).

The functionalisation of MLA (**4.8**) at the alkene moiety was explored using several methods. A thiol-Michael addition was initially carried out using 1,6-hexanethiol in the presence of Et_3N following a procedure described by Fuoco *et al.* (Scheme 4.13).[35] After removal of any excess NEt_3 and its corresponding salts by washing the reaction mixture with dilute HCl, the crude product was analysed by ^{1}H and ^{13}C NMR spectroscopy. The ^{1}H NMR spectrum indicated a singlet at δ = 2.47 ppm, which indicates the presence of an isolated moiety, although all signals in the product were expected to have higher multiplicities due to neighbouring protons (Figure 4.8a). In addition, the ^{13}C NMR spectrum showed two carbonyl signals at δ = 197.9, 190.8, which is atypical for lactide derivatives (δ = 160 – 170 ppm) (Figure 4.8b).[24,35] These observations supported the presence of other carbonyl moieties that were formed from the ring-opening of MLA (**4.8**) by the thiol and resulted in an enol that further equilibrated to the corresponding ketone (Scheme 4.14). A similar observation was reported by Miyake *et al.* that demonstrated the regioselective ring-opening of MLA (**4.8**) by methanol on the carbonyl next to the methyl group, which formed the corresponding pyruvic ester.[32] Moreover, the authors observed that MLA (**4.8**) hydrolysed under ambient conditions (complete after 7 days) and in the presence of excess methanol (complete after 2 days), which demonstrated the susceptibility of the ring of compound **4.8** to be attacked by nucleophiles. Although our results seem to contrast with the successful thiol-Michael addition reported by Fuoco *et al.*, the

authors utilised a sterically demanding thiol and this likely prevented attack to the carbonyl moiety in MLA (**4.8**) (Scheme 4.6).[35]

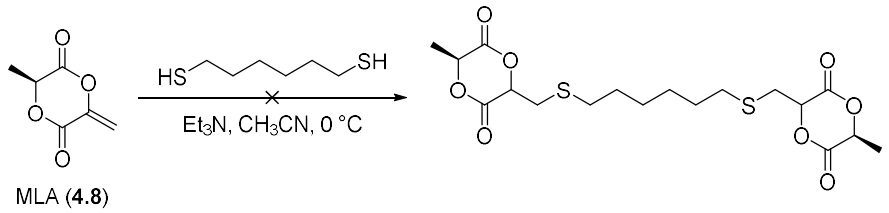

Scheme 4.13. Attempted thiol-Michael addition of MLA (**4.8**) and 1,6-hexanedithiol.

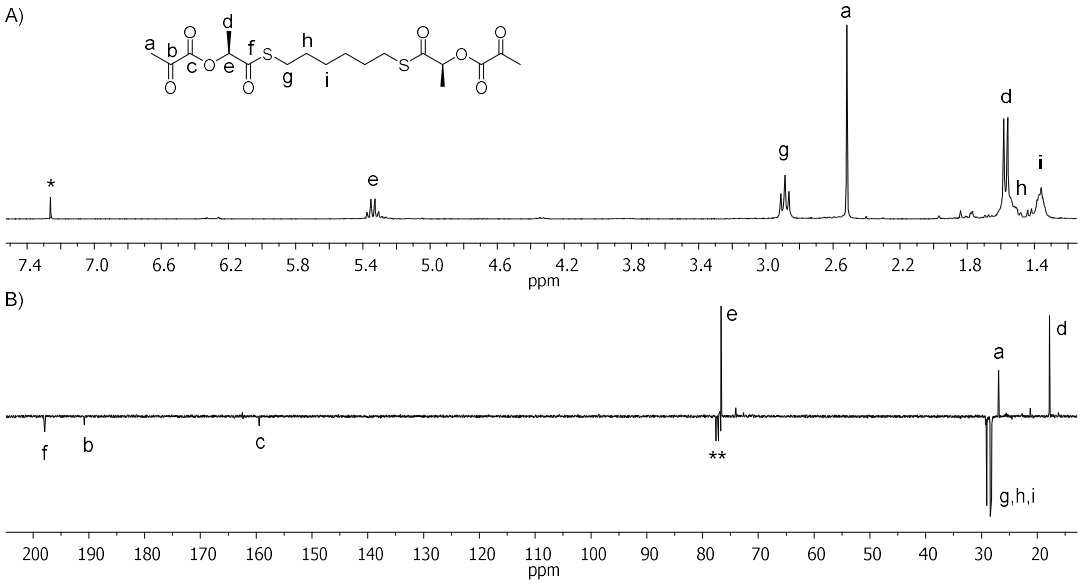

Figure 4.8. A) ^{1}H (300 MHz) and B) ^{13}C APT (75 MHz) NMR spectra of product from reaction between MLA (**4.8**) and 1,6-hexanedithiol ($CDCl_3$, 298 K, * = $CHCl_3$, ** = $CDCl_3$).

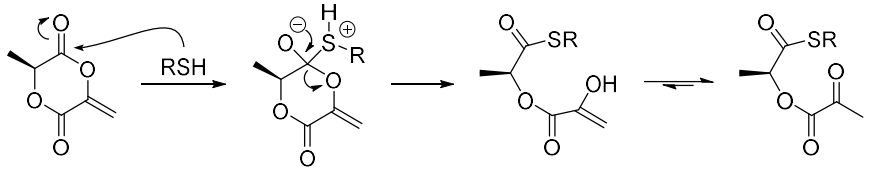

Scheme 4.14. Mechanism for the ring-opening reaction of MLA (**4.8**) with a thiol.

Since MLA was sensitive to a nucleophilic ring-opening, the radical thiol-ene reaction was considered as an alternative methodology. As such, the reaction was carried out with 2,2-dimethoxy-2-phenylacetophenone (DMPA) as photoinitiator and 1-hexanethiol as a model compound in 1,4-dioxane, using an irradiation source of λ =

254 nm for 16 hours (Scheme 4.15).[37] Analysis of the crude products by ^{1}H NMR spectroscopy showed the disappearance of the methylene proton resonances at δ = 5.55 and 5.95 ppm, whereas the signals corresponding to 1-hexanethiol remained unchanged (Figure 4.9). However, the appearance of broad signals around δ = 5.1, 3.0 and 1.7 ppm indicated that MLA had undergone radical homopolymerisation, according to comparison with previously reported data.[32] This was further confirmed by size exclusion chromatography (SEC) analysis that revealed the presence of polymers with a number-average molecular weight (M_n) of 3.5 kg mol^{-1} (Figure 4.10). This observation indicated that MLA (**4.8**) was more susceptible to radical homopolymerisation than to thiol additions, which has been previously reported for thiol-acrylate reactions.[38] Moreover, the radical polymerisation of MLA (**4.8**) was also observed in the presence of 2,2'-azobis(isobutyronitrile) (AIBN) as a thermal initiator.[31,32,39,40]

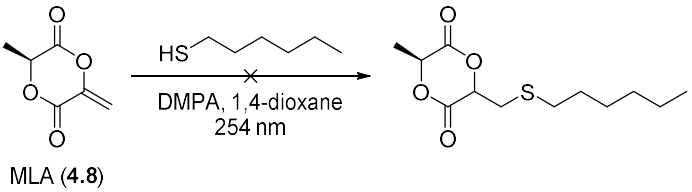

Scheme 4.15. Attempted radical thiol-ene reaction between MLA (**4.8**) and 1-hexanethiol.

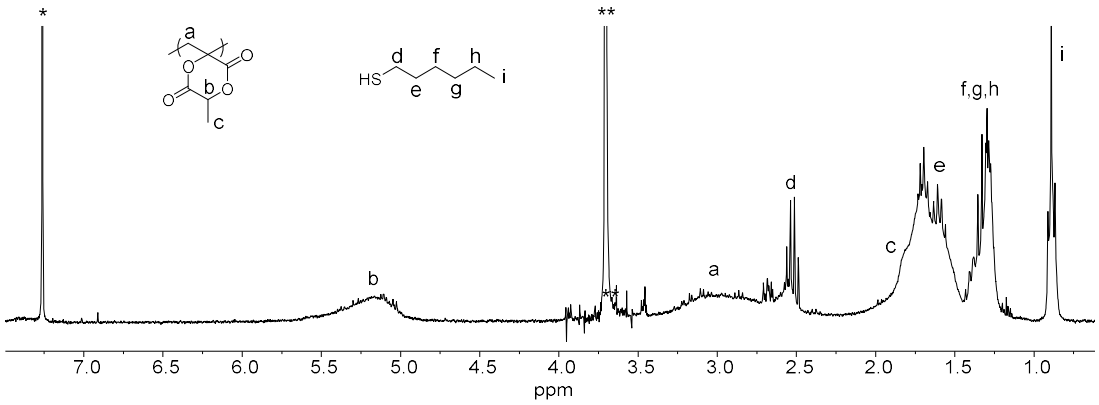

Figure 4.9. ^{1}H NMR spectrum of crude product obtained from the reaction of MLA (**4.8**) and 1-hexanethiol catalysed by DMPA ($CDCl_3$; 300 MHz; 298 K, * = $CHCl_3$, ** = 1,4-dioxane).

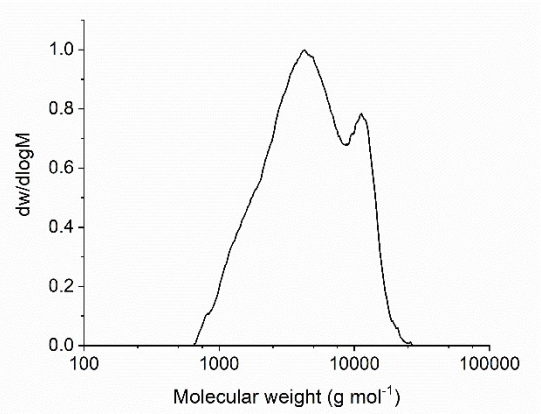

Figure 4.10. Size exclusion chromatogram of PMLA (M_n = 3.5 kg mol^{-1}, $Đ_M$ = 1.7) (DMF, RI, calibrated against poly(methyl methacrylate) standards).

Facing the challenges of functionalising MLA (**4.8**) with thiols, the Diels-Alder method previously reported by Hillmyer and coworkers was investigated.[33,34] However, in order to use MLA as a dienophile to synthesise a bicyclic crosslinker, a compound containing two 1,3-diene moieties would be necessary. As such, the synthesis of the tetraene **4.9** was accomplished using sorbic alcohol (**4.10**) and sorbic bromide (**4.11**), as previously described (Scheme 4.16).[41,42] Firstly, compound **4.11** was synthesised from sorbic alcohol (**4.10**) and phosphorous tribromide, and subsequently reacted with sorbic alcohol (**4.10**) in the presence of NaOH and a phase transfer agent, tetrabutylammonium bromide (TBAB). However, attempts to isolate a pure compound **4.9** using column chromatography failed, because both the starting materials and resultant product displayed sensitivity to air and light.

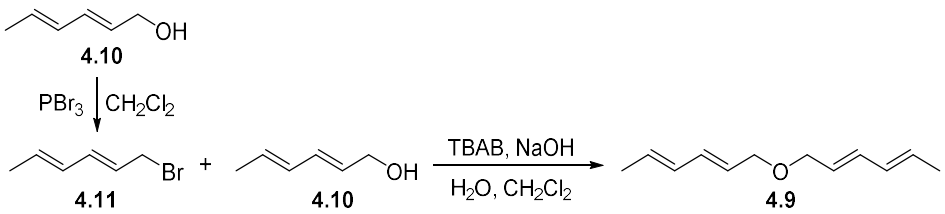

Scheme 4.16. Attempted synthesis of the bis(1,3-diene) **4.9**.

4.2.3 Synthesis of a Bis(cyclic diester) from Glyoxylic Acid

Considering the challenges in functionalising MLA, a similar monomer containing a reactive functional group less susceptible to ring-opening and radical homopolymerisation was envisioned. As such, the allyl-functional lactide (allyl-LA) reported by Leemhuis *et al*. was explored as a reactive intermediate that could undergo

a thiol-ene addition to provide a bis(cyclic diester) (Scheme 4.17).[29] In this case, the double bond moiety in allyl-LA is not very 'activated' and thus should suppress the radical polymerisation as previously observed for other thiol-allyl reactions.[38,43]

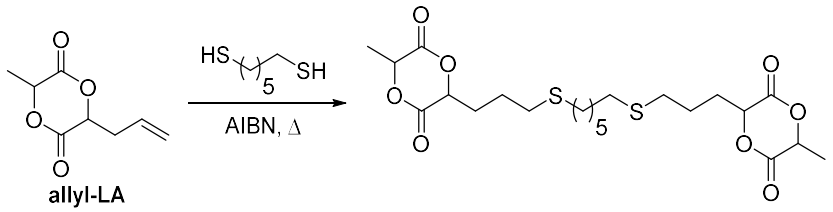

Scheme 4.17. Proposed synthesis of a bis(cyclic diester) from allyl-LA.

Allyl-LA (**4.12**) was prepared according to a previously described procedure by Delle Chiaie *et al*. (Scheme 4.18).[44] The allylation of glyoxylic acid (**4.13**) was performed using allyl bromide in the presence of zinc and bismuth chloride to afford α-hydroxy acid **4.14** in 64% yield. The ^{1}H NMR spectrum of **4.14** indicated the presence of a methine proton resonance at δ = 4.36 ppm, while the allyl group was identified by the characteristic olefinic resonances at δ = 5.81 and 5.19 ppm and the methylene signals at δ = 2.64 and 2.50 ppm, which corroborated previously reported data (Figure 4.11a).[44] Then, compound **4.14** was reacted with 2-bromopropionyl bromide and Et_3N to provide the acid intermediate **4.15**. After removal of the Et_3N.HBr salts, the crude acid **4.15** was subsequently cyclised under pseudo-dilution conditions in the presence of Na_2CO_3 in DMF. The resultant product was purified by column chromatography to provide allyl-LA (**4.12**). Two small fractions of pure diastereomers were isolated from the chromatographic separation and were analysed by ^{1}H NMR spectroscopy (Figure 4.11b and c). The spectra of both isomers showed a shift of the methine signal from δ = 4.36 in the α-hydroxy acid **4.14** to δ ~ 5.0 ppm in allyl-LA. Furthermore, the methyl and methine proton resonances at δ ~ 1.6 and 5.0 ppm indicated the displacement of the bromine atom. The NMR spectroscopic data was found to be in agreement with previously reported assignments for allyl-LA.[44]

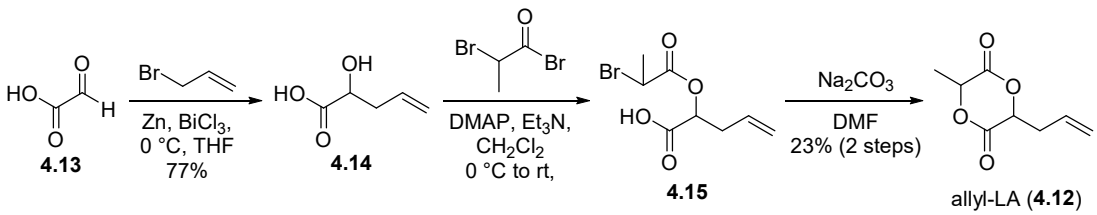

Scheme 4.18. Preparation of allyl-LA (**4.12**).

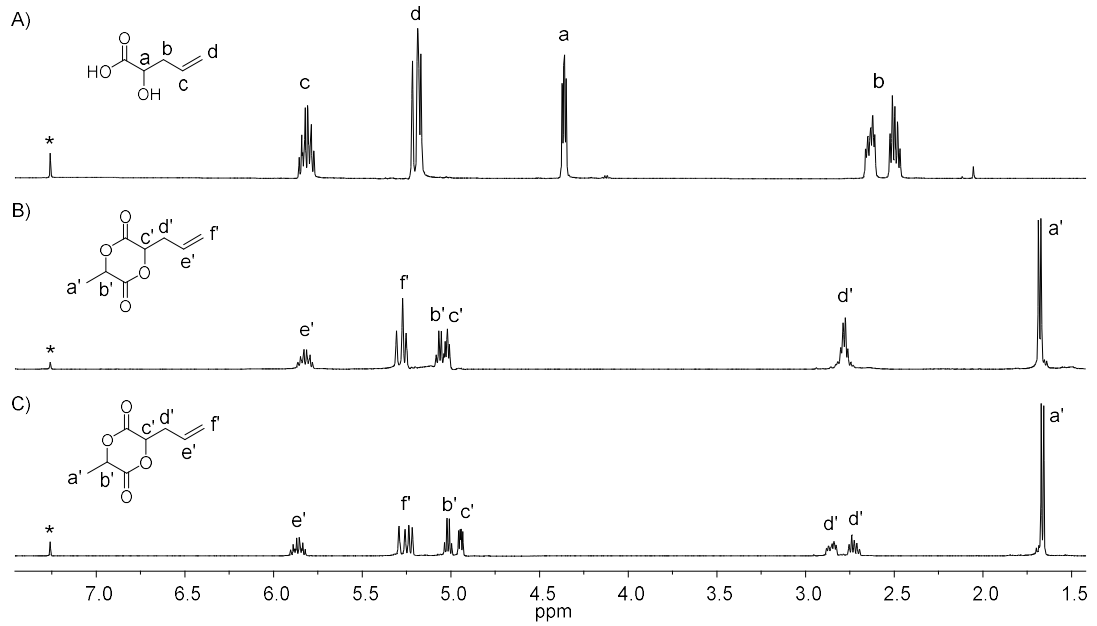

Figure 4.11. A) ^{1}H NMR spectra of A) allyl α-hydroxy acid **4.14**, B) and C) allyl-LA diastereomers (**4.12**) ($CDCl_3$, 500 MHz, 298 K, * = $CHCl_3$).

To prepare the bicyclic monomer, the radical thiol-ene reaction between allyl-LA (**4.12**) and 0.5 equivalent of 1,6-hexanedithiol was performed with AIBN as a thermal initiator at 55 °C (Scheme 4.19). The resultant solid was washed with hexane to furnish bis(thiol-lactide) (BTLA, **4.16**) in 96% yield. The ^{1}H NMR spectrum displayed the disappearance of olefinic proton resonances at δ = 5.8 and 5.3 ppm associated with allyl-LA and the appearance of characteristic thioether signals at δ = 2.57 and 2.50 ppm (Figure 4.12a). In addition, the integration of signals was in agreement with the reaction of one dithiol with two allyl-LA molecules. Finally, ^{13}C NMR analysis showed the expected signals for the carbonyl moiety of the cyclic structure at δ =167.5 and 166.8 ppm and the aliphatic carbons from the thiol at δ = 32.0, 19.5 and 28.4 ppm, which further confirmed the preparation of a novel bis(cyclic diester) (Figure 4.12b). With the synthesis of this monomer, further studies on the formation of polyester

networks using a photocatalyst could be carried out and will be discussed in detail in Chapter 5.

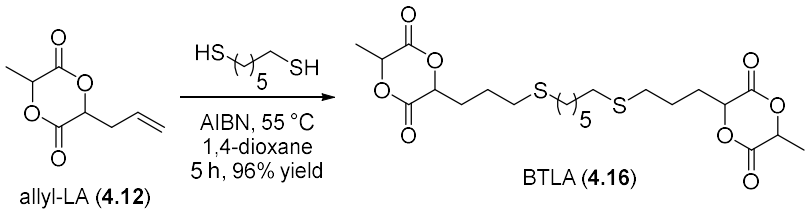

Scheme 4.19. Synthesis of BTLA (**4.16**).

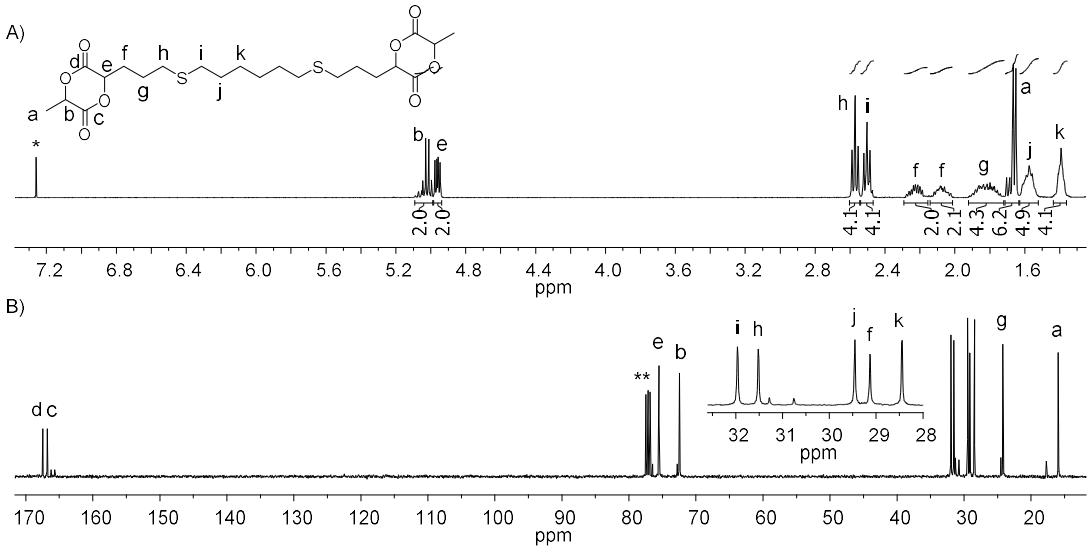

Figure 4.12. ^{1}H (400 MHz) and ^{13}C (100 MHz) NMR spectra of BTLA (**4.16**) ($CDCl_3$, 298 K, * = $CHCl_3$, ** = $CDCl_3$).

4.3 Conclusions

The synthesis of a bis(cyclic diester) monomer that could be polymerised and crosslinked by ROP for preparing biodegradable networks was investigated using several approaches. Initially, the modification of L-malic acid was performed in order to insert a second α-hydroxy acid functionality that would provide a bis(cyclic diester) after ring closure. However, the cyclisation step proved challenging with significant oligomer formation resulting from intermolecular reactions even when employing diluted reaction conditions.

Alternatively, L-LA was modified to produce the reactive methylene derivative MLA, which was then utilised as an intermediate for further functionalisation. The attempted thiol-Michael addition reaction between 1,6-hexanedithiol and MLA

resulted in the undesirable ring-opening, as a consequence of the high electrophilicity of the carbonyl moiety. On the other hand, an attempt using radical thiol-ene conditions favoured the homopolymerisation of MLA, in which no formation of the desired product was observed. These results were in agreement with other reports in the literature that outlined the challenges in modifying L-LA without concomitant ring-opening,[32,45] in addition to the propensity of the methylene group to undergo radical homopolymerisation.[39,40]

At this point, the synthesis of a cyclic intermediate similar to MLA, but less susceptible to ring-opening and radical polymerisation was explored. As such, an allyl-functional lactide was synthesised in two steps from glyoxylic acid, which allowed further modification *via* a radical thiol-ene reaction with 1,6-hexanedithiol to successfully provide a bis(cyclic diester). Although this work demonstrated the challenges associated with the preparation of a functional lactide, the synthesis of a bifunctional lactide will allow investigation on the synthesis of crosslinked materials for spatial control by ROP.

4.4 References

1. D. Bratton, D. Yang, J. Dai and C. K. Ober, *Polym. Adv. Technol.*, 2006, **17**, 94.
2. D. Wöll, J. Smirnova, M. Galetskaya, T. Prykota, J. Bühler, K.-P. Stengele, W. Pfleiderer and U. E. Steiner, *Chem. Eur. J.*, 2008, **14**, 6490.
3. D. Wöll, S. Walbert, K.-P. Stengele, T. J. Albert, T. Richmond, J. Norton, M. Singer, R. D. Green, W. Pfleiderer and U. E. Steiner, *Helv. Chim. Acta*, 2004, **87**, 28.
4. A. del Campo and E. Arzt, *Chem. Rev.*, 2008, **108**, 911.
5. W. Xi, H. Peng, A. Aguirre-Soto, C. J. Kloxin, J. W. Stansbury and C. N. Bowman, *Macromolecules*, 2014, **47**, 6159.
6. E. C. Hagberg, M. Malkoch, Y. Ling, C. J. Hawker and K. R. Carter, *Nano Lett.*, 2007, **7**, 233.
7. A. S. Quick, J. Fischer, B. Richter, T. Pauloehrl, V. Trouillet, M. Wegener and C. Barner-Kowollik, *Macromol. Rapid Commun.*, 2013, **34**, 335.
8. S. Huang, M. Podgórski, X. Zhang, J. Sinha, M. Claudino, J. W. Stansbury and C. N. Bowman, *J. Dent. Res.*, 2018, **97**, 530.

9. A. Hoffmann, H. Leonards, N. Tobies, L. Pongratz, K. Kreuels, F. Kreimendahl, C. Apel, M. Wehner and N. Nottrodt, *J. Tissue Eng.*, 2017, **8**, 2041731417744485.
10. M. Podgórski, E. Becka, S. Chatani, M. Claudino and C. N. Bowman, *Polym. Chem.*, 2015, **6**, 2234.
11. R. P. Brannigan and A. P. Dove, *Biomater. Sci.*, 2017, **5**, 9.
12. K. Fukushima, *Biomater. Sci.*, 2016, **4**, 9.
13. F. P. Melchels, J. Feijen and D. W. Grijpma, *Biomaterials*, 2009, **30**, 3801.
14. L. Elomaa, S. Teixeira, R. Hakala, H. Korhonen, D. W. Grijpma and J. V. Seppälä, *Acta Biomater.*, 2011, **7**, 3850.
15. I. K. Kwon and T. Matsuda, *Biomaterials*, 2005, **26**, 1675.
16. S. M. Oskui, G. Diamante, C. Liao, W. Shi, J. Gan, D. Schlenk and W. H. Grover, *Environ. Sci. Technol. Lett.*, 2016, **3**, 1.
17. R. Palmgren, S. Karlsson and A.-C. Albertsson, *J. Polym. Sci., Part A: Polym. Chem.*, 1997, **35**, 1635.
18. L.-Q. Yang, B. He, S. Meng, J.-Z. Zhang, M. Li, J. Guo, Y.-M. Guan, J.-X. Li and Z.-W. Gu, *Polymer*, 2013, **54**, 2668.
19. X. Jiang, E. B. Vogel, M. R. Smith III and G. L. Baker, *Macromolecules*, 2008, **41**, 1937.
20. X. Jiang, M. R. Smith III and G. L. Baker, *Macromolecules*, 2008, **41**, 318.
21. R. Tong, *Ind. Eng. Chem. Res.*, 2017, **56**, 4207.
22. Y. Kimura, K. Shirotani, H. Yamane and T. Kitao, *Macromolecules*, 1988, **21**, 3338.
23. T. Trimaille, M. Möller and R. Gurny, *J. Polym. Sci., Part A: Polym. Chem.*, 2004, **42**, 4379.
24. R. J. Pounder and A. P. Dove, *Biomacromolecules*, 2010, **11**, 1930.
25. S. Deechongkit, S.-L. You and J. W. Kelly, *Org. Lett.*, 2004, **6**, 497.
26. W. W. Gerhardt, D. E. Noga, K. I. Hardcastle, A. J. García, D. M. Collard and M. Weck, *Biomacromolecules*, 2006, **7**, 1735.
27. Y. Yu, J. Zou, L. Yu, W. Ji, Y. Li, W.-C. Law and C. Cheng, *Macromolecules*, 2011, **44**, 4793.
28. F. Coumes, V. Darcos, D. Domurado, S. Li and J. Coudane, *Polym. Chem.*, 2013, **4**, 3705.

29. M. Leemhuis, N. Akeroyd, J. A. W. Kruijtzer, C. F. van Nostrum and W. E. Hennink, *Eur. Polym. J.*, 2008, **44**, 308.
30. J. Zou, C. C. Hew, E. Themistou, Y. Li, C.-K. Chen, P. Alexandridis and C. Cheng, *Adv. Mater.*, 2011, **23**, 4274.
31. A. S. Scheibelhoffer, W. A. Blose and H. J. Harwood, *Polym. Prepr. (Am. Chem. Soc., Div. Polym. Chem.)*, 1969, **10**, 1375.
32. G. M. Miyake, Y. Zhang and E. Y. X. Chen, *J. Polym. Sci., Part A: Polym. Chem.*, 2015, **53**, 1523.
33. F. Jing and M. A. Hillmyer, *J. Am. Chem. Soc.*, 2008, **130**, 13826.
34. G. L. Fiore, F. Jing, J. V. G. Young, C. J. Cramer and M. A. Hillmyer, *Polym. Chem.*, 2010, **1**, 870.
35. T. Fuoco, A. Finne-Wistrand and D. Pappalardo, *Biomacromolecules*, 2016, **17**, 1383.
36. F. Sinclair and M. P. Shaver, *J. Polym. Sci., Part A: Polym. Chem.*, 2018, **56**, 741.
37. M. Uygun, M. A. Tasdelen and Y. Yagci, *Macromol. Chem. Phys.*, 2010, **211**, 103.
38. N. B. Cramer and C. N. Bowman, *J. Polym. Sci., Part A: Polym. Chem.*, 2001, **39**, 3311.
39. J. Britner and H. Ritter, *Macromolecules*, 2015, **48**, 3516.
40. T. C. Mauldin, J. T. Wertz and D. J. Boday, *ACS Macro Lett.*, 2016, **5**, 544.
41. R. Hertel, J. Mattay and J. Runsink, *J. Am. Chem. Soc.*, 1991, **113**, 657.
42. T. Kim, G. A. Mirafzal, J. Liu and N. L. Bauld, *J. Am. Chem. Soc.*, 1993, **115**, 7653.
43. D. E. Borchmann, N. T. Brummelhuis and M. Weck, *Macromolecules*, 2013, **46**, 4426.
44. K. R. D. Chiaie, L. M. Yablon, A. B. Biernesser, G. R. Michalowski, A. W. Sudyn and J. A. Byers, *Polym. Chem.*, 2016, **7**, 4675.
45. J.-B. Zhu, X. Tang, L. Falivene, L. Caporaso, L. Cavallo and E. Y. X. Chen, *ACS Catal.*, 2017, **7**, 3929.

Chapter 5

Studies Towards the Spatial Control *via* Photoinduced Ring-Opening Polymerisation

5.1 Introduction

The use of bicyclic monomers as crosslinkers in ring-opening polymerisations is an interesting strategy to produce biodegradable elastomers without introducing non-degradable content into the polymer.[1] This approach was first explored by Pitt *et al.*, who described the incorporation of the bicyclic compound during the polymerisation of another monomer, thus acting as a crosslinker (Scheme 5.1).[2] The authors investigated the copolymerisation of ε-caprolactone (ε-CL) and a 2,2'-bis-(3-caprolactone-4-yl)propane (BCP) to eliminate the crystallinity of polycaprolactone (PCL) by restricting the interaction between chain segments upon crosslinking. This approach was utilised as a means to increase the rate of degradation of PCL while maintaining its form stability. The networks obtained were shown to be amorphous and started degrading after 2 weeks *in vivo* while presenting a surface degradation profile until 102 weeks. This result contrasted with uncrosslinked PCL of similar molecular weight (MWt) that presented a bulk erosion process with a mass loss being observed only after one year.[3]

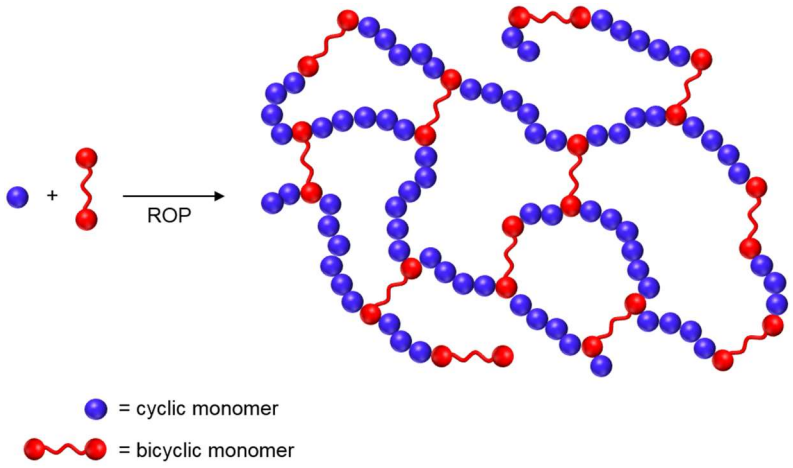

Scheme 5.1. Formation of a network by ring-opening polymerisation of a cyclic monomer with a crosslinker.

This crosslinking approach was further explored with other monomers (*e.g.* trimethylene carbonate (TMC), L-lactide (L-LA), 1.5-dioxepan-2-one (DXO)), as well as different bicyclic compounds as crosslinkers (Figure 5.1).[4-14] For instance, Albertsson and coworkers prepared crosslinked films from the (co)polymerisation of ε-CL and 1,5-dioxepan-2-one (DXO) and BCP as the crosslinker, with varied monomer fractions and crosslinking densities (Scheme 5.2).[4] The authors observed

that the Young's modulus of the resultant films increased with the PCL content, while the elongation at break decreased, which was attributed to the presence of crystalline domains in the PCL segments. In addition, similar enhancement in the mechanical performance was observed with higher crosslinking densities, which is a result of the increased interconnectivity between the chain segments.[15]

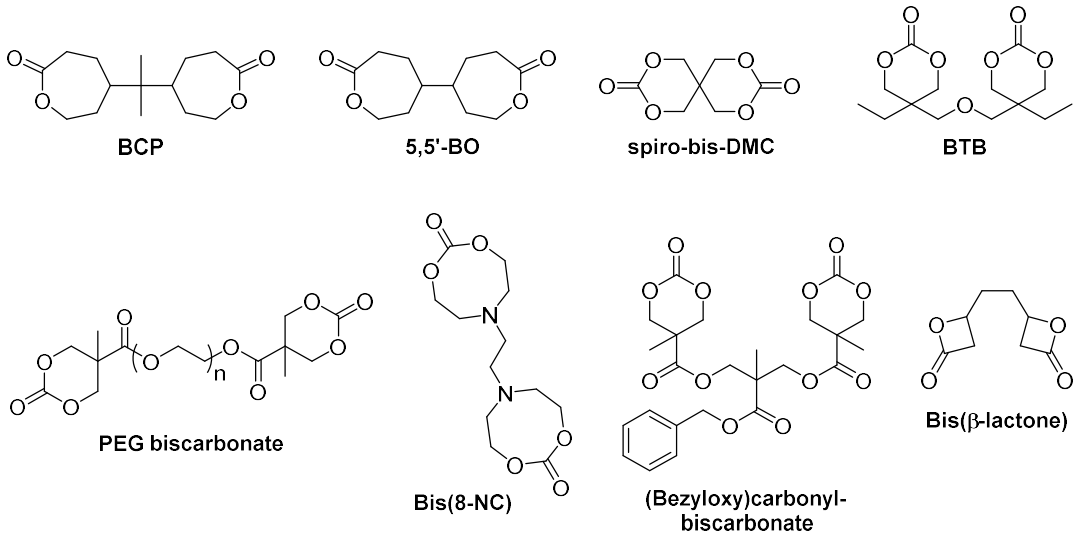

Figure 5.1. Bicyclic monomers utilised as crosslinkers for ROP.

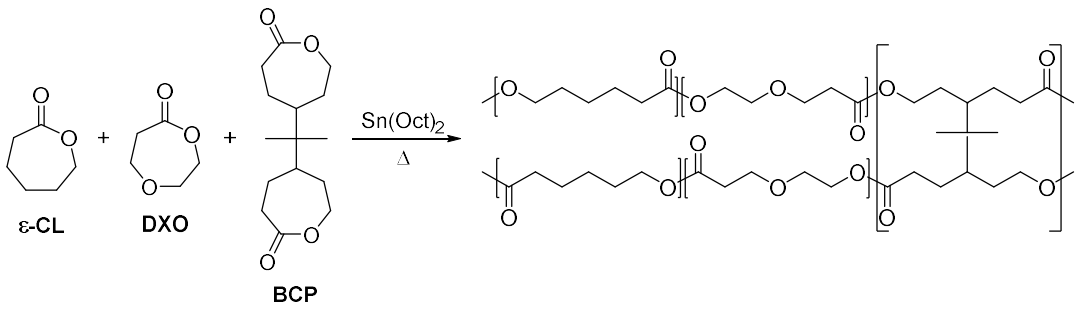

Scheme 5.2. Network formation by the ROP of ε-CL and DXO using BCP as a crosslinker.

Pennings and coworkers also investigated L-LA in the preparation of networks from 5,5'-bis(oxepane-2-one) (5,5'-BO, Figure 5.1).[6] This crosslinker presented reactivity much lower than that of L-LA in the presence of $Sn(Oct)_2$ as catalyst and, as a result, the crosslinker could not be fully incorporated into the polymer when the reaction was carried out at 110 °C. The crosslinking of L-LA could be improved by the use of spiro-bis-trimethylene carbonate (spiro-bis-TMC), which showed higher reactivity than 5,5'-BO and, therefore, a more efficient crosslinking was observed.[7]

Amsden and coworkers reported a different approach for the preparation of networks, which involved two stages: firstly, 3-arm pre-copolymers of ε-CL and D,L-LA were synthesised utilising glycerol as initiator and $Sc(Oct)_2$ as catalyst.[16,17] Then, taking the advantage that the prepolymers presented living characteristics, further polymerisation with BCP as crosslinker in the presence of ε-CL, as both solvent and comonomer, provided networks (Scheme 5.3). The authors observed that, for a prepolymer with a fixed MWt, tougher materials were obtained with increasing amounts of BCP, as a consequence of higher crosslinking densities. A similar effect was observed when the BCP:prepolymer ratio was kept constant and the molecular weight of prepolymers decreased, once the interconnection points became closer and resulted in an increased crosslinking density.

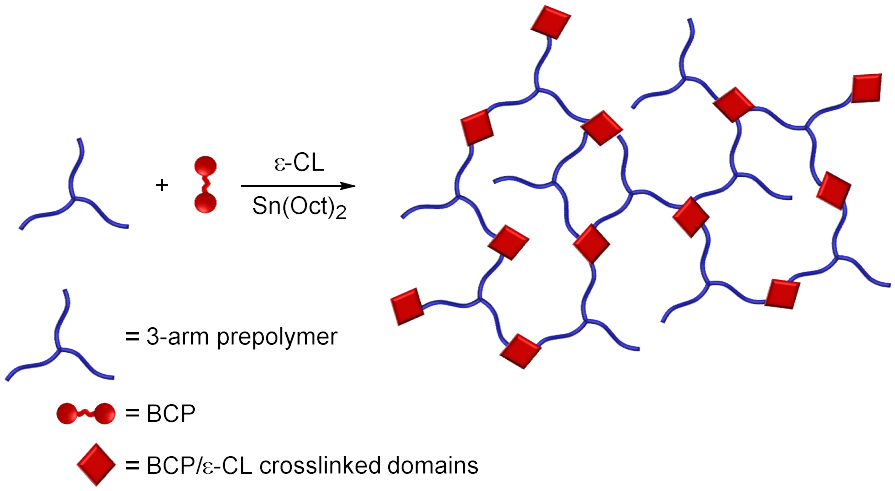

Scheme 5.3. Formation of a network from the ROP of a BCP by a prepolymer in the presence of ε-CL as a solvent and copolymer.

Although these strategies allowed tuning the properties of biodegradable materials, while providing form-stability, the network formation required the addition of metal or organocatalysts in a traditional manner. Nevertheless, the exploration of more advanced methodologies based on a suitable catalyst that could be produced by an external stimulus would introduce temporal and spatial control to the system. In this regard, the photocatalyst developed in Chapter 3, namely 2-(2-nitrophenyl)propoxycarbonyl 1,1,3,3-tetramethylguanidine (NPPOC-TMG), would allow the photochemically controlled release of TMG, a ROP catalyst that showed to be efficient especially for L-LA, although ineffective for ε-CL and TMC. Therefore,

to obtain spatial control utilising this photocatalyst, the polymerisation of L-LA in combination with a bicyclic monomer was envisioned. As demonstrated in previous works, ε-CL derivatives are ineffective in the copolymerisation with L-LA,[6] whereas TMC crosslinkers, although allowed the formation of network materials, is still considerably less reactive than LA.[7,18,19] In this regard, the bis(cyclic diester) synthesised in Chapter 4 (*i.e.* (bis(thiol-lactide) (BTLA)) was expected to provide comparable reactivities. As such, herein we investigate the preparation of PLLA networks utilising BTLA as a crosslinker *via* photoinduced ROP. This approach is especially interesting as it would provide alternatives to current methodologies for the production of biodegradable cured materials that typically involves the use of toxic acrylates.[20]

5.2 Results and Discussion

5.2.1 Ring-Opening Polymerisation of Functional Lactide and Glycolide Monomers

Prior to the investigation of the formation of crosslinked materials from the photopolymerisation of BTLA, similar monofunctional monomers were synthesised and polymerised to allow simple characterisation of the resultant linear polymers. In addition, free TMG was utilised to investigate the control of the polymerisation system. Accordingly, dodecanethiol-lactide (DTLA, **5.3**) and the corresponding functional glycolide (DTGA, **5.4**) were synthesised from glyoxylic acid (**4.13**), following a strategy described in Chapter 4 (Scheme 5.4). The ^{1}H NMR spectra of the resultant monomers showed the characteristic peaks of the long aliphatic chain at δ = 1.36 and 1.26 ppm and the terminal methyl group at δ = 0.88 ppm (Figure 5.2). Specifically, DTLA (**5.3**) presented the methine proton resonances at δ = 5.01 and 4.95 ppm and the methyl group signal in the monomer ring at δ = 1.67 ppm, whereas DTGA (**5.4**) displayed the methine signals at δ = 4.94 and the methylene proton resonances at δ = 4.92 ppm. The solid monomers were dried in a desiccator over P_2O_5 in a static vacuum and then transferred into a glove box. The ROP studies were then carried out in $CDCl_3$ or CH_2Cl_2 ($[M]_0$ = 1 M) at room temperature using 4-methoxybenzyl alcohol as initiator and TMG as a catalyst (Scheme 5.5).

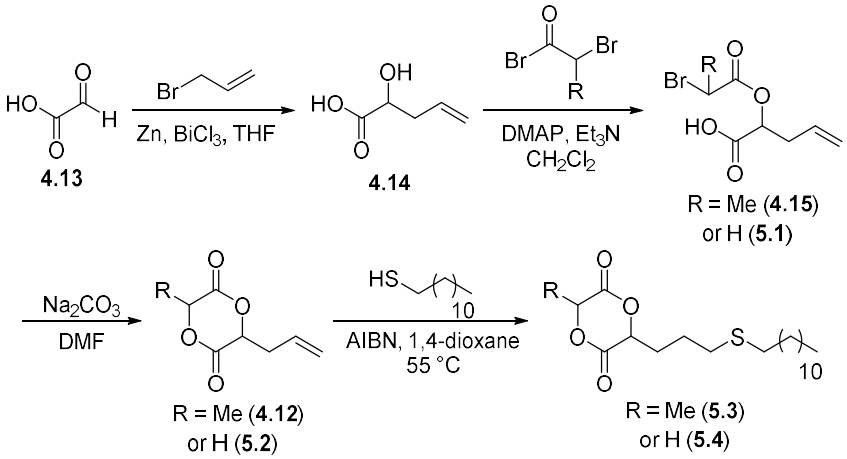

Scheme 5.4. Synthesis of DTLA (R = Me, **5.3**) and DTGA (R = H, **5.4**).

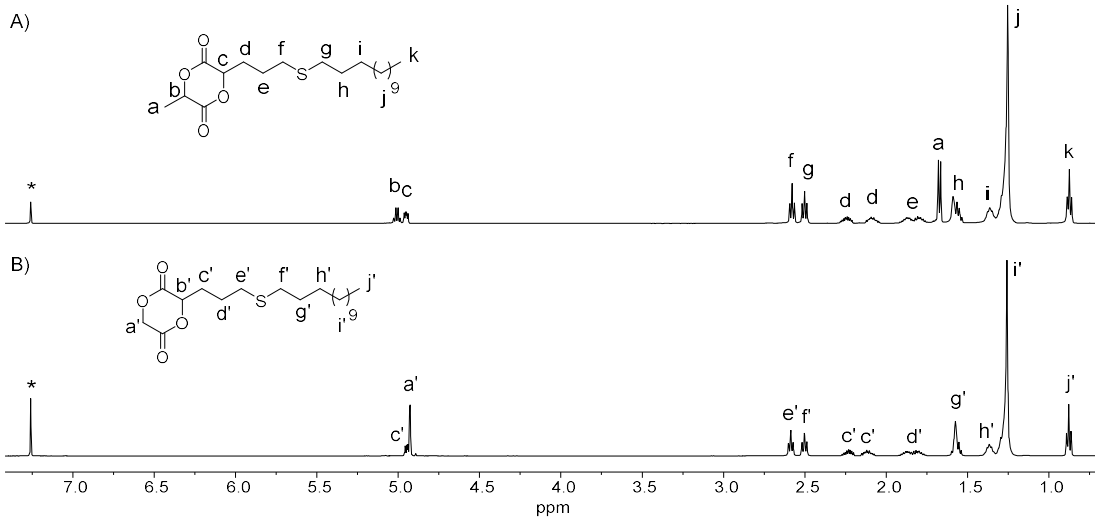

Figure 5.2. ^{1}H NMR spectra of A) DTLA (**5.3**) and B) DTGA (**5.4**) ($CDCl_3$, 500 MHz, 298 K, * = $CHCl_3$).

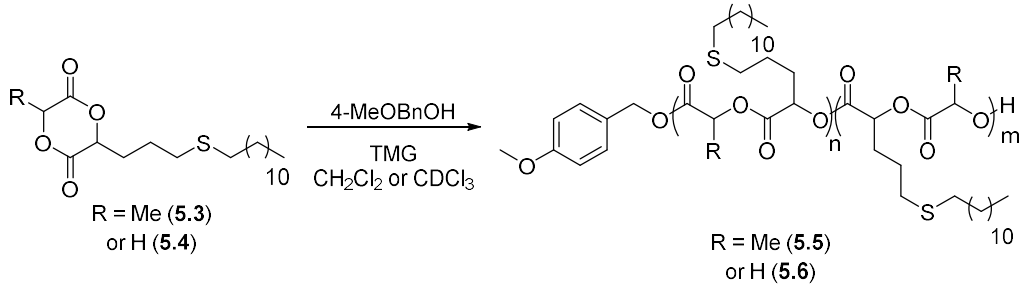

Scheme 5.5. Synthesis of PDTLA (R = Me, **5.5**) and PDTGA (R = H, **5.6**) *via* ROP catalysed by TMG.

The ROP of DTLA (**5.3**) was monitored by ^{1}H NMR spectroscopy, which showed the disappearance of the methine signals in the monomer at δ =4.95 and 5.01 ppm and

the appearance of the corresponding proton resonances in the polymer at δ = 5.11 (Figure 5.3). For an initial monomer-to-initiator concentration ratio ($[M]_0/[I]_0$) of 25 and using 5 mol% TMG, full monomer conversion was obtained in 75 minutes. The polymerisation was quenched by adding acidic Amberlyst resin, and PDTLA (**5.5**) was purified by precipitation in methanol. Analysis of the resultant polymer by size exclusion chromatography (SEC) revealed a monomodal distribution with a number-average molecular weight (M_n) of 9.3 kg mol^{-1} and narrow dispersity values ($Đ_M$ = 1.1) that indicated a good control over the polymerisation (Figure 5.4). Interestingly, the ^{1}H NMR signals were shown to be relatively broad, which could indicate a lack of regio-selectivity during the ring-opening. Although studies by Yin and Baker had demonstrated that the polymerisation rates of alkyl-substituted cyclic diesters would decrease as the size of the alkyl chain increased (*e.g.* rate for lactide: 6.2 × 10^3 s^{-1}, ethyl-substituted glycolide: 4.8 × 10^3 s^{-1}, hexyl-substituted glycolide: 3.7 × 10^3 s^{-1}), the rates are in the same order of magnitude and, therefore either ester groups on the monomer ring could have been opened in a competitive manner.[21]

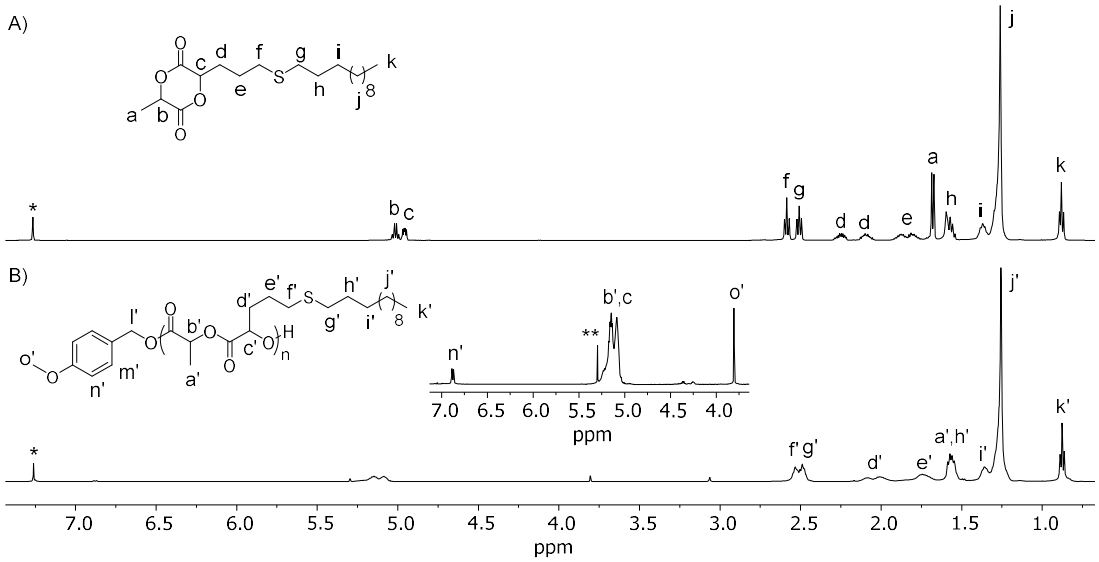

Figure 5.3. ^{1}H NMR spectra of A) DTLA (**5.3**) and B) PDTLA (**5.5**) ($CDCl_3$, 500 MHz, 298 K, * = $CHCl_3$, ** = CH_2Cl_2). Conditions: $[M]_0$ = 1 M, $[M]_0/[I]_0/[cat]_0$= 25:1:1.25 using TMG as catalyst and 4-methoxybenzyl alcohol as initiator.

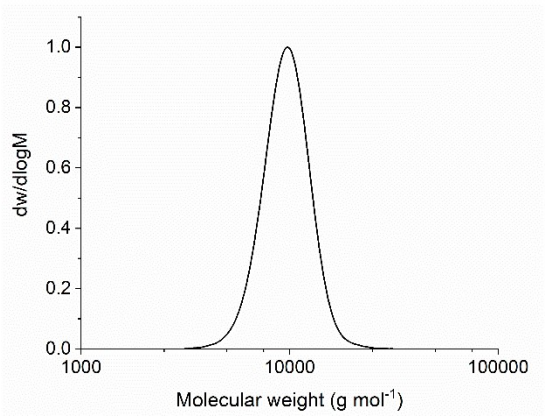

Figure 5.4. Size exclusion chromatogram of PDTLA (**5.5**) (M_n = 9.3 kg mol^{-1}, $Đ_M$ = 1.1) ($CHCl_3$, RI, calibrated against polystyrene standards). Conditions: $[M]_0$ = 1 M, $[M]_0/[I]_0/[cat]_0$ = 25:1:1.25, using TMG as catalyst and 4-methoxybenzyl alcohol as initiator.

Further analysis by matrix-assisted laser desorption/ionisation time-of-flight mass spectrometry (MALDI-ToF MS) revealed two distributions, the major one corresponding to the sodium charged PDTLA (**5.5**) and the second one for the potassium charged polymer, with both showing a spacing of 372 *m*/*z* corresponding to the monomer unit (Figure 5.5). In addition, the signal at 2767 *m*/*z* was assigned to the sodium charged PDTLA (**5.5**) with a degree of polymerisation (DP) of 7, initiated from 4-methoxybenzyl alcohol, which corroborated a high end-group fidelity. This feature was also confirmed by ^{1}H NMR spectroscopy that displayed the characteristic signals from the end group at δ = 3.79 and 6.86 ppm (Figure 5.3b). Finally, the number-average molecular weight (M_n) was shown to increase linearly with the monomer-to-initiator ratio ([M]/[I]), while the dispersity values remained low throughout the polymerisation (Figure 5.6a). However, a minor high MWt shoulder was observed for polymers with higher DPs, which could be originated from undesirable transesterification reactions (Figure 5.6b). As the polymers were purified by precipitation, the low MWt polymers would be removed and result in a high MWt shoulder. Nevertheless, this profile demonstrated that this polymerisation system was well controlled, allowing the synthesis of PDTLA (**5.5**) with predictable M_n according to the $[M]_0/[I]_0$.

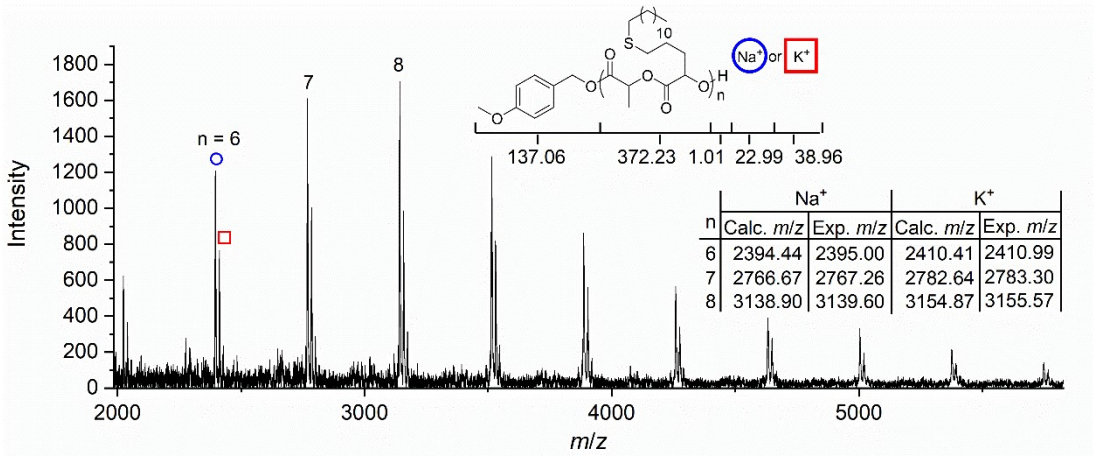

Figure 5.5. MALDI-ToF MS analysis of PDTLA (**5.5**). Conditions: $[M]_0$ = 1 M, $[M]_0/[I]_0$ = 10, using 5 mol% TMG and 4-methoxybenzyl alcohol as initiator.

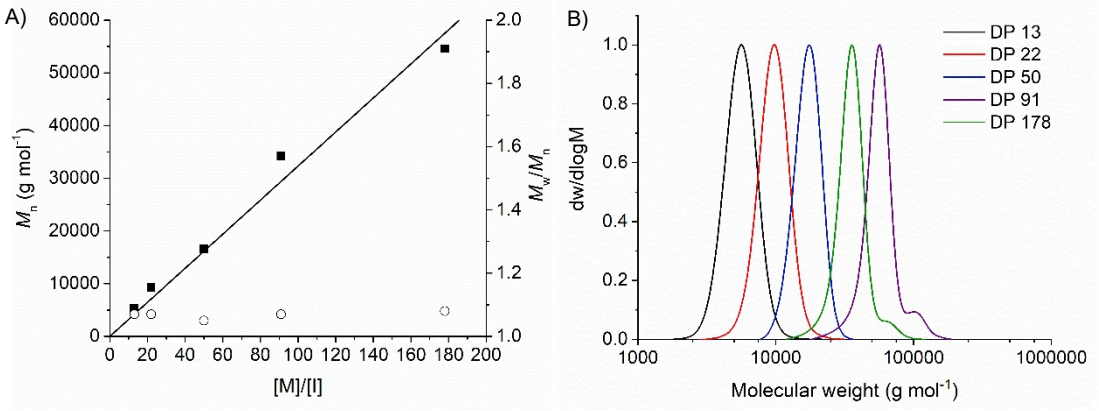

Figure 5.6. Plots of A) number-average molecular weight (M_n; ■) and dispersity ($Đ_M$ = M_w/M_n; ○) against monomer-to-initiator concentration ratio ([M]/[I]) and B) evolution of size exclusion chromatograms of PDTLA (**5.5**) with DPs varying from 13 to 178 ($CHCl_3$, RI, calibrated against polystyrene standards). Conditions: $[M]_0$ = 1 M, using 5 mol% TMG and 4-methoxybenzyl alcohol as initiator.

As with DTLA (**5.3**), the polymerisation progress of DTGA (**5.4**) was monitored by ^{1}H NMR spectroscopy, where the formation of the polymer was confirmed by the disappearance of the methine signal of the monomer at δ = 4.95 ppm and the appearance of the corresponding proton resonance in the polymer at δ = 5.17 ppm (Figure 5.7). The ROP of DTGA was carried out using 2 mol% of TMG, which provided 85% monomer conversion in 20 minutes for a $[M]_0/[I]_0$ = 100. SEC analysis of PDTGA (**5.6**) revealed a narrow and monomodal distribution, although it became broader at prolonged polymerisation times, which indicated the incidence of

transesterification of the polymer (Figure 5.8). In an attempt to avoid this undesirable reaction, the catalyst loading was reduced to 1 mol%; however, almost no monomer conversion was observed after 24 hours. Therefore, the TMG loading was maintained at 2 mol%, and the polymerisations were quenched at monomer conversions below 90%, which was before the onset of transesterification.

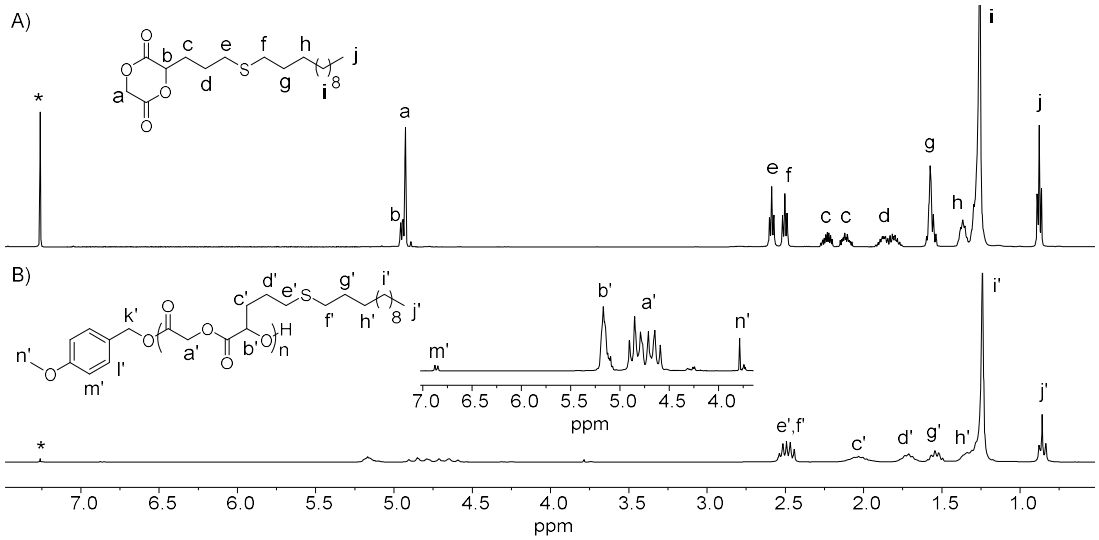

Figure 5.7. ^{1}H NMR spectra of A) DTGA (**5.4**) and B) PDTGA (**5.6**) ($CDCl_3$, 500 MHz, 298 K, * = $CHCl_3$). Conditions: $[M]_0$ = 1 M, $[M]_0/[I]_0/[cat]_0$ = 50:1:1, using TMG as catalyst and 4-methoxybenzyl alcohol as initiator.

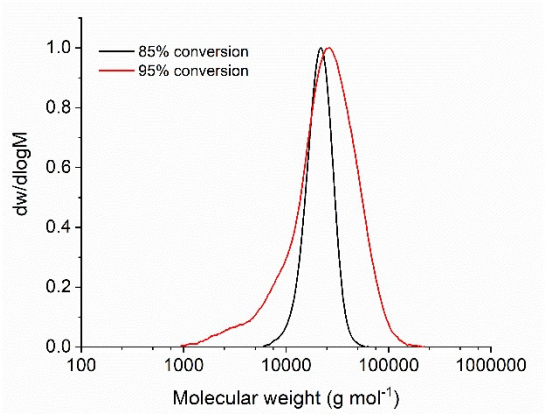

Figure 5.8. Size exclusion chromatograms of PDTGA (**5.6**) at monomer conversions of 85% (M_n = 19.9 kg mol^{-1}, $Đ_M$ = 1.10) and 95% (M_n = 15.9 kg mol^{-1}, $Đ_M$ = 1.87) ($CHCl_3$, RI, calibrated against polystyrene standards). Conditions: $[M]_0$ = 1 M, $[M]_0/[I]_0/[cat]_0$ = 100:1:2 using TMG as catalyst and 4-methoxybenzyl alcohol as initiator.

The MALDI-ToF MS analysis of a low molecular weight polymer displayed a main distribution attributed to a sodium charged PDTGA (**5.6**) and a second one with increments of 16 *m*/*z* corresponding to the potassium charged polymer (Figure 5.9). The distributions showed a spacing of 358 *m*/*z* that corresponds to the monomer unit and a peak at 2311 *m*/*z* attributed to the sodium charged PDTGA (**5.6**) with DP of 6, initiated from 4-methoxybenzyl alcohol. The end-group fidelity was also demonstrated in the ^{1}H NMR spectrum that showed the aromatic signal at δ = 6.86 ppm and the methoxy protons resonance at δ = 3.79 ppm (Figure 5.7). Further investigation of the polymerisation control revealed a linear increase of the molecular weight with the [M]/[I] along with narrow dispersity values. (Figure 5.10). However, a non-zero intercept was observed, which could indicate that the rate of propagation is higher than the that of initiation.

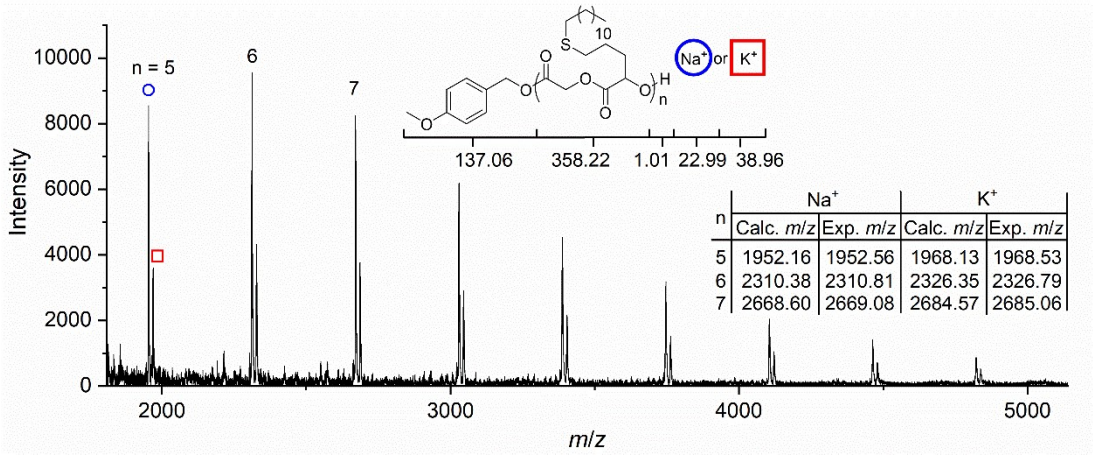

Figure 5.9. MALDI-ToF MS analysis of PDTGA (**5.6**). Conditions: $[M]_0$ = 1 M, $[M]_0/[I]_0$ = 10, using 2 mol% TMG and 4-methoxybenzyl alcohol as initiator.

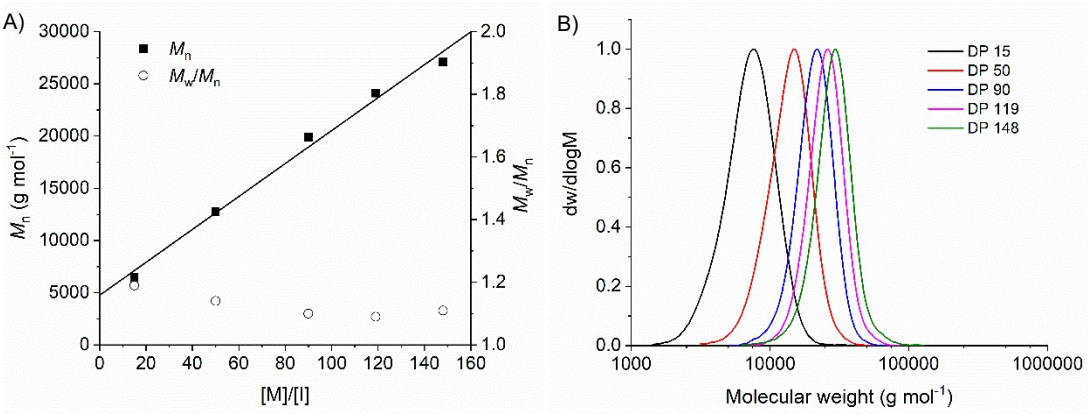

Figure 5.10. Plots of A) Number-average molecular weight (M_n; ■) and dispersity ($Đ_M = M_w/M_n$; ○) against monomer-to-initiator concentration ratio ([M]/[I]) and B) evolution of size exclusion chromatograms of PDTGA (**5.6**) with DPs varying from 15 to 148 ($CHCl_3$, RI, calibrated against polystyrene standards). Conditions: $[M]_0 = 1$ M, using 2 mol% TMG and 4-methoxybenzyl alcohol as initiator.

These results showed the good levels of control in the polymerisation of thiol-functional cyclic diesters catalysed by TMG, although DTGA (**4.4**) is more susceptible to transesterification reactions, probably as a result of the low steric hindrance of the glycolide unit.

5.2.2 Resin Formulation and Materials Characterisation

As the polymerisation of the thiol-lactide monomer was shown to be well controlled, the next studies focused on the use of a bifunctional analogue of lactide as a crosslinker. As such, the synthesis of bis(thiol-lactide) (BTLA) described in Chapter 4 was scaled up to allow the preparation of PLA thermosets (Scheme 5.6) and the preparation of a suitable resin composition for photopatterning was studied. We initially investigated the formation of a network by the copolymerisation of L-LA with BTLA, where the crosslinker would be incorporated into the growing PLLA chains. Considering that both monomers are solids, the use of a diluent was necessary to obtain a liquid resin at room temperature. This diluent would be further removed after the polymerisation to provide the crosslinked material. However, networks formed under these conditions result in swollen and fragile structures and, therefore, the amount of diluent should be kept to a minimum.[22] While diluents previously utilised for PLLA resins (*i.e.* ethyl lactate[23] and propylene carbonate[24]) provided low solubility for L-LA and BTLA (> 60 wt% diluent), less typical solvents were then considered (*i.e.* ethyl

acetate, dioxane, and *N*,*N*-dimethylformamide (DMF)), with DMF providing the best solubility (50 wt%). Finally, residual water present in the resin was considered as the initiator, once this would avoid the extensive drying procedures typically required to obtain well-defined polymers by ROP and thus, enable performing the polymerisation under more practical conditions.

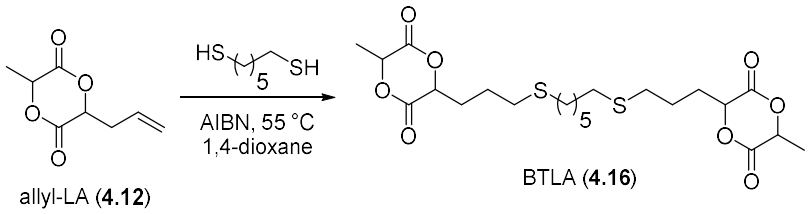

Scheme 5.6. Synthesis of BTLA (**4.16**).

The preparation of crosslinked materials was initially investigated using TMG as a catalyst in order to determine the appropriate loadings necessary to obtain short curing times. Accordingly, a resin containing L-LA/BTLA ratio of 8:2 in DMF was prepared, and 5 mol% TMG (related to L-LA + BTLA) was added into the solution. Under these conditions, the resin became viscous, although no curing was observed in 10 minutes. The catalyst loading was increased to 10 mol%, and the resin stopped flowing after 4 minutes. The resultant polymer was insoluble in CH_2Cl_2, a good solvent for PLLA and PDTLA, which indicated the materials were crosslinked.

To characterise the mechanical properties of the PLA network, dogbone-shaped samples were prepared by adding TMG into the formulation containing L-LA/BTLA (8:2) in DMF and immediately transferring into Teflon moulds. To remove the diluent, the materials were placed in a vacuum oven at 60 °C until the weight stopped decreasing and constant measurements were obtained (~ 24 hours). The resultant dogbone-shaped samples were submitted to a tensile test, which was carried out at room temperature (~ 26 °C) at a rate of 3 mm min^{-1}. The tests showed an ultimate tensile strength of 1.8 ± 0.2 MPa, a strain at peak of 286 ± 24% and a Young's modulus of 5.8 ± 0.3 MPa (Figure 5.11, black curve). However, materials prepared on different days presented inconsistent properties: while some samples were inefficiently cured and resulted in the materials not being able to maintain their shape, others presented higher stiffness. This divergence was more clearly evidenced in the tensile test that showed, for example, a material with an ultimate tensile strength of 2.7 MPa and a

Young's modulus of 12.9 MPa, values that were considerably higher than those initially tested (Figure 5.11, red curve). This inconsistency is likely to be caused by a variation in the water content in the resin, which would provide different degrees of polymerisation and ultimately modify the mechanical properties of the resultant material.

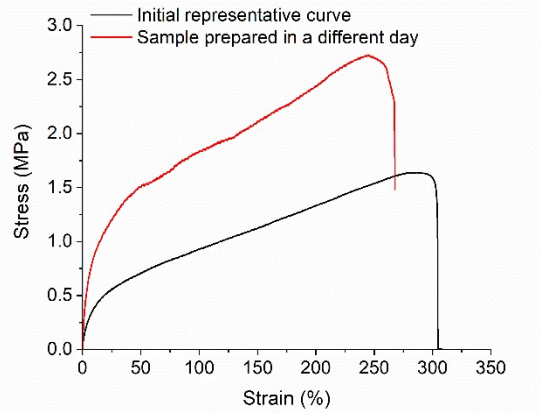

Figure 5.11. Plot of stress against strain for networks prepared from L-LA/BTLA (8:2) in different days.

To avoid the issues caused by the different quantities of water in the formulation, the preparation of lactide oligomers as macroinitiators was envisioned. This strategy would lead to a high initiator content in the resin and allow the crosslinker to react preferentially with the macroinitiator rather than water. As such, 2-arm PLLA (**5.7**) and 3-arm PLLA (**5.8**) were prepared by using 1,3-propanediol or glycerol as initiators, respectively, with target DPs of 10 and 20. Again, to avoid the laborious removal of water and simplify the preparation of oligomers in large quantities, no preliminary drying procedure was performed. In this case, the ROP of L-LA was carried out under bulk conditions at 175 °C in the presence of 4-dimethylaminopyridine (DMAP) as a catalyst, which provided full monomer conversions in only 5 minutes. The purification of the resultant oligomers was attempted by precipitation in methanol; however, high solubilities were observed in this solvent. As such, a solution of hexane/ethanol (10:1) was utilised, although the complete removal of catalyst proved to be challenging as a consequence of its low solubility in hexane. After consecutive precipitation steps and removal of volatiles under reduced pressure, the ^{1}H NMR spectra of resultant oligomers displayed

negligible amounts of DMAP (< 1%) and were therefore utilised without further purification (Figure 5.12).

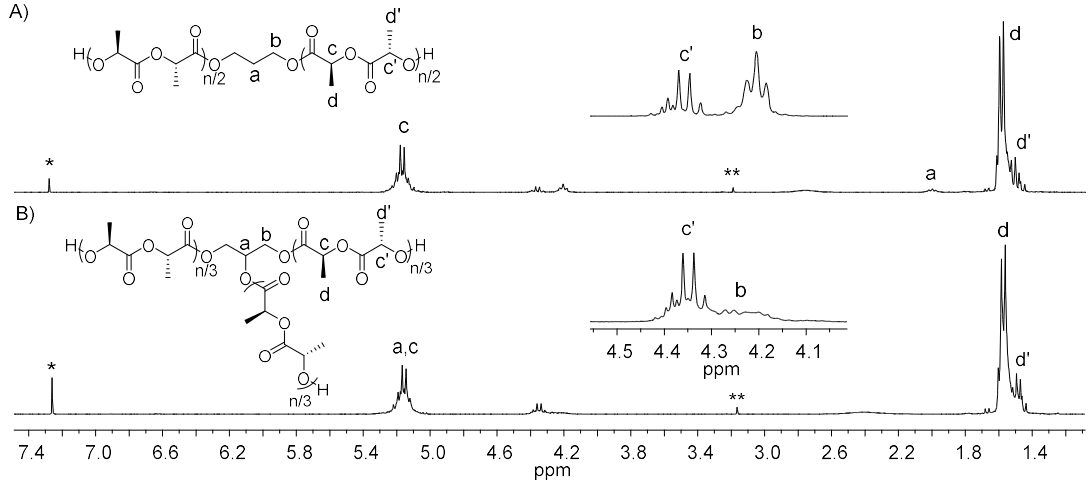

Figure 5.12. ^{1}H NMR spectra of A) 2-arm $PLLA_{17}$ and B) 3-arm $PLLA_{18}$ ($CDCl_3$, 300 MHz, 298 K, * = $CHCl_3$, ** = DMAP).

Additional analysis of the ^{1}H NMR spectra allowed calculation of the DP of PLLAs. Specifically for the 2-arm oligomers, comparison of the methylene signal in the initiator at δ = 4.21 ppm and the methine proton resonance in the polymer at δ = 5.16 ppm revealed DPs of 10 and 17 (Example of DP 17 showed in Figure 5.12a). Regarding the 3-arm PLLAs, the methylene signals in the glycerol ester appeared at δ = 4.27 ppm and comparison with the methine signals in the polymer at δ = 5.16 ppm showed DPs of 9 and 18 (Example of DP 18 showed in Figure 5.12b). Further analysis by SEC showed a monomodal distribution for 2-arm PLLAs, whereas the 3-arm polymers presented a low MWt shoulder (Figure 5.13). As the polymerisation was carried out without any drying process, this bimodality is believed to be originated from competitive water initiation that would lead to the propagation in a single direction, while the polymers initiated from glycerol would propagate in 3 directions, thus providing higher MWt.

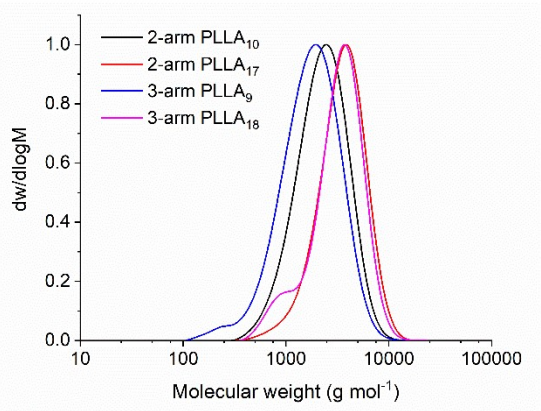

Figure 5.13. Size exclusion chromatograms of 2-arm $PLLA_{10}$ (M_n = 1.9 kg mol^{-1}, $Đ_M$ = 1.4), 2-arm $PLLA_{17}$ (M_n = 2.9 kg mol^{-1}, $Đ_M$ = 1.3), 3-arm $PLLA_9$ (M_n = 1.3 kg mol^{-1}, $Đ_M$ = 1.6) and 3-arm $PLLA_{18}$ (M_n = 2.5 kg mol^{-1}, $Đ_M$ = 2.4) prepared from 1,3-propanediol and glycerol (RI, THF, calibrated against polystyrene standards).

The resins containing PLLA oligomers were then prepared utilising 1:0.5 ratio of PLLA hydroxy chain end to BTLA (*i.e.* one hydroxy chain end per cycle in BTLA) in DMF as a diluent. The TMG loading was investigated for this system, which required less catalyst than the previous resins utilising L-LA as a monomer, once only BTLA would be polymerised in the new resin formulation. As such, cured materials were obtained in less than 10 minutes utilising 20 mol% catalyst (related to BTLA). The networks were then dried in a vacuum oven at 60 °C for 24 hours until complete removal of DMF and were labelled as NXarm-$PLLA_Y$, where X is the number of arms and Y is the DP of the PLLA oligomer.

The thermal properties of the PLLA precursors and the resultant network materials were characterised by differential scanning calorimetry (DSC). The thermograms of PLLA oligomers revealed glass transition temperatures (T_g) of around 30 °C, which was consistent with previously reported data for low MWt PLLA (37 °C, DP = 15) (Table 5.1, Entries 1-4).[25] As for the network materials, all samples presented a T_g slightly lower than the original PLLA oligomers, a result that contrasts with the reduced mobility on the chain segments upon crosslinking that typically leads to an increase on the T_g (Table 5.1, Entries 5-8, Figure 5.14, see other DSC thermograms in Figures A.6−A.8 in Appendix).[9,23] However, the BTLA crosslinker presents a long carbon chain that provides flexibility to the network and ultimately contributes for a greater mobility, thus reducing the T_g.[15,25] In addition, no melting peak was observed

in the first or second scan, which indicated the amorphous nature of the polymer networks.

Table 5.1. Thermal properties of PLLA precursors and networks formed from PLLA and BTLA.

Entry	Sample	T_g[a] (°C)	T_d 1%[b] (°C)	T_d 5%[c] (°C)
1	2-arm $PLLA_{10}$	26	196	241
2	2-arm $PLLA_{17}$	32	179	245
3	3-arm $PLLA_{9}$	28	182	235
4	3-arm $PLLA_{18}$	36	141	251
5	N2-arm $PLLA_{10}$	20	138	221
6	N2-arm $PLLA_{17}$	26	132	208
7	N3-arm $PLLA_{9}$	26	125	202
8	N3-arm $PLLA_{18}$	32	111	182
9	BTLA	-	200	270

[a] Determined by DSC analysis from the second heating scan. [b] Determined by TGA at 1% weight loss. [c] Determined by TGA at 5% weight loss.

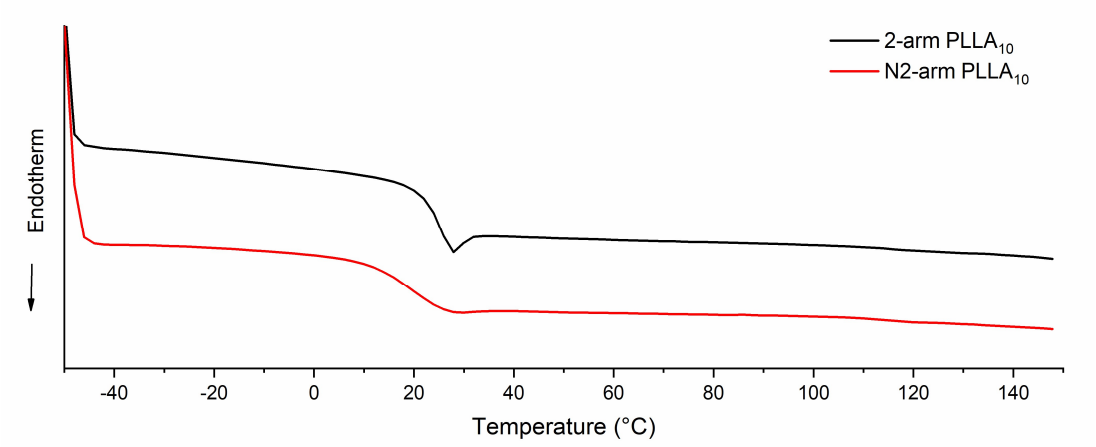

Figure 5.14. DSC thermograms of second heating scan of 2-arm $PLLA_{10}$ and its corresponding network. Conditions: heating and cooling cycles between −50 and 150 °C under N_2 atmosphere at a rate of +/− 10 °C min^{-1}.

The thermogravimetric analysis (TGA) showed a weight loss of 5% at around 245 °C for the PLLA oligomers, although they gradually degraded from temperatures below 200 °C (Table 5.1, Entries 1-4, Figure 5.15a). This effect was more pronounced

for the networks, which showed the start of degradation at ~120 °C and slowly progressed until ~200 °C, after what there was a sharper mass loss (Table 5.1, Entries 5-8 and Figure 5.15b). This gradual weight loss could be a result of small amounts of DMAP catalyst present in the oligomer that would accelerate the degradation of the network at elevated temperatures. Nonetheless, the PLLA oligomers and the corresponding networks were shown to be stable at room temperature for up to three months, enough time scale to allow the preparation and characterisation of the materials. In case further studies were required, a silica plug could be utilised to remove any residual DMAP. Finally, the crosslinker BTLA showed a higher degradation temperature (T_d 5% = 270 °C) that would contribute to a greater thermal stability to the network.

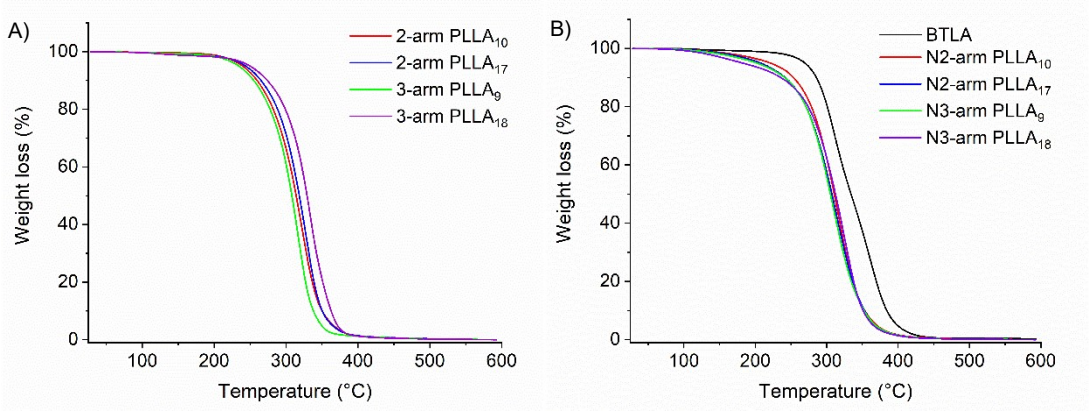

Figure 5.15. TGA thermograms of A) PLLA oligomers and B) PLLA networks and BTLA.

To evaluate the mechanical properties of the networks, dogbone-shaped structures were prepared and analysed by tensile test at room temperature (26 °C). The materials obtained showed consistent results independently on the day of preparation, which suggested that water initiation was indeed minimised when using PLLAs as macroinitiators. Interestingly, the networks presented Young's modulus and tensile strength significantly lower than that of high MWt PLLAs (*e.g.* PLLA of M_W = 66 kg mol^{-1}: Young's modulus = 3500 MPa, tensile strength = 59 MPa) (Table 5.2, Figure 5.16).[26] The decrease in the Young's modulus and tensile strength (13−34 MPa and 1.4−3.9 MPa, respectively) could be a result of the proximity of the T_g of the materials to room temperature that would cause an increased flexibility of the polymer chains, and therefore, a reduced rigidity during the mechanical characterisation.[15] In addition,

PLA is known for presenting an intrinsic relationship between the crystallinity and the mechanical strength of the material.[27] Since the networks produced herein indicated an amorphous nature, the reduction in tensile performance can be related to the decreased contributions associated with strong interactions present in crystalline segments of PLLA.

Table 5.2. Mechanical properties of PLLA networks prepared from PLLA oligomers and BTLA.[a]

Entry	Network	Young's Modulus (MPa)	Elongation at Peak (%)	Tensile Strength (MPa)
1	N2-arm $PLLA_{10}$	19 ± 4	173 ± 118	1.6 ± 0.3
2	N2-arm $PLLA_{17}$	34 ± 3	48 ± 12	3.9 ± 0.6
3	N3-arm $PLLA_{9}$	13 ± 1	268 ± 31	1.9 ± 0.1
4	N3-arm $PLLA_{18}$	19 ± 2	26 ± 6	1.4 ± 0.1

[a] Mechanical properties were determined by uniaxial tensile test at a rate of 3 mm min^{-1}.

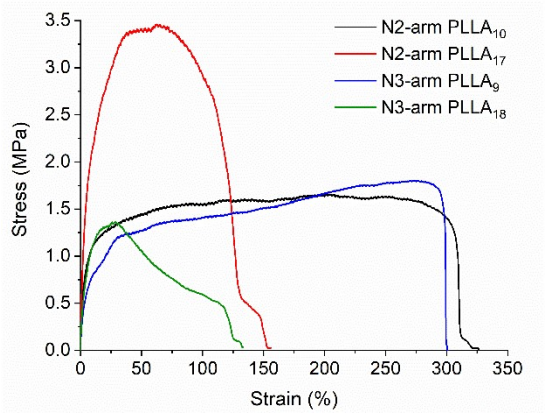

Figure 5.16. Representative plots of stress against strain of PLLA networks.

Comparison of the mechanical properties of the different networks produced showed that materials formed with PLLA of higher DP presented superior tensile performance when compared to analogues produced with short PLLA chains. This characteristic was attributed to stronger interactions between the hard PLLA chains as the molecular weight between the segments is increased. Interestingly, N2-arm PLLA presented higher Young's modulus than N3-arm PLLA of similar DP, which is a result of the more irregular profile of the 3-arm networks that hinders effective interactions

between the PLLA segments. Thus, these results indicate that the stronger interactions provided by PLLA have a higher contribution to the mechanical strength of the materials than the production of more tightly connected networks by using N3-arms or shorter PLLA moieties. This kind of behaviour has been previously observed in similar systems produced with PCL as the main backbone, in which less crystalline networks resulted in poorer mechanical properties.[9]

Remarkably, all samples presented high elongation at peak, especially those originated from PLLAs with lower DPs, characteristics that contrast with those of high MWt PLLA (*e.g.* PLLA of M_W = 66 kg mol^{-1}: elongation at break = 7%)[26] (Table 5.2, Figure 5.16). This feature is associated with the higher flexibility provided by the long carbon chain in BTLA that reflects in an increased mobility of the polymer network.[25] This effect was more pronounced when using low MWt oligomers as the amount of crosslinker per lactide repeating unit is higher, which provides an increased content of flexible segments in the network. These studies demonstrated that networks of different mechanical properties could be efficiently produced by utilising PLLA oligomers in combination with BTLA as a crosslinker. Moreover, the use of preformed polymers allowed the preparation of materials in an open atmosphere, which simplified the procedure when compared to previous reports that utilised strictly dried conditions.

5.2.3 Studies on the Preparation of Networks by Photoactivation

5.2.3.1 Use of a TMG Photobase Generator

Once the preparation of PLLA networks from BTLA crosslinker catalysed by TMG was demonstrated, the photobase generator (PBG) NPPOC-TMG, was investigated to generate TMG upon irradiation and ultimately lead to a temporal and spatial control in the formation of crosslinked materials. As such, resins composed of PLLA and BTLA (1:0.5) in DMF and 20 mol% NPPOC-TMG (relative to BTLA) were prepared and exposed to λ = 320–400 nm light. However, no curing was observed after irradiating the samples for up to 20 minutes, even after increasing the catalyst loadings to 40 mol%.

Analysis of the resins by ^{1}H NMR spectroscopy revealed that, while determining the TMG release was impractical because its signal overlapped with the DMF resonance, the presence of small quantities of nitrostyrene byproduct at δ = 7.85 ppm indicated that the photolysis occurred only to a small extent (Scheme 5.7, Figure 5.17).

This corroborates the lower TMG release efficiency in highly concentrated solutions (*i.e.* 100 mM NPPOC-TMG in this resin), as demonstrated in Chapter 3. Those studies showed that a 100 mM NPPOC-TMG solution required 3 hours to release 86% TMG, whereas a 20 mM solution was able to produce the same percentage of free catalyst in 1 hour. This was attributed to the scattering and absorption effects that disturb the photolysis process and are more pronounced as the concentration of chromophore increases.[28,29] These results showed that NPPOC-TMG was inefficient for the system as a consequence of the relatively low catalytic activity of TMG that required the use of high catalyst concentrations.

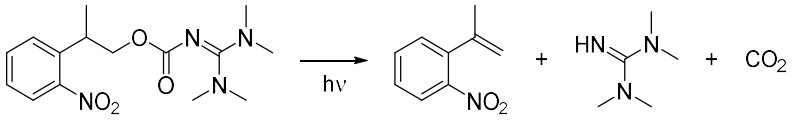

Scheme 5.7. Photolysis of NPPOC-TMG.

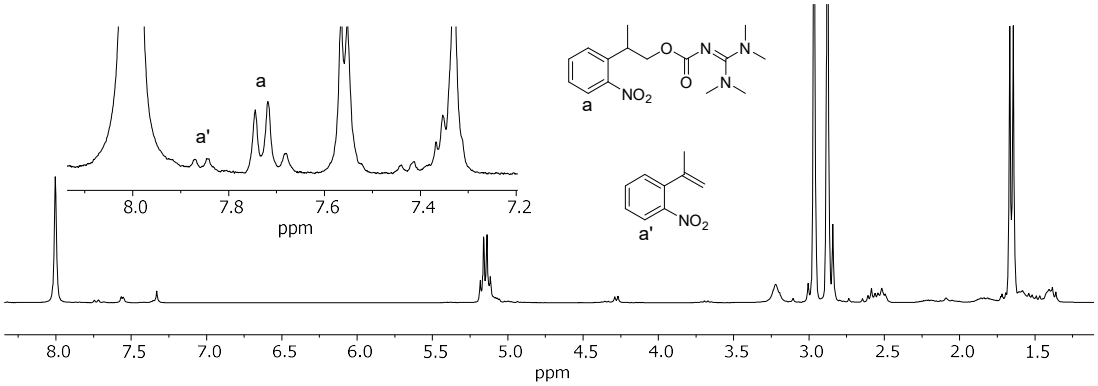

Figure 5.17. ^{1}H NMR of PLLA/BTLA resin in the presence of NPPOC-TMG after λ = 320–400 nm irradiation ($CDCl_3$, 300 MHz, 298 K).

5.2.3.2 Investigation of TBD Photocatalysts

Given the challenges observed with the use of NPPOC-TMG, we envisioned the use of more efficient PBGs that could be photocleaved more quickly and release a more active catalyst. In this regard, several PBG of carboxylate salts of TBD with thioxanthone or anthraquinone chromophores were investigated (Figure 5.18).[i] The use of TBD as a ROP catalyst has been reported by Lohmeijer *et al*. and was shown

[i] This work was done in collaboration with Dr Haritz Sardon and Dr Nicolas Zivic, from the University of the Basque Country, who prepared the PBGs.

to polymerise LA to full monomer conversion in 20 seconds for a $[M]_0/[I]_0$ of 100 and catalyst loading of only 0.1 mol% (*i.e.* ~1000 times faster than TMG (5 hours using 1 mol%)).[18] Therefore, we envisioned that the higher catalytic activity provided by TBD would allow a decrease in the catalyst loadings in the resin and minimise the side effects caused by the use in high concentrations.

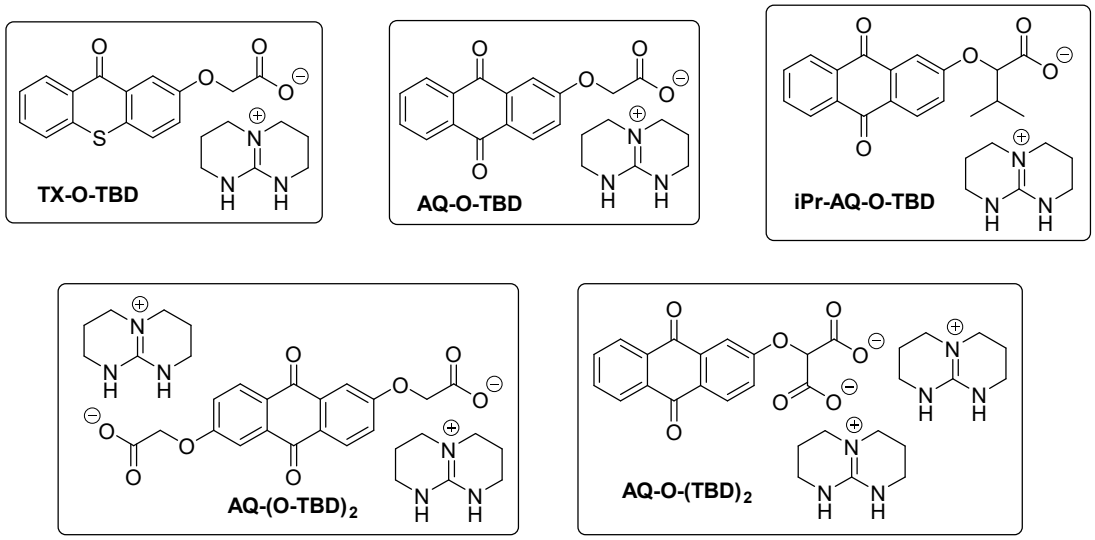

Figure 5.18. PBGs based on carboxylate salt of TBD investigated in this work.[i]

The UV-Vis spectrum of TX-O-TBD showed maximum absorption at 400 nm, while the anthraquinone analogues' maximum absorption was found to be 375 nm and, therefore, photolysis studies were carried out using a λ = 320–400 nm light (Figure 5.19). The PBGs photolyses were monitored by ^{1}H NMR spectroscopy that allowed calculating the catalyst release from the decrease in the integration of methylene signal in the carboxylate chromophore, that varied from δ = 4.4 to 5.2 ppm depending on the PBG, as the photocatalyst decomposed over irradiation time (Scheme 5.8, Figure 5.20 and Figures A.9−A.12 in Appendix). Overall, the anthraquinone PBGs displayed higher photolysis efficiency than the thioxanthone derivative, (> 90% *vs* 44% release in 20 minutes, respectively) (Table 5.3). However, the PBGs containing two TBD molecules presented lower solubility in $CDCl_3$, with AQ-(O-TBD)$_2$ being slightly insoluble even at a concentration of 10 mM.

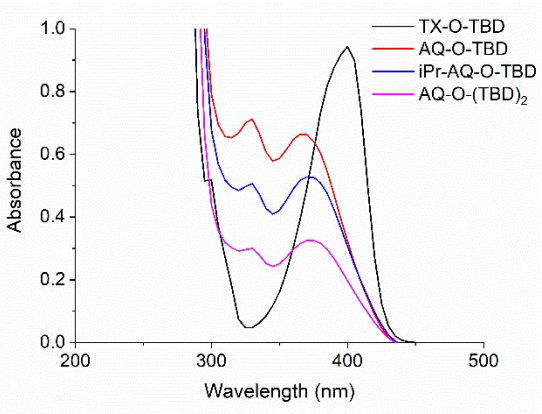

Figure 5.19. UV-Vis spectra of TX-O-TBD (0.13 mM in MeCN), AQ-O-TBD (0.24 mM in MeCN), iPr-AQ-O-TBD (0.22 mM) and AQ-O-$(TBD)_2$ (0.17 mM in MeCN).

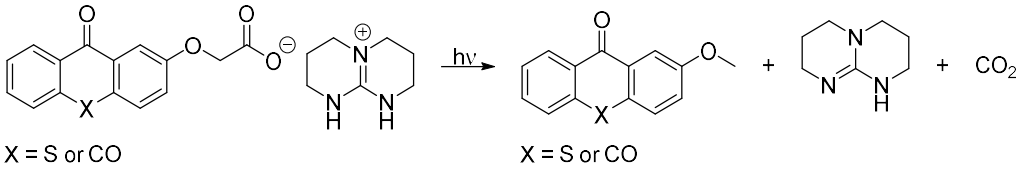

Scheme 5.8. Photolysis of PBGs based on carboxylate salts of TBD.

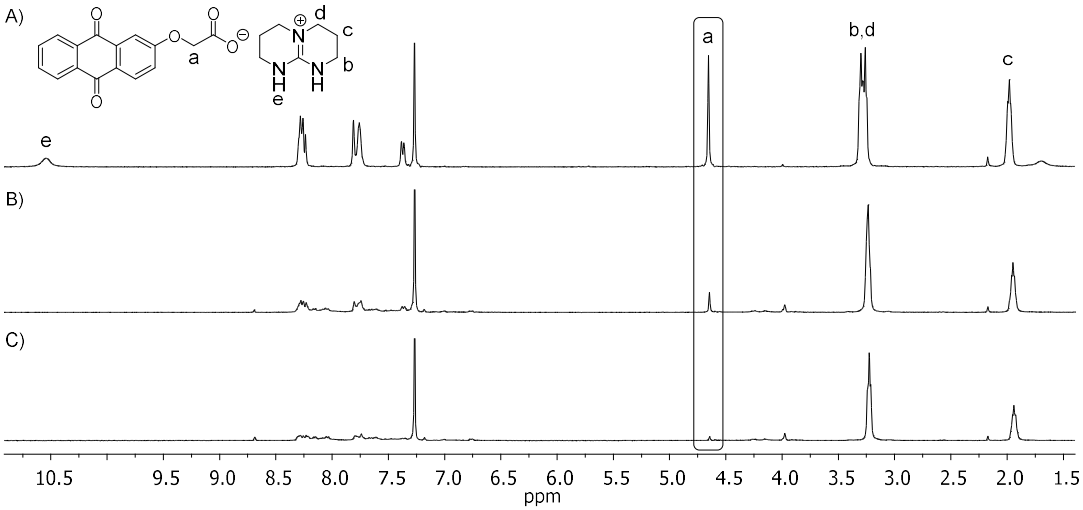

Figure 5.20. ^{1}H NMR spectra of AQ-O-TBD in $CDCl_3$ (10 mM) A) before and after λ = 320–400 nm irradiation for B) 10 minutes and C) 20 minutes ($CDCl_3$, 300 MHz, 298 K).

Table 5.3. TBD release for PBGs solutions in $CDCl_3$ (10 mM) under λ = 320–400 nm irradiation.

	TBD Release[a] (%)				
Irradiation Time (min)	**TX-O-TBD**	**AQ-O-TBD**	**iPr-AQ-O-TBD**	**AQ-(O-TBD)$_2$[b]**	**AQ-O-(TBD)$_2$**
10	27	91	79	79	84
20	44	> 95	94	90	> 95

[a] Determined by ^{1}H NMR spectroscopy. [b] Slightly insoluble at 10 mM in $CDCl_3$.

The anthraquinone PBGs were then investigated in the photoinduced ROP of L-LA, which was carried out in $CDCl_3$ ($[M]_0$ = 1 M) at room temperature, with $[M]_0/[I]_0$ of 125 and 0.1 mol% photocatalyst (except by AQ-(O-TBD)$_2$ that was shown to be insoluble under these conditions and therefore was not investigated). The polymerisation solution was initially maintained in the absence of light and analysed by ^{1}H NMR spectroscopy, which showed no polymerisation occurring under these conditions, as evidenced by the presence of the methylene signal of benzyl alcohol at δ = 4.65 pm (Example using AQ-O-(TBD)$_2$ in Figure 5.21a). The sample was then irradiated with λ = 320−400 nm light for 5 minutes and quenched by adding acidic Amberlyst after 2 minutes. Further analysis by ^{1}H NMR spectroscopy allowed calculation of the monomer conversion by comparing the integration of the methine signal in the monomer at δ = 5.03 ppm and in the polymer at δ = 5.14 ppm (Figure 5.21b). AQ-O-TBD provided higher monomer conversions than the isopropyl analogue (68% *vs* 44%, respectively), which corroborated the higher TBD release by the former (Table 5.4). On the other hand, AQ-O-(TBD)$_2$ yielded almost full monomer conversion even though it presented lower TBD release than AQ-O-TBD after 10 minutes irradiation. This was attributed to the release of two catalyst molecules by AQ-O-(TBD)$_2$, which would provide a higher overall TBD concentration, thus a faster polymerisation. Remarkably, all PBGs were shown to induce the polymerisation when the solution was kept in ambient light, which indicated the high susceptibility to photolysis even with low-intensity irradiation. Finally, the resultant polymers were analysed by SEC, which displayed narrow molecular weight distributions, although the PLLA obtained from AQ-O-(TBD)$_2$ presented a high molecular weight shoulder assigned to the well-known transesterification reactions that occur for TBD catalysed ROP of LA at high monomer conversions (Figure 5.22).[30]

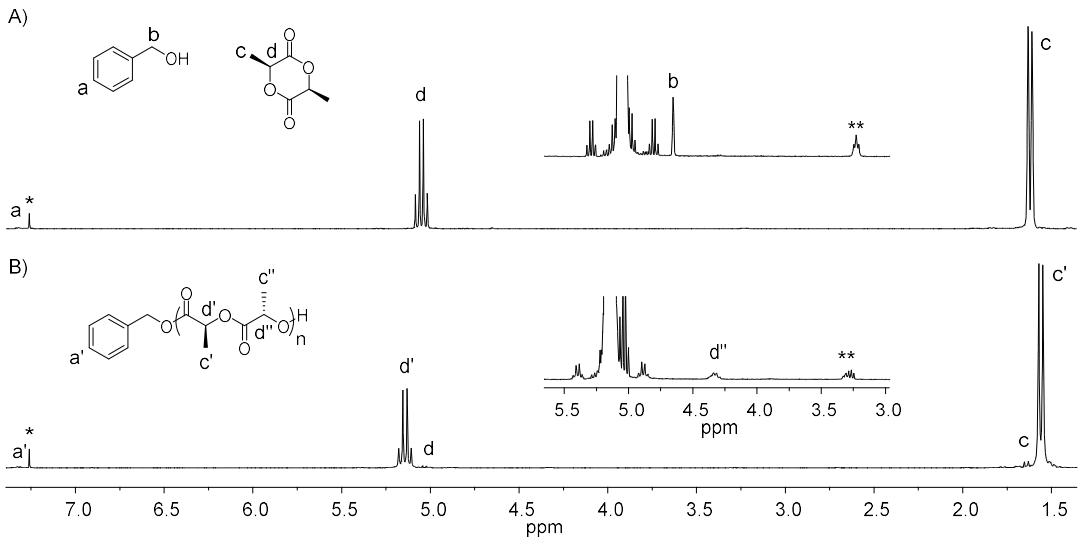

Figure 5.21. ^{1}H NMR spectra of polymerisation of L-LA catalysed by AQ-O-(TBD)$_2$ A) before and B) after λ = 320−400 nm irradiation for 5 minutes and quenched after 2 minutes ($CDCl_3$, 300 MHz, 298 K, * = $CHCl_3$, ** = TBD). Conditions: $[M]_0$ = 1 M in $CDCl_3$, $[M]_0/[I]_0$ = 125, using 0.1 mol% AQ-O-(TBD)$_2$ and benzyl alcohol as initiator.

Table 5.4. Photoinduced ROP of L-LA using different PBGs.[a]

Entry	Catalyst	Monomer Conversion[b] (%)	M_n[c] (kg mol^{-1})	$Đ_M$[c]
1	AQ-O-TBD	68	23.8	1.06
2	iPr-AQ-O-TBD	44	20.4	1.06
3	AQ-O-(TBD)$_2$	> 95	34.0	1.09

[a] Polymerisation carried out in $CDCl_3$ ($[M]_0$ = 1 M, $[M]_0/[I]_0$ = 125) with 0.1 mol% PBG under λ = 320−400 nm irradiation for 5 minutes and quenched after 7 minutes from start of irradiation. [b] Determined by ^{1}H NMR spectroscopy. [c] Determined by SEC analysis in $CHCl_3$ using RI detector, calibrated against polystyrene standards.

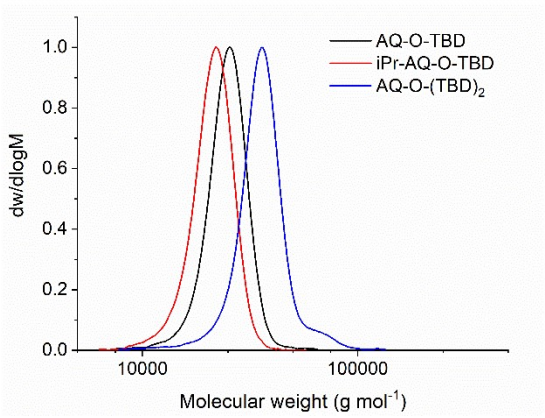

Figure 5.22. Size exclusion chromatograms of PLLA prepared with AQ-O-TBD (M_n = 23.8 kg mol^{-1}, $Đ_M$ = 1.06), iPr-AQ-O-TBD (M_n = 20.4 kg mol^{-1}, $Đ_M$ = 1.06), and AQ-O-(TBD)$_2$ (M_n = 34.0 kg mol^{-1}, $Đ_M$ = 1.09) ($CHCl_3$, RI, calibrated against polystyrene standards). Conditions: $[M]_0$ = 1 M in $CDCl_3$, $[M]_0/[I]_0/[cat]_0$ = 125:1:0.125, using benzyl alcohol as initiator, 5 minutes under λ = 320–400 nm irradiation, quenched after 7 minutes from start of irradiation.

The fast photolysis of the anthraquinone PBGs, combined with the high activity of the released TBD allowed the ROP of L-LA to occur up to 50 times faster than utilising NPPOC-TMG (6 hours for a $[M]_0/[I]_0$ = 100, 15 minutes irradiation), while utilising a catalyst loading as low as 0.1 mol%. With these promising results, AQ-O-TBD and AQ-O-(TBD)$_2$ were selected for further investigation on the preparation of networks from PLLA and BTLA, as they demonstrated greater photolysis efficiency.

5.2.3.3 Use of TBD Photobase Generators

As previously investigated with TMG, the preparation of crosslinked materials was initially studied with free TBD using a resin composition of PLLA/BTLA (1:0.5) and 50 wt% DMF. However, the resins cured almost instantaneously after the addition of a diluted solution of TBD in DMF, and produced heterogeneous materials, even using catalyst loadings of 0.01 mol%. Nevertheless, homogeneous networks were expected to be produced by utilising the photoinduced crosslinking strategy, as the photocatalyst would be evenly spread across the resin prior to irradiation. As such, AQ-O-TBD was added to the resin at loadings of 0.1 to 0.5 mol% (relative to BTLA) and exposed to λ = 320–400 nm light for up to 10 minutes. However, no curing occurred under these conditions, with the same results being observed when utilising AQ-O-(TBD)$_2$ at loadings of 0.1 to 0.25 mol% (maximum value defined by the

solubility of the PBG in DMF). Although the use of small amounts of PBG limited the visualisation of appropriate signals in the ^{1}H NMR spectrum to calculate the catalyst release, complete photolysis was expected to have occurred within 10 minutes irradiation, once the concentration of PBG in solution was below 5 mM, and preliminary studies showed a release of 84% for 10 mM AQ-O-(TBD)$_2$ solution.

These unexpected results can be rationalised by the reaction of the CO_2 released after photolysis of the PBG with TBD to form an inactive adduct. Villiers *et al*. have previously demonstrated that TBD-CO_2 adducts present a zwitterionic structure that, while stable in the solid state or polar solvents such as acetonitrile, undergo CO_2 dissociation in less polar solvents such as THF (Figure 5.23).[31] This stability goes in line with observations in our work that showed the successful polymerisation of L-LA in a non-polar solvent ($CDCl_3$), and the non-reactivity of the catalyst in the resins containing highly polar DMF. In addition, PBGs that releases CO_2 and a guanidine have been successfully applied to thiol-epoxy[32,33] and thiol-Michael polymerisations,[34,35] which could be a result of the less polar characteristics of the systems. In this regard, while less polar solvents such as CH_2Cl_2 and $CHCl_3$ could be utilised as diluents for the resins, the low solubility of BTLA (> 70 wt%) prevented further investigation.

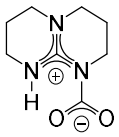

Figure 5.23. Zwitterionic structure of TBD-CO_2 adduct.

5.3 Conclusions

In this study, we investigated the preparation of networks by combining the strategy of photoinduced ROP demonstrated in Chapter 3 and the crosslinker BTLA prepared in Chapter 4. To evaluate the reactivity of the crosslinker towards ROP, monofunctional monomers analogous to LA (DTLA) and glycolide (DTGA) were synthesised and polymerised in the presence of TMG as a catalyst. The polymerisation of DTGA was shown to be fast, with a $[M]_0/[I]_0$ of 100 taking 20 minutes to reach 85% monomer conversion. However, the high reactivity of the monomers resulted in a loss of control when achieving high monomer conversions, which is attributed to transesterification side reactions that are facilitated by the low steric hindrance of the

glycolide unit. Nonetheless, polymers with narrow dispersities could be obtained by quenching the polymerisation with the addition of acidic Amberlyst at conversions below 90%. On the other hand, the ROP of DTLA was demonstrated to be well controlled, which allowed the preparation of polymers with low dispersity values and predicted M_n based on the $[M]_0/[I]_0$. Although the ROP of DTLA required higher catalyst loading than L-LA, the reactivities of both monomers were comparable, and therefore, the copolymerisation of L-LA and the BTLA crosslinker was expected to be effective.

In order to prepare crosslinked materials from BTLA, a suitable resin formulation was investigated, and TMG was utilised as a catalyst. As such, a strategy involving the incorporation of the crosslinker during the polymerisation of L-LA was considered, while utilising residual water as an initiator. However, materials with irreproducible properties were obtained, as the amount of water present in the resins depended on the environmental humidity. To avoid this inconsistency, PLLA oligomers were prepared and utilised as macroinitiators for the ROP of BTLA. This methodology not only provided reproducible results but also allowed the preparation of materials with varied mechanical properties by changing the oligomer length and architecture.

Considering that BTLA showed to provided crosslinked materials when utilising TMG as a catalyst, NPPOC-TMG was investigated as a means to generate the active ROP catalyst under UV light. However, the quantity of TMG released upon irradiation was insufficient to allow the polymerisation of BTLA, which resulted in no formation of crosslinked materials. This low catalyst release was attributed to the high concentrations of photocatalyst required in the resin that enhances undesirable scattering and absorption effects, which finally reduces the overall photolysis efficiency.

In order to obtain photocatalysts with improved efficiency and catalyst activity, PBGs based on thioxanthone and anthraquinone that release TBD as a catalyst were investigated. Initially, analysis of the PBGs photolyses revealed that the anthraquinone derivatives were more effective than thioxanthone, showing a catalyst release above 90% in 20 minutes. As such, these PBGs were utilised in the ROP of L-LA to enable comparison of activity with TMG. When utilising AQ-O-TBD or AQ-O-$(TBD)_2$ with loadings only 0.1 mol%, monomer conversions of 68 and > 95%, respectively, were obtained after 5 minutes irradiation and further 2 minutes before quenching the reaction. The low catalyst loadings along with the short irradiation times demonstrated

the high efficiency of these PBGs and the potential in the preparation of crosslinked materials.

Finally, these photocatalysts were applied to the resins of PLLA and BTLA, and again no crosslinking was observed even after increasing the catalyst loadings or irradiation times. This was believed to be originated from the formation of inactive TBD-CO_2 adducts that are stabilised in polar solvents such as DMF. Further investigation on the use of less polar solvents to decrease the adduct stability would potentially enable the desirable spatial control investigated herein. Nonetheless, we demonstrated the development of a strategy to produce crosslinked biodegradable materials under practical conditions that require no drying procedures. In addition, several highly active photocatalysts were investigated and showed great activity for ROP L-LA when utilising non-polar solvents.

5.4 References

1. B. Amsden, *Soft Matter*, 2007, **3**, 1335.
2. C. G. Pitt, R. W. Hendren, A. Schindler and S. C. Woodward, *J. Control. Release*, 1984, **1**, 3.
3. C. G. Pitt, F. I. Chasalow, Y. M. Hibionada, D. M. Klimas and A. Schindler, *J. Appl. Polym. Sci.*, 1981, **26**, 3779.
4. N. Andronova, R. K. Srivastava and A.-C. Albertsson, *Polymer*, 2005, **46**, 6746.
5. R. Palmgren, S. Karlsson and A.-C. Albertsson, *J. Polym. Sci., Part A: Polym. Chem.*, 1997, **35**, 1635.
6. A. J. Nijenhuis, D. W. Grijpma and A. J. Pennings, *Polymer*, 1996, **37**, 2783.
7. D. W. Grijpma, E. Kroeze, A. J. Nijenhuis and A. J. Pennings, *Polymer*, 1993, **34**, 1496.
8. L.-Q. Yang, B. He, S. Meng, J.-Z. Zhang, M. Li, J. Guo, Y.-M. Guan, J.-X. Li and Z.-W. Gu, *Polymer*, 2013, **54**, 2668.
9. L. Yang, J. Li, Y. Jin, M. Li and Z. Gu, *Polym. Degrad. Stab.*, 2015, **112**, 10.
10. L. Yang, J. Li, Y. Jin, J. Zhang, M. Li and Z. Gu, *Polymer*, 2014, **55**, 6686.
11. T. F. Al-Azemi and K. S. Bisht, *Polymer*, 2002, **43**, 2161.
12. F. Nederberg, V. Trang, R. C. Pratt, A. F. Mason, C. W. Frank, R. M. Waymouth and J. L. Hedrick, *Biomacromolecules*, 2007, **8**, 3294.

13. A. Pascual, J. P. Tan, A. Yuen, J. M. Chan, D. J. Coady, D. Mecerreyes, J. L. Hedrick, Y. Y. Yang and H. Sardon, *Biomacromolecules*, 2015, **16**, 1169.
14. G. X. De Hoe, M. T. Zumstein, B. J. Tiegs, J. P. Brutman, K. McNeill, M. Sander, G. W. Coates and M. A. Hillmyer, *J. Am. Chem. Soc.*, 2018, **140**, 963.
15. L. E. Nielsen and R. F. Landel, *Mechanical Properties of Polymers and Composites*, Marcel Dekker, New York, 2nd edn., 1994.
16. H. M. Younes, E. Bravo-Grimaldo and B. G. Amsden, *Biomaterials*, 2004, **25**, 5261.
17. B. Amsden, S. Wang and U. Wyss, *Biomacromolecules*, 2004, **5**, 1399.
18. B. G. G. Lohmeijer, R. C. Pratt, F. Leibfarth, J. W. Logan, D. A. Long, A. P. Dove, F. Nederberg, J. Choi, C. Wade, R. M. Waymouth and J. L. Hedrick, *Macromolecules*, 2006, **39**, 8574.
19. F. Nederberg, B. G. G. Lohmeijer, F. Leibfarth, R. C. Pratt, J. Choi, A. P. Dove, R. M. Waymouth and J. L. Hedrick, *Biomacromolecules*, 2007, **8**, 153.
20. S. M. Oskui, G. Diamante, C. Liao, W. Shi, J. Gan, D. Schlenk and W. H. Grover, *Environ. Sci. Technol. Lett.*, 2015, **3**, 1.
21. M. Yin and G. L. Baker, *Macromolecules*, 1999, **32**, 7711.
22. S. Schüller-Ravoo, J. Feijen and D. W. Grijpma, *Macromol. Biosci.*, 2011, **11**, 1662.
23. F. P. Melchels, J. Feijen and D. W. Grijpma, *Biomaterials*, 2009, **30**, 3801.
24. D. Quintanar-Guerrero, H. Fessi, E. Allémann and E. Doelker, *Int. J. Pharm.*, 1996, **143**, 133.
25. J. E. Báez, Á. Marcos-Fernández and P. Galindo-Iranzo, *J. Polym. Res.*, 2010, **18**, 1137.
26. S. Farah, D. G. Anderson and R. Langer, *Adv. Drug Deliv. Rev.*, 2016, **107**, 367.
27. G. Perego, G. D. Cella and C. Bastioli, *J. Appl. Polym. Sci.*, 1996, **59**, 37.
28. S. C. Ligon, R. Liska, J. Stampfl, M. Gurr and R. Mülhaupt, *Chem. Rev.*, 2017, **117**, 10212.
29. R. Göstl, A. Senf and S. Hecht, *Chem. Soc. Rev.*, 2014, **43**, 1982.
30. R. C. Pratt, B. G. G. Lohmeijer, D. A. Long, R. M. Waymouth and J. L. Hedrick, *J. Am. Chem. Soc.*, 2006, **128**, 4556.
31. C. Villiers, J. P. Dognon, R. Pollet, P. Thuery and M. Ephritikhine, *Angew. Chem. Int. Ed.*, 2010, **49**, 3465.

32. Z. Li, W. Shen, X. Liu and R. Liu, *Polym. Chem.*, 2017, **8**, 1579.
33. M. Bouzrati-Zerelli, M. Frigoli, F. Dumur, B. Graff, J. P. Fouassier and J. Lalevée, *Polymer*, 2017, **124**, 151.
34. W. Xi, H. Peng, A. Aguirre-Soto, C. J. Kloxin, J. W. Stansbury and C. N. Bowman, *Macromolecules*, 2014, **47**, 6159.
35. X. Zhang, W. Xi, C. Wang, M. Podgórski and C. N. Bowman, *ACS Macro Lett.*, 2016, **5**, 229.

Chapter 6

Conclusions and Future Work

6.1 Conclusions

This thesis describes strategies for the synthesis of biodegradable polycarbonates and polyesters, which are promising alternatives for more sustainable materials and for the application in the biomedical field. The first approach investigated comprised the synthesis of an epoxy-functionalised polycarbonate (PTMOC) and its post-polymerisation modifications as a strategy to tune the polymer properties. The ROP of TMOC showed to be selective for the carbonate moiety by using 1,5,7-triazabicyclo[4.4.0]dec-5-ene (TBD) as the catalyst. In addition, this system provided well-defined polycarbonates with controlled molecular weight and narrow dispersity values. The unreacted pendent epoxide functionality of the polycarbonate was further explored in post-polymerisation modifications by nucleophilic reactions. Despite the susceptibility of the carbonate moiety in undergoing competitive nucleophilic attack, the epoxide group in PTMOC was modified without degrading the backbone by optimising the reaction conditions. Indeed, the complete functionalisation of the polymer was achieved with benzylamine and chlorine at high temperatures, which yielded well-defined polycarbonates. However, the reaction of PTMOC with iodine was shown to be prone to crosslinking, as a consequence of the higher leaving capability of the group.

Further post-polymerisation modification of PTMOC with thiols provided varying degrees of functionalisation depending on the thiol nature, being especially high when employing aryl thiols. In addition, no side reactions or degradation of the polymer was observed when using excess thiol and low catalyst loadings. Hence, the pendent epoxy functionality allowed the efficient insertion of a series of groups into a polycarbonate, which results in a promising platform for tuning the polymer properties. However, the reactivity of the side group was shown to be relatively low, so that the competitive reactions with the carbonate moiety in the polymer backbone could occur, and therefore the system required an attentive optimisation of conditions.

In a second approach, photopolymerisation systems were explored in the preparation of biodegradable polymers with temporal and spatial control. Initially, the use of a photobase generator that releases the superbase 1,1,3,3-tetramethylguanidine (TMG) was envisioned to provide the desired temporal regulation. As this compound had not been reported for ROP, its catalytic activity was investigated in the polymerisation of a series of cyclic monomers. TMG provided well-defined polymers from L-LA with reactivity comparable to the highly active 1,8-

diazabicyclo[5.4.0]undec-7-ene (DBU) catalyst. In addition, the controlled ROP of δ-VL and ε-CL was achieved by using TMG in combination with a thiourea cocatalyst. As such, this commercially available superbase resulted in a great addition to the class of organocatalysts for ROP. TMG was then photocaged with 2-(2-nitrophenyl)propoxycarbonyl (NPPOC) group and released in a controlled manner upon irradiation. By using this photocatalyst, no polymerisation of L-LA was observed after 9 days in the absence of light, whereas the polymerisation was triggered after irradiation, which illustrated the excellent temporal control of the system. This method was shown to be more efficient than previously reported approaches regarding the use of benign UV light ($\lambda > 300$ nm), although slower than photocatalysts that release the highly active 1,5,7-triazabicyclo[4.4.0]dec-5-ene (TBD).

To expand the use of this photocatalyst to obtain a spatial resolution, the synthesis of a bicyclic monomer that could be used as a crosslinker was investigated. As TMG was more active in the ROP of L-LA, a series of methodologies for the preparation of its functional analogue were explored. While the methylene-lactide derived from modifications of L-LA demonstrated to be susceptible to undesirable ring-opening or homopolymerisations, the functionalisation of L-malic acid and further cyclisation provided oligomers from intermolecular side reactions. Still, a bis(cyclic diester) was successfully prepared through the synthesis of allyl-functional lactide, followed by a thiol-ene reaction with a dithiol to form bis(thiol lactide) (BTLA). However, it is noteworthy that the synthesis of allyl-lactide on a large scale is demanding, as a large volume of solvent is required, and the final yield is relatively low (< 20%). Nonetheless, the polymerisability of this monomer with TMG was investigated using monocyclic lactide and glycolide derivatives to prepare linear polymers and allow easier characterisation. Indeed, the ROP of the lactide analogue catalysed by TMG showed to be controlled and provided well-defined polymers, thus demonstrating that BTLA should be an effective crosslinker.

Finally, the preparation of a resin composition with the crosslinker BTLA was investigated in the presence of free TMG as a catalyst. PLLA oligomers were shown to be effective as macroinitiators to form polymer networks with BTLA, and materials with different mechanical properties were obtained by changing the oligomer length and architecture. However, no curing was observed when applying the photocatalyst NPPOC-TMG, which was attributed to the slow release of TMG under the high concentrations applied in the resin. Therefore, photocatalysts that release the more

active TBD catalyst were utilised and demonstrated to be considerably more efficient than NPPOC-TMG, thus providing exceptional temporal control over the ROP of L-LA. However, these photocatalysts were also unable to promote the crosslinking of the resin, a fact that was associated with the deactivation of the released catalyst by the formation of a stable TBD-CO_2 complex in the polar solvent utilised in the resin. Therefore, obtaining spatial control with the resin formulation employed and the photocatalysts explored was shown to be challenging.

6.2 Future Work

The methodologies developed for the post-polymerisation modification of an epoxy-functional polycarbonate provide opportunities for further exploring the introduction of other functionalities and more complex structures. Moreover, the hydroxy group formed after ring-opening the epoxide provides an additional handle for conducting other modifications and preparing multifunctional polymers. Regarding the preparation of quarternised polymers from halide-functionalised polycarbonates, the utilisation of bromine as a pendent group provides a promising alternative to the functionalities investigated herein (*i.e.* chlorine and iodine). This group is a better leaving group than chlorine and is expected to provide a more efficient functionalisation. Moreover, the crosslinking observed with the polymer containing pendent iodine should be minimised, as a consequence of the lower leaving ability of bromine. In this case, the additional use of lower concentrations is expected to avoid these undesirable intermolecular reactions. Finally, a screening of other solvents could potentially promote the functionalisation reactions under milder conditions, which would avoid the degradation of the polymer backbone caused by the use of high temperatures, and also contribute to higher degrees of functionalisation.

The reactivity of the epoxide pendent group in the polycarbonate could also be increased, as a means to prevent the competitive nucleophilic reactions with the polymer backbone and enable introducing a greater variety of functionalities to the polymer. A potential approach would be utilising more electron-withdrawing groups next to the epoxide group, such as an ester in the β position. This pendent functionality is similar to that of poly(glycidyl acrylate)s, which has demonstrated to be rather susceptible to nucleophilic reactions and, therefore, has been extensively utilised in modifications of the polymer. Hence, the preparation of such a polymer would broaden the applicability of epoxides as pendent groups for post-polymerisation modifications,

especially those involving the incorporation of amines into polycarbonates, considering the incompatibility of these compounds with ROP and the limited approaches to insert these functionalities into polycarbonates.

The photobase generators investigated in Chapter 5 provided a fast release of a very active ROP organocatalyst upon irradiation and, although curing the resins with this system could not be demonstrated, these catalysts still represent a great potential to achieve spatial control. However, considering the stability of the inactive TBD-CO_2 complex in polar solvents, the use of less polar diluents would be required to release the catalyst and allow the polymerisation to proceed. As such, the preparation of a crosslinker that is more soluble in apolar solvents is desirable. In principle, a series of compounds derived from allyl-lactide could be synthesised from different dithiols, allowing the investigation of their suitability in the resin. However, as the synthesis of allyl-lactide is rather challenging and the corresponding crosslinker was mainly utilised because of the higher reactivity of lactide with TMG, other classes of crosslinkers polymerizable by TBD also become open to further exploration. For instance, the monomers derived from 6- and *N*-substituted 8-membered cyclic carbonates have demonstrated fast polymerisation in the presence of TBD and could be suitable for the resin. In addition, other oligomers employed as macroinitiators could be investigated, such as PVL or PTMC, in order to obtain improved solubilities of the crosslinker in the resin. As such, there is a range of parameters to modify that could result in the preparation of an appropriate resin, which would expand the application of the photocatalyst systems developed herein to potentially provide a spatial resolution for biodegradable polymers.

Chapter 7

Experimental

7.1 Materials

All chemicals and solvents, unless otherwise stated, were purchased from Sigma-Aldrich or Fisher Scientific and used without further purification. Benzyl alcohol, δ-valerolactone (δ-VL), ε-caprolactone (ε-CL), 1,8-diazabicyclo[5.4.0]undec-7-ene (DBU), and 1,1,3,3-tetramethylguanidine were dried over CaH_2, distilled, and stored under an inert atmosphere. 1,5,7-Triazabicyclo[4.4.0]dec-5-ene (TBD) was dried by sublimation and stored under an inert atmosphere. 4-Methoxybenzyl alcohol, 1,4-benzenedimethanol (1,4-BDM), $CDCl_3$ (Apollo Scientific), C_6D_6 were dried and stored over 3 Å molecular sieves under an inert atmosphere. L-Lactide (L-LA, Purac) was dissolved in CH_2Cl_2 and passed through a silica plug. The solution was transferred to a Schlenk flask and concentrated under vacuum. The resultant solid was recrystallised twice from dry hot toluene (70 °C), sublimed and stored in a glovebox. 1-(3,5-Bis(trifluoromethyl)phenyl)-3-cyclohexylthiourea (TU) was synthesised as previously reported[1] and dried over CaH_2 in dry THF. Trimethylenepropane oxirane ether carbonate (TMOC) was synthesised as previously reported[2] and dried over CaH_2 in dry CH_2Cl_2. 7-Dimethylamino-methoxycarbonylcoumarin-1,1,3,3-tetramethylguanidine (coumarin-TMG),[3] 2-(nitrophenyl)propoxycarbonyl-1,1,3,3-tetramethylguanidine (NPPOC-TMG)[4] were prepared as previously reported and dried over P_2O_5 in a vacuum desiccator for one week, in which P_2O_5 was replaced every day. 3-(3-(Dodecylthio)propyl)-6-methyl-1,4-dioxane-2,5-dione (DTLA), 3-(3-(dodecylthio)propyl)-1,4-dioxane-2,5-dione (DTGA), and all photobase generators derived from thioxanthone and anthraquinone[1] were dried over P_2O_5 in a vacuum desiccator for one week, in which P_2O_5 was replaced every day. Silica gel (pore size = 40 Å) was obtained from Fisher Scientific and used as received. Dry solvents were obtained by purification over an Innovative Technology SPS alumina solvent column and degassed by repeated freeze-pump-thaw cycles prior to use.

7.2 General Considerations

7.2.1 Techniques

All polymerisations were performed under an inert N_2 atmosphere in a glovebox unless otherwise stated. Photopolymerisations were performed in a Metalight Classic

[1] The photobase generators were provided by Dr. Haritz Sardon and Dr. Nicolas Zivic, from the University of the Basque Country.

lightbox containing 12 × 9 W bulbs with spectrum at λ = 320–400 nm. Samples were typically placed 10 cm away from the source with the bulbs arranged concentrically around them.

7.2.2 Nuclear Magnetic Resonance (NMR) Spectroscopy

NMR spectra were recorded on a Bruker Avance III HD 300, 400 or 500 MHz spectrometer at 298 K and kinetics studies were recorded on a Bruker Avance III 400 MHz spectrometer. Chemical shifts are reported as δ in parts per million (ppm) and referenced to the residual solvent signal ($CDCl_3$: ^1H, δ = 7.26 ppm, ^{13}C, δ = 77.2 ppm, C_6D_6, ^1H, δ = 7.16 ppm, ^{13}C, δ = 128.1 ppm, $(CD_3)SO$: ^1H, δ = 2.50 ppm, ^{13}C, δ = 39.5 ppm, $(CD_3)CO$: ^1H, δ = 2.05 ppm, ^{13}C, δ = 29.8 ppm, TMS: ^1H, δ = 0.00 ppm). Multiplicities are reported as s = singlet, brs = broad singlet, d = doublet, t = triplet, q = quartet, quin = quintuplet, m = multiplet. Multiplicity is followed by coupling constant (*J*) in Hz, and integration.

7.2.3 Mass Spectrometry

High-resolution mass spectrometry (HRMS) was performed on a Waters Xevo-G2-XS-ToF mass spectrometer with electrospray ionisation (ESI). The electrospray analysis was performed in ESI positive mode with a capillary voltage of 3000 V, a cone voltage of 40 V, a source temperature of 120 °C, a desolvation temperature of 350 °C and a desolvation gas (N_2) flow of 500 L h^{-1}. The samples were diluted to appropriate concentrations in acetonitrile and injected with a Waters Alliance e2695 by direct injection. The parent ions ($[M + H]^+$) are quoted.

Matrix-assisted laser desorption/ionisation time-of-flight mass spectrometry (MALDI-ToF MS) analysis was performed on a Bruker Autoflex Speed or Bruker Ultraflex Extreme mass spectrometer using a nitrogen laser delivering 2 ns pulses at 337 nm with positive ion ToF detection performed using an accelerating voltage of 25 kV. *Trans*-2-[3-(4-tertbutylphenyl)-2-methyl-2-propylidene]malonitrile (DCTB) was used as a matrix (a 40 g L^{-1} solution in THF), with sodium trifluoroacetate (NaTFA) used as a cationic agent (10 g L^{-1} solution in THF). Analyte (1 g L^{-1} solution in THF) was mixed with the DCTB and NaTFA solutions (20 μL of each) and applied to form a thin matrix-analyte film. All samples were measured in reflectron mode and calibrated against a 3000 to 8000 g mol^{-1} poly(ethylene glycol) standard.

7.2.4 Elemental Analysis

Elemental analysis was performed in duplicate by Warwick Analytical Services or Birmingham Analytical Team.

7.2.5 Size Exclusion Chromatography (SEC)

SEC was conducted on systems composed of a Varian 390-LC-Multi detector suite fitted with differential refractive index, light scattering, and ultraviolet detectors, equipped with a guard column (Varian Polymer Laboratories PLGel 5 μM, 50 × 7.5 mm) and two mixed D columns (Varian Polymer Laboratories PLGel 5 μM, 300 × 7.5 mm). The mobile phase was either $CHCl_3$ (HPLC grade) with 2% Et_3N, DMF with 5 mM NH_4BF_4, or THF with 2% Et_3N at 40 °C with a flow rate of 1.0 mL min^{-1}. SEC samples were calibrated against Varian Polymer Laboratories Easi-Vials linear polystyrene standards (162 – 2.4 × 10^5 g mol^{-1}) ($CHCl_3$ and THF SEC), linear poly(methyl methacrylate) standards (556 – 1.8 × 10^6 g mol^{-1}) (DMF SEC) using Cirrus v3.3 software.

7.2.6 Fourier-Transform Infrared Spectroscopy (FT-IR)

FT-IR spectra for the new compounds were obtained using a Perkin-Elmer Spectrum 100 or Agilent Cary 600 Series FT-IR spectrometer. Observed spectra were acquired from ν = 4000 to 550 cm^{-1} with an accumulation of 16 scans with a background scan subtracted, and the representative transmittance values are reported in cm^{-1}.

7.2.7 Ultraviolet-Visible (UV-Vis) Spectroscopy

UV-Vis spectra were obtained for using a Varian Cary 50 UV-Vis Spectrophotometer. All samples were analysed in acetonitrile using quartz cuvettes with 1 cm light path length. Absorbance data were acquired from λ = 200 to 800 nm, and the maximum absorption value is reported in nm.

7.2.8 Mechanical Testing

Uniaxial tensile testing was performed at ambient temperature using a Tensiometric M350-5CT system with a load cell capacity of 10 kgf and a crosshead speed of 3 mm min^{-1} with a pre-measured grip-to-grip separation. Uniform dog-bone samples were prepared by placing the resins in a Teflon mould immediately after the

addition of catalyst to allow samples to cure. After curing, the samples were removed from the mould and placed in a vacuum oven at 60 °C for 24 h to remove the diluent. Samples were loaded axially into the apparatus, with a minimum of 5 samples of each material tested, and results recorded using winTest Analysis v5.0.34 software.

7.2.9 Thermal Analysis

Differential scanning calorimetry (DSC) was performed using Mettler Toledo DSC1 Star or Mettler Toledo DSC 3+ Star systems, and thermogravimetric analysis (TGA) was performed using TGA/DSC Star system. DSC heating and cooling cycles were run in triplicate in series between -50 and 150 °C under a nitrogen atmosphere at a heating rate of +/- 10 °C min^{-1} in a 40 μL aluminium crucible. TGA was conducted between 20 and 600 °C at a heating rate of 10 °C min^{-1} in a 40 μL aluminium crucible.

7.3 Experimental Procedures for Chapter 2

7.3.1 Synthesis of 5-((Allyloxy)methyl)-5-ethyl-1,3-dioxan-2-one (2.3)

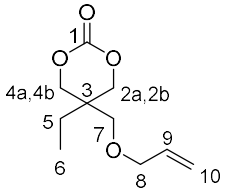

2.3

Trimethylolpropane allyl ether (60.0 mL, 0.348 mol) and ethyl chloroformate (100 mL, 1.04 mol) were dissolved in THF (1 L) in a 2 L round-bottomed flask. The solution was cooled to 0 ºC, and triethylamine (145 mL, 1.04 mol) was added dropwise. The reaction was allowed to warm to room temperature and stirred for 15 h. After this period, the white solid was removed by filtration and the filtrate was concentrated under reduced pressure. The resultant oil was dissolved in ethyl acetate (200 mL) and washed with an aqueous solution of 1 M HCl (2 × 200 mL) and water (200 mL). The organic layer was dried over $MgSO_4$, filtered and concentrated under reduced pressure to yield a yellow oil. The crude oil was purified by vacuum distillation to yield compound **2.3** (56.2 g, 0.281 mol, 81%) as a clear oil. The ^{1}H and ^{13}C NMR spectroscopic data were in agreement with those reported in literature.[2]

^{1}H NMR (300 MHz, $CDCl_3$) δ 5.84 (ddt, ^{3}J = 17.3, 10.4 and 5.6 Hz, 1H, H^{9}), 5.28-5.16 (m, 2H, H^{10}), 4.31 (d, ^{2}J = 10.9 Hz, 2H, $H^{2a,4a}$), 4.12 (d, ^{2}J = 10.9 Hz, 2H $H^{2b,4b}$), 3.96 (dt, ^{3}J = 5.6 and ^{4}J = 1.4 Hz, 2H, H^{8}), 3.38 (s, 2H, H^{7}), 1.52 (q, ^{3}J = 7.6 Hz, 2H, H^{5}), 0.90 (t, ^{3}J = 7.6 Hz, 3H, H^{6}).

^{13}C NMR (75 MHz, $CDCl_3$) δ 148.6 (C^{1}), 134.1 (C^{9}), 117.6 (C^{10}), 72.9 ($C^{2,4}$), 72.5 (C^{8}), 68.3 (C^{7}), 35.5 (C^{3}), 23.4 (C^{5}), 7.4 (C^{6}).

7.3.2 Synthesis of 5-Ethyl-5-((oxiran-2-ylmethoxy)methyl)-1,3-dioxan-2-one (TMOC, 2.1)

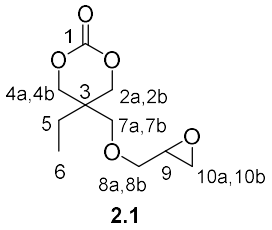

2.1

A solution of 5-((allyloxy)methyl)-5-ethyl-1,3-dioxan-2-one (**2.3**) (9.00 g, 44.9 mmol) in CH_2Cl_2 (400 mL) was prepared in a 1 L round-bottomed flask. The solution was cooled to 0 ºC and *m*-chloroperbenzoic acid (15.5 g, 62.9 mmol) was carefully added to the reaction medium. The mixture was allowed to warm to room temperature and stirred for 21 h. The reaction was quenched at 0 ºC by the addition of solid potassium carbonate, leading to the production of a white precipitate. The mixture was filtered to remove the solid and the filtrate was washed with saturated aqueous solution of $NaHCO_3$ (3 × 150 mL) and saturated brine (150 mL). The combined organic layer was dried over $MgSO_4$, filtered and concentrated under reduced pressure. The crude oil was purified by column chromatography using hexane:EtOAc (1:1) as eluent (R_f = 0.34) to yield TMOC (**2.1**) (7.46 g, 34.5 mmol, 77%) as a clear oil. Characterization data was found to be in agreement with those reported in literature.[2]

Mixture of isomers:

^{1}H NMR (300 MHz, $CDCl_3$) δ 4.30 (ddd, ^2J = 6.1, ^4J = 4.9 and 2.0 Hz, 2H, $H^{2a, 4a}$), 4.11 (m, 2H, $H^{2b, 4b}$), 3.78 (dd, ^2J = 11.7 and ^3J = 2.6 Hz, 1H, H^{8a}), 3.52, (d, ^2J = 9.7 Hz, 1H, H^{7a}), 3.43 (d, ^2J = 9.7 Hz, 1H, H^{7b}), 3.32, (dd, ^2J = 11.7 and ^3J = 6.1 Hz, 1H, H^{8b}), 3.09 (ddt, ^3J = 6.7, 4.2 and 2.6 Hz, 1H, H^9), 2.76 (t, $^{2,3}J$ = 5.5 Hz, 1H, H^{10a}), 2.55 (dd, ^2J = 5.0 and ^3J = 2.7 Hz, 1H, H^{10b}), 1.51 (q, ^3J = 7.7 Hz, 2H, H^5), 0.90 (t, ^3J = 7.6 Hz, 3H, H^6).

^{13}C NMR (75 MHz, $CDCl_3$) δ 148.4 (C^1), 72.6 ($C^{2,}$), 72.5 (C^4), 72.0 (C^8), 69.5 (C^7), 50.4 (C^9), 43.6 (C^{10}), 35.3 (C^3), 23.0 (C^5), 7.2 (C^6).

7.3.3 General Procedure for the Polymerization of TMOC (PTMOC, 2.4)

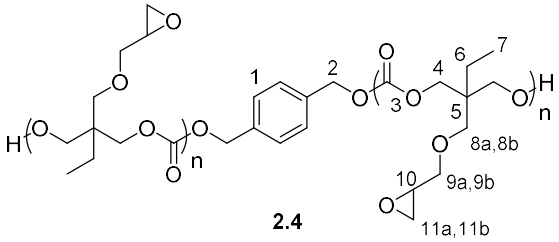

2.4

Within a glovebox, 5-ethyl-5-((oxiran-2-ylmethoxy)methyl)-1,3-dioxan-2-one (TMOC, **2.1**) (130 mg, 0.600 mmol) was dissolved in dry $CDCl_3$ (564 µL). A solution of the initiator 1,4-benzenedimethanol (27.4 µL of a 100 g L^{-1} solution in THF, 19.8 µmol) was added to the monomer solution, followed by 1,5,7-triazabicyclo[4.4.0]dec-5-ene (8.35 µL of a 100 g L^{-1} solution in $CDCl_3$; 6.00 µmol). The reaction solution was transferred to a

NMR tube and monitored by ^{1}H NMR spectroscopy. The reaction was quenched by the addition of 3.5 mg of benzoic acid and purified by precipitation in Et_2O or by column chromatography using Et_2O as eluent to remove excess monomer, followed by ethyl acetate to yield poly(ethyl-5-((oxiran-2-ylmethoxy)methyl)-1,3-dioxan-2-one) (PTMOC, **2.4**) as a viscous clear liquid.

^{1}H NMR (500 MHz, $CDCl_3$) δ 7.38 (s, H^1), 5.13 (s, H^2), 4.09 (s, H^4), 3.70 (dd, ^{2}J = 11.7 and ^{3}J = 2.8 Hz, H^{9a}), 3.44 (d, ^{2}J = 9.3 Hz, H^{8a}), 3.35 (m, $H^{8b,9b}$), 3.08 (m, H^{10}), 2.76 (m, H^{11a}), 2.57 (dd, ^{2}J = 5.0 and ^{3}J = 2.7 Hz, H^{11b}), 1.48 (q, ^{3}J = 7.5 Hz, H^6), 0.88 (t, ^{3}J = 7.6 Hz, H^7).

^{13}C NMR (125 MHz, $CDCl_3$) δ 155.2 (C^3); 128.7 (C^1), 72.2 (C^9); 70.9 (C^8); 67.7 (C^4); 50.9 (C^{10}); 44.1 (C^{11}); 42.1 (C^5); 22.6 (C^6); 7.6 (C^7).

GPC (DMF, LS, *dn/dc* = 0.0375) DP = 30, M_n = 4.9 kg mol^{-1}, $Đ_M$ = 1.20.

7.3.4 General Procedure for the Post-polymerisation Functionalisation of PTMOC with Amines (PTMOC-amine, 2.5)

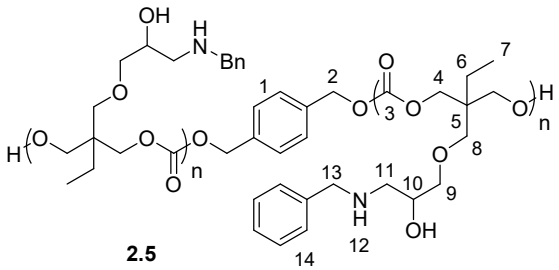

2.5

To a solution of PTMOC (**2.4**) (25 mg, 0.115 mmol) in DMSO (0.50 mL) was added benzylamine (63 µL, 0.575 mmol). The reaction medium was heated to 70 °C and stirred for 24 h. After this period the solution was cooled to room temperature and purified by precipitation in Et_2O to provide PTMOC-amine (**2.5**) as a viscous clear oil.

^{1}H NMR (500 MHz, $CDCl_3$, TMS) δ 7.29 (m, H^{14}), 5.11 (s, H^2), 4.07 (s, H^4), 3.91 (br s, H^{10}), 3.83 (m, H^{13}), 3.62 (br s, H^{12}), 3.37 (s, H^9), 3.31 (m, H^8), 2.69 (m, H^{11}), 1.42 (m, H^6), 0.84 (m, H^7).

^{13}C NMR (125 MHz, $CDCl_3$) δ 155.3 (C^3), 129.1-127.6 (C^{14}), 74.2 (C^9), 70.9 (C^8), 68.4 (C^{10}), 67.7 (C^4), 53.4 (C^{13}), 51.2 (C^{11}), 42.2 (C^5), 22.7 (C^6), 7.6 (C^7).

SEC (DMF, RI) DP = 34, M_n = 11.4 kg mol^{-1}, $Đ_M$ = 1.18.

7.3.5 General Procedure for the Post-polymerisation Functionalisation of PTMOC with Chlorine (PTMOC-Cl, 2.6)

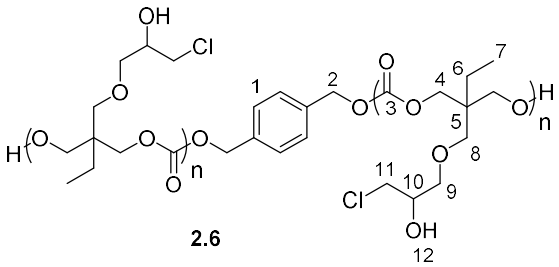

2.6

To a round bottom flask containing a solution of PTMOC (**2.4**) (25 mg; 0.115 mmol) in DMSO (0.50 mL), Et_3NHCl (32 mg; 0.230 mmol) was added, and a condenser was adapted before heating the solution to 70 °C. The reaction mixture was stirred under these conditions for 24 h and after this period, the mixture was diluted with EtOAc (5 mL) and washed with H_2O (3 × 2 mL) to remove excess Et_3NHCl. The organic phase was dried over $MgSO_4$, filtered and dried over reduced pressure to provide PTMOC-Cl (**2.6**) as a viscous liquid.

^{1}H NMR (400 MHz, $CDCl_3$) δ 7.39 (s, H^1), 5.15 (s, H^2), 4.11 (s, H^4), 3.94 (quin, ^3J = 5.1 Hz, H^{10}), 3.56 (m, $H^{9,11}$), 3.41 (m, H^8), 2.73 (br s, H^{12}), 1.47 (q, ^3J = 7.3 Hz, H^6), 0.89 (t, ^3J = 7.3, H^7).

^{13}C NMR (75 MHz, $CDCl_3$) δ 155.4 (C^3), 128.8 (C^1), 72.3 (C^9), 71.1 (C^8), 70.3 (C^{10}), 67.9 (C^4), 45.9 (C^{11}), 42.2 (C^5), 22.8 (C^6), 7.6 (C^7).

SEC (DMF, RI) DP = 34, M_n = 12.4 kg mol^{-1}, $Đ_M$ = 1.16.

7.3.6 General Procedure for the Post-polymerisation Functionalisation of PTMOC with Thiols (PTMOC-thiophenol, 2.9)

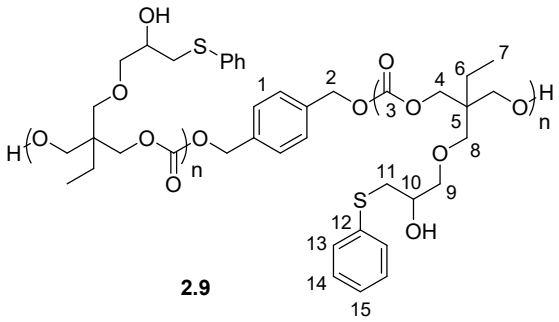

2.9

To a solution of PTMOC (50 mg; 0.231 mmol) and thiophenol (47 µL; 0.462 mmol) in THF (1.0 mL) at 0 °C, was added a solution of DBU in THF (42 µL of a 0.22 M solution in THF; 9.24 µmol). The ice bath was removed, and the reaction medium was stirred for 7 h. The product was purified by precipitation in Et_2O, providing poly(5-ethyl-5-((2-hydroxy-3-(phenylthio)propoxy)methyl)-1,3-dioxan-2-one) (PTMOC-thiophenol, **2.9**) as a white solid.

^{1}H NMR (500 MHz, $CDCl_3$, TMS) δ 7.35 (m, H^{13}), 7.26 (m, H^{14}), 7.17 (m, H^{15}), 5.12 (s H^2), 4.10 (s, H^4), 3.84 (m, H^{10}), 3.48 (m, H^9), 3.32 (m, H^8), 3.03 (m, H^{11}), 1.44 (q, J = 7.3 Hz, H^6), 0.85 (t, J = 0.85 Hz, H^7).

^{13}C NMR (125 MHz, $CDCl_3$) δ 155.4 (C^3); 136.0 (C^{12}); 129.4 (C^{13}); 129.2 (C^{14}); 126.4 (C^{15}); 73.9 (C^9); 71.0 (C^8); 69.2 (C^{10}); 67.8 (C^4); 42.2 (C^5); 37.1 (C^{11}); 22.8 (C^6); 7.6 (C^7).

GPC (DMF, RI) DP = 73, M_n = 20.2 kg mol^{-1}, $Đ_M$ = 1.19.

7.4 Experimental Procedures for Chapter 3

7.4.1 General Procedure for the Synthesis of PLLA (3.1) by the ROP of L-Lactide Catalysed by 1,1,4,4-Tetramethylguanidine (TMG)

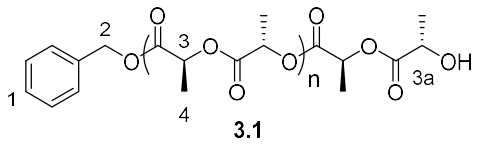

3.1

Within a glovebox, benzyl alcohol (25.9 µL of a 100 g L^{-1} solution in $CDCl_3$) was added to a solution of L-lactide (173 mg; 1.20 mmol) in $CDCl_3$ (600 µL), followed by TMG (13.8 µL of a 100 g L^{-1} solution in $CDCl_3$; 12 µmol). The polymerisation was stopped after 90 min by the addition of benzoic acid (7 mg) and purified by precipitation in cold petroleum ether and cold MeOH to provide PLLA (**3.1**) as a white solid.

^{1}H NMR (300 MHz, $CDCl_3$) δ 7.34 (m, H^1), 5.16 (q, ^3J = 7.1 Hz, H^3), 4.35 (q, ^3J = 7.1, H^{3a}), 1.58 (d, ^3J = 7.1 Hz, H^4).

SEC ($CHCl_3$, RI) DP = 37, M_n = 11.7 kg mol^{-1}, $Đ_M$ = 1.05.

7.4.2 General Procedure for the Synthesis of PVL (3.2) or PCL (3.3) by the ROP of δ-Valerolactone or ε-Caprolactone Catalysed by TMG and 1-(3,5-Bis(trifluoromethyl)phenyl)-3-cyclohexylthiourea (TU)

Within a glovebox, benzyl alcohol (25.9 µL of a 100 g L^{-1} solution in C_6D_6) was added to a solution of δ-valerolactone (120 mg; 1.20 mmol) in C_6D_6 (600 µL), followed by a solution of TMG and TU (88.8 µL of a solution containing 17 µL of TMG and 50 mg of TU in 200 µL of C_6D_6; 60 µmol). The polymerisation was stopped after 23 h by the addition of benzoic acid (5 mg) and purified by precipitation in cold MeOH to provide PVL as a white solid.

PVL (**3.2**):

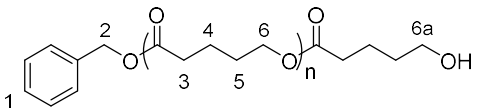

^{1}H NMR (300 MHz, $CDCl_3$) δ 7.35 (m, H^1), 5.11 (s, H^2), 4.08 (m, H^6), 3.65, (m, H^{6a}), 2.34 (m, H^3), 1.67 (m, $H^{4,5}$).

SEC ($CHCl_3$, RI) DP = 24, M_n = 3.7 kg mol^{-1}, $Đ_M$ =1.10.

PCL (**3.3**):

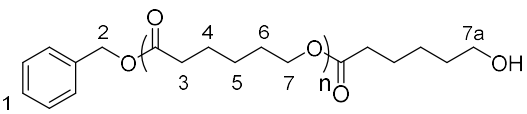

^{1}H NMR (300 MHz, $CDCl_3$) δ 7.34 (m, H^1), 5.11 (s, H^2), 4.05 (t, ^3J = 6.6 Hz, H^7), 3.64 (t, ^3J = 6.6 Hz, H^{7a}), 2.30 (t, ^3J = 7.5 Hz, H^3), 1.64 (m, $H^{4,6}$), 1.37 (m, H^5).

SEC ($CHCl_3$, RI) DP = 19, M_n = 4.8 kg mol^{-1}, $Đ_M$ =1.12.

7.4.3 Synthesis of 7-Dimethylamino-hydroxymethylcoumarin (Coumarin-OH, 3.6)

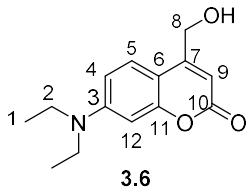

3.6

To a solution of 7-diethylamino-methylcoumarin (**3.5**) (1.00 g; 4.32 mmol) in xylene (21 mL) was added selenium dioxide (719 mg; 6.48 mmol). The mixture was heated to reflux and stirred under these conditions for 24 h. After this period, the mixture was cooled to room temperature, filtered in Celite and concentrated under reduced pressure to provide the corresponding aldehyde.

To a solution of the crude aldehyde in methanol (29 mL) was added sodium borohydride (245 mg; 6.48 mmol). The reaction mixture was stirred for 4 h before being neutralised by the addition of 1 M HCl solution (7 mL). After removing the solvent, the crude product was diluted in H_2O (10 mL) and extracted with CH_2Cl_2 (3 × 20 mL). The combined organic layer was dried over $MgSO_4$, filtered and concentrated under reduced pressure. The residue was purified by column chromatography in silica gel using CH_2Cl_2:hexane:MeOH (8:1:1) as eluent (R_f = 0.56) to provide coumarin-OH (**3.6**) (238 mg; 0.962 mmol; 22%) as an orange solid. The ^{1}H and ^{13}C NMR spectroscopic data were in agreement with those reported in literature.[3]

^{1}H NMR (300 MHz, $CDCl_3$) δ 7.32 (d, ^3J = 9.0 Hz, 1H, H^5), 6.56 (dd, ^3J = 9.0 and ^4J = 2.6 Hz, 1H, H^4), 6.51, (d, ^4J = 2.6 Hz, 1H, H^{12}), 6.26 (s, 1H, H^9), 4.83 (s, 2H, H^8), 3.40 (q, ^3J = 7.1 Hz, 4H, H^2), 1.20 (t, ^3J = 7.1 Hz, 6H, H^1).

^{13}C NMR (75 MHz, $CDCl_3$) δ 162.9 (C^{10}), 156.3 (C^{11}), 155.0 (C^3), 150.6 (C^7), 124.5 (C^5), 108.7 (C^9), 106.4 (C^6), 105.5 (C^4), 97.9 (C^{12}), 61.1 (C^8), 44.9 (C^2), 12.6 (C^1).

7.4.4 Synthesis of 7-Dimethylamino-methoxycarbonylcoumarin-1,1,3,3-tetramethylguanidine (Coumarin-TMG, 3.4)

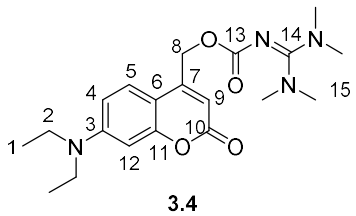

3.4

Coumarin-OH (**3.6**) (238 mg; 0.962 mmol) e carbonyldiimidazole (186 mg; 1.15 mmol) were dissolved in CH_2Cl_2 (8.0 mL) and the solution was stirred under reflux during 4 h. Then, a solution of DMAP (26 mg; 0.202 mmol) and TMG (51 µL; 0.404 mmol) in CH_2Cl_2 (0.5 mL) was added and the reaction mixture was stirred in the dark for 17 h. After this period, the mixture was washed with saturated aqueous solution of NaCl (10 mL) and extracted

with CH_2Cl_2 (3 × 20 mL). The combined organic layer was dried over $MgSO_4$, filtered and concentrated under reduced pressure. The crude product was purified by column chromatography in silica gel using CH_2Cl_2:hexane:MeOH (8:1:1) as eluent (R_f = 0.38) to provide coumarin-TMG (**3.4**) (200 mg; 0.515 mmol; 54%) as an orange solid. The ^1H and ^{13}C NMR spectroscopic data were in agreement with those reported in literature.[3]

^{1}H NMR (500 MHz, $CDCl_3$) δ 7.34 (d, ^3J = 9.0 Hz, 1H, H^5), 6.51 (dd, ^3J = 9.0 and ^4J = 2.4 Hz, 1H, H^4), 6.50, (d, ^4J = 2.4 Hz, 1H, H^{12}), 6.24 (s, 1H, H^9), 5.25 (s, 2H, H^8), 3.35 (q, ^3J = 7.1 Hz, 4H, H^2), 2.86 (s, 12H, H^{13}), 1.14 (t, ^3J = 7.1 Hz, 6H, H^1).

^{13}C NMR (125 MHz, $CDCl_3$) δ 166.6 (C^{14}), 162.2 (C^{10}), 159.2 (C^{13}), 156.2 (C^{11}), 151.8 (C^7), 150.5 (C^3), 124.7 (C^5), 108.6 (C^4), 106.4 (C^6), 106.0 (C^9), 97.7 (C^{12}), 62.0 (C^8), 44.7 (C^2), 40.0 (C^{15}), 12.4 (C^1).

UV-Vis λ_{max} 380.

7.4.5 Synthesis of 2-(2-Nitrophenyl)propoxycarbonyl-1,1,3,3-tetramethylguanidine (NPPOC-TMG, 3.7)

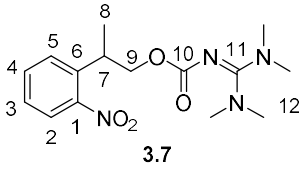

3.7

To a solution of TMG (314 µL; 2.50 mmol) in CH_2Cl_2 (20 mL) at 0 °C in the dark was added a solution of 2-(2-nitrophenyl)propyl chloroformate (**3.8**) (487 mg; 2.00 mmol) in CH_2Cl_2 (10 mL). The reaction medium was warmed to room temperature and stirred under these conditions for 14 h. After this period, the mixture was washed with saturated aqueous solution of NaCl (3 × 30 mL) and the organic layer was dried over $MgSO_4$, filtered and concentrated under reduced pressure. The crude product was purified in the dark by column chromatography in silica gel using CH_2Cl_2:MeOH (10:1) as eluent (R_f = 0.32) to provide NPPOC-TMG (**3.7**) (336 mg; 1.20 mmol; 60%) as a yellow solid. The ^1H and ^{13}C NMR spectroscopic data were in agreement with those reported in literature.[4]

^{1}H NMR (500 MHz, $CDCl_3$) δ 7.72 (d, ^3J = 8.1 Hz, 1H, H^2), 7.53 (m, 2H, $H^{4,5}$), 7.31 (m, 1H, H^3), 4.28 (d, ^3J = 6.8 Hz, 2H, H^9), 3.69 (h, ^3J= 6.8 Hz, 1H, H^7), 2.79 (s, 12H, H^{12}), 1.36 (d, ^3J = 6.9 Hz, 3H, H^8).

^{13}NMR (125 MHz, $CDCl_3$) δ 166.3 (C^{11}), 160.3 (C^{10}), 150.5 (C^1), 138.5 (C^6), 132.6 (C^4), 128.6 (C^5), 127.1 (C^3), 124.2 (C^2), 68.6 (C^9), 39.9 (C^{12}), 34.0 (C^7), 18.7 (C^8).

UV-Vis λ_{max} 345.

7.4.6 General Procedure for the Synthesis of PLLA (3.1) by the Photoactivated ROP of L-Lactide Catalysed by NPPOC-TMG

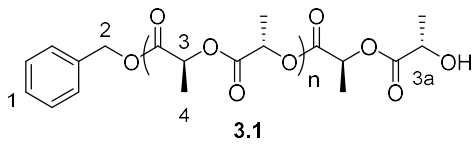

3.1

Within a glovebox, benzyl alcohol (25.9 µL of a 100 g L^{-1} solution in $CDCl_3$) was added to a solution of L-lactide (173 mg; 1.20 mmol) in $CDCl_3$ (600 µL), followed by NPPOC-TMG (**3.7**) (38.7 µL of a 100 g L^{-1} solution in $CDCl_3$; 12 µmol). The solution was transferred to an NMR tube, sealed and removed from the glovebox. The sample was irradiated for 15 minutes in a Metalight Classic light box, with the sample placed 10 cm away from the source and the bulbs arranged concentrically around them.

was stopped after 90 min by the addition of benzoic acid (7 mg) and purified by precipitation in cold petroleum ether and cold MeOH to provide PLLA (**3.1**) as a white solid.

^{1}H NMR (300 MHz, $CDCl_3$) δ 7.34 (m, H^1), 5.16 (q, ^3J = 7.1 Hz, H^3), 4.35 (q, ^3J = 7.1, H^{3a}), 1.58 (d, ^3J = 7.1 Hz, H^4).

SEC ($CHCl_3$, RI) DP = 37, M_n = 11.7 kg mol^{-1}, $Đ_M$ = 1.05.

7.5 Experimental Procedures for Chapter 4

7.5.1 Synthesis of (*S*)-2-(2,2-Dimethyl-5-oxo-1,3-dioxolan-4-yl)acetic acid (4.2)

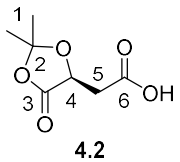

4.2

To a solution of L-malic acid (**4.1**) (10 g; 74.6 mmol) in 2,2-dimethoxypropane (73 mL; 597 mmol) was added *p*-toluene sulfonic acid monohydrate (142 mg; 0.746 mol). The solution was purged with N_2 and stirred at room temperature for 4 h. After this period, an aqueous solution of $NaHCO_3$ (63 mg in 50 mL H_2O; 0.75 mmol) was added and the reaction mixture was extracted with CH_2Cl_2 (5 × 50 mL). The combined organic layer was washed with saturated aqueous solution of NaCl (100 mL), dried over $MgSO_4$, filtered and concentrated under reduced pressure. The resultant white solid was recrystallised with Et_2O/hexane to provide (*S*)-2-(2,2-dimethyl-5-oxo-1,3-dioxolan-4-yl)acetic acid (**4.2**) (8.2 g; 47.1 mmol; 63%) as white crystals. The ^{1}H and ^{13}C NMR spectroscopic data were in agreement with those reported in literature.[5]

^{1}H NMR (500 MHz, $CDCl_3$) δ 4.71 (dd, ^3J = 6.5 and 3.8 Hz, 1H, H^4), 3.00 (dd, ^2J = 17.3 and ^3J =3.8 Hz, 1H, H^{5a}), 2.86 (dd, ^2J = 17.3 and ^2J = 6.5 Hz, 1H, H^{5b}), 1.62 (s, 3H, H^{1a}), 1.57 (s, 3H, H^{1b}).

^{13}C NMR (125 MHz, $CDCl_3$) δ 174.7 (C^6), 172.0 (C^3), 111.5 (C^2), 70.5 (C^4), 36.1 (C^5), 26.9 (C^{1a}), 26.0 (C^{1b}).

7.5.2 Synthesis of 1,4-Phenylenebis(methylene) bis(2-((*S*)-2,2-dimethyl-5-oxo-1,3-dioxolan-4-yl)acetate) (4.3)

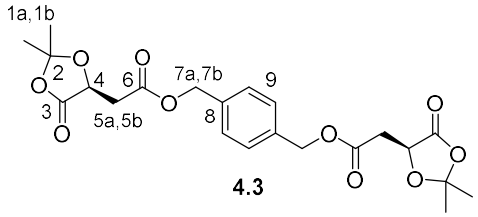

4.3

To a solution of (*S*)-2-(2,2-dimethyl-5-oxo-1,3-dioxolan-4-yl)acetic acid (**4.2**) (8.20 g; 47.1 mmol) in dry acetone (50 mL) under atmosphere of N_2 were added Et_3N (7.9 mL; 56.5 mmol) and *α*,*α*'-dibromo-*p*-xylene (6.23 g; 23.6 mmol). The reaction mixture was heated to reflux at 50 °C and stirred under these conditions for 13 h. After this period, the solids were removed by filtration and the filtrate was concentrated under reduced pressure. The residue was dissolved in EtOAc (200 mL) and H_2O (100 mL) and the aqueous layer was extracted with EtOAc (2 × 100 mL). The combined organic layer was dried over $MgSO_4$, filtered and concentrated under reduced pressure. The crude product was purified by column chromatography in silica gel using hexane/EtOAc (6:4) as eluent to provide 1,4-phenylenebis(methylene) bis(2-((*S*)-2,2-dimethyl-5-oxo-1,3-dioxolan-4-yl)acetate) (**4.3**) (5.94 g; 13.2 mmol, 56%) as a white solid.

^{1}H NMR (500 MHz, $CDCl_3$) δ 7.35 (s, 4H, H^9), 5.17 (d, ^2J = 12.4 Hz, 2H, H^{7a}), 5.15 (d, ^2J = 12.4 Hz, 2H, H^{7b}), 4.73 (dd, ^{3}J = 6.4 and 3.9 Hz, 2H, H^4), 2.98 (dd, ^2J = 17.0 and ^3J =3.9 Hz, 2H, H^{5a}), 2.85 (dd, ^2J = 17.0 and ^3J = 6.5 Hz, 2H, H^{5b}), 1.58 (s, 6H, H^{1a}), 1.56 (s, 6H, H^{1b}).

^{13}C NMR (125 MHz, $CDCl_3$) δ 172.1 (C^3), 169.1 (C^6), 135.7 (C^8), 128.7 (H^9), 111.4 (C^2), 70.8 (C^4), 66.7 (C^7), 36.4 (C^5), 26.9 (C^{1a}), 26.0 (C^{1b}).

FT-IR ν_{max}/cm^{-1} 3006 (*ν* C–H), 2990(*ν* C–H), 2944(*ν* C–H), 1793(*ν* C=O, ring), 1730 (*ν* C=O), 1524(*ν* C=C), 1449(*ν* C=C), 1177(*ν* C–O), 1103 (*ν* C–O).

7.5.3 Synthesis of (2*S*,2'*S*)-4,4'-((1,4-Phenylenebis(methylene))bis(oxy))bis(2-hydroxy-4-oxobutanoic acid) (4.4)

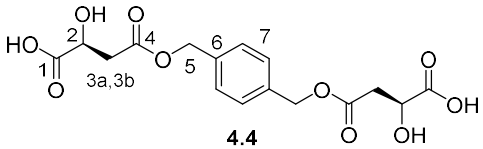

4.4

1,4-phenylenebis(methylene) bis(2-((*S*)-2,2-dimethyl-5-oxo-1,3-dioxolan-4-yl)acetate) (**4.3**) (1.32 g; 2.93 mmol) was dissolved in AcOH/THF/H_2O (1:1:1; 10.8 mL) and heated to 40 °C for 24 h. After this period, the

solvent was removed under reduced pressure and the crude product was freeze-dried to provide (2*S*,2'*S*)-4,4'-((1,4-phenylenebis(methylene))bis(oxy))bis(2-hydroxy-4-oxobutanoic acid) (**4.4**) (1.07 g; 2.89 mmol, 99%) as a white solid.

^{1}H NMR (500 MHz, $(CD_3)_2CO$) δ 7.41 (s, 4H, H^7), 5.16 (s, 4H, H^5), 4.56 (dd, ^3J = 7.4 and 4.5 Hz, 2H, H^2), 2.90 (dd, ^2J = 15.9 and ^3J = 4.5 Hz, 2H, H^{3a}), 2.76 (dd, ^2J = 15.9 and ^3J = 7.4 Hz, 2H, H^{3b}).

^{13}C NMR (125 MHz, $(CD_3)_2CO$) δ 174.6 (C^1), 170.8 (C^4), 137.1 (C^6), 128.9 (C^7), 68.0 (C^2), 66.4 (C^5), 39.9 (C^3).

FT-IR ν_{max}/cm^{-1} 3414 (*v* O–H), 3258 (*v* O–H), 2959 (*v* C–H), 1735 (*v* C=O, ester), 1720(*v* C–H, carboxylic acid), 1520 (*v* C=C), 1458 (*v* C=C), 1342 (*v* C–O), 1158 (*v* C–O), 1090 (*v* C–O).

Anal. Calcd for $C_{16}H_{18}O_{10}$: C 51.9; H 4.9%. Found: C 51.9; H 4.9.

7.5.4 Synthesis of (6*S*)-3-Bromo-3,6-dimethyl-1,4-dioxane-2,5-dione (Bromo-lactide, 4.7)

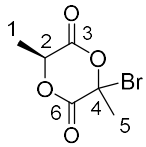

4.7

To a two-neck round bottom flask containing a mixture of L-lactide (9.73 g; 67.5 mmol) in benzene (49 mL) was added *N*-bromosuccinimide (13.2 g; 74.3 mmol). The mixture was heated to reflux under an atmosphere of N_2, and a solution of benzoyl peroxide (327 mg; 1.35 mmol) in benzene (5 mL) was added to the reaction medium. After 4 h 30 min, the mixture was cooled to room temperature and the solid was removed by filtration and the filtrate was concentrated under reduced pressure. The solid formed was dissolved in CH_2Cl_2 (75 mL) and washed with a saturated aqueous solution of sodium metabisulfite (3 × 50 mL) and a saturated aqueous solution of NaCl (50 mL). The organic layer was dried over $MgSO_4$, filtered and concentrated under reduced pressure. The yellow solid was recrystallised from EtOAc/hexane to provide bromo-lactide (**4.7**) (7.06 g; 31.7 mmol, 47%) as white crystal needles. The ^{1}H and ^{13}C NMR spectroscopic data were in agreement with those reported in literature.[6]

^{1}H NMR (500 MHz, $CDCl_3$) δ 5.50 (q, ^3J = 6.8 Hz, 1H, H^2), 2.34 (s, 3H, H^5), 1.73 (d, ^3J = 6.8 Hz, 3H, H^1).

^{13}C NMR (125 MHz, $CDCl_3$) δ 164.8 (C^6); 161.3 (C^3); 81.5 (C^4); 73.9 (C^2); 29.8 (C^5); 16.6 (C^1).

7.5.5 Synthesis of (*S*)-3-Methyl-6-methylene-1,4-dioxane-2,5-dione (methylene-lactide (MLA), 4.8)

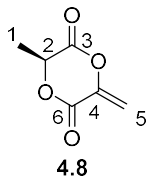

4.8

To a solution of bromo-lactide (**4.7**) (8.41 g; 37.7 mmol) in dry CH_2Cl_2 (54 mL) at 0 °C under an atmosphere of N_2 was added Et_3N (5.8 mL; 41.5 mmol) dropwise, observing the formation of white solids. After 1 h, the reaction medium was warmed to room temperature and stirred for another 1 h. Then, the mixture was washed with a saturated aqueous solution of 1 M HCl (3 × 30 mL) and a saturated aqueous solution of NaCl (30 mL). The organic layer was dried over $MgSO_4$, filtered and concentrated under reduced pressure. The resultant orange solid was purified by sublimation at 40 °C and 5×10^{-2} Torr to provide methylene-lactide (**4.8**) (3.48 g; 24.5 mmol, 65%) as white crystal needles. The ^{1}H and ^{13}C NMR spectroscopic data were in agreement with those reported in literature.[6]

^{1}H NMR (500 MHz, $CDCl_3$) δ 5.95 (d, ^2J = 2.4 Hz, 1H, H^{5a}), 5.55 (d, ^2J = 2.4 Hz, 1H, H^{5b}), 5.03 (q, ^3J = 7.0 Hz, 1H, H^2), 1.71 (d, ^3J = 7.0 Hz, 3H, H^1).

^{13}C NMR (125 MHz, $CDCl_3$) δ 163.1 (C^3); 157.9 (C^6); 143.1 (C^4); 110.7 (C^5); 72.6 (C^2); 17.5 (C^1).

7.5.6 Synthesis of 2-Hydroxypent-4-enoic Acid (4.14)

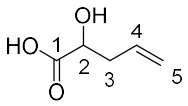

4.14

To a solution of glyoxylic acid monohydrate (**4.13**) (30.0 g; 326 mmol) in dry THF (890 mL) at 0 °C under an atmosphere of N_2 was added zinc dust (44.8 g; 685 mmol) in 2 portions, followed by $BiCl_3$ (143.8 g; 456 mmol) in 4 portions. The mixture was stirred under these conditions for 3 h and then allyl bromide (40.0 mL; 456 mmol) was added dropwise. The reaction mixture was allowed to stir for 15 h at 0 °C before being quenched by the addition of 1M HCl (1.5 L). The suspension was stirred for 3 h at room temperature and then the solids were removed by filtration. The filtrate was extracted with Et_2O (4 × 700 mL) and the organic layer was washed with a saturated aqueous solution of NaCl (3 × 500 mL) to remove bismuth salts. The organic layer dried over $MgSO_4$, filtered and concentrated under reduced pressure to provide 2-hydroxypent-4-enoic acid (**4.14**) (29.3 g; 252 mmol; 77%) as a white solid. The ^{1}H and ^{13}C NMR spectroscopic data were in agreement with those reported in literature.[7]

^{1}H NMR (500 MHz, $CDCl_3$) δ 5.81 (ddt, ^3J = 17.2, 10.1 and 7.1 Hz, 1H, H^4), 5.19 (m, 2H, H^5), 4.36 (dd, ^3J = 6.5 and 4.6 Hz, 1H, H^2), 2.64 (m, 1H, H^{3a}), 2.50 (m, 1H, H^{3b}).

^{13}C NMR (125 MHz, $CDCl_3$) δ 178.9 (C^1), 132.0 (C^4), 119.6 (C^5), 69.9 (C^2), 38.4 (C^3).

7.5.7 Synthesis of 2-((2-Bromopropanoyl)oxy)pent-4-enoic Acid (4.15)

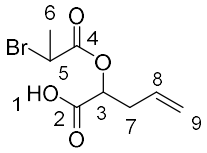

4.15

To a solution of DMAP (2.83 mg; 25.2 mmol) in CH_2Cl_2 (645 mL) was added 2-bromopropionyl bromide (26.4 mL; 252 mmol) dropwise at 0 °C under atmosphere of N_2. Then, a solution of 2-hydroxypent-4-enoic acid (**4.14**) (29.3 g; 252 mmol) and Et_3N (35.1 mL; 252 mmol) in CH_2Cl_2 (320 mL) was transferred dropwise *via* cannula to the reaction mixture. The reaction medium was stirred for 17 h at room temperature. After this period, the solvent was removed under reduced pressure, and the excess salt was removed by filtration. The crude oil was diluted with EtOAc (300 mL) and washed with H_2O (200 mL). The aqueous layer was extracted with EtOAc (3 × 300 mL) and the combined organic layer was dried over $MgSO_4$, filtered and concentrated under reduced pressure to provide crude 2-((2-bromopropanoyl)oxy)pent-4-enoic acid (**4.15**) as a yellow oil. The ^{1}H and ^{13}C NMR spectroscopic data were in agreement with those reported in literature.[7]

Mixture of isomers:

^{1}H NMR (500 MHz, $CDCl_3$) δ 10.93 (brs, 1H, H^1), 5.77 (m, 1H, H^8), 5.18 (m, 3H, $H^{3,9}$), 4.42 (m, 1H, H^5), 2.67 (m, 2H), H^7), 1.84 (m, 3H, H^6).

^{13}C NMR (125 MHz, $CDCl_3$) δ 175.1 and 175.0 (C^2), 169.9 and 169.6 (C^4), 131.3 and 131.2 (C^8), 119.6 (C^9), 72.4 and 72.3 (C^3), 39.5 and 39.2 (C^5), 35.2 and 35.1 (C^7), 21.8 and 21.6 (C^6).

7.5.8 Synthesis of 3-Allyl-6-methyl-1,4-dioxane-2,5-dione (Allyl-LA, 4.12)

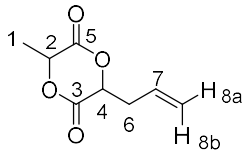

4.12

To a suspension of Na_2CO_3 (9.5 mg; 90 mmol) in dry DMF (4.2 L) under atmosphere of N_2 was added a solution of crude 2-((2-bromopropanoyl)oxy)pent-4-enoic acid (**4.15**) (252 mmol) in DMF (800 mL) *via* syringe pump (rate = 1.5 mL min^{-1}) at room temperature. After this period, the reaction mixture was stirred for 7 h before removing the solvent under reduced pressure. Then, acetone was added to precipitate the salts, which were removed by filtration. The filtrate was concentrated under reduced pressure and purified by column chromatography in silica gel using hexane/EtOAc

(8:2) as eluent (R_f = 0.25 and 0.18) to provide allyl-LA (**4.12**) (9.65 g; 56.7 mmol, 23% for 2 steps) as a yellow oil. The ^{1}H and ^{13}C NMR spectroscopic data were in agreement with those reported in literature.[7]

Isomer 1:

^{1}H NMR (500 MHz, $CDCl_3$) δ 5.82 (ddt, ^{3}J = 17.1, 10.0 and 7.1 Hz, 1H, H^{7}), 5.28 (m, 2H, H^{8}), 5.06 (q, ^{3}J = 7.1 Hz, 1H, H^{2}), 5.02 (t, ^{3}J = 6.0 Hz, 1H, H^{4}), 2.78 (m, 2H, C^{6}), 1.68, (d, ^{3}J = 7.1 Hz, 3H, H^{1}).

^{13}C NMR (125 MHz, $CDCl_3$) δ 166.0 (C^{5}), 165.3 (C^{3}), 130.0 (C^{7}), 121.5 (C^{8}), 76.2 (C^{4}), 72.9 (C^{2}), 36.4 (C^{6}), 17.9 (C^{1}).

Isomer 2:

^{1}H NMR (500 MHz, $CDCl_3$) δ 5.86 (ddt, ^{3}J = 17.1, 10.2 and 6.9 Hz, 1H, H^{7}), 5.28 (dd, ^{3}J = 17.1 and ^{4}J =1.0 Hz, 1H, H^{8b}), 5.23 (d, ^{3}J = 10.2 Hz, 1H H^{8a}), 5.02 (q, ^{3}J = 6.7 Hz, 1H, H^{2}), 4.95 (dd, ^{3}J = 7.2 and 4.5 Hz, 1H, H^{4}), 2.86 (m, 1H, H^{6a}), 2.73 (m, 1H H^{6b}), 1.66, (d, ^{3}J = 6.7 Hz, 3H, H^{1}).

^{13}C NMR (125 MHz, $CDCl_3$) δ 167.3 (C^{5}), 166.4 (C^{3}), 130.7 (C^{7}), 120.4 (C^{8}), 75.5 (C^{4}), 72.5 (C^{2}), 34.3 (C^{5}), 16.0 (C^{1}).

7.5.9 Synthesis of 6,6'-((Hexane-1,6-diylbis(sulfanediyl))bis(propane-3,1-diyl))bis(3-methyl-1,4-dioxane-2,5-dione) (BTLA, 4.16)

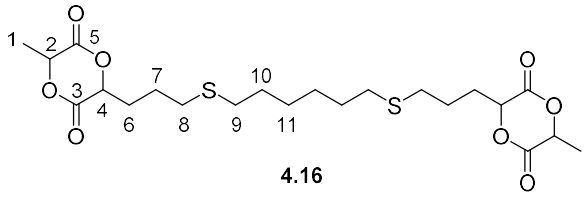

4.16

To a solution of allyl-LA (**4.12**) (1.5 g; 8.82 mmol) in 1,4-dioxane (3.8 mL) was added 1,6-hexanedithiol (0.71 mL; 4.63 mmol), followed by AIBN (72 mg; 1.44 mmol). The solution was transferred to an ampoule and degassed by freeze-pump-thaw cycles (3 ×). The flask was filled with N_2 and then heated to 55 °C. After stirring the solution for 5 h at this temperature, the solvent was evaporated and the product was washed with hexane (5 × 10 mL) to provide 6,6'-((hexane-1,6-diylbis(sulfanediyl))bis(propane-3,1-diyl))bis(3-methyl-1,4-dioxane-2,5-dione) (**4.16**) (2.07 g; 4.22 mmol, 96%) as a white solid.

^{1}H NMR (400 MHz, $CDCl_3$) δ 5.02 (q, ^{3}J = 6.7 Hz, 2H, H^{2}), 4.96 (dd, ^{3}J = 7.5 and 4.4 Hz, 2H, H^{4}), 2.57 (t, ^{3}J = 7.0 Hz, 4H, H^{8}), 2.50 (t, ^{3}J = 7.3 Hz, 4H, H^{9}), 2.23 (m, 2H, H^{6a}), 2.08 (m, 2H, H^{6b}), 1.82 (m, 2H, H^{7}), 1.66 (d, ^{3}J = 6.7 Hz, 6H, H^{1}), 1.58 (m, 4H, H^{10}), 1.39 (m, 4H, H^{11}).

^{13}C NMR (100 MHz, $CDCl_3$) δ 167.5 (C^5), 166.8 (C^3), 75.5 (C^4), 72.4 (C^2), 32.0 (C^9), 31.5 (C^8), 29.5 (C^{10}), 29.1 (C^6), 28.4 (C^{11}), 24.2 (C^7), 15.9 (C^1).

7.6 Experimental Procedures for Chapter 5

7.6.1 Synthesis of 3-(3-(Dodecylthio)propyl)-6-methyl-1,4-dioxane-2,5-dione (DTLA, 5.3)

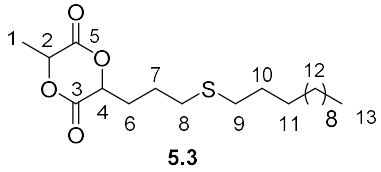

5.3

To a solution of allyl-LA (**4.15**) (783 mg; 4.60 mmol) in 1,4-dioxane (1.9 mL) was added 1-dodecanethiol (1.15 mL; 4.83 mmol), followed by AIBN (38 mg; 0.23 mmol). The solution was transferred to an ampoule and degassed by freeze-pump-thaw cycles (3 ×). The flask was filled with N_2 and then heated to 55 °C. After stirring the solution for 5 h at this temperature, the solvent was evaporated and the product was washed with hexane (5 × 2 mL) to provide 3-(3-(dodecylthio)propyl)-6-methyl-1,4-dioxane-2,5-dione (**5.3**) (1.06 g; 2.85 mmol, 62%) as a white solid.

^{1}H NMR (500 MHz, $CDCl_3$) δ 5.01 (q, ^3J = 6.7 Hz, 1H, H^2), 4.95 (dd, ^3J = 7.5 and 4.4 Hz, 1H, H^4), 2.58 (t, ^3J = 7.1 Hz, 2H, H^8), 2.50 (t, ^3J = 7.4 Hz, 2H, H^9), 2.24, (m, 1H, H^{6a}), 2.09 (m, 1H, H^{6b}), 1.87 (m, 1H, H^{7a}), 1.80 (m, 1H, H^{7b}), 1.67 (d, ^3J = 6.7 Hz, 3H, H^1), 1.59 (m, 2H, H^{10}), 1.36 (m, 2H, H^{11}), 1.25 (brs, 16H, H^{12}), 0.87 (t, ^3J = 6.8 Hz, 3H, H^{13}).

^{13}C NMR (125 MHz, $CDCl_3$) δ 167.4 (C^5), 166.7 (C^3), 75.6 (C^4), 72.5 (C^2), 32.2 (C^9), 32.1 (C^{12}), 31.6 (C^8), 29.8-29.7 (C^{12}), 29.5 (C^{10}), 29.4 (C^{12}), 29.2 (C^6), 29.1 (C^{11}), 24.2 (C^7), 22.8 (C^{12}), 16.0 (C^1), 14.3 (C^{13}).

FT-IR ν_{max}/cm^{-1} 2920 (ν C–H), 2850 (ν C–H), 1770 (ν C=O), 1741 (ν C=O), 1258 (ν C–O), 1085 (ν C–O).

HRMS: Calculated for $C_{20}H_{37}O_4S$ ($M+H^+$) 373.2413, found 373.2415 ($M+H^+$) *m*/*z*.

Anal. Calcd for $C_{20}H_{36}O_4S$: C 64.5; H 9.7; S 8.6%. Found: C 64.5; H 9.7 S 8.7.

7.6.2 Synthesis of 2-(2-Bromoacetoxy)pent-4-enoic Acid (5.1)

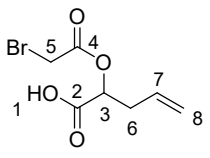

5.1

To a solution of DMAP (452 mg; 4.03 mmol) in CH_2Cl_2 (106 mL) was added bromoacetyl bromide (3.51 mL; 40.3 mmol) dropwise at 0 °C under an atmosphere of N_2. Then, a solution of 2-hydroxypent-4-enoic acid (**4.14**) (4.68 g; 40.3 mmol) and Et_3N (5.6 mL; 40.3 mmol) in CH_2Cl_2 (50 mL) was transferred dropwise *via* cannula to the reaction mixture. After this period, the solvent was removed under reduced pressure, and the

excess salt was removed by filtration. The crude oil was diluted with EtOAc (50 mL) and washed with H_2O (30 mL). The aqueous layer was extracted with EtOAc (3 × 50 mL) and the combined organic layer was dried over $MgSO_4$, filtered and concentrated under reduced pressure to provide crude 2-(2-bromoacetoxy)pent-4-enoic acid (**5.1**) as a yellow oil. The ^{1}H and ^{13}C NMR spectroscopic data were in agreement with those reported in literature.[8]

^{1}H NMR (300 MHz, $CDCl_3$) δ 11.12 (brs, 1H, H^{1}), 5.79 (ddt, ^{3}J = 17.0 Hz, 10.2 and 6.9 Hz, 1H, H^{7}), 5.19 (m, 3H, H^{3} and H^{8}), 3.94 (d, ^{2}J = 12.7 Hz, 1H, H^{5a}), 3.90 (d, ^{2}J = 12.7 Hz, 1H, H^{5b}), 2.67 (m, 2H, H^{6}).

^{13}C NMR (75 MHz, $CDCl_3$) δ 174.7 (C^{2}), 166.9 (C^{4}), 131.2 (C^{7}), 119.7 (C^{8}), 72.7 (C^{3}), 35.2 (C^{6}), 25.2 (C^{5}).

7.6.3 Synthesis of 3-Allyl-1,4-dioxane-2,5-dione (Allyl-glycolide, 5.2)

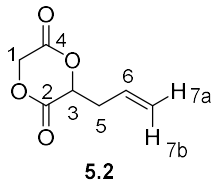

5.2

To a suspension of Na_2CO_3 (1.77g; 16.7 mmol) in dry DMF (1.2 L) under atmosphere of N_2 was added a solution of 2-(2-bromoacetoxy)pent-4-enoic acid (**5.1**) (40.3 mmol) in DMF (230 mL) *via* syringe pump (rate = 1.5 mL min^{-1}) at room temperature. After this period, the reaction mixture was stirred for 13 h before removing the solvent under reduced pressure. Then, acetone was added to precipitate the salts, which were removed by filtration. The filtrate was concentrated under reduced pressure and purified by column chromatography in silica gel using hexane:EtOAc (7:3) as eluent (R_f = 0.32) to provide allyl-glycolide (**5.2**) (3.61 g; 23.1 mmol, 57% for 2 steps) as a yellow oil. The ^{1}H and ^{13}C NMR spectroscopic data were in agreement with those reported in literature.[8]

^{1}H NMR (500 MHz, $CDCl_3$) δ 5.84 (ddt, ^{3}J = 17.2, 10.2, 7.0 Hz, 1H, H^{6}), 5.29 (d, ^{3}J = 17.1 Hz, 1H, H^{7b}), 5.26 (d, ^{3}J = 10.2 Hz, 1H, H^{7a}), 4.98 (dd, ^{3}J = 6.7 and 5.0 Hz, 1H, H^{3}), 4.94 (d, ^{2}J = 16.7 Hz, 1H, H^{1}), 4.89 (d, ^{2}J = 16.7 Hz, 1H, H^{1}), 2.84 (m, 1H, H^{5a}), 2.75 (m, 1H, H^{5b}).

^{13}C NMR (125 MHz, $CDCl_3$) δ 165.2 (C^{2}), 164.1 (C^{4}), 130.2 (C^{6}), 121.1 (C^{7}), 75.2 (C^{3}), 65.5 (C^{1}), 35.3 (C^{5}).

FT-IR ν_{max}/cm^{-1} 2940 (*v* C–H), 2921 (*v* C–H), 2852 (*v* C–H), 1768 (*v* C=O), 1739 (*v* C=O), 1255 (*v* C–O), 1087 (*v* C–O).

HRMS: Calculated for $C_{22}H_{35}O_8S_2$ ($M+H^+$) 491.1773, found 491.1772 ($M+H^+$) *m*/*z*.

Anal. Calcd for $C_{22}H_{34}O_8S_2$: C 53.9; H 7.0; S 13.1%. Found: C 54.1; H 7.0 S 13.1.

7.6.4 Synthesis of 3-(3-(Dodecylthio)propyl)-1,4-dioxane-2,5-dione (DTGA, 5.4)

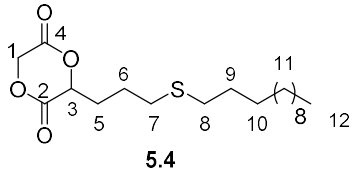

5.4

To a solution of allyl-glycolide (**5.2**) (2.00 g; 12.8 mmol) in 1,4-dioxane (5.3 mL) was added 1-dodecanethiol (3.2 mL; 13.4 mmol), followed by AIBN 105 mg; 0.64 mmol). The solution was transferred to an ampoule and degassed by freeze-pump-thaw cycles (3 ×). The flask was filled with N_2 and then heated to 55 °C. After stirring the solution for 5 h at this temperature, the solvent was evaporated and the product was washed with hexane (5 × 10 mL) to provide 3-(3-(dodecylthio)propyl)-1,4-dioxane-2,5-dione (**5.4**) (4.50 g; 12.6 mmol, 98%) as a white solid.

^{1}H NMR (500 MHz, $CDCl_3$) δ 4.94 (dd, ^3J = 4.7 and 7.9 Hz, 1H, H^3), 4.95 (d, ^3J = 16.7 Hz, 1H, H^{1a}), 4.91, (d, ^3J = 16.7 Hz, 1H, H^{1b}), 2.59 (t, ^3J = 7.0 Hz, 2H, H^7), 2.50 ^3J = 7.4 Hz, 2H, H^8), 2.23 (m, 1H, H^{5a}), 2.11 (m, 1H, H^{5b}), 1.83 (m, 2H, H^6), 1.57 (m, 2H, H^9), 1.37 (m, 2H, H^{10}), 1.26 (brs, 16H, H^{11}), 0.88 (t, ^3J = 6.9 Hz, 3H, H^{12}).

^{13}C NMR (125 MHz, $CDCl_3$) δ 165.5 (C^2), 164.3 (C^4), 75.4 (C^3), 65.5 (C^1), 32.2 (C^8), 32.1 (C^{11}), 31.4 (C^7), 29.9 (C^5), 29.8-29.7 (C^{11}), 29.5 (C^9), 29.4 (C^{11}), 29.2 (C^{10}), 24.3 (C^6), 22.8 (C^{11}), 14.3 (C^{12}).

FT-IR ν_{max}/cm^{-1} 2913 (ν C–H), 2848 (ν C–H), 1764 (ν C=O), 1741 (ν C=O), 1245 (ν C–O), 1087(ν C–O).

HRMS: Calculated for $C_{19}H_{35}O_4S$ ($M+H^+$) 359.2256, found 359.2255 ($M+H^+$) *m*/*z*.

Anal. Calcd for $C_{19}H_{34}O_4S$: C 63.5; H 9.6; S 8.9%. Found: C 63.5; H 9.6 S 9.2.

7.6.5 General Procedure for the Synthesis of PDTLA (5.5) or PDTGA (5.6) by the ROP of DTLA (5.3) or DTGA (5.4) Catalysed by TMG

Within a glovebox, 4-methoxybenzyl alcohol (3.7 µL of a 100 g L^{-1} solution in $CDCl_3$) was added to a solution of DTLA (**5.3**) (50 mg; 0.134 mmol) in CH_2Cl_2 (600 µL), followed by TMG (7.7 µL of a 100 g L^{-1} solution in $CDCl_3$). The polymerisation was stopped after 75 min by the addition of acidic Amberlyst and purified by precipitation in MeOH to provide DTLA as a viscous polymer.

PDTLA (**5.5**):

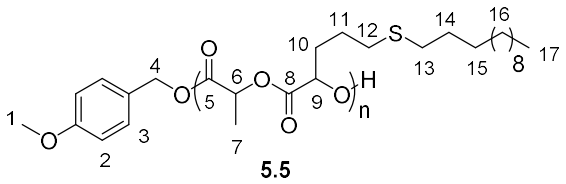

5.5

^{1}H NMR (500 MHz, $CDCl_3$) δ 7.25 (m, 1H, H^3), 6.87 (s, 1H, H^2), 5.15 (m, 1H, H^6), 5.09, (m, 1H, H^9), 3.81 (s, 3H, H^1), 2.53 (m, 2H, H^{12}), 2.49 (m, 2H, H^{13}), 2.05 (m, 2H, H^{10}), 1.74 (m, 2H, H^{11}), 1.57 (m, 5H, $H^{7,14}$), 1.36 (m, 2H, H^{15}), 1.27 (brs, 16H, H^{16}), 0.88 (t, ^3J = 6.7 Hz, 3H, H^{17}).

^{13}C NMR (125 MHz, $CDCl_3$) δ 169.8-169.4 (C^5), 169.1-168.4 (C^8), 130.3 (C^3), 114.1 (C^2), 72.4 (C^9), 69.2 (C^6), 67.2 (C^4), 55.4 (C^1), 32.2 (C^{13}), 32.1 (C^{16}), 31.6 (C^{12}), 30.1 (C^{10}), 29.8 (C^{16}), 29.5 ($C^{14,16}$), 29.1 (C^{15}), 25.0 (C^{11}), 22.8 (C^{16}), 16.9 (C^7), 14.3 (C^{17}).

SEC ($CHCl_3$, RI) DP = 50, M_n = 16.5 kg mol^{-1}, $Đ_M$ =1.05.

PDTGA (**5.6**):

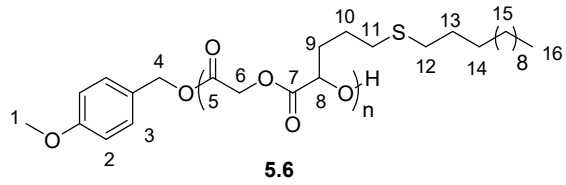

5.6

^{1}H NMR (400 MHz, $CDCl_3$) δ 7.24 (m, 1H, H^3), 6.86 (s, 1H, H^2), 5.13 (m, 1H, H^8), 4.75, (m, 2H, H^6), 3.79 (s, 3H, H^1), 2.51 (t, ^3J = 7.1 Hz, 2H, H^{11}), 2.47 (t, ^3J = 7.4 Hz, 2H, H^{12}), 2.03 (m, 2H, H^9), 1.71 (m, 2H, H^{10}), 1.54 (m, 2H, H^{13}), 1.34 (m, 2H, H^{14}), 1.24 (brs, 16H, H^{15}), 0.86 (t, ^3J = 6.7 Hz, 3H, H^{17}).

^{13}C NMR (100 MHz, $CDCl_3$) δ 168.7-168.5 (C^7), 166.6-166.5 (C^5), 130.3 (C^3), 114.1 (C^2), 72.5 (C^8), 67.3 (C^4), 60.9 (C^6), 55.3 (C^1), 32.1 (C^{12}), 32.0 (C^{15}), 31.4 (C^{11}), 30.0 (C^9), 29.7 ($C^{13,15}$), 29.4 (C^{15}), 29.0 (C^{14}), 24.9 (C^{10}), 22.8 (C^{16}), 14.2 (C^{16}).

SEC ($CHCl_3$, RI) DP = 50, M_n = 12.8 kg mol^{-1}, $Đ_M$ =1.14.

7.6.6 General Procedure for the Synthesis of 2- (5.7) and 3-Arm (5.8) Poly(L-Lactide) Oligomers

L-Lactide was purified by recrystallisation from hot toluene and used without further drying procedures. L-Lactide (15 g; 104 mmol) and DMAP (635 mg; 5.2 mmol) were added to a flask and purged with N_2. The flask was heated to 170 °C until L-lactide was molten and glycerol (0.38 mL; 5.2 mmol) was added in one portion. The solution was stirred for 5 minutes and cooled to room temperature. The polymer was dissolved

in CH_2Cl_2 and precipitated in hexane/EtOH (10:1; 3 × 200 mL) to provide PLLA as a white solid.

2-arm PLLA (**5.7**):

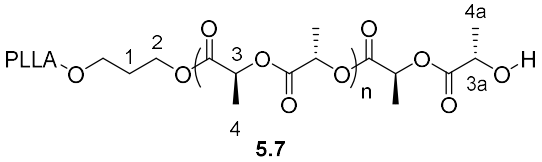

5.7

^{1}H NMR (300 MHz, $CDCl_3$) δ 5.15 (m, H^3), 4.35 (m, H^{3a}), 4.20 (t, ^3J = 6.9 Hz, H^2), 1.99 (m, H^1), 1.57 (d, ^3J = 6.9 Hz, H^4), 1.48 (m, H^{4a}).

SEC ($CHCl_3$, RI) DP = 17, M_n = 2.9 kg mol^{-1}, $Đ_M$ = 1.34.

3-arm PLLA (**5.8**):

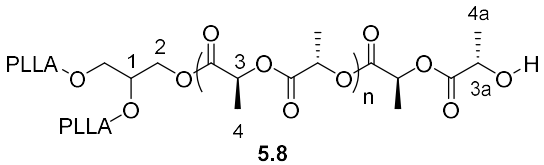

5.8

^{1}H NMR (300 MHz, $CDCl_3$) δ 5.15 (m, $H^{1,3}$), 4.35 (m, H^{3a}), 4.24 (m, H^2), 1.99 (m, H^1), 1.57 (m, H^4), 1.48 (m, H^{4a}).

SEC ($CHCl_3$, RI) DP = 18, M_n = 2.5 kg mol^{-1}, $Đ_M$ = 1.45.

7.7 References

1. R. C. Pratt, B. G. G. Lohmeijer, D. A. Long, P. N. P. Lundberg, A. P. Dove, H. Li, C. G. Wade, R. M. Waymouth and J. L. Hedrick, *Macromolecules*, 2006, **39**, 7863.
2. Y. He, H. Keul and M. Möller, *React. Funct. Polym.*, 2011, **71**, 175.
3. X. Zhang, W. Xi, C. Wang, M. Podgórski and C. N. Bowman, *ACS Macro Lett.*, 2016, **5**, 229.
4. W. Xi, H. Peng, A. Aguirre-Soto, C. J. Kloxin, J. W. Stansbury and C. N. Bowman, *Macromolecules*, 2014, **47**, 6159.
5. R. J. Pounder and A. P. Dove, *Biomacromolecules*, 2010, **11**, 1930.
6. F. Jing and M. A. Hillmyer, *J. Am. Chem. Soc.*, 2008, **130**, 13826.
7. K. R. D. Chiaie, L. M. Yablon, A. B. Biernesser, G. R. Michalowski, A. W. Sudyn and J. A. Byers, *Polym. Chem.*, 2016, **7**, 4675.
8. M. Leemhuis, N. Akeroyd, J. A. W. Kruijtzer, C. F. van Nostrum and W. E. Hennink, *Eur. Polym. J.*, 2008, **44**, 308.

Appendix

Supplementary Information

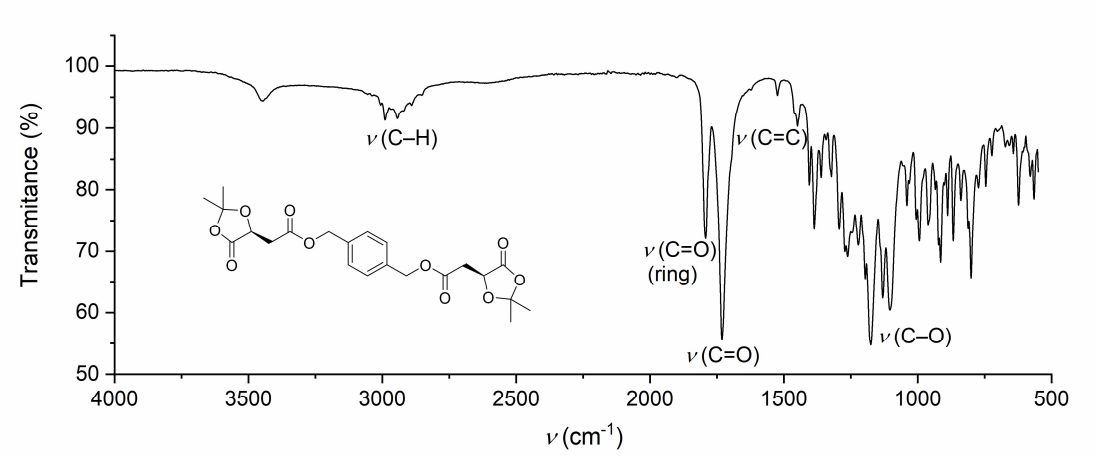

Figure A.1. FT-IR spectrum of bisacetonide prepared from L-malic acid in Chapter 4.

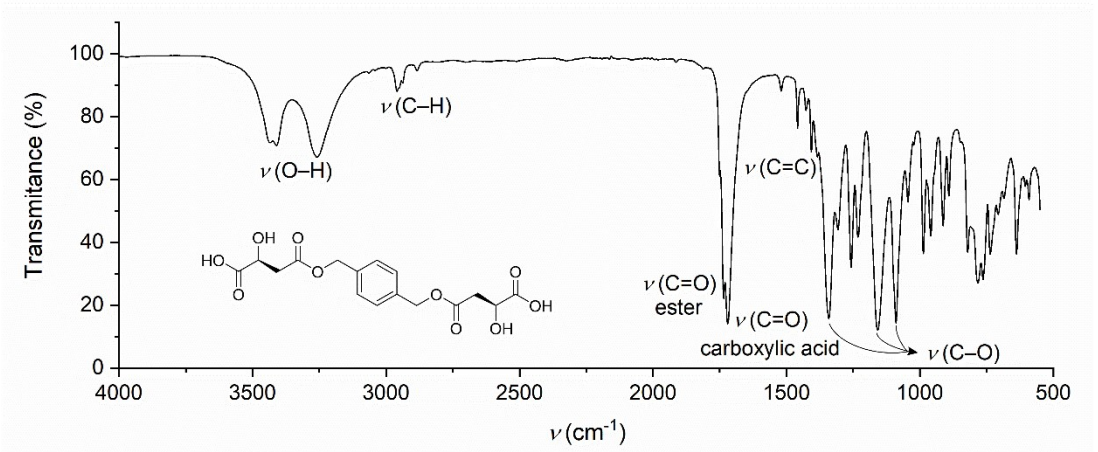

Figure A.2. FT-IR spectrum of bis(α-hydroxy acid) prepared from L-malic acid in Chapter 4.

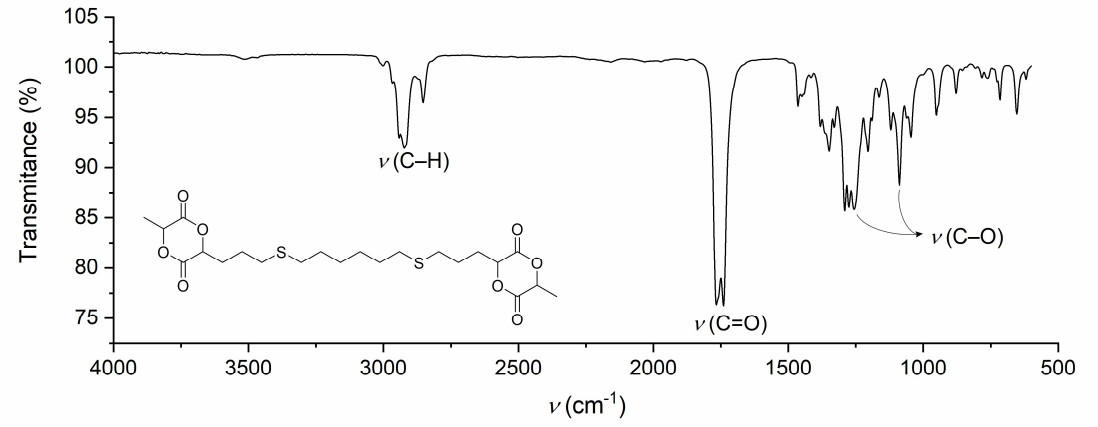

Figure A.3. FT-IR spectrum of BTLA prepared from allyl-LA in Chapter 4.

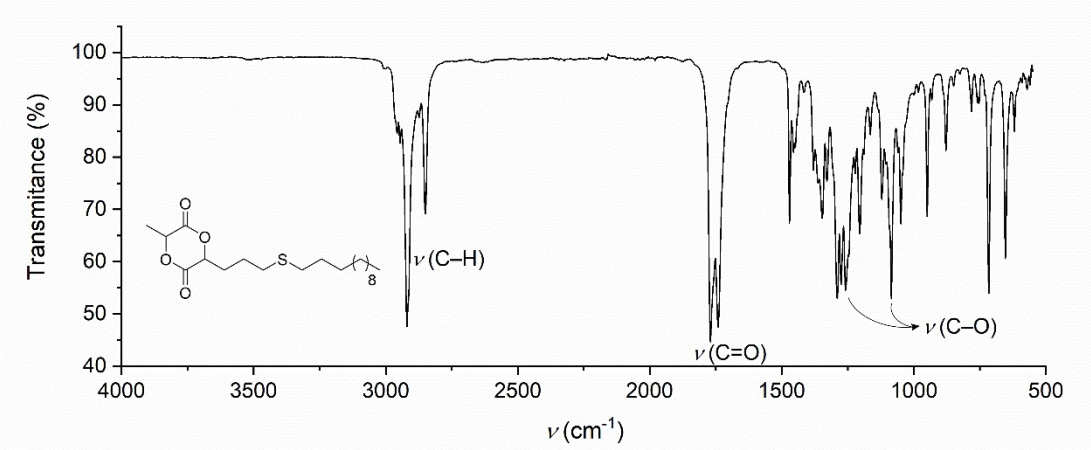

Figure A.4. FT-IR spectrum of TLA prepared from allyl-LA in Chapter 5.

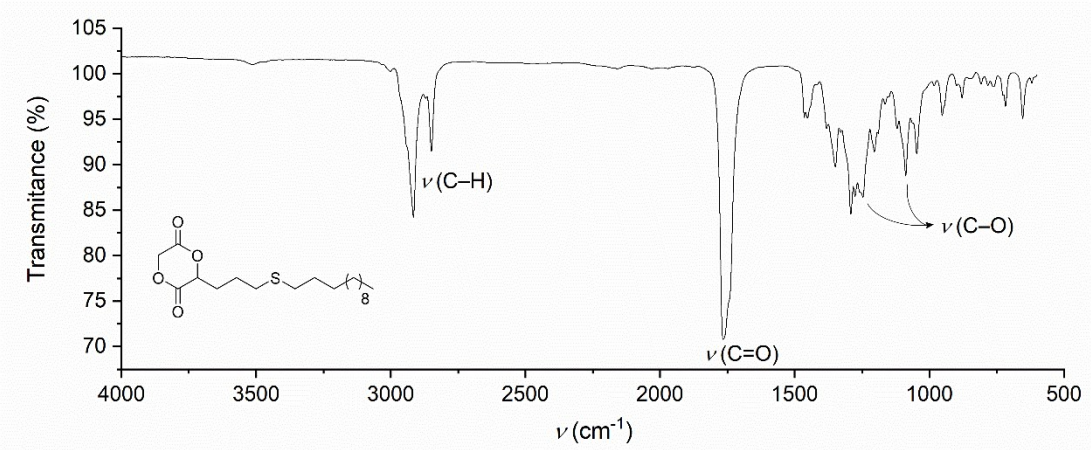

Figure A.5. FT-IR spectrum of TGA prepared from allyl-glycolide in Chapter 5.

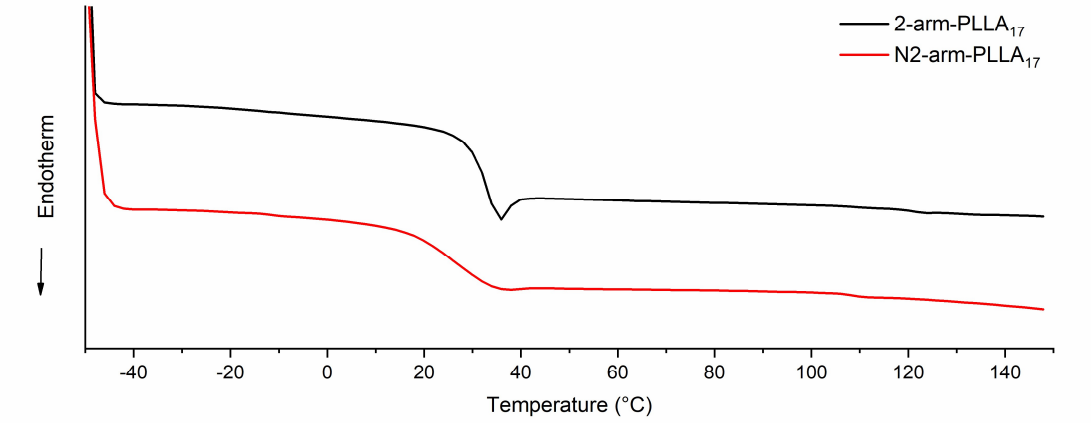

Figure A.6. DSC thermograms of second heating scan of 2-arm $PLLA_{17}$ and its corresponding network. Conditions: heating and cooling cycles between −50 and 150 °C under N_2 atmosphere at a rate of +/− 10 °C min^{-1}.

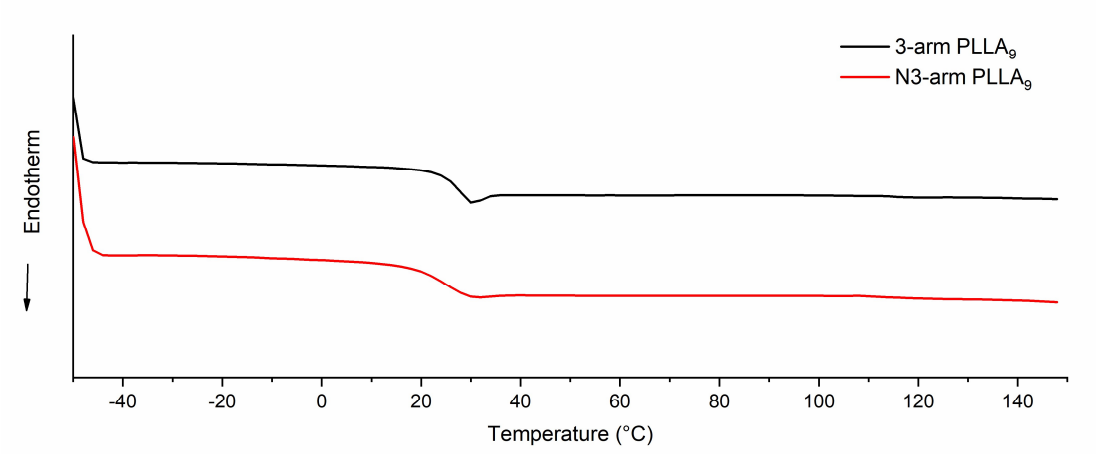

Figure A.7. DSC thermograms of second heating scan of 3-arm $PLLA_9$ and its corresponding network. Conditions: heating and cooling cycles between −50 and 150 °C under N_2 atmosphere at a rate of +/− 10 °C min^{-1}.

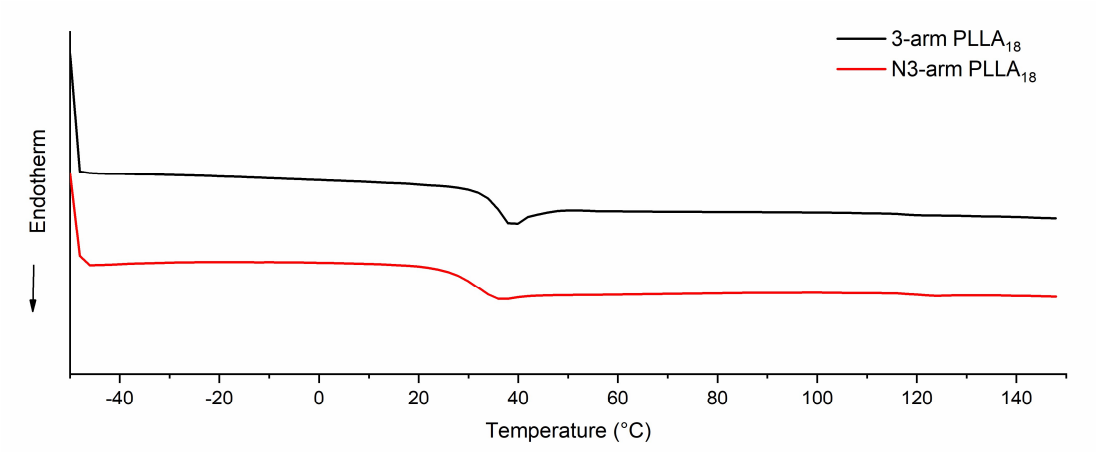

Figure A.8. DSC thermograms of second heating scan of 3-arm $PLLA_{18}$ and its corresponding network. Conditions: heating and cooling cycles between −50 and 150 °C under N_2 atmosphere at a rate of +/− 10 °C min^{-1}.

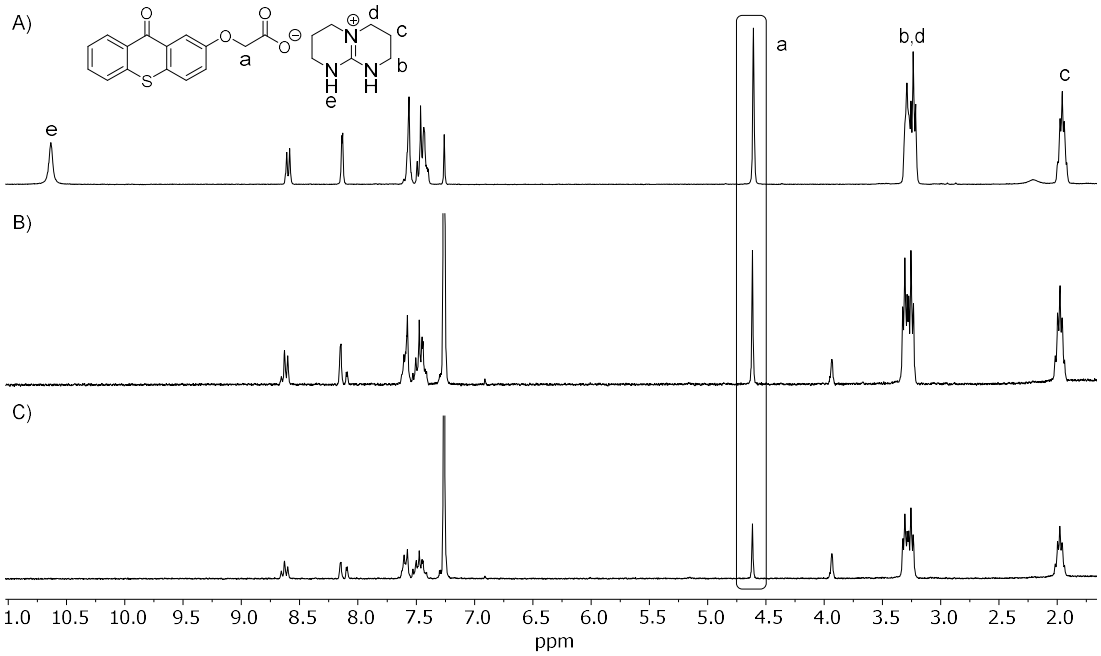

Figure A.9. ^{1}H NMR spectra of TX-O-TBD in $CDCl_3$ (10 mM) A) before and after λ = 320–400 nm irradiation for B) 10 minutes and C) 20 minutes ($CDCl_3$, 300 MHz, 298 K).

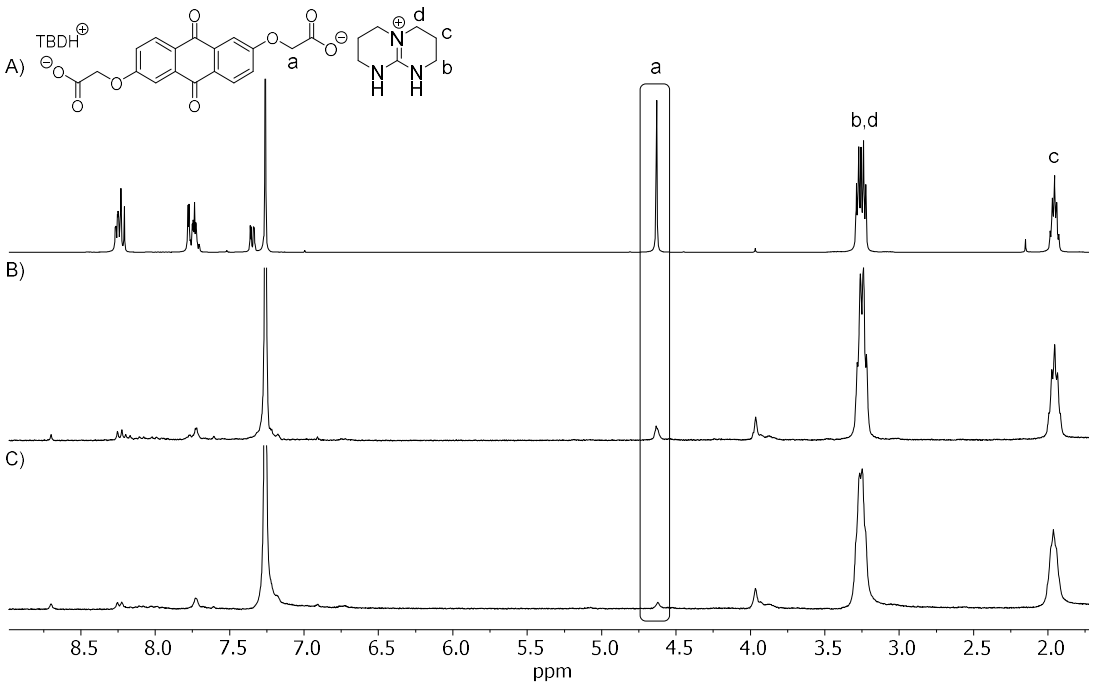

Figure A.10. ^{1}H NMR spectra of AQ-(O-TBD)$_2$ in $CDCl_3$ (10 mM) A) before and after λ = 320–400 nm irradiation for B) 10 minutes and C) 20 minutes ($CDCl_3$, 300 MHz, 298 K).

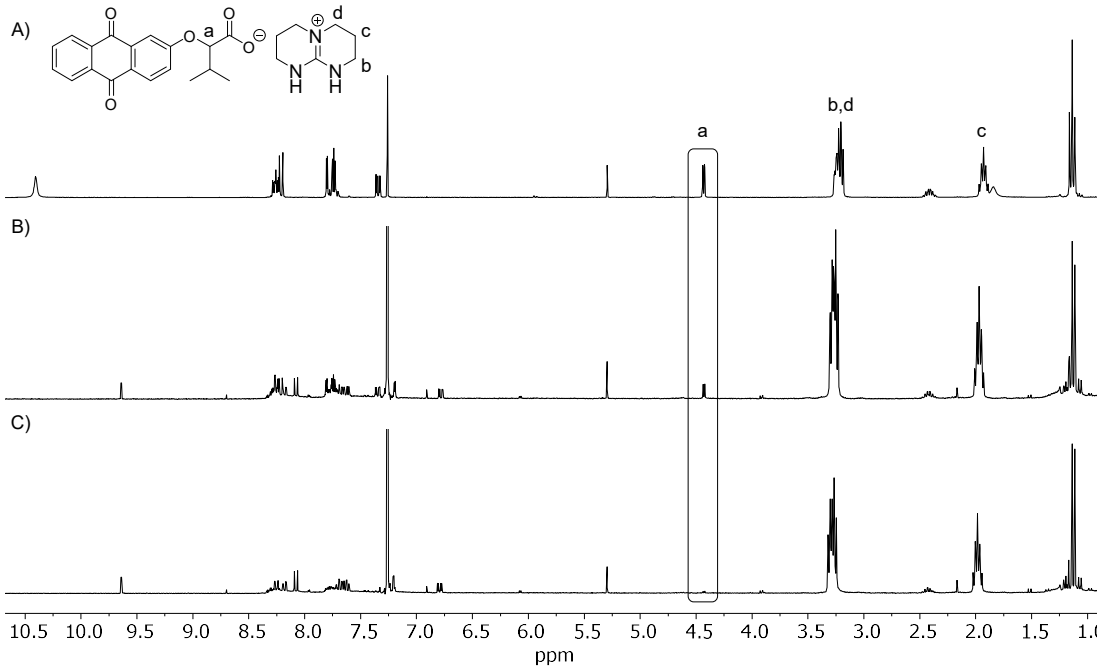

Figure A.11. ^{1}H NMR spectra of iPr-AQ-O-TBD in $CDCl_3$ (10 mM) A) before and after λ = 320–400 nm irradiation for B) 10 minutes and C) 20 minutes ($CDCl_3$, 300 MHz, 298 K).

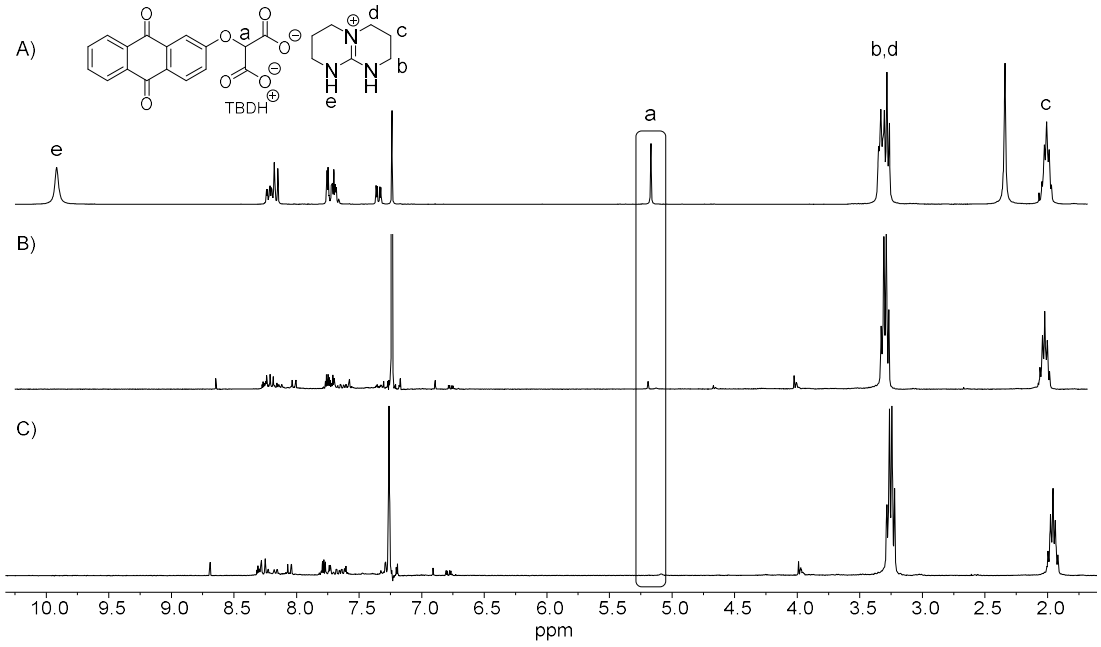

Figure A.12. ^{1}H NMR spectra of AQ-O-$(TBD)_2$ in $CDCl_3$ (10 mM) A) before and after λ = 320–400 nm irradiation for B) 10 minutes and C) 20 minutes ($CDCl_3$, 300 MHz, 298 K).